

SCHOOL OF CHEMISTRY

CARDIFF UNIVERSITY



Microporous Polymers for Carbon Dioxide Capture

Thesis submitted for the degree of Doctor of Philosophy by:

Matthew James Croad

Supervisor: Neil B. McKeown

2013

DECLARATION

This work has not previously been accepted in substance for any degree and is not concurrently submitted in candidature for any degree.

Signed..... (candidate)

Date.....

STATEMENT 1

This thesis is being submitted in partial fulfilment of the requirements for the degree of Doctor of Philosophy.

Signed..... (candidate)

Date.....

STATEMENT 2

This thesis is the result of my own independent work/investigation, except where otherwise stated. Other sources are acknowledged by explicit references.

Signed..... (candidate)

Date.....

STATEMENT 3

I hereby give consent for my thesis, if accepted, to be available for photocopying and for interlibrary loan, and for the title and summary to be made available to outside organisations.

Signed..... (candidate)

Date.....

Table of Contents

Acknowledgements.....	6
Abstract	7
Abbreviations	8
Chapter 1: Introduction	26
1.1 Microporous materials.....	26
1.2 Surface area measurement.....	26
1.3 The adsorption isotherm.....	29
1.4 A survey of nanoporous materials	30
1.4.1 Metal organic frameworks (MOFs)	30
1.4.2 Covalent organic frameworks (COFs).....	32
1.4.3 Zeolites	34
1.4.4 Activated carbon	35
1.4.5 Hypercrosslinked polymers	37
1.4.6 Conjugated microporous polymers.....	39
1.4.7 Porous aromatic frameworks.....	41
1.4.8 Polymers of intrinsic microporosity	43
1.5 The Robeson plot	53
1.6 Carbon capture and storage.....	55
1.7 Tröger's base	58
1.8 Project introduction	60
Chapter 2: Monomer synthesis and discussion	61
2.1 Discussion of TB reaction and initial optimisation	61
2.2 Design and synthesis of a novel TB derivative	64
2.3 Triptycene chemistry.....	65
2.4 Dibromotriptycene chemistry	72
2.5 Methyl substituted triptycenes.....	74
2.6 Crown ether chemistry.....	87
2.7 Naphthalene chemistry.....	88
2.8 1,4-Dimethylbenzene chemistry	89
2.9 1,4-Dimethoxybenzene chemistry	90
2.10 9,9'-Spirobisfluorene chemistry.....	92

2.11	Bis-aniline chemistry	94
2.12	Coumaron chemistry	102
2.13	Summary of monomer yields	111
Chapter 3:	Polymer synthesis	115
3.1	PIM polymerisation reactions	115
3.2	The development and optimisation of TB polymerisation	120
3.3	TB PIMs based on the triptycene unit.....	127
3.3.1	TB triptycene ladder polymers (82 - 84)	127
3.3.2	Discussion of solubility properties	132
3.3.3	TB triptycene network polymers (85 - 86)	132
3.4	Other TB polymers (87 – 92)	133
3.4.1	TB dibenzo-18-crown-6 ladder polymer (87).....	134
3.4.2	TB naphthalene ladder polymer (88) and its derivatives (89 – 90).....	134
3.4.3	TB 1,4-dimethylbenzene ladder polymer (91)	136
3.4.4	Attempted preparation of TB 1,4-dimethoxybenzene ladder polymer	137
3.4.5	TB spirobisfluorene network polymer (92)	138
3.4.6	Discussion of solubility properties	138
3.5	Bis-aniline TB polymers (93 – 103).....	139
3.5.1	Synthesis of polymers 93 - 103	139
3.5.2	Discussion of solubility properties	145
3.6	Polymerisation of coumaron derivatives	147
3.6.1	Attempted preparation of a polymer using a coumaron-forming condensation reaction	147
3.6.2	Attempted polymerisation of 2,3,8,9-tetrahydroxy-5a,10b-diphenylcoumarano-2,2',3,3'-coumaron	150
Chapter 4:	Discussion of polymer properties	152
4.1	Microporosity.....	152
4.2	Thermal stability.....	157
4.3	Film formation.....	160
4.4	Gas permeation properties	162
4.5	Carbon dioxide capacity	171
4.6	TB network polymers as heterogeneous catalysts	174
Chapter 5:	Future work.....	177
Chapter 6:	Experimental	180

6.1	Experimental techniques	180
6.2	Monomer and model compound synthesis	183
6.3	Polymer synthesis	247
Bibliography		264
Appendix 1: Solid state crystal structure analysis		272
A1.1	Crystal structures from TB model compounds	272
A1.2	Bis-aniline monomers.....	280
A1.3	Coumaron derivatives	288

Acknowledgements

First and foremost I would like to thank the EPSRC for funding my research through research grant EP/G062129/1. Special mention must also go to my supervisor Professor Neil McKeown for the opportunity to work within his research group and for initially approaching me about the PhD. He has been a constant source of help and support throughout my PhD. Great thanks must also go to Doctor Mariolino Carta, who has helped me on a regular basis, with everything from experimental problems to reaction mechanisms and even took the time to proof-read my thesis, which was very much appreciated. Doctor Grazia Bezzu also deserves many thanks, since she has been so helpful with X-ray crystallography and many other everyday issues that I encountered in the laboratory. I must thank Doctor Kadhun Msayib for being kind enough to share his fume cupboard with me and for offering his advice when I needed it. I owe gratitude to Doctor Yulia Rogan for her help and support during my studies. Thank you to my fellow students in the laboratory: Alaa, Alex, Ian, Mike, James, Jono, Richard, Rhodri, Rhys, Rupert, Sabeeha and Sadiq who made the laboratory a much more enjoyable place to work.

I must also mention the administrative and technical staff at Cardiff. They have been helpful and friendly over the years, especially Gary Coleman, Simon James, Doctor Rob Jenkins, Robin Hicks and Sham Ali. Thanks to you all.

Many thanks go to my friends in Cardiff and elsewhere, who have made life over the past three and a half years really enjoyable and who provided me with a much needed distraction from the laboratory work. I would like to say a special thanks to my family for supporting me through my education and during the problematic year that was 1998, despite everything they never gave up on me.

Finally, I would like to say a big thank you to my girlfriend Amy, for her support, patience and love over the years. Without her life wouldn't be so good and the future a lot less bright.

Abstract

The research described in this thesis relates to the development and optimisation of a novel polymerisation reaction and its subsequent use in the generation of novel ‘Polymers of Intrinsic Microporosity’ (PIMs). The polymerisation reaction takes monomers containing two or more aromatic amines and fuses them together by the synthesis of a bridged bicyclic heterocyclic link called *Tröger’s base* (TB). This link not only strongly holds the polymer chain together, but also provides a site of contortion, which is necessary for a PIM to exhibit microporosity.

The first part of this work introduces the background to the research, detailing the reasons behind the development of a new class of PIM and the competitor materials. Following this is detailed the optimisation of the TB forming condensation reaction and the synthesis of a variety of amine functionalised monomers. Also described in this section is the optimisation of a second condensation reaction used for the synthesis of a family of compounds based around a coumaron framework, all of which lack amine functionality. This precedes discussion of X-ray crystal structure analysis of several TB model compounds, amine functionalised monomers and coumaron-based compounds. After this is a description of the development of the novel TB polymerisation reaction, the results of the TB polymerisation of the amine functionalised monomers, characterisation of the successful polymers and the attempted polymerisation of two coumaron-based monomers. The final part of this work reports the experimental procedure for each compound together with full characterisation.

In closing, the TB polymerisation reaction has successfully used for the production of highly stable and soluble PIMs exhibiting a wide range of microporosity, with BET surface areas ranging from 0 m²/g to 1035 m²/g. A few of these PIMs have been found to have excellent molecular weight, capable of forming strong membranes, suitable for gas separation, most notably for the purification of oxygen, hydrogen and carbon dioxide from nitrogen. Conversely, the synthesis of coumaron-based PIMs proved unsuccessful, but nevertheless this research should allow the future synthesis of a coumaron-based PIM.

The research on TB polymerisation detailed in this thesis has contributed towards an International Patent¹²² and a paper in *Science*¹²³ so can be deemed to have been successful by that measure.

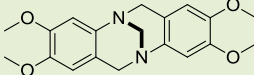
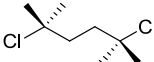
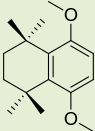
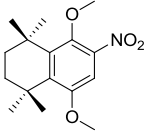
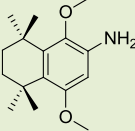
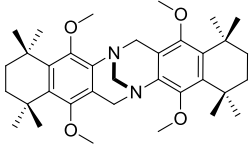
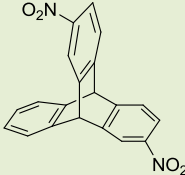
Abbreviations

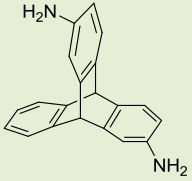
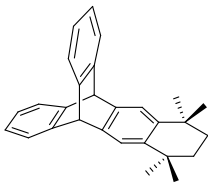
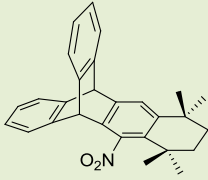
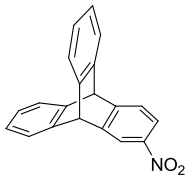
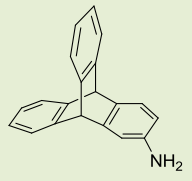
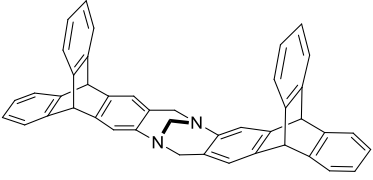
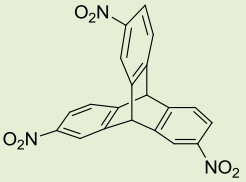
Abbreviation	Meaning
Å	Angstrom
AcCl	Acetyl chloride
AlCl ₃	Aluminium trichloride
Aq.	Aqueous
BBr ₃	Boron tribromide
BET	Brunauer, Emmett and Teller
Br.	Broad
BuLi	n-Butyllithium
Calc.	Calculated
CCS	Carbon capture and storage
CHCl ₃	Chloroform
CMP	Conjugated microporous polymer
COF	Covalent-organic framework
CrO ₃	Chromium trioxide
CS ₂	Carbon disulphide
D	Doublet
DCE	Dichloroethane
DCM	Dichloromethane
DMAc	N,N-Dimethylacetamide
DMF	N,N-Dimethylformamide
DMSO	Dimethyl sulphoxide
EI	Electron impact
Equiv. or Eq.	Equivalents
ES	Electrospray
Et.	Ethyl group
Et ₂ O	Diethyl ether
EtOH	Ethanol
F _{AV}	Average functionality
G	Grams
GHG	Greenhouse gas(es)
GPC	Gel Permeation Chromatography
H	Hour(s)
HCl	Hydrochloric acid

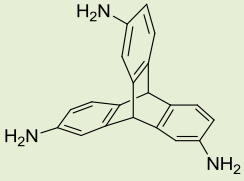
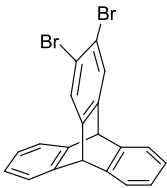
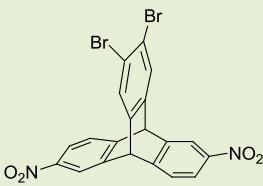
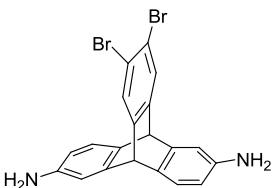
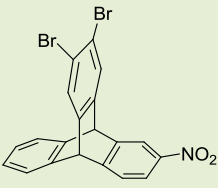
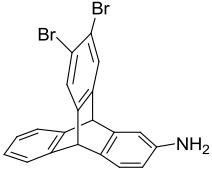
Abbreviation	Meaning
HI	Hydroiodic acid
HCP	Hypercrosslinked polymer
HNO ₃	Nitric acid
HRMS	High resolution mass spectrometry
H ₂ SO ₄	Sulphuric acid
Hz	Hertz
IR	Infra-red
IPr	Iso-propyl group
IUPAC	International union of pure and applied chemistry
J	Coupling constant
K(ads)	Rate of adsorption
K(des)	Rate of desorption
KNO ₃	Potassium nitrate
Lit.	Literature
LRMS	Low resolution mass spectrometry
M	Multiplet
Me	Methyl group
MeCN	Acetonitrile
MeCOOH	Acetic acid
MHz	Mega hertz
ml	Millilitres
MeMgBr	Methylmagnesium bromide
MeOH	Methanol
MeNO ₂	Nitromethane
Mmol	Millimole(s)
M_n	Number-average molecular weight
MOF	Metal-organic framework
Mp	Melting point
M_w	Mass-average molecular weight
M_z	Z-average molecular weight
NH ₃	Ammonia
NaOCl	Sodium hypochlorite
NaOH	Sodium hydroxide
Nm	Nanometre(s)
NMP	N-methyl pyrrolidone

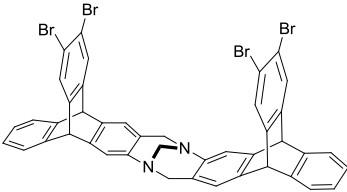
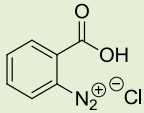
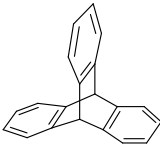
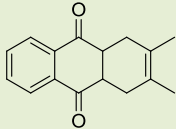
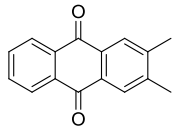
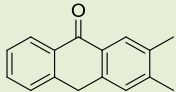
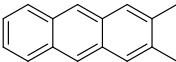
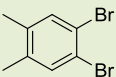
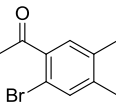
Abbreviation	Meaning
NMR	Nuclear magnetic resonance
OMIM	Oligomeric material of intrinsic microporosity
P	Pressure
PAF	Porous aromatic framework
Ph	Phenyl group
Ph ₂ O	Diphenyl ether
Ph-Cl	Chlorobenzene
PIM	Polymer of intrinsic microporosity
Ppm	Parts per million
Q	Quartet
R.t.	Room temperature
S	Singlet
T	Triplet
TB	Tröger's base
TFA	Trifluoroacetic acid
TFAA	Trifluoroacetic anhydride
TGA	Thermogravimetric analysis
THF	Tetrahydrofuran
TON	Turnover number
TOF	Turnover frequency
UV	Ultra-violet
V(ads)	Volume of adsorbed gas
XRD	X-ray diffraction
Z	The number of chemical formula units per unit cell
Zlc	Zero-length column

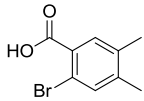
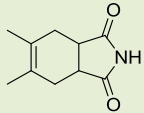
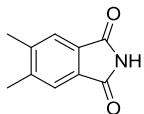
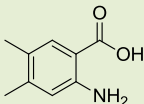
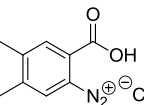
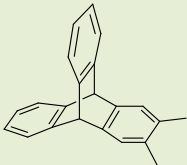
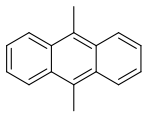
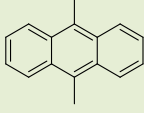
Table of molecules

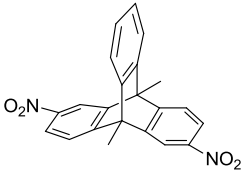
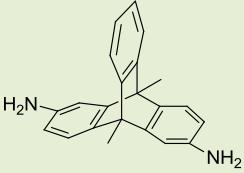
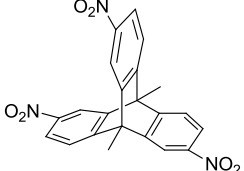
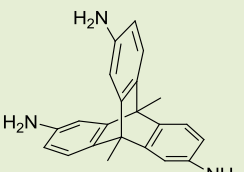
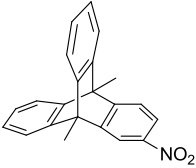
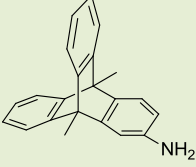
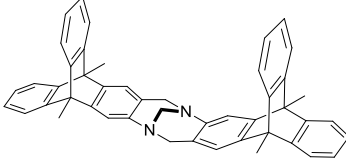
Chemical name	Structure	Number
(5S,11S)-2,3,8,9-tetramethoxy-6,12-dihydro-5,11-methanodibenzo[b,f][1,5]diazocine		1
2,5-Dichloro-2,5-dimethylhexane		2
5,8-Dimethoxy-1,1,4,4-tetramethyl-1,2,3,4-tetrahydronaphthalene		3
5,8-Dimethoxy-1,1,4,4-tetramethyl-6-nitro-1,2,3,4-tetrahydronaphthalene		4
5,8-Dimethoxy-1,1,4,4-tetramethyl-6-amino-1,2,3,4-tetrahydronaphthalene		5
(6S,14S)-5,8,13,16-Tetramethoxy-1,1,4,4,9,9,12,12-octamethyl-1,2,3,4,7,9,10,11,12,15-decahydro-6,14-methanodinaphtho[2,3-b:2',3'-f][1,5]diazocine		6
2,6(7)-Dinitrotritycene		7

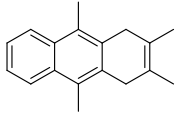
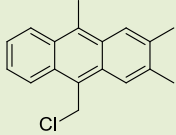
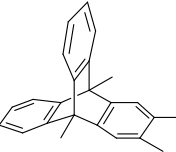
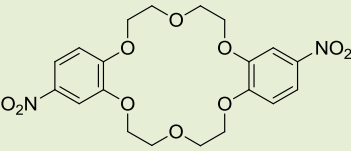
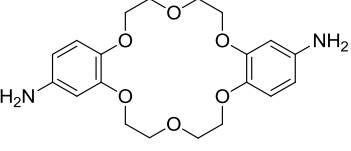
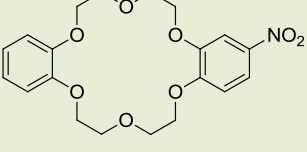
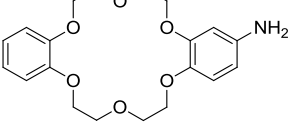
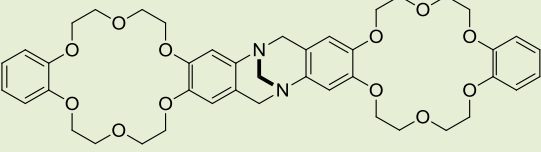
Chemical name	Structure	Number
2,6(7)-Diaminotriptycene		8
2,2,5,5-Tetramethyl-2,3,4,5-tetrahydrobenzotriptycene		9
2,2,5,5-Tetramethyl-1-nitro-2,3,4,5-tetrahydrobenzotriptycene		10
2-Nitrotriptycene		11
2-Aminotriptycene		12
(5S,7R,10R,15S,17R,20R)-5,8,10,15,18,20-Hexahydro-5,20:10,15-bis([1,2]benzeno)-7,17-methanodianthra[2,3-b:2',3'-f][1,5]diazocine		13
2,6(7),14-Trinitrotriptycene		14

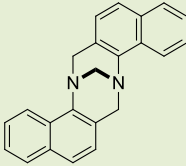
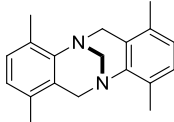
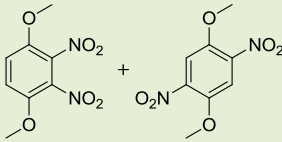
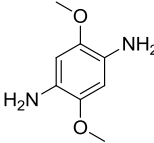
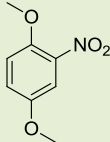
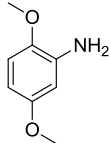
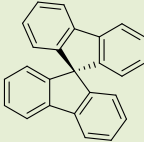
Chemical name	Structure	Number
2,6(7),14-Triaminotriptycene		15
2,3-Dibromotriptycene		16
2,3-Dibromo-6(7),14-dinitrotriptycene		17
2,3-Dibromo-6(7),14-diaminotriptycene		18
2,3-Dibromo-6(7)-nitrotriptycene		19
2,3-Dibromo-6(7)-aminotriptycene		20

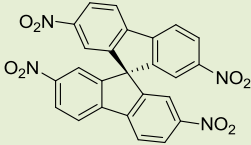
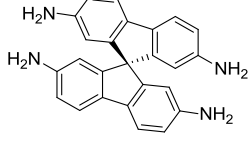
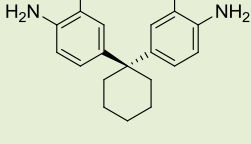
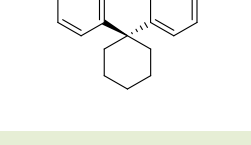
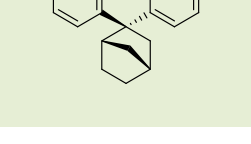
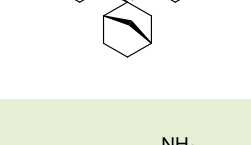
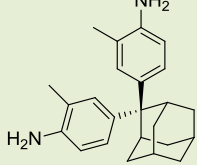
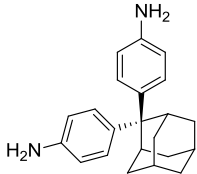
Chemical name	Structure	Number
(5S,7R,10R,15S,17R,20R)- 2,3,12,13-Tetrabromo- 5,8,10,15,18,20-hexahydro- 5,20:10,15-bis([1,2]benzeno)-7,17- methanodianthra[2,3-b:2',3'- f][1,5]diazocine		21
Benzenediazonium-2- carboxylatechloride		22
Triptycene		23
2,3-Dimethylbutadiene-α- naphthoquinone		24
2,3-Dimethylantraquinone		25
2,3-Dimethylanthrone		26
2,3-Dimethylanthracene		27
1,2-Dibromo-4,5-dimethylbenzene		28
2-Bromo-4,5- dimethylacetophenone		29

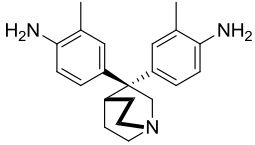
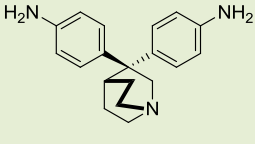
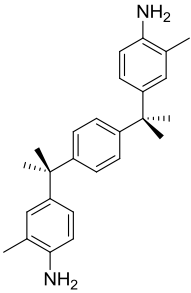
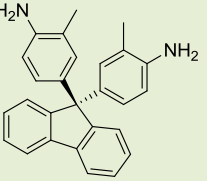
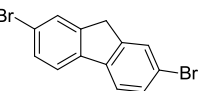
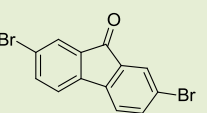
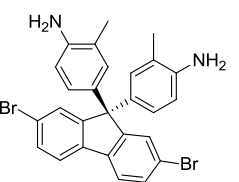
Chemical name	Structure	Number
<i>2-Bromo-3,4-dimethylbenzoic acid</i>		30
<i>3,4-Dimethyltetrahydrophthalimide</i>		31
<i>3,4-Dimethylphthalimide</i>		32
<i>4,5-Dimethylantranilic acid</i>		33
<i>4,5-Dimethylbenzenediazonium-2-carboxylatechloride</i>		34
<i>2,3-Dimethyltriptycene</i>		35
<i>9,10-Dimethylantracene</i>		36
<i>9,10-Dimethylantracene</i>		36
<i>9,10-Dimethyltriptycene</i>		37

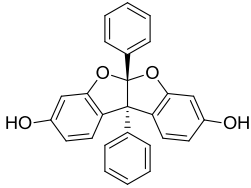
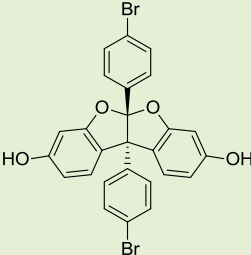
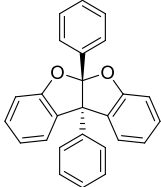
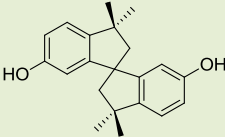
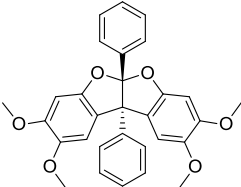
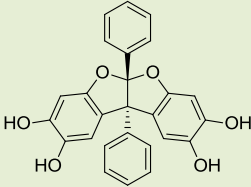
Chemical name	Structure	Number
2,6(7)-Dinitro-9,10-dimethyltriptycene		38
2,6(7)-Diamino-9,10-dimethyltriptycene		39
2,6(7),14-Trinitro-9,10-dimethyltriptycene		40
2,6(7),14-Triamino-9,10-dimethyltriptycene		41
2-Nitro-9,10-dimethyltriptycene		42
2-Amino-9,10-dimethyltriptycene		43
TB 9,10-dimethyltriptycene model compound		44

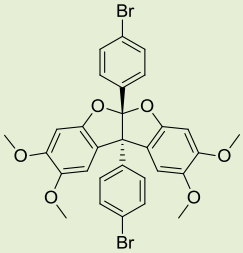
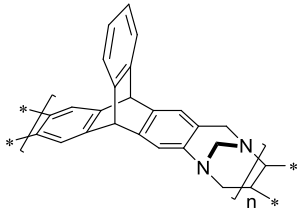
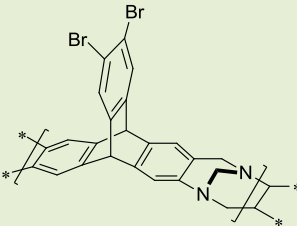
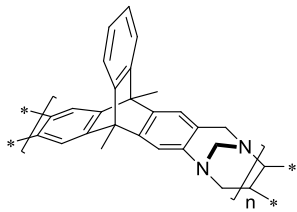
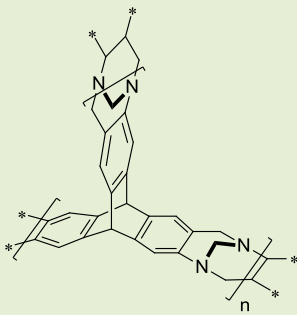
Chemical name	Structure	Number
2,3,9,10-Tetramethyl-1,4-dihydroanthracene		45
2,3,9-Trimethyl-10-chloromethylanthracene		46
2,3,9,10-Tetramethylanthracene		47
2,13(14)-Dinitrodibenzo-18-crown-6		48
2,13(14)-Diaminodibenzo-18-crown-6		49
2-Nitrodibenzo-18-crown-6		50
2-Aminodibenzo-18-crown-6		51
TB dibenzo-18-crown-6 model compound		52

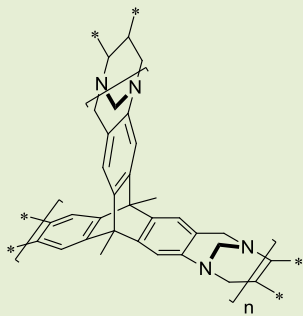
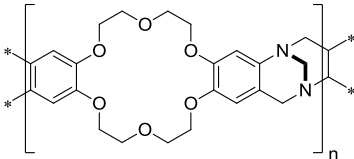
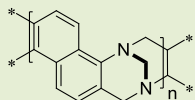
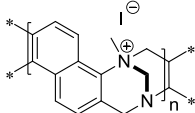
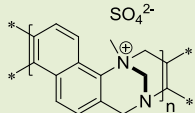
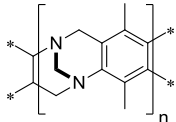
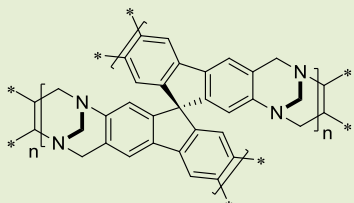
Chemical name	Structure	Number
<i>TB naphthalene model compound</i>		53
<i>TB 1,4-dimethylbenzene model compound</i>		54
<i>1,4-Dimethoxy-2,3-dinitrobenzene (A)</i> <i>1,4-Dimethoxy-2,5-dinitrobenzene (B)</i>		55
<i>1,4-Dimethoxy-2,5-phenylenediamine</i>		56
<i>1,4-Dimethoxy-2-nitrobenzene</i>		57
<i>1,4-Dimethoxy-2-aminobenzene</i>		58
<i>9,9'-Spirobisfluorene</i>		59

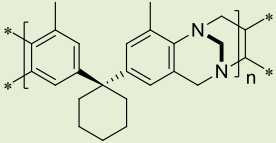
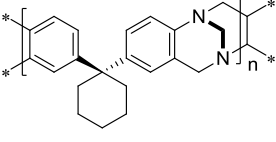
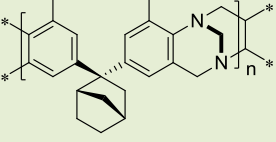
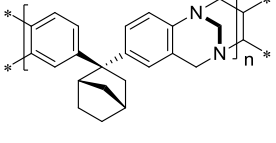
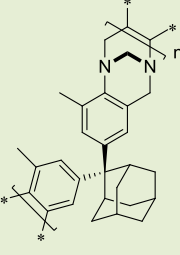
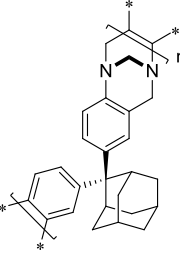
Chemical name	Structure	Number
2,2',7,7'-Tetranitro-9,9'-spirobisfluorene		60
2,2',7,7'-Tetraamino-9,9'-spirobisfluorene		61
2,2-Bis(3-methyl-4-aminophenyl)cyclohexane		62
2,2-Bis(4-aminophenyl)cyclohexane		63
2,2-Bis(3-methyl-4-aminophenyl)bicyclo[2.2.1]heptane		64
2,2-Bis(4-aminophenyl)bicyclo[2.2.1]heptane		65
2,2-Bis(3-methyl-4-aminophenyl)adamantane		66
2,2-Bis(4-aminophenyl)adamantane		67

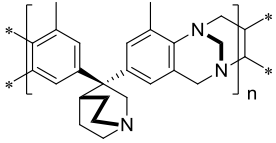
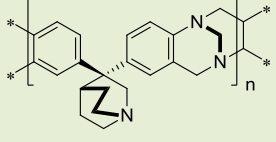
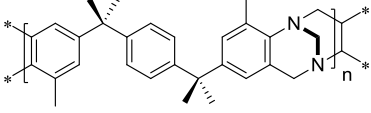
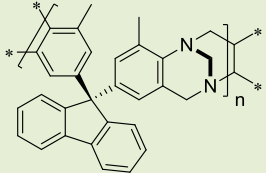
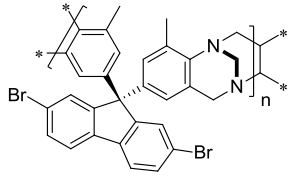
Chemical name	Structure	Number
3,3-Bis(3-methyl-4-aminophenyl)-1-azabicyclo[2,2,2]octane		68
3,3-Bis(4-aminophenyl)-1-azabicyclo[2,2,2]octane		69
1,1',4,4'-Tetramethyl-1,4-(3-methyl-4-aminophenyl)benzene		70
9,9'(3-Methyl-4-aminophenyl)fluorene		71
2,7-Dibromo-9-fluorene		72
2,7-Dibromo-9-fluorenone		73
2,7-Dibromo-9,9'-(3-methyl-4-aminophenyl)fluorene		74

Chemical name	Structure	Number
<p>3,8-Dihydroxy-5a,10b-diphenylcoumarano-2,2',3,3'-coumaron</p>		75
<p>3,8-Dihydroxy-(4,4'-dibromo)-5a,10b-diphenylcoumarano-2,2',3,3'-coumaron</p>		76
<p>5a,10b-Diphenylcoumarano-2,2',3,3'-coumaron</p>		77
<p>3,3,3',3'-Tetramethyl-2,2',3,3'-tetrahydro-1,1'-spirobi[indene]-6,6'-diol</p>		78
<p>2,3,8,9-Tetramethoxy-5a,10b-diphenylcoumarano-2,2',3,3'-coumaron</p>		79
<p>2,3,8,9-Tetrahydroxy-5a,10b-diphenylcoumarano-2,2',3,3'-coumaron</p>		80

Chemical name	Structure	Number
<p>2,3,8,9-Tetramethoxy-(4,4'-dibromo)-5a,10b-diphenylcoumarano-2,2',3,3'-coumaron</p>		81
<p>TB triptycene ladder polymer</p>		82
<p>TB 2,3-dibromotriptycene ladder polymer</p>		83
<p>TB 9,10-dimethyltriptycene ladder polymer</p>		84
<p>TB triptycene network polymer</p>		85

Chemical name	Structure	Number
TB 9,10-dimethyltritycene network polymer		86
TB dibenzo-18-crown-6 ladder polymer		87
TB naphthalene ladder polymer		88
Iodine stabilised quaternary naphthalene TB polymer		89
Sulphate stabilised quaternary naphthalene polymer		90
TB 1,4-dimethylbenzene ladder polymer		91
TB 9,9'-spirobisfluorene network polymer		92

Chemical name	Structure	Number
<i>TB bis-aniline polymer 1</i>		93
<i>TB bis-aniline polymer 2</i>		94
<i>TB bis-aniline polymer 3</i>		95
<i>TB bis-aniline polymer 4</i>		96
<i>TB bis-aniline polymer 5</i>		97
<i>TB bis-aniline polymer 6</i>		98

Chemical name	Structure	Number
<i>TB bis-aniline polymer 7</i>		99
<i>TB bis-aniline polymer 8</i>		100
<i>TB bis-aniline polymer 9</i>		101
<i>TB bis-aniline polymer 10</i>		102
<i>TB bis-aniline polymer 11</i>		103

Chapter 1: Introduction

1.1 Microporous materials

Most materials cannot be classified as being porous¹, since they lack minute surface openings, through which gases, liquids, or microscopic particles may pass. For porous materials it is the structure of these openings or pores that determines physical properties such as density, thermal conductivity and strength of a material. Hence, controlling porosity is very important in the design of catalysts, adsorbents, membranes and ceramics².

Pores can be classified according to their size³: pores with diameters greater than 50 nm are called macropores, pores with diameters between 2 nm and 50 nm are known as mesopores and pores with diameters less than 2 nm are defined as micropores. The smaller a pore the greater its surface area to volume ratio, so it is perhaps not surprising that micropores constitute the largest proportion of a materials surface area. Hence, a material with a lot of micropores, a microporous material, generally has a high surface area. It is such materials that the work covered in this thesis is concerned with.

Over the past fifty years microporous materials have become an increasingly important and developed area of chemistry. There are many academic and industrial research groups now investigating these materials for applications including adsorbent technology⁴, catalysis⁵, gas purification⁶, hydrogen storage⁷ and carbon dioxide capture⁸. The reason behind this interest comes from microporous materials possessing accessible and high surface areas.

1.2 Surface area measurement

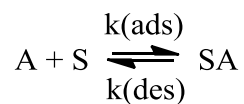
A surface is a boundary between two phases and hence where the phases can interact with one another. For a microporous material this interaction happens between gas molecules and the surface of the micropores. In this example, the gas molecule can interact with the surface in two ways: chemisorption or physisorption. By studying this gas sorption it is possible to gather information about the material, such as its apparent surface area and its pore size distribution.

Chemisorption is the phenomenon that occurs when a chemical bond is formed between a gas molecule and a surface. It often involves activation energy and the resulting bond is

strong, thus the process is often irreversible. Physisorption is the phenomenon that occurs when a Van der Waals bond is formed between a gas molecule and a surface. As the interaction does not involve activation energy the resulting bond is only weak and the process is readily reversible.

In 1916 Irving Langmuir developed a mathematical model known today as the Langmuir isotherm⁹, to describe physisorption in a gas/solid system. In this system equilibrium is established between the gas molecules adsorbed onto the surface and the free gas molecules. The position of this equilibrium depends on the relative stabilities of the species, the temperature of the system and the pressure of the gas above the surface. High pressure and low temperature are necessary to keep the surface saturated with gas molecules.

The system is described by the following equation:



Where: A = the gas molecules, S = vacant surface sites, SA = occupied surface sites, k(ads) = rate of adsorption and k(des) = rate of desorption.

As previously stated, the pressure of the system is important to the position of the equilibrium; higher pressure will force more gas molecules onto the surface of the material. Thus [A] is proportional to the pressure of gas (P). [SA] is proportional to the amount of the surface covered by adsorbed molecules (θ), and [S] is proportional to the number of vacant sites ($1 - \theta$). Using this, equations for the rates of sorption can be described:

$$\text{Rate of adsorption} = k_{ads}P(1 - \theta)$$

$$\text{Rate of desorption} = k_{des}\theta$$

Where: P = pressure and θ = fractional monolayer coverage.

In a dynamic equilibrium the rate of adsorption equals the rate of desorption, so the Langmuir isotherm can be written as:

$$\theta = \frac{KP}{1 + KP} \quad \text{where } K = \frac{k_{ads}}{k_{des}}$$

The Langmuir isotherm makes a number of assumptions; the surface is uniform and all sites of adsorption are equal, the adsorbed molecules do not interact, and the surface is considered saturated once a single monolayer has formed. In many real systems this is not true, so the model was modified in 1938 by Brunauer, Emmett and Teller to give a new model known as the BET isotherm model⁹. It assumes that once a monolayer becomes saturated a further monolayer can form on top, and that the rates of evaporation and condensation are equal for each layer. The BET isotherm model can be described as follows:

$$V = \frac{V_m c P}{P_0 - P \left[1 + \frac{(c-1)P}{P_0} \right]}$$

Where: P = adsorption pressure, P₀ = saturation vapour pressure, c = the BET constant, V = volume of adsorbed gas, V_m = monolayer volume.

This can then be rearranged to:

$$\frac{P}{V(P_0 - P)} = \frac{c-1}{cV_m} \left(\frac{P}{P_0} \right) + \frac{1}{cV_m}$$

When $P/V(P_0 - P)$ is plotted against P/P_0 the values of V_m and c can be obtained from the slope $[(c-1)/V_m c]$ and intercept $[1/(V_m c)]$ of the line from the plotted points. Knowing the monolayer volume and the area occupied by one adsorbate molecule the BET surface area (S) can be derived:

$$S = N_A V_m \sigma$$

Where: S = BET surface area, N_A = Avogadro's number, V_m = monolayer volume and σ = area occupied by one adsorbate molecule.

Therefore, by knowing the amount of material (adsorbent), the amount of gas adsorbed (adsorbate) and the area occupied by one adsorbate molecule the surface area of any

sample can be measured. Nitrogen (N₂) is the most commonly used for BET measurements, and one N₂ molecule has an area of 16.2 Å². This method allows the calculation of BET surface area for materials ranging from 0.01 to 6000 m²/g. Pore size and pore size distribution can also be calculated from the isotherm using an assessment model, based on size and shape, for pores ranging in size from a few Angstroms to half a micron. For an accurate measurement of surface area, pore size and pore size distribution it is essential to remove all contaminant gas molecules from the surface of a material.

1.3 The adsorption isotherm

The complete adsorption/desorption process is known as an adsorption isotherm. Each class of material (microporous, macroporous and nonporous) has a different adsorption isotherm profile². This is illustrated below in Figure 1.

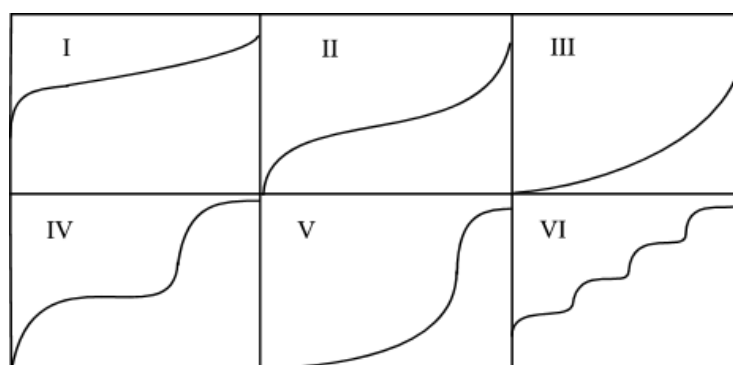


Figure 1: The IUPAC classification of adsorption isotherms². Type I is microporous, type IV and V are mesoporous and type II, III and VI are macroporous.

This nomenclature is solely concerned with pore width, whilst neglecting hysteresis and pore shape, which become important when investigating shape selective molecular sieve behaviour. Fluid-solid and fluid-fluid attractive forces account for the differences between types II and III and types IV and V. Stronger interactions help the gas to adsorb at lower pressures, resulting in the isotherm climbing the y-axis faster. The shape of the type VI isotherm can be explained by adsorption on a macroporous material, with stepwise multilayer adsorption occurring. Desorption of N₂ gas from a material can either be completely reversible (types I, II, III and VI) or not fully reversible (types IV and V), which results in hysteresis loops in the isotherm. These loops are associated with capillary condensation in the mesopores, which dominates the adsorption. Meanwhile, adsorption in

a micropore is dominated by stronger interactions between the adsorbate and the pore walls¹⁰.

The work detailed in this thesis is concerned solely with microporous materials (type I isotherms). In such systems a large amount of nitrogen can be adsorbed at low pressures, and it is this part of the isotherm that is called the microporous region (Figure 2). The blue line represents gas adsorption and the red line represents gas desorption. In this example, desorption does not follow the line of adsorption and consequently there is what is referred to as a hysteresis. This behaviour arises because for some materials adsorption of gas is not readily reversible under the conditions used for BET analysis. Data from such an isotherm can be used to determine the structure and size of pores in an adsorbent.

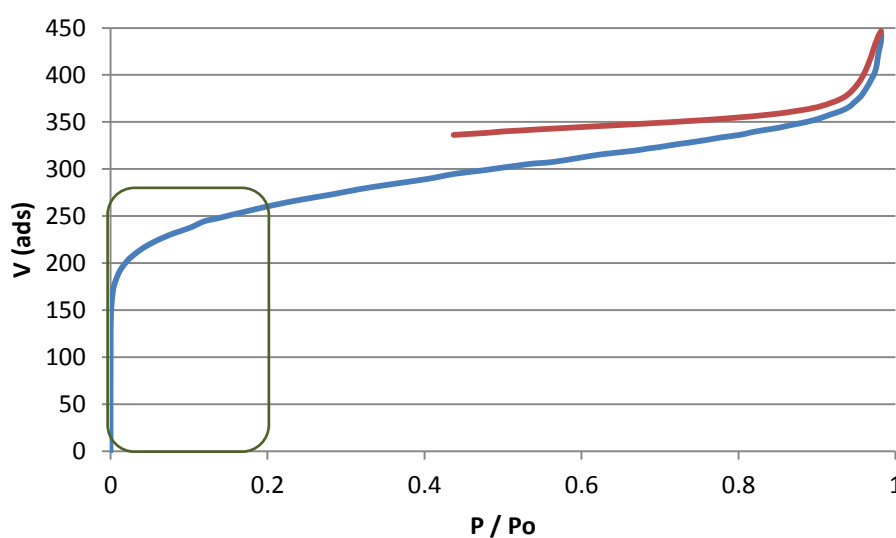


Figure 2: A BET isotherm for a microporous material, the microporous region is outlined in green.

1.4 A survey of nanoporous materials

1.4.1 Metal organic frameworks (MOFs)

Metal organic frameworks (MOFs) are a family of crystalline porous materials comprised of ordered networks formed from organic electron donor linkers and metal cations. They are synthesised using either a solvothermal or sonochemical reaction in which organic ligands form coordination bonds to metal-based nodes (either a single ion or cluster) in a self-assembly process. This process creates a 3D framework (Figure 3) possessing

extremely high surface area, up to 7000 m²/g, and pore volume, up to 4.40 cm³/g¹¹. Most importantly, these frameworks can be synthesised so that they do not collapse when guest molecules, such as solvent, are removed¹², allowing for the use of MOFs in a range of applications.

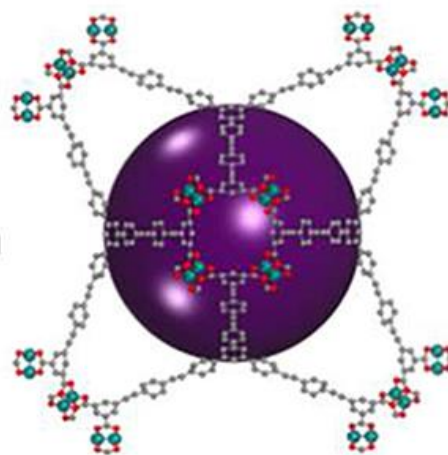


Figure 3: The structure of MOF NU-110¹², showing the large pore volume in purple.

Fuelling interest in MOFs is their extraordinary compositional and structural variety; there are greater than 10,000 MOFs known¹¹, many of which display permanent porosity, ultralow densities and well-defined pores and channels. This variety arises from the synthetic flexibility MOFs possess due to having organic components, which can be designed and synthesised to a certain specification, this offers a freedom that inorganic synthesis cannot compete with. Thus by careful design of the ligand linker and choosing the right cation it is possible to tailor the pore size and chemical properties of a MOF to suit a desired application¹³.

The properties of a MOF may be further tuned by post-synthetic modification; this involves functionalising the organic linker (covalent modification), metal-based node (coordinate covalent modification) or both by chemical reaction. This modification leads to MOFs with improved gas sorption, catalytic activity, bioactivity and more robust physical properties¹⁴. MOFs are such useful materials because of their extremely high porosity, well-defined pore structure, design freedom and ability to be tuned. These properties have made MOFs attractive materials for study and have led to a range of potential applications, including catalysis¹⁵, drug delivery¹⁶, gas separation and purification¹⁷, hydrogen storage¹⁸, sensors¹⁹ and carbon dioxide capture²⁰.

MOFs are currently being investigated for post combustion carbon dioxide capture owing to their extremely high surface areas, which provide an opportunity for large carbon dioxide adsorption capacities to be achieved²¹. For example, MOF-177 has an adsorption capacity for carbon dioxide of 320 cm³/cm³ under standard conditions of temperature and pressure. To improve CO₂/N₂ selectivity a range of amine containing organic linkers are being investigated for use in MOFs, with such materials achieving ratios of up to 115:1, with carbon dioxide loadings up to 22.2 cm³/g, at standard flue gas conditions²².

The main problems encountered with MOFs are their low stability towards heat, moisture and chemical environment²². MOFs can collapse when heated to remove guest molecules; this causes loss of porosity and order, resulting in an amorphous solid. Some MOFs become amorphous simply by exposure to air. The oxygen-metal coordination bonds in MOFs often undergo hydrolysis in presence of water, even at low levels, irreversibly destroying the framework and rendering the material useless. MOFs can also undergo structural changes by the metal ions interacting with adsorbed molecules, such as carbon dioxide, or gas stream impurities, such as SO_x and NO_x.

1.4.2 Covalent organic frameworks (COFs)

Covalent organic frameworks (COFs) are a family of porous crystalline macromolecules made solely from organic building blocks. They are made from only light element (C, H, N, B and O) building blocks linked together with strong covalent bonds²³. Compared to inorganic materials they are less dense and more robust towards dry air and organic solvents. COFs possess rigid structures, long-range order, high thermal stability (up to 600 °C) and permanent porosity with extremely high surface areas, up to 6450 m²/g²⁴.

COFs are most commonly derived from condensation reactions of polyfunctional boronic acids and built from boron-containing connectors and hydrocarbon linkers (Figure 4). Each connector/linker combination forms a specific framework with topology based on the geometry of reactive functional groups²⁵. The voids within the framework provide COFs with their microporous and macroporous adsorption sites. Their organic nature offers remarkable synthetic flexibility as new COFs can be synthesised by varying the molecular building blocks and explains why COFs offer a staggering number of potentially useful materials.

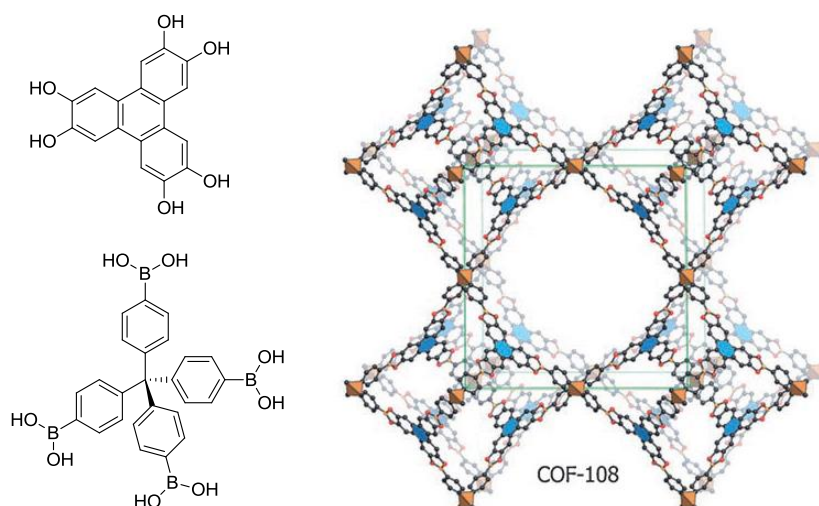


Figure 4: The building blocks and structure model for COF-108²³.

The selection of the right solvent is important to the formation of a uniform and highly ordered structure²³. This is because the condensation reaction that forms the COF framework is reversible, so that solvents are chosen in which the reactants are freely soluble. Furthermore, the reactions are carried out in sealed Pyrex tubes, which slows down the reverse reaction and minimises defects by self-healing.

COFs are an attractive group of materials because their organic nature allows total control over their structural parameters, including composition and porosity. This makes them useful for a variety of applications including catalysis²⁶, filtration²⁷, hydrogen storage²⁸, optoelectronics²⁹ and carbon dioxide capture³⁰.

Several COFs have been studied for their use as potential materials for carbon dioxide capture³¹. This study found that COFs with smaller pore volumes became saturated with carbon dioxide at lower pressure than those with larger pore volumes, a similar relationship to that seen in MOFs. COFs exhibit large carbon dioxide adsorption capacities (up to 1200 mg/g at 50 bar and 298K), but generally low selectivity due to the large pore size. Research has also looked at the theoretical effect of doping of metals in COFs on carbon dioxide adsorption²⁸. This found that Lithium doped COFs had significantly enhanced carbon dioxide adsorption capacities, with Li-doped COF-105 having a predicted capacity of 2266 mg/g at 40 bar and 298K.

As previously mentioned, COFs generally suffer from poor gas selectivities, as the large pore size does not usually provide a site of adsorption for one gas preferentially over

another. Similarly to MOFs, COFs tend not to be particularly stable to temperature and moist air, which is obviously a problem and limits their potential as useful materials.

1.4.3 Zeolites

Zeolites are a family of microporous crystalline materials with well-defined structures that rank amongst the most widespread of chemical materials used today. They were discovered by Alex Fredick Cronstedt, a Swedish mineralogist, in 1756 when he heated the mineral stilbene and noticed that it gave off steam. Consequently he named the minerals zeolites, derived from the Greek words 'zein' (to boil) and 'lithos' (rock)³².

The zeolites are a family of aluminosilicate materials made from silicate $[\text{SiO}_4]^{4-}$ and aluminate $[\text{AlO}_4]^{5-}$ tetrahedrons connected through oxygen atoms. The resulting box-like framework (Figure 5) has channels of molecular dimensions (0.1 – 2.0 nm) running throughout the three dimensional structure of the material. The large structural cavities and associated entry channels contain water molecules, which form hydration spheres around alkali or alkali earth metal cations. This microporous structure provides zeolites with a surface areas ranging from 400 – 900 m^2/g ³³.

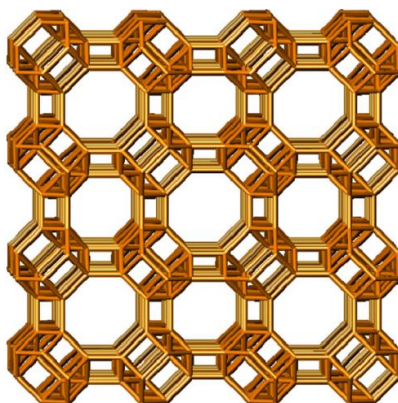


Figure 5: The aluminosilicate framework of ZK-5³³.

Since their discovery 250 years ago, zeolites have enjoyed much scientific interest and have benefited many industries with their numerous uses. Some of their applications include purification of gases and liquids by adsorption of impurities³⁴⁻³⁵, catalysis in petrochemical industries³⁶, molecular sieves³⁷, gas sensors³⁸, gas separation membranes³⁹

(including carbon dioxide separation) and hydrogen storage⁴⁰. So far over 170 unique zeolite frameworks have been reported³⁸.

All zeolites are able to undergo cation exchange without change in crystal structure, because the included metal cation is not part of the supramolecular framework. This is a useful tool for tuning the properties of a chosen zeolite, thus making it more suitable for a particular application⁴¹. Water can be removed from a zeolite without changing its crystal structure, and is performed by heating the material at 350-400 °C; this allows small molecules to pass through entry channels, but blocks larger molecules, creating the molecular sieve property of zeolites¹⁶. Zeolites are currently being investigated for use in post-combustion carbon dioxide capture technology⁴². Zeolites 13X and 4A have been found to possess a carbon dioxide capacity of 160 and 135 mg/g adsorbent, respectively, at 25 °C and 1 atmosphere carbon dioxide partial pressure. However, the adsorption capacity quickly decreases with increasing temperature so there is a demand to modify these zeolites to enhance carbon dioxide adsorption and enable them to perform at the elevated temperatures required. For example, immobilising a primary or secondary amine within the zeolite framework leads to an enhanced carbon dioxide adsorption capacity.

It is important to recognise that zeolites present some problems³⁷. Often they deactivate rapidly, due to poisoning, and catalytic turnover numbers greater than 100 are rarely reported when working in the liquid phase, resulting in the material needing frequent regeneration. Reaction rates for zeolite catalysts are dependent on diffusion, thus for fast reaction rate very small particles (<0.1 µm) and high amounts of catalysts are required.

1.4.4 Activated carbon

Activated carbons are a family of synthetically modified carbon-based materials containing very small graphite crystallites and amorphous carbon. These materials generally possess pores less than 1 nm in size and surface areas up to 3000 m²/g⁴³. An activated carbon is prepared from a carbon-rich precursor by a thermal treatment (dry distillation) forming a carbonised organic material, which can be activated by either thermal or chemical treatment, further increasing the pore volume. Thermal treatment is performed by treating the material at 700 – 1000 °C in the presence of oxidising gases, such as steam and carbon

dioxide. Chemical treatment is performed by treating the material at 500 – 800 °C in the presence of a dehydrating species, such as potassium hydroxide or phosphoric acid.

The structure of activated carbons is not completely understood, but one theory suggests that they are made up of small carbon sheets curled back upon themselves and linked together by aliphatic units, creating a network that cannot pack space efficiently (Figure 6)⁴⁴. These sheets provide multiple surfaces upon which adsorption can occur, and hence give the materials their high surface areas.

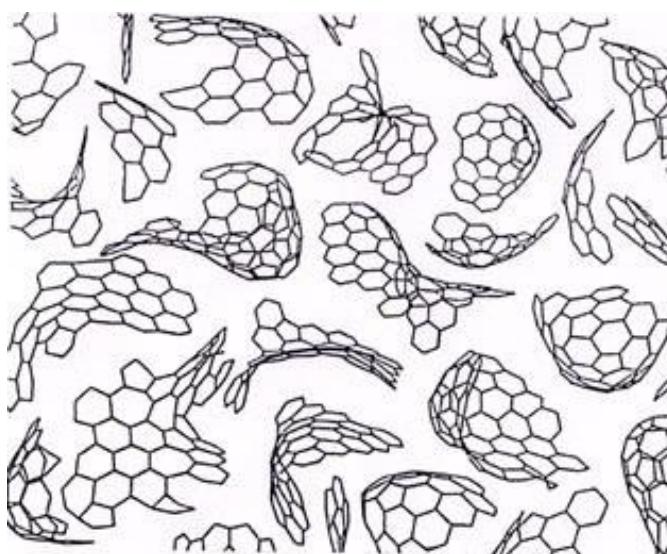


Figure 6: The proposed structure of activated carbons⁴⁴.

Activated carbons are excellent adsorbents, which have been used for centuries. Their applications include water purification⁴⁵, liquid decolourisation⁴⁶, fish oil purification⁴⁷, medical adsorbents⁴⁸, hydrogen storage⁴⁹ and carbon dioxide capture⁵⁰. The specific properties of an activated carbon are the net result of the raw material used and the activation process, allowing design for a specific application.

A wide variety of carbon-rich precursors are used as raw materials for activated carbons, these include coal, coconut shell, and wood. This makes activated carbons abundant, cheap and versatile family of materials. Recently, other porous materials, such as zeolites⁴⁹ and mesoporous silicas⁵⁰ have been used as templates for activated carbon production. The resulting materials show great potential thanks to their regular pore size and large surface areas. Polymers, such as polyimides, have been used as the carbon precursors to activated carbons⁵⁰; this produces activated carbons with low inorganic impurities and well developed porous structures.

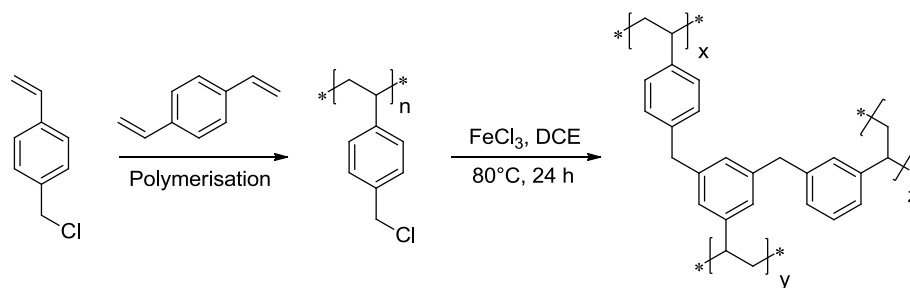
Several activated carbons are being developed for carbon dioxide capture. This is an application well suited to the materials, which have high surface areas, good thermal and chemical stabilities, easy to control pore structures and low-costs for production and regeneration⁵⁰. Carbon dioxide adsorption capabilities for these materials are typically 2-3 mmol/g at 25 °C and 1 atmosphere pressure⁵¹, but recently an activated carbon was prepared from sawdust, AC-2-600, which showed an enhanced carbon dioxide adsorption capacity of 4.8 mmol/g under the same conditions⁵². These materials usually suffer from poor carbon dioxide selectivity, but the incorporation of nitrogen-containing groups has been proven to boost selectivity towards carbon dioxide⁵⁰.

Activated carbons do have a couple of inherent problems. Due to their method of production most activated carbons have a wide distribution of pores sizes ranging from microporous to macroporous. Additionally, the surface of activated carbons is chemically ill-defined, with a mixture of oxygen and nitrogen functional groups present. These two factors combine to give a material that is an excellent adsorbent for a wide range of species, but suffers from poor selectivity for specific species.

1.4.5 Hypercrosslinked polymers

Hypercrosslinked polymers (HCPs) are a broad group of amorphous organic materials, made from light elements (C, H, N, O), and consisting of polymer chains cross-linked together. The crosslinking produces a highly rigid network structure that is unable to collapse, giving insoluble materials with small pore sizes, micropore volumes and very high surface areas⁵³.

The first HCPs, known as ‘Davankov resins’, were based on cross-linked polystyrene⁵⁴ and synthesised by a simple two-step procedure. Initially, vinylbenzyl chloride is polymerised in the presence of a small amount of divinylbenzene cross-linker, producing a lightly cross-linked copolymer. When swollen in a suitable solvent the copolymer is ‘hypercross-linked’ via a Friedel-Crafts alkylation reaction using a Lewis acid, such as iron (III) chloride, forming a HCP (Scheme 1). These materials display interesting swelling properties in both polar and non-polar solvents, and have a surface area of between 600 – 2000 m²/g, dependent upon the hypercross-linking procedure used⁵⁵.



Scheme 1: Davankov resin synthesis.

Friedel-Crafts alkylation has been successfully used to prepare HCPs with high surface areas, without the need to synthesise the precursor cross-linked polymer⁵⁶. This direct approach uses bis(chloromethyl) aromatic monomers, such as bis(chloromethyl)anthracene to produce materials with surface areas up to 1900 m²/g. Interestingly, the surface areas were found to increase when more Lewis acid was used during the hypercross-linking.

Various other reactions have been used successfully for the synthesis of hypercross-linked materials. One such group of materials are known as element-organic frameworks (EOFs) and are synthesised by reacting tetrakis(4-bromophenyl)silane with dilithiated aromatics. EOFs are thermally and moisture stable, with surface areas up to 1046 m²/g⁵⁷. The pore size of the resulting framework (Figure 7) can be tailored by using different organic linkers. Furthermore, it is possible to prepare EOFs with antimony, bismuth or tin instead of silicon. These materials show lower surface areas (423, 261 and 445 m²/g, respectively), but have potential as catalysts⁵⁸.

The properties of HCPs can be fine-tuned for a specific purpose by postsynthetic modification⁵⁹. This is possible because the hypercross-linking reaction does not occur at every possible site, resulting in residual chloromethyl groups being present in the polymeric matrix. Thus, functional groups, such as amines or alcohols, can be transferred to the polymer matrix by replacing these residual chlorine atoms. This has resulted in the widespread applicability of HCPs, with applications including adsorbents for toxic organic⁶⁰ and inorganic⁶¹ contaminants, chromatography⁶², hydrogen storage⁶³ and carbon capture⁶⁴.

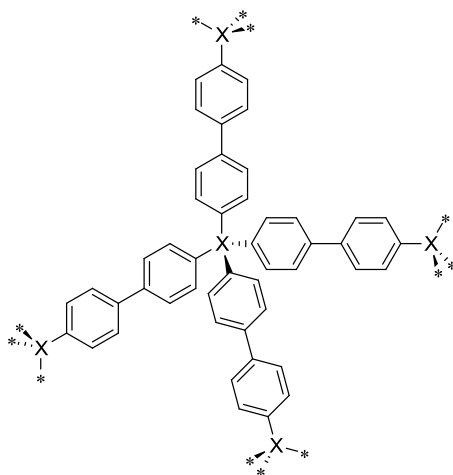
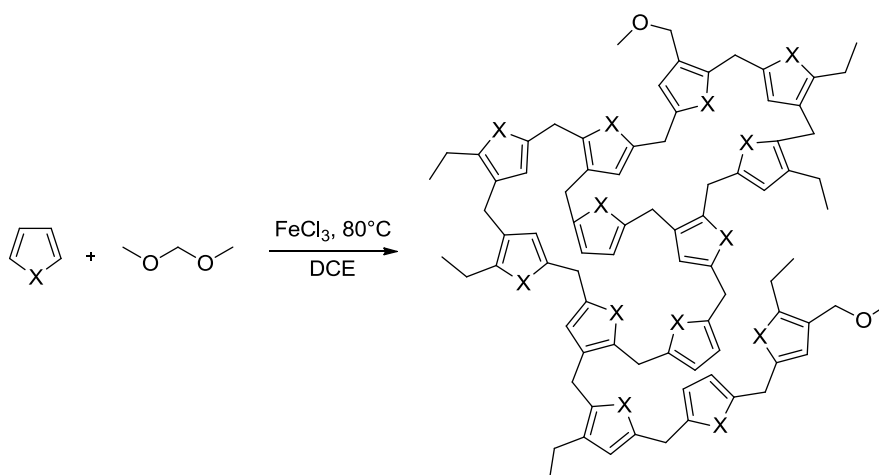


Figure 7: The structure of an elemental-organic framework, X = Si or Sn.

A series of recently developed HCPs for carbon dioxide capture⁶⁴ were made from the Friedel-Crafts alkylation between formaldehyde dimethyl acetal and furan, pyrrole or thiophene (Scheme 2). The resulting polymers were found to have surface areas of 437 – 726 m²/g, carbon dioxide adsorption capacities up to 12.7 wt% (298 K, 1 bar) and N₂:CO₂ selectivities of up to 117:1 (273K, 1.13 bar).



Scheme 2: The synthesis of a HCP designed for carbon dioxide capture, where X = O, NH or S.

1.4.6 Conjugated microporous polymers

Conjugated microporous polymers (CMPs) are another group of HCPs, but they differ significantly from others because their framework is made up of multiple carbon-carbon bonds and/or aromatic rings, forming an extended conjugated network⁶⁵. CMPs are made

using various metal mediated cross-coupling reactions⁶⁶, resulting in a framework of 1,3,5-substituted benzene nodes connected directly via a covalent bond or alkyne units (Figure 8). These polymers have been found to have surface areas exceeding 1000 m²/g⁵³.

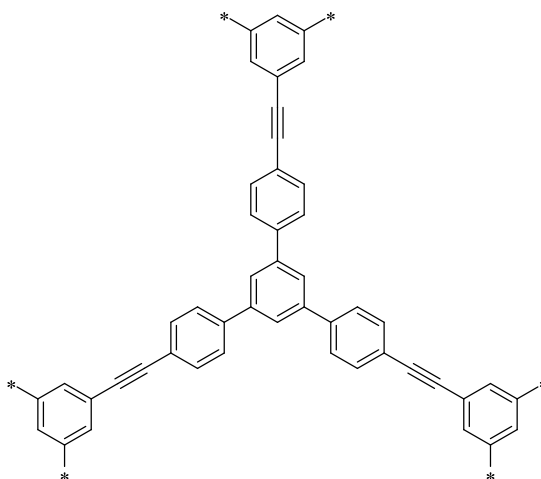


Figure 8: The structure of CMP-O.

CMPs are formed under kinetic control and display no long-range order, but despite this their pore size is well-defined and can be controlled by careful consideration of which monomers to use⁶⁷. Surface area can also be controlled by changing the linker length, with the number of micropores decreasing with increasing linker length. This behaviour can be understood by the extra flexibility granted to the framework by having longer linkers, thereby allowing it to pack more efficiently and decreasing the available surface area.

CMPs are attracting considerable interest as materials that combine the mechanical stability of polymers with adjustable optoelectronic properties of organic molecules. They are currently being investigated for applications in areas such as catalysis⁶⁸, hydrogen storage⁶⁹, light-harvesting networks⁷⁰, metal nano-particle composites⁷¹, supercapacitors⁷² and carbon dioxide capture⁷³.

Much of the research performed on CMPs has focussed on broadening the range of functional groups that can be incorporated into the frameworks, towards the aim of tuning the properties of the materials for different applications. It was recently reported that 2,4,6-triphenyl-1,3,5-triazine has been used instead of 1,3,5-triphenylbenzene as a CMP building block for materials for carbon dioxide capture⁷³. The resulting networks are analogous to conventional CMPs (Figure 9) and show similar surface areas, but show improvements in thermal stability and carbon dioxide adsorption capacities. The most successful of these

materials is TNCMP-2, a polymer made from 2,4,6-triphenyl-1,3,5-triazine and tris(4-ethynylphenyl)amine. This polymer, with a high surface area of 995 m²/g, shows excellent carbon dioxide capacity (up to 2.62 mmol/g at 273K and 1 bar or 1.45 mmol/g at 298K and 1 bar) and high CO₂:N₂ selectivity (up to 25.2:1 at 298K and 1 bar). Furthermore, as the polymer is constructed with both an electron donor (triazine) and an electron acceptor (triphenylamine) it has interesting optoelectronic properties and could have potential use as a photocatalyst.

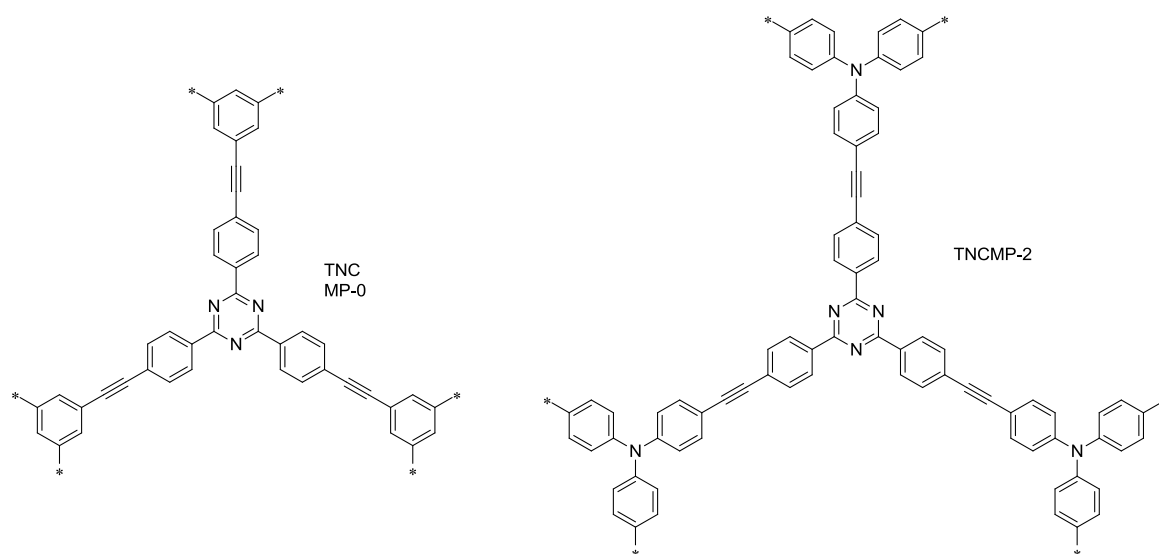


Figure 9: The structures of CMPs built from 1,3,5-triazine derived building blocks.

1.4.7 Porous aromatic frameworks

Porous aromatic frameworks (PAFs) are a family of materials similar to CMPs, but with diamond-like structures. They are made using a nickel(0)-catalysed Yamamoto-type Ullmann cross-coupling reaction on a tetrahedral monomer, such as tetrakis(4-bromophenylmethane)⁷⁴. The cross-coupling reaction links the phenyl groups of monomers together, in a substitution reaction where bromide is eliminated, forming an amorphous framework. These networks possess high thermal and hydrothermal stability, due to their diamond-like structures, low densities and extremely high surface areas, but no long-range order.

The first PAF created from the nickel(0)-catalysed Yamamoto-type Ullmann cross-coupling reaction on tetrakis(4-bromophenylmethane) was called PAF-1⁷⁵ (Figure 10). It shows exceptional stability to heat and water, due to its hydrophobic nature, a density of 0.315 g/cm³ and an exceptionally high surface area, 5640 m²/g. PAF-1 demonstrates high adsorption capacity for hydrogen (10.7 wt% at 77K and 48 bar) and carbon dioxide (1300 mg/g at 298K and 40 bar).

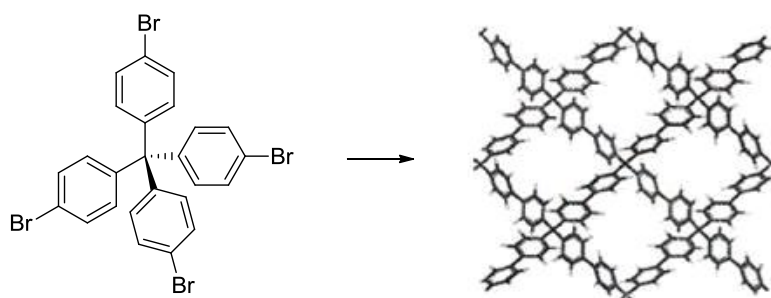


Figure 10: The reaction and model structure of PAF-1⁷⁵. *Reagents and conditions:* Ni(COD)₂, COD, DMF, 2,2'-bipyridyl at 80 °C.

The surface area of PAFs exceeds those for all other polymeric materials and is comparable with the best performing MOFs. It is believed that PAF networks are so much more microporous than other polymeric materials because the cross-coupling reaction occurs at nearly every possible site. This has been proven by NMR, FTIR and elemental analysis studies, which do not show any evidence of remaining bromine atoms⁷⁴.

Despite the high gas capacity possessed by PAF-1, it only weakly interacts with gas molecules, due to the purely hydrocarbon skeleton it possesses, limiting both the operating temperature and overall capacity of the material. One possible way to remedy this is to lithiate PAF-1 post-synthetically by reductive lithiation with lithium naphthalenide⁷⁶. This activates PAF-1 by reduction with lithium ions, which are subsequently bound within the pores of the framework, lowering the pore volume. This activation drastically lowers the surface area, from 3639 m²/g down to 479 m²/g, but greatly enhances gas storage capacities for H₂, CO₂ and CH₄ (11.03 mmol/g at 77 K and 1.22 bar; 8.99 mmol/g at 273 K and 1.22 bar; 1.30 mmol/g at 273 K and 1.22 bar, respectively, for 5 wt% Li).

Another method for improving gas adsorption capacity in PAFs is to synthesise frameworks from metal-based monomers⁷⁷, where instead of a central carbon atom the monomer unit is built around either a silicon or germanium atom. The silicon-based

framework shows the most potential with high surface area (2932 m²/g) and enhanced adsorption capacity for hydrogen (2.07 wt% at 77K and 1 atm, increasing to 5.5 wt% at 60 bar), methane (1.9 wt% at 273 K and 1 atm) and carbon dioxide (15.3 wt% at 273 K and 1 atm).

1.4.8 Polymers of intrinsic microporosity

Polymers of intrinsic microporosity (PIMs) are a group of polymeric materials made from light elements (C, H, N, O) and were originally developed as an organic version of activated carbons⁷⁸. Polymers are not usually microporous because they normally possess sufficient flexibility to bend and twist into a space efficient packing, but PIMs are an exception to this due to their highly rigid and contorted structures, which greatly restricts their flexibility. Hence, PIMs are not able to pack space efficiently, which leaves molecular-sized interconnected voids in the material, resulting in high microporosity.

The rigidity of PIMs is a direct consequence of their fused-ring skeletons, but this alone would not be enough to account for the high microporosity. PIMs also possess sites of contortion, which are structural features (Figure 11) that force the polymer chain to bend in a different direction, contributing massively towards the microporous character.

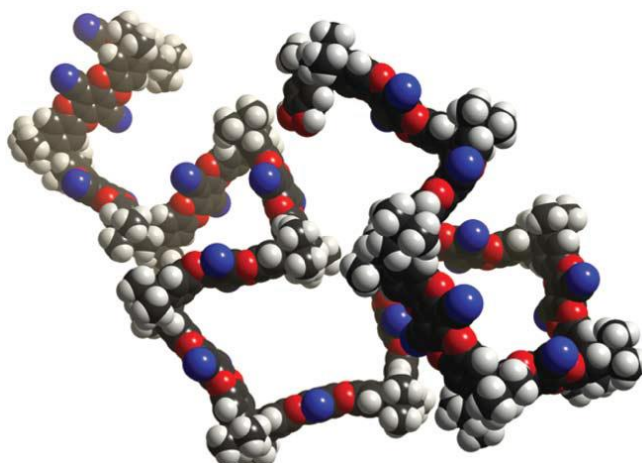


Figure 11: The modelled structure of PIM-1⁸⁰.

PIMs are amorphous solids due to their random packing and lack of long-range order, but possess surface areas in the range of 400 – 1760 m²/g⁷⁹. Usually they are formed by a double nucleophilic aromatic substitution reaction between a tetrahydroxylated monomer

and a tetrafluorinated monomer, resulting in the formation of dioxane links between monomer units (Figure 12). It is essential for the production of a microporous PIM for one of the monomers to have a highly rigid and contorted structure; if this is not the case then the resulting polymer will not be microporous⁸⁰.

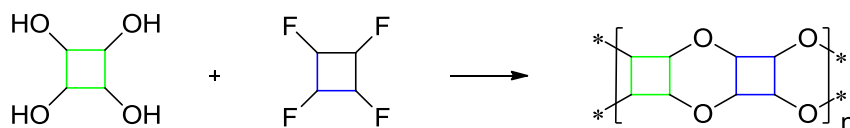


Figure 12: The synthesis of a PIM.

As is usual for a polymerisation reaction between two monomers the form of the polymer produced from this reaction depends upon the average number of reactive groups possessed by both monomers, which is termed the average functionality (f_{av}). A polymerisation reaction between two monomers each with a functionality of two will produce a “ladder polymer”, with the collective polymer chains held together by only weak intramolecular forces that can be reversibly disrupted by solvent molecules, usually resulting in the polymer being soluble. A reaction where one or both monomers possess a functionality of greater than two results in significant cross-linking between polymer chains, creating a network polymer. The higher the f_{av} of a pair of monomers the more cross-linked the resulting network polymer will be. Cross-linking involves the production of strong covalent bonds between polymer chains and results in the polymer being insoluble as solvent molecules cannot disrupt these strong links holding the polymer framework together. Therefore, when designing a PIM it is important to consider the f_{av} of the mixture of monomers, to ensure that the resulting polymer exhibits the desired properties.

The simple dibenzodioxane reaction has led to the development of three distinct classes of PIMs (Figure 13): insoluble network PIMs, soluble ladder PIMs and oligomeric molecules of intrinsic microporosity (OMIMs)⁸¹. Network PIMs are insoluble polymers with chains held together by several strong covalent bonds, ladder PIMs are soluble polymers with unconnected polymer chains and OMIMs are discrete molecules with highly accessible surface areas. Each class of PIM has differing properties, which makes them useful for different applications; network PIMs possess the highest surface areas of the three and are useful as adsorbents⁸², heterogeneous catalysts⁸³ and hydrogen storage materials⁸⁴, ladder PIMs are solution processable and can be used in gas sensors⁸⁵ and for gas separation

membranes⁸⁶. OMIMs are a developing class of PIMs, but show potential as soluble discrete molecules possessing surface area.



Figure 13: Cartoon structures of network PIMs, ladder PIMs and OMIMs⁸¹.

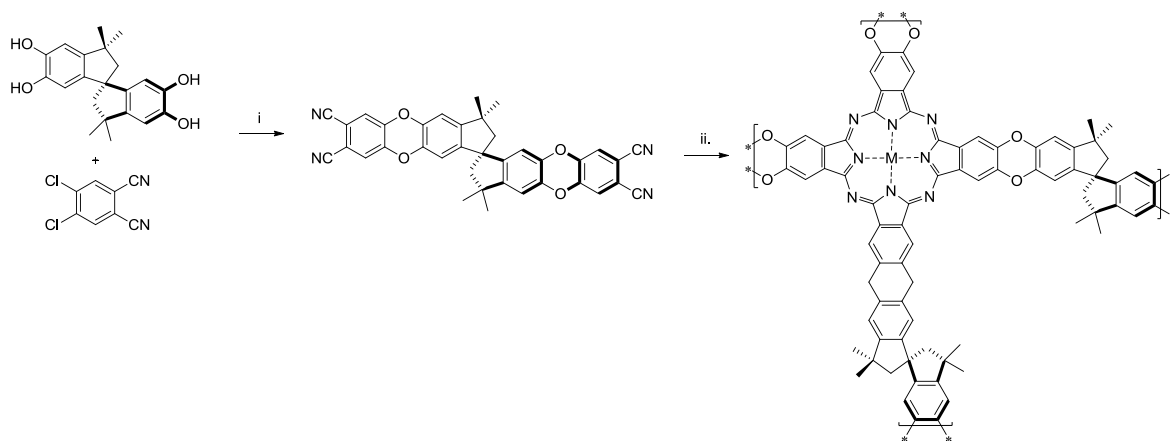
1.4.8.1 Network PIMs

Network PIMs are a class of polymers made from monomers with at least 3 sets of reactive groups ($f_{av} > 2$) suitable for undergoing the polymerisation reaction. This means that the polymer grows in at least three directions and creates a framework where a typical monomer unit is linked to at least three others by strong covalent bonds. This structure gives the polymer high stability (up to 400 °C) and surface areas (500 – 1760 m²/g)⁷⁸, but results in the polymer being insoluble, as solvent molecules cannot disrupt the strong covalent bonds. Several types of network PIM exist, including phthalocyanine and porphyrin based polymers.

1.4.8.2 Phthalocyanine network PIMs

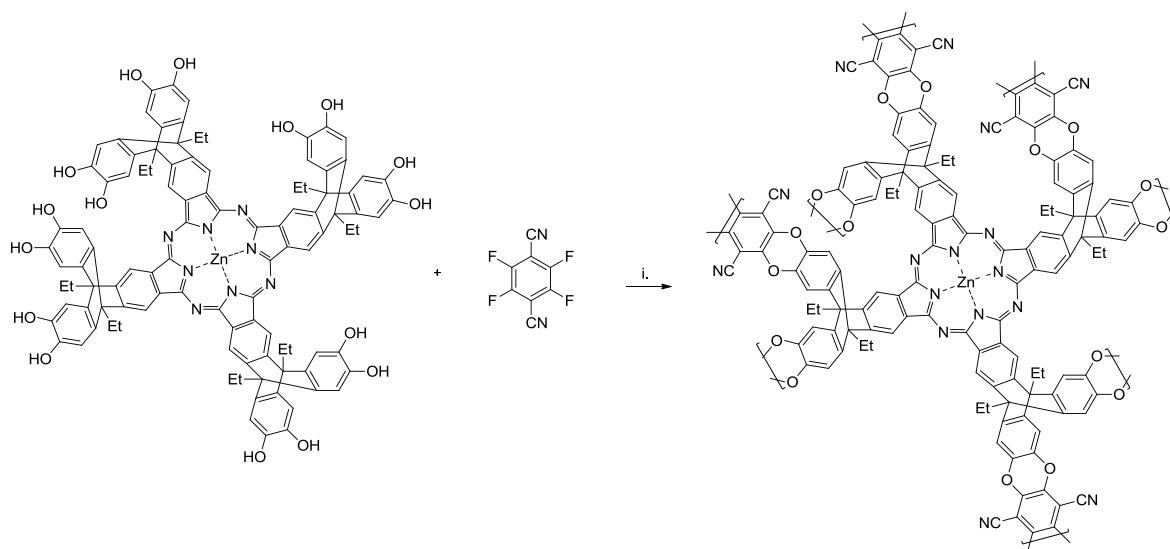
Phthalocyanine network PIMs were developed from the idea that nanoporous organic materials could result from linking together large planar molecules with rigid, fused ring spacers. It was essential that the spacer contain a site of contortion, to prevent the planar components from aggregating due to strong π - π interactions and resulting in nonporous solids, a trend seen in other phthalocyanine network polymers⁸⁷. Phthalocyanines were selected as the planar component due to their range of useful properties, including size, rigidity and stability⁹⁰. As expected phthalocyanine network polymers are colourful, due to the presence of a metal and conjugated electron system, they have found use in applications such as catalysis and as absorbents⁸³.

One of the first phthalocyanine network PIMs synthesised was the product of a multi-step synthesis starting with the aromatic nucleophilic substitution reaction between 4,5-dichlorophthalonitrile and 5,5',6,6'-tetrahydroxy-3,3,3',3'-tetramethyl-1,1'-spirobisindane, both of which are commercially available. The spirobisindane provides the site of contortion necessary to prevent aggregation, hence ensuring the polymer exhibits microporosity. This reaction occurs with high yield, 80 – 90%, producing the contorted bis(phthalonitrile), which when heated in the presence of a metal salt and quinoline produces the network polymer (Scheme 3). The surface area of the polymer depends upon the metal template used, but falls within the range of 489 m²/g – 895 m²/g⁸⁸ and shows little reproducibility, even when the same template is used.



Scheme 3: A phthalocyanine network PIM (M = Zn, Cu, Co or 2H⁺). *Reagents and conditions:* i. K₂CO₃, DMF, 70 °C, ii. Metal salt, quinoline, lithium pentoxide, 220 °C.

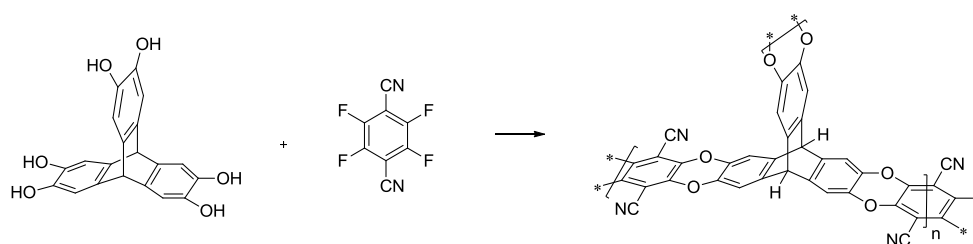
The framework for phthalocyanine network PIMs can also be synthesised using the dibenzodioxane link forming reaction used for PIMs. An example of this is the PIM synthesised using the bulky triptycene unit to prevent aggregation during network formation. This PIM is formed by the nucleophilic substitution reaction between 2,3,6,7-tetrahydroxytriptycene-substituted phthalocyanine and 2,3,5,6-tetrafluoroterephthalonitrile, in which dibenzodioxane links are formed (Scheme 4)⁸⁹. This phthalocyanine network PIM requires a more time consuming synthesis, since the triptycene-substituted phthalocyanine is not commercial, but exhibits a surface area of 806 m²/g and the synthesis gives reproducible results.



Scheme 4: The structure of a triptycene-substituted phthalocyanine network PIM. *Reagents and conditions:* K_2CO_3 , DMF, 80 °C, 48 h.

1.4.8.3 Triptycene network PIM

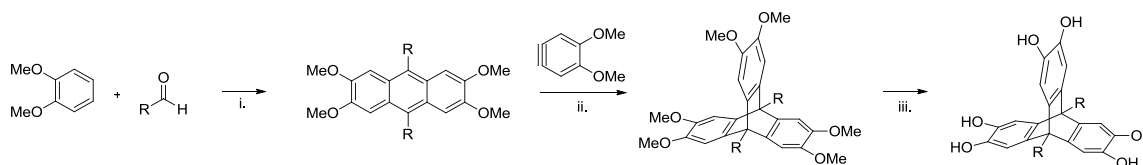
Triptycene was identified as a useful building block for making PIMs because of its rigid fused-ring skeleton and three-fold symmetry⁹⁰, which provides a site of contortion. The network made using the dibenzodioxane forming reaction between 2,3,6,7,13,14-hexahydroxytriptycene and 2,3,5,6-tetrafluoroterephthalonitrile produced a PIM (Scheme 5) with a high surface area, 1318 m^2/g and excellent capacity for hydrogen, 7.46 mmol/g at 1 bar and 77K.



Scheme 5: The preparation of triptycene network PIM. *Reagents and conditions:* K_2CO_3 , DMF, 120 °C, 2 days.

Following the success of this polymer a series of similar triptycene based network PIMs were synthesised, with various alkyl and benzyl groups replacing the bridgehead hydrogen atoms on each triptycene unit. This was achieved by synthesising the alkyl substituted

tetrahydroxyanthracene, and performing a Diels-Alder reaction upon it using dihydroxybenzynes to give the hexahydroxytriptycene, which was demethylated to produce the triptycene monomer (Scheme 6). The monomer was then polymerised under the same conditions as above. These PIMs showed a wide range of surface areas (618 – 1760 m²/g) and excellent hydrogen capacities (up to 1.83% at 1 bar and 77K)⁹⁰.



Scheme 6: The synthesis of alkyl-substituted triptycenes. *Reagents and conditions:* i. c. H₂SO₄, 5 °C, 2 h; ii. 1,2-epoxypropane, CH₂Cl₂, reflux, 12 h; iii. BBr₃, CH₂Cl₂, room temperature, 3 h.

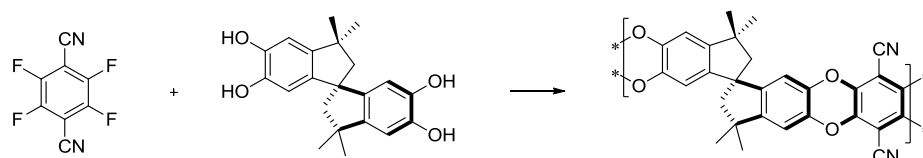
From this series an interesting trend was observed, the surface area of the PIM increased by changing R from hydrogen to methyl groups, but decreased when longer or bulkier groups than methyl groups were used. It is thought that the methyl groups help to force the polymer chains apart more than the smaller hydrogen atoms do, but longer or bulkier groups have more flexibility, allowing the substituents to occupy some of the free volume of the polymer. The methyl-substituted triptycene network PIM possesses the highest surface area of all PIMs to date, 1760 m²/g.

1.4.8.4 Ladder (soluble) PIMs

It is possible to create non-network (ladder) PIMs using the same dibenzodioxane forming polycondensation reaction as discussed above in the synthesis of network PIMs. To avoid creating a network PIM it is essential to only use suitable monomers with two sets of reactive groups ($f_{av} = 2$), which prevents cross-linking between polymer chains. Ladder PIMs show the same high thermal stability observed in network PIMs, but can have significantly lower surface areas (430 – 850 m²/g)⁸⁶, which is due to the polymer chains possessing more flexibility than network frameworks, allowing more efficient packing. However, the solubility that some ladder polymers display is a useful property that allows the solution processing of a PIM from a powder into a thin but robust membrane, and is a clear advantage over alternative microporous materials, which are usually held together by strong covalent bonds.

1.4.8.5 PIM-1

The most useful ladder PIM to date, denoted as PIM-1, is the product of the polymerisation reaction between two commercially available monomers, 2,3,5,6-tetrafluoroterephthalonitrile and 5,5',6,6'-tetrahydroxy-3,3,3',3'-tetramethyl-1,1'-spirobisindane (Scheme 7)⁹¹. The site of contortion is provided by the spirobisindane monomer, which contributes massively towards the high surface area (850 m²/g) that PIM-1 possesses. The polymerisation reaction is very efficient, giving an extremely high molecular weight ($M_w = 270,000 \text{ gmol}^{-1}$, $M_w/M_n = 2.8$). PIM-1 is completely soluble in some organic solvents and robust self-standing membranes can be cast from it. Therefore PIM-1 is an attractive material for a range of potential applications, including sensors⁸⁵ and gas-separation membranes⁸⁶.



Scheme 7: The synthesis of PIM-1. *Reagents and conditions:* K₂CO₃, DMF, 65 °C.

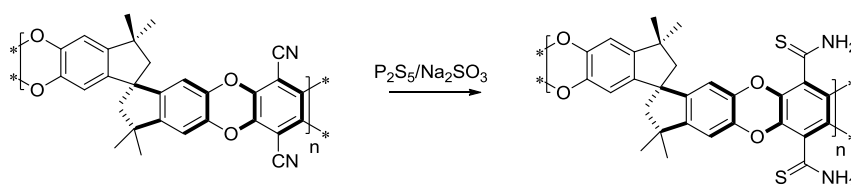
Building on the success of PIM-1 there have been numerous attempts to modify the polymer in order to tune the properties for a particular application and enhance the performance, particularly since PIM-1 possesses high permeability and moderate selectivity for a range of gases (Table 1)⁹².

Gas	Diffusivity (cm ² /sec)	Solubility (cm ³ (STP)/cm ³ cmHg)	Permeability (Barrer)	Perm.-Selectivity (P _x /P _{N2})
O ₂	388	39.30	1530	2.50
N ₂	163	37.30	610	1.00
He	6800	1.95	1320	2.16
H ₂	5000	6.60	3300	5.40
CO ₂	160	699.00	11200	18.80
CH ₄	71	162.00	1160	1.90

Table 1: The gas permeation properties of a PIM-1 membrane. *Conditions:* Feed pressure = 4.5 psi, permeate pressure = 0 psi, temperature = 30 °C. 1 Barrer = 10⁻¹⁰ [cm³(STP)•cm]/(cm²•s•cmHg).

A research group at the National University of Singapore recently reported their attempts to tune the permeability and selectivity of PIM-1 towards oxygen and carbon dioxide by blending it with Matrimid⁹³. Matrimid was chosen due to its availability, high thermal stability and good processability. Matrimid also exhibits excellent gas-pair selectivity towards CO₂/CH₄ (34), CO₂/N₂ (30) and moderate for O₂/N₂ (6.4), but suffers from low permeability towards oxygen (2.1 Barrer) and carbon dioxide (9.6 Barrer). Matrimid was found to be completely miscible in PIM-1 only at low concentrations, but a PIM-1:Matrimid (9:1) polymer blend was created that displays enhanced properties. This includes good permeability for oxygen and carbon, 400 and 1953 Barrer respectively, and moderate selectivity for O₂/N₂ (4.0), CO₂/N₂ (20) and CO₂/CH₄ (16).

The Budd research group at Manchester University took a different approach towards improving PIM-1 CO₂/N₂ selectivity⁹⁴. They performed postsynthetic modification on PIM-1 by reaction with phosphorous pentasulphide in the presence of sodium sulphite, which converted the nitrile groups to thioamide groups (Scheme 8). This efficient reaction (80% conversion) gave a polymer with a significantly lower surface area (263 m²/g) and lower carbon dioxide permeability (1120 Barrer), but an improved CO₂/N₂ selectivity (30.3).



Scheme 8: The postsynthetic modification of PIM-1. *Reagents and conditions:* P₂S₅, Na₂SO₃, dioxane, EtOH, reflux, 20 h.

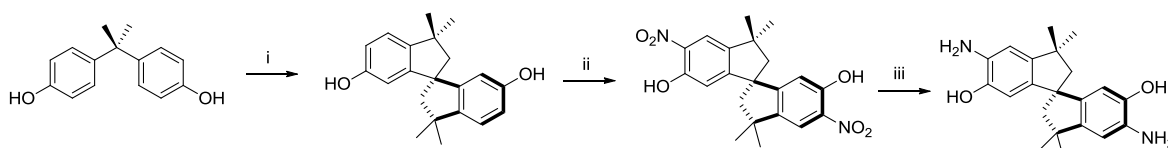
1.4.8.6 PIM-polyimides

Polyimides are an important group of polymers used in a range of applications including adhesives, dielectrics, membrane separations and opto-electronics⁹⁵. They have been extensively studied due to their thermo-oxidative stability, unique electrical properties, high resistance to radiation and solvent effects and excellent mechanical strength. Polyimides allow a great degree of freedom in their synthesis, allowing the incorporation of a variety of functional groups, and the tuning of their properties to a particular function.

However, they generally suffer from low solubility in common solvents, particularly when made using rigid aromatic components, which makes their processing difficult and expensive.

Therefore, a family of polymers were created that contain both polyimide and PIM components, which helps to improve the solubility of the resulting polymer whilst making them microporous. PIM-polyimides are formed by the polycondensation reaction between a dianhydride and a diamine, one of which must possess a site of contortion, which normally requires synthesis using an appropriate method. The resulting polymers exhibit significantly increased permeability compared to conventional polyimides, and enhanced selectivities compared to conventional PIMs⁹⁶⁻⁹⁷.

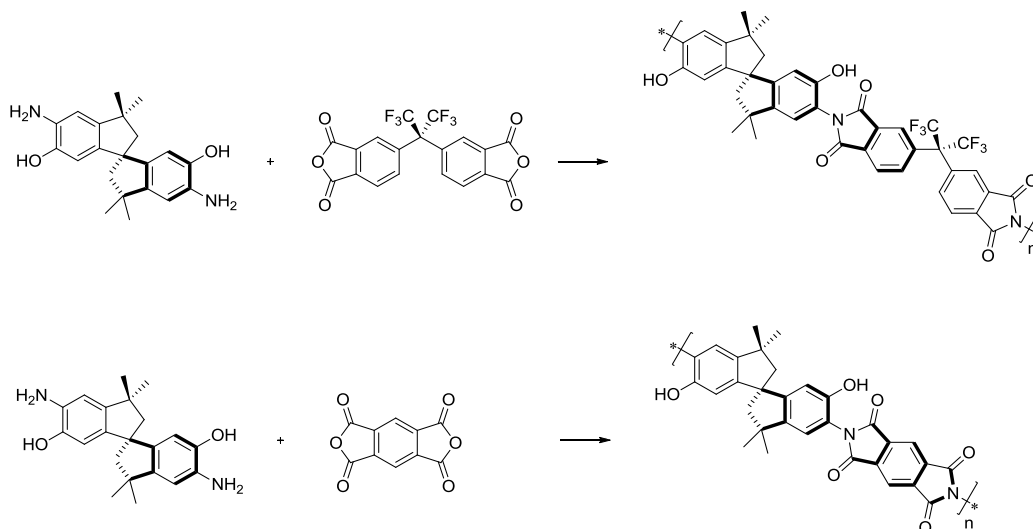
The Pinnau research group based at King Abdullah University of Science and Technology in Saudi Arabia recently published a paper discussing two PIM-polyimides showing high permeability and selectivity for carbon dioxide⁹⁶. They devised a multi-step synthesis to produce a diamine derived from Bisphenol A (Scheme 9), which was reacted with two different dianhydrides to give the two PIM-polyimides. A condensation reaction on Bisphenol A gives 3,3,3',3'-tetramethyl-1,1'-spirobisindane-6,6'-diol, which is nitrated and subsequently reduced to give 3,3,3',3'-tetramethyl-1,1'-spirobisindane-5,5'-diamino-6,6'-diol.



Scheme 9: The synthesis of 3,3,3',3'-tetramethyl-1,1'-spirobisindane-5,5'-diamino-6,6'-diol. *Reagents and conditions:* i. methylsulphonic acid, 135 °C, 5 h; ii. HNO₃, HAc, 12 h; iii. dichlorotin, HCl, methanol, reflux, 6 h.

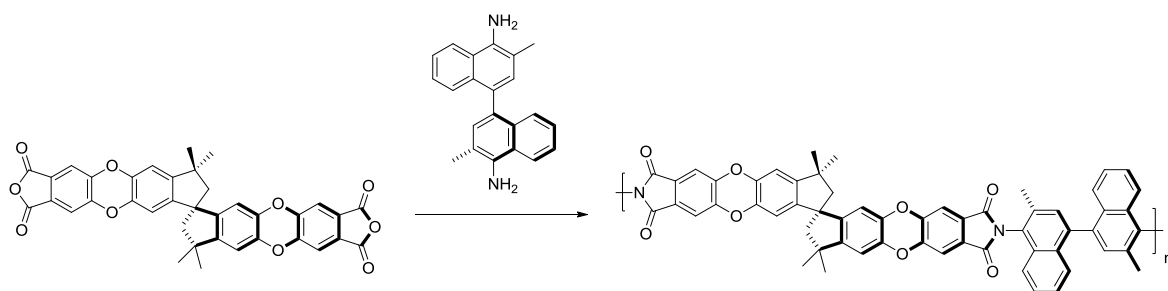
The polycondensation reaction between 3,3,3',3'-tetramethyl-1,1'-spirobisindane-5,5'-diamino-6,6'-diol and 4,4'-(hexafluoroisopropylidene)diphthalic anhydride or pyromellitic dianhydride gives the PIM-polyimide, PIM-6FDA-OH and PIM-PMDA-OH, respectively (Scheme 10). Both polymers show good solubility and high thermal stability, as expected. PIM-6FDA-OH exhibits moderate surface area (225 m²/g), high molecular weight ($M_w = 165,000$, $M_n = 85,400$ gmol⁻¹), moderate permeability for carbon dioxide (263 Barrer) and

hydrogen (259 Barrer) with high selectivities for CO₂/N₂ (24), H₂/N₂ (24) and CO₂/CH₄(29). PIM-PMDA-OH exhibits lower surface area (190 m²/g), but higher molecular weight ($M_w = 356,000$ and $M_n = 130,000$ gmol⁻¹), lower permeability for carbon dioxide (198 Barrer) and hydrogen (190 Barrer), with higher selectivity for CO₂/N₂ (29) and H₂/N₂ (28), but lower selectivity for CO₂/CH₄ (26).



Scheme 10: The synthesis of PIM-6FDA-OH and PIM-PMDA-OH. *Reagents and conditions:* pyridine, toluene, reflux, 12 h.

An alternative strategy was used by the McKeown group at Cardiff University to produce a series of PIM-polyimides, they synthesised a dianhydride possessing a site of contortion before performing the polycondensation reaction using a range of commercial diamines⁹⁷. Starting with a dibenzodioxane condensation reaction on 5,5',6,6'-tetrahydroxy-3,3,3',3'-tetramethyl-1,1'-spirobisindane, a tetranitrile compound was prepared, which was hydrolysed to a tetracarboxylic acid before being converted to the bisanhydride. This was reacted with a range of diamines for the preparation of a series of PIM-polyimides, each of which exhibited high surface area (471 – 680 m²/g), moderate to high molecular weight ($M_w = 31,000 – 116,000$ gmol⁻¹ and $M_n = 11,000 – 54,000$ gmol⁻¹), with moderate to high membrane permeabilities and selectivities for a range of gases. The best of the series, PIM-PI-8 (Scheme 11), had high permeability for hydrogen (1600 Barrer), helium (660 Barrer), oxygen (545 Barrer) and carbon dioxide (3700 Barrer). PIM-PI-8 also displayed high selectivity for H₂/N₂ (10), CO₂/CH₄ (14.2) and CO₂/N₂ (23.1).



Scheme 11: The synthesis of PIM-PI-8. *Reagents and conditions:* m-cresol, quinoline, toluene, reflux, 5 h.

1.5 The Robeson plot

Soluble polymers are attracting considerable interest as microporous materials, especially since this solubility allows for the production of robust and self-standing membranes from polymer powders. Polymeric membranes have been used for the separation of gas mixtures since the late 1970s and have attracted significant academic and industrial interest, particularly since membrane separation has high initial cost but low energy cost compared to more conventional systems, such as cryogenic distillation. Membranes can be used for a variety of useful gas separations, such as O₂/N₂ for oxygen enrichment, CO₂/CH₄ for the purification of biogas and CO₂/N₂ for carbon dioxide capture.

Gas separation has two key parameters, the permeability of a specific component of the gas mixture and the separation factor between the gases. However, these are trade-off parameters meaning that generally as the separation factor decreases the permeability of the more permeable gas component increases, and vice versa. In 1991 Robeson published a paper that showed that this trade-off relationship could be represented graphically for various gas pairs by plotting the log of the separation factor versus the log of the permeability for the more permeable gas (Figure 14). This graph was given an upper bound performance limit, determined by data from numerous permeability studies for different polymers, which no polymer at that time was able to exceed⁹⁸. However, it was predicted that following structure/property optimisation studies the various upper bounds would shift slightly higher, but that the slope of the line would remain constant.

Indeed, since that time significant research has been directed towards exceeding the upper bound for various gas pairs and making progress towards optimising structure/property relationships. A large number of polymer membranes, including several PIMs, have been

created that exceed the original 1991 upper bound for certain gas pairs, and in 2008 Robeson published a paper discussing a revised upper bound limits⁹⁹. It is likely that as better understanding of the structure/property relationship of polymers is gained, new polymer membranes that exceed even this revised upper bound limit will be created. This is especially likely since the 2008 upper bound was created using very few examples of ladder-type polymers, which are able to behave as molecular sieves due to their greater rigidity and so therefore potentially offer better materials for gas separation than other polymers.

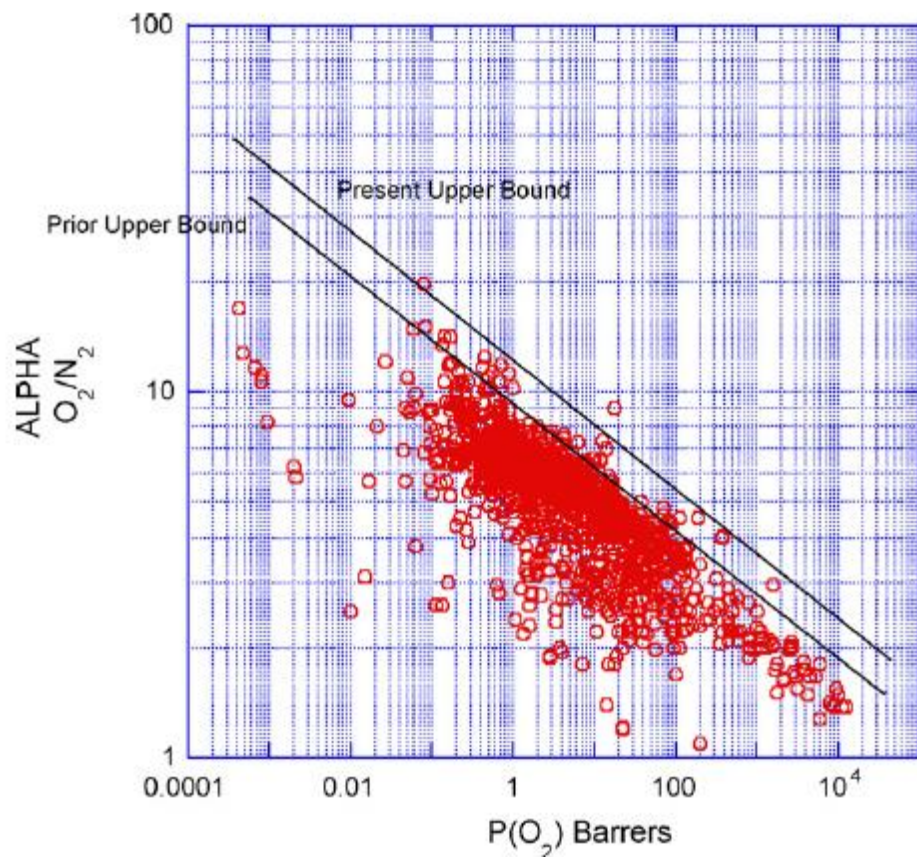


Figure 14: The Robeson plot for O₂/N₂, showing the 1991 and 2008 upper bounds⁹⁹.

The position of a polymer membrane on the Robeson plot for a particular gas pair is a good indicator of how useful for gas separation it may be. A good polymer membrane must possess both high permeability and high selectivity towards a particular gas, and therefore the best materials lie towards the top right of the Robeson plot, although, in practice very few materials exceed the upper bound limit.

1.6 Carbon capture and storage

The surface temperature of the Earth has increased by about 0.8 °C over the past century, with the increase particularly pronounced over the past three decades¹⁰⁰. This is well outside what can be considered normal for natural climate fluctuations and is instead, thought to be linked to the increased levels of greenhouse gases (GHGs). These gases, known to include water vapour, carbon dioxide, methane, ozone, nitrous oxide, hydrofluorocarbons, perfluorocarbons and sulphur hexafluoride, are thought to absorb the infrared radiation emitted by the Earth's surface as it is heated by solar radiation. This infrared radiation is then re-emitted in all directions, further heating the surface of the Earth. This is a natural process, helping to make the Earth habitable, but becomes a problem as the levels of GHGs rise, meaning that more radiation is trapped and the surface of the Earth is further heated.

Carbon dioxide (CO₂) does not cause the most severe global warming impact amongst GHGs, but is considered the most important because its emission is notably higher than the others¹⁰¹. CO₂ is naturally absorbed by the Earth, either by rock weathering or by photosynthesis in land or ocean plant life, for centuries these natural sinks have controlled the level of atmospheric CO₂, but since the Industrial Revolution these sinks have proven insufficient. Therefore since that time the level of atmospheric CO₂ has increased dramatically by over 37%, until the present 383 ppm level¹⁰². It has already been shown that the rise in atmospheric CO₂ levels over the past few centuries has been closely followed by a rise in global temperature¹⁰³ and ocean acidification¹⁰⁴, but scientists have predicted that if the CO₂ concentration reaches 450 ppm the polar ice sheet will melt, causing severe flooding and species extinction¹⁰⁵. Therefore, it is essential to drastically reduce the emission of CO₂ into the atmosphere.

The energy supply sector contributes heavily towards CO₂ emissions, particularly from fossil fuel power plants, which are dominant in generating and supplying electricity¹⁰¹. Hence this has been a target area for emission reduction, and has attracted much research interest. Renewable energy sources are being developed to reduce or eliminate the emission of GHGs by replacing traditional fossil fuel plants, but these systems are still at a preliminary stage and require further substantial financial investment. So for the next century fossil fuels, coal, natural gas and oil, will remain the most important source of energy, due to their high availability and low financial cost. Hence, the current challenge

is to develop and implement CO₂ capture systems in existing and new fossil fuel power plants, then use or store the CO₂.

Carbon capture and storage (CCS) is the name given to the wide range of technologies designed to remove and store CO₂ in a safe manner, preventing its release into the atmosphere. CCS involves the capture, compression, transport and storage of CO₂ from large emission sources, and requires less energy than other CO₂ removal systems, whilst drastically reducing emissions¹⁰⁶. Carbon capture can be achieved in one of three manners: post-combustion capture, pre-combustion capture and oxy-fuel combustion capture (Figure 15).

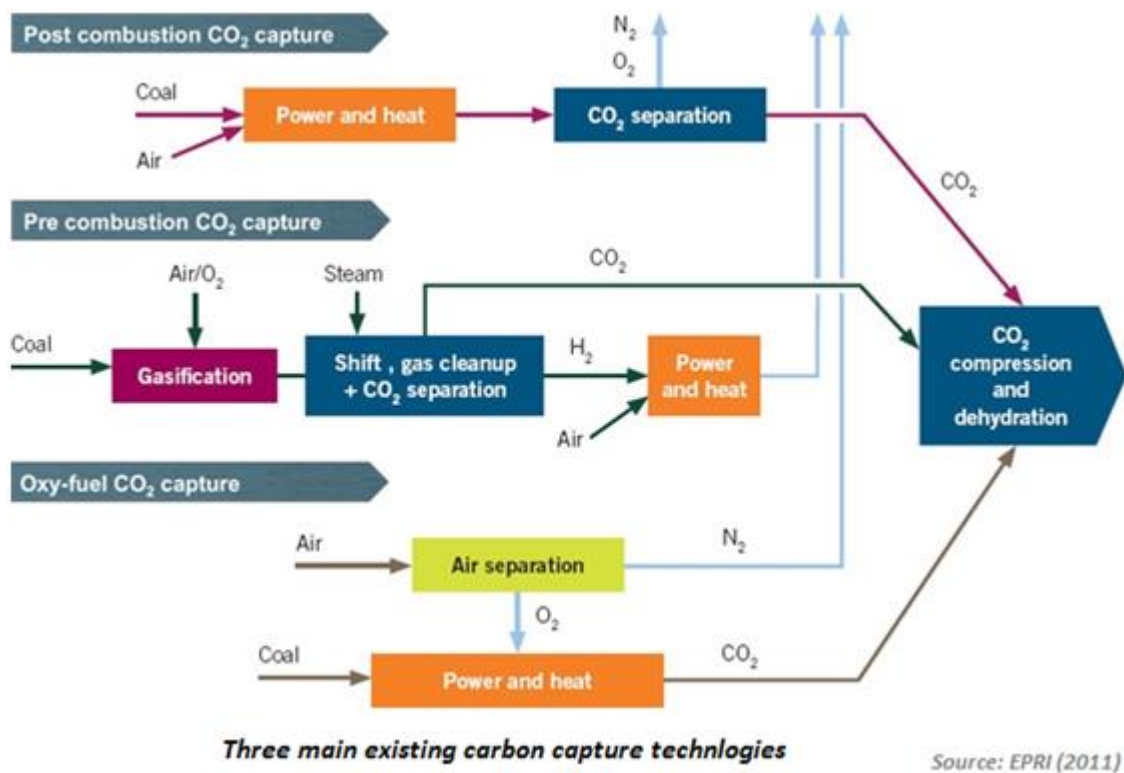


Figure 15: The different CCS methods.

Post-combustion capture is the process where CO₂ is removed from the flue gas after fossil fuel combustion. Pre-combustion capture is a process by which CO₂ is captured and stored prior to the combustion process on the fossil fuel, meaning that the fuel is decarbonised before it is used for the production of energy. Oxy-fuel capture uses high purity oxygen, about 95%, instead of natural air for fuel combustion, which produces a mixture of CO₂ and water from which CO₂ is separated from the gas stream. Of the three capture methods

post-combustion has the advantage that it can be retrofitted into existing power plant systems, avoiding the high cost of replacing power plants¹⁰⁷.

Presently, post-combustion capture systems have three main problems: they have not been demonstrated on a large scale, the CO₂ capture process reduces power generation capacity by roughly one-third and it would not be cost-effective to scale up present developing systems¹⁰⁸. Current amine-based chemical absorption technologies that use alkaline amine-based solvents, such as monoethanolamine and diglycol-amine, to achieve the capture of CO₂ from flue gas (Figure 16) have some major problems: high thermal energy requirement for solvent regeneration, the necessity of flue gas pre-treatment to remove SO₂ and NO to prevent irreversible reaction with the solvent, a low limit to concentration of the amine solution to avoid foaming and corrosion caused by products of the process¹⁰⁹.

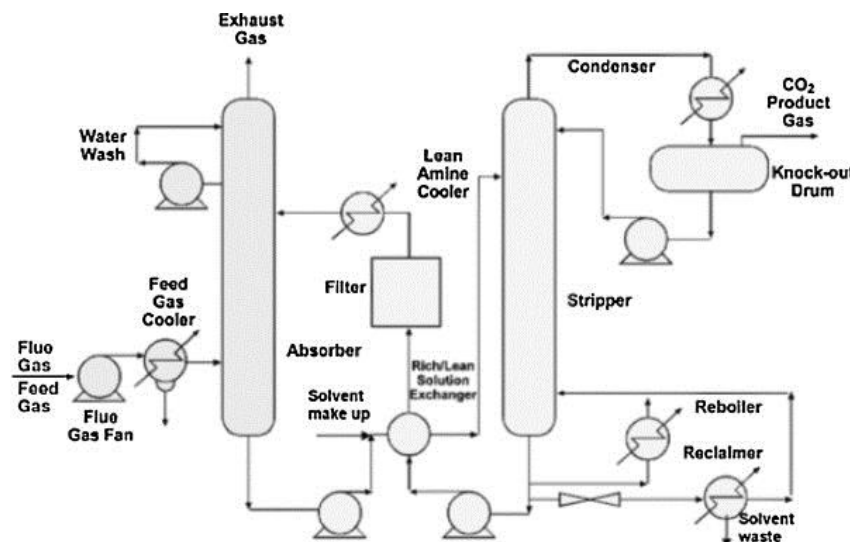


Figure 16: The solvent absorption system for post-combustion CO₂ capture¹⁰⁹.

Thus, current research on post-combustion capture is focussing on alternative technologies to deliver a cost-effective system, with growing interest developing in adsorption processes to separate the flue gas mixture. Adsorption using solid sorbents for the reversible capture of CO₂ has many potential advantages¹⁰⁸: reduced energy cost for regeneration, greater capacity, increased selectivity and improved ease of handling. In such a system desorption is achieved by a pressure and/or temperature swing approach that lowers the regeneration energy requirement significantly compared to the amine-based technologies¹¹⁰. However, any material designed for this purpose must have high CO₂ adsorption capacity, high selectivity, quick adsorption/desorption kinetics, high stability (thermal, pressure and

chemical), be low cost to produce and have a low energy requirement for regeneration¹⁰⁹. This last property is particularly important, since a material with a high adsorption capacity would not be practical for CO₂ capture if it did not release a large proportion of the captured gas at a reasonable temperature and/or pressure because its regeneration would be too expensive.

High adsorption capacity, quick adsorption/desorption, low energy requirement for regeneration and high selectivity can be achieved by the incorporation of organic amines in large surface area porous solids through impregnation, post-synthetic modification or direct condensation reactions, which is why this research area has attracted interest in the last decade¹¹¹. Amine-containing materials capture CO₂ by a reversible reaction thought to occur via the formation of a carbamate, with two moles of amine reacting with one mole of CO₂ through a zwitterion mechanism¹¹² (Figure 17).

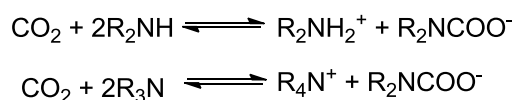


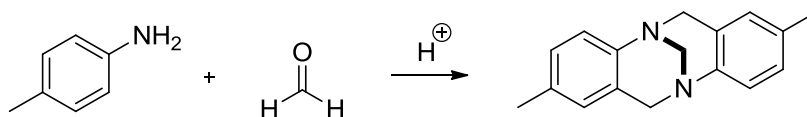
Figure 17: The formation of the carbamate species.

1.7 Tröger's base

The challenge of designing a PIM for the post-combustion capture of CO₂ meant incorporating amine functionality into the polymer chain whilst maintaining high rigidity, surface area, solubility and stability. Two options existed for this problem: altering an existing PIM to include amine functionality or developing a new range of PIMs. The first was initially attempted within the McKeown group, but the materials synthesised displayed poor solubility, low surface area or low molecular weight and possessed low amine content. It was anticipated that the use of Tröger's base as a component for novel PIMs would provide the desired high amine content.

Tröger's base (TB) is a bridged bicyclic molecule originally isolated by Julius Tröger in 1887 whilst he was studying the acid-catalysed condensation of p-toluidine and formaldehyde¹¹³ (Scheme 12), but its structure puzzled chemists for decades until it was correctly assigned in 1935¹¹⁴. It was the first molecule to be resolved whose chirality is

entirely attributable to asymmetric nitrogen atoms because unlike most other chiral tertiary amines the enantiomers of TB are greatly hindered from inversion due to the great ring strain it would create.



Scheme 12: The synthesis of Tröger's base.

TB displays a rigid V-shaped structure (Figure 18) with C_2 symmetry around two stereogenic bridgehead nitrogen atoms and a total length of about 1 nm¹¹⁵. This makes TB an ideal building block for nanometre molecular designs, and explains why it has been utilised as a scaffold for systems investigating molecular recognition¹¹⁶.

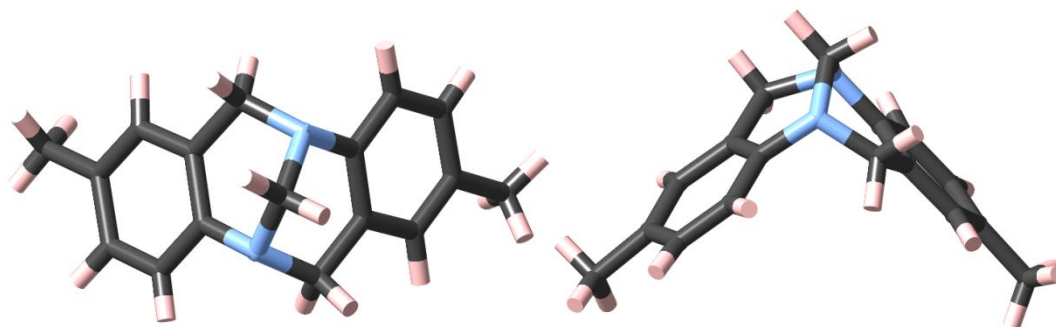


Figure 18. Tröger's base solid state crystal structure¹¹⁷.

TB was initially believed to be only weakly basic¹¹⁸, but a recent study on hydrogen bonding acceptor strength found that it is actually strongly basic relative to other aromatic amines ($pK_{HB}(N) = 1.15$), due to the low degree of conjugation between the lone pairs of the nitrogen atoms and the connected aromatic rings resulting from the rigidity of the molecule¹¹⁹. This property has been used successfully for catalysis¹²⁰, but also makes TB attractive for use in CO₂ capture materials, where the basicity is predicted to increase the affinity for CO₂.

TB and its simple derivatives can be prepared in excellent yields (> 85%) from a condensation reaction between a suitable amine and a source of formaldehyde in the presence of trifluoroacetic acid (TFA), which acts as both acid catalyst and solvent¹¹⁵. More recently, TB oligomers have been synthesised in good yields (50 – 80%) that feature two or three TB links between benzene units¹²¹. However, previous to the research described in this thesis, there were no reports on the use of TB formation for making polymers.

1.8 Project introduction

PIMs show remarkable potential as gas separation materials, but none have so far been designed specifically for carbon capture. The incorporation of amine functionality into materials was anticipated to increase affinity towards CO₂ significantly due to the interaction between basic nitrogen and CO₂. Hence, a PIM possessing a high amount of basic nitrogen would potentially be a very useful CO₂ capture material. Tröger's base was chosen as a building block for PIM synthesis due to its rigidity, size and two basic nitrogens, but clearly any PIM built from this unit will require a very different synthesis to existing PIMs. So a new synthetic strategy was needed to make TB-containing PIMs (Figure 19).

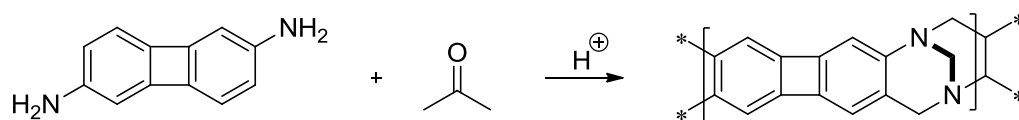


Figure 19: The preparation of TB-PIMs.

As previously mentioned, TB is made from the condensation reaction between an amine and formaldehyde in the presence of acid. This reaction occurs with excellent yield, and has already been proven to work with diamines to make TB oligomers¹²²⁻¹²³. The extension of this reaction for making PIMs is detailed along with the properties of the resulting polymers within the rest of this thesis.

Chapter 2: Monomer synthesis and discussion

2.1 Discussion of TB reaction and initial optimisation

As previously discussed, there is great interest in the incorporation of amine functionality into a PIM to produce a competitive, highly selective and permeable material for carbon dioxide capture. The structure known as Tröger's base (TB) was chosen as the linker between monomer units to produce novel polymers for this application. This involved the development of a novel polymerisation reaction, which began with the optimisation of the TB condensation reaction.

Significant study has been previously made into analysing TB formation, with several mechanisms proposed for how the reaction proceeds, but mass spectrometric experiments were recently used to devise a generally accepted mechanism¹²⁴ for the preparation of TB analogues from derivatives of aniline and formaldehyde (Figure 20). The mechanism proceeds by a series of in situ Friedel-Crafts alkylation reactions. The reaction begins with the transformation of the aniline derivative into the unstable imine intermediate, existing in equilibrium with the iminium intermediate (A). Secondly, an electrophilic attack occurs from the ortho-position of another molecule of aniline onto the iminium intermediate, giving ortho-aminobenzylamine (B), which undergoes cyclisation with another molecule of formaldehyde, through a series of proton transfer and dehydration steps, to form tetrahydroquinazoline (C). This species picks up a third molecule of formaldehyde, by electrophilic attack, to form an iminium intermediate (D), which finally undergoes intramolecular electrophilic substitution to give the TB analogue (E).

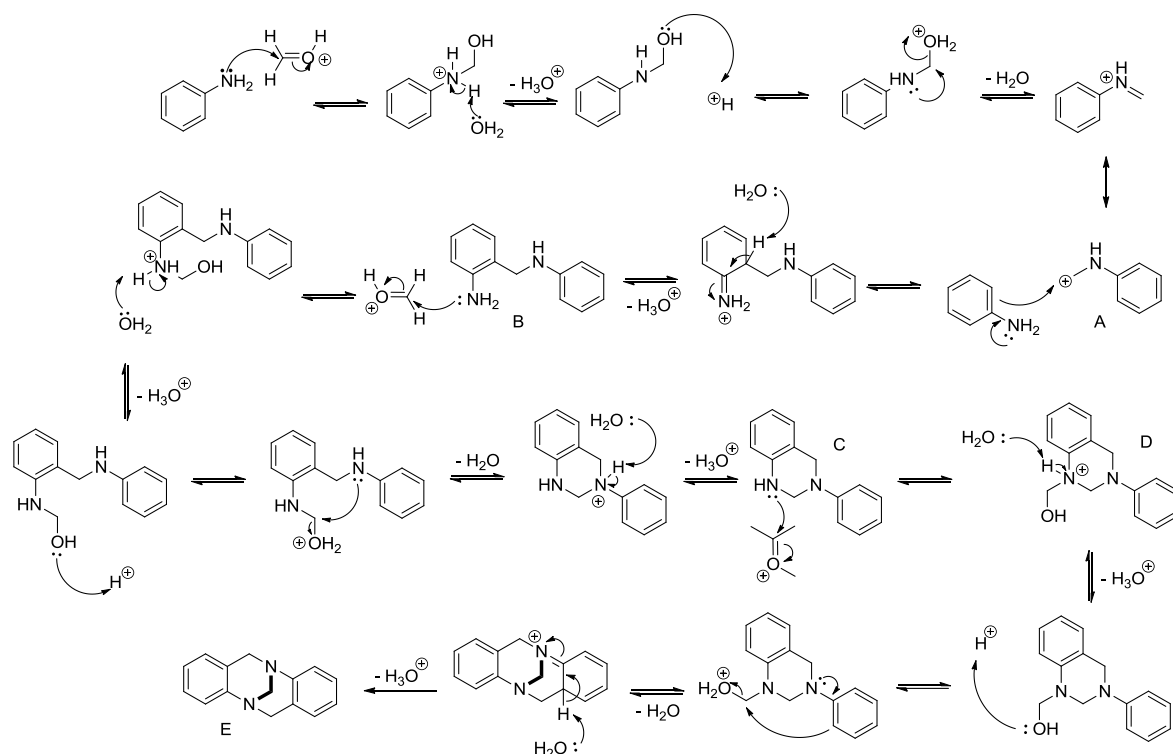
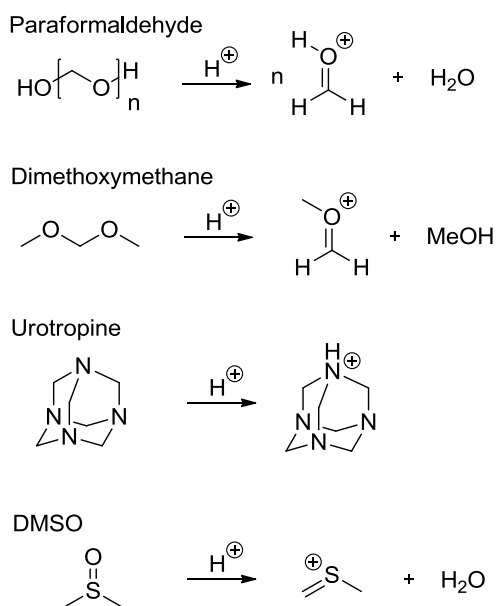


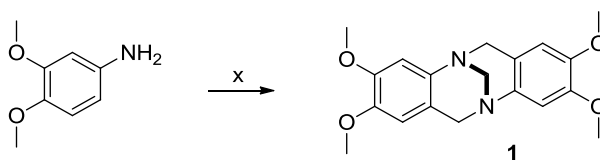
Figure 20: The TB condensation mechanism from an aniline derivative and formaldehyde.

The mechanism clearly shows that to make a molecule of TB two molecules of aniline and three equivalents of methylene are required. The source of the aniline derivative is obviously important for the synthesis to produce the desired product, but no systematic approach has previously studied the importance of the methylene source. So this was an important aspect of the reaction to optimise and a study was carried out to assess reaction yield with different methylene sources: paraformaldehyde¹²¹, dimethoxymethane¹²⁵, urotropine¹²⁶ and dimethyl sulphoxide (DMSO)¹²⁷, each of which can form a species capable of donating a methylene group to the aniline derivative (Scheme 13).



Scheme 13: The production of methylene from different sources.

Each of these precursors was tested for efficiency in forming TB under similar reaction conditions (Scheme 14) to make results reliable. The aniline reagent chosen for this test was 3,4-dimethoxyaniline, which is activated towards TB formation by the electron donating methoxy substituents.



Scheme 14: The production of TB from 3,4-dimethoxyaniline (**1**), x = methylene precursor. *Reagents and conditions:* 3,4-dimethoxyaniline (1 g), TFA (10 ml), 0 °C, 16 hours.

The results of the reaction varied greatly between the different methylene sources (Table 2), but dimethoxymethane and paraformaldehyde were clearly the best reagents, giving a product yield of 90%. Urotropine performed surprisingly poorly, since each molecule can potentially provide more than a single methylene, which should have meant all of the 3,4-dimethoxyaniline quickly reacting. Finally, DMSO performed extremely poorly, with only trace amounts of the product being formed. This indicated that the TB forming reaction was very efficient when either dimethoxymethane or paraformaldehyde were used.

Methylene precursor (x)	Yield (%)
Dimethoxymethane	90
Paraformaldehyde	90
Urotropine	42.5
Dimethyl sulphoxide	< 5

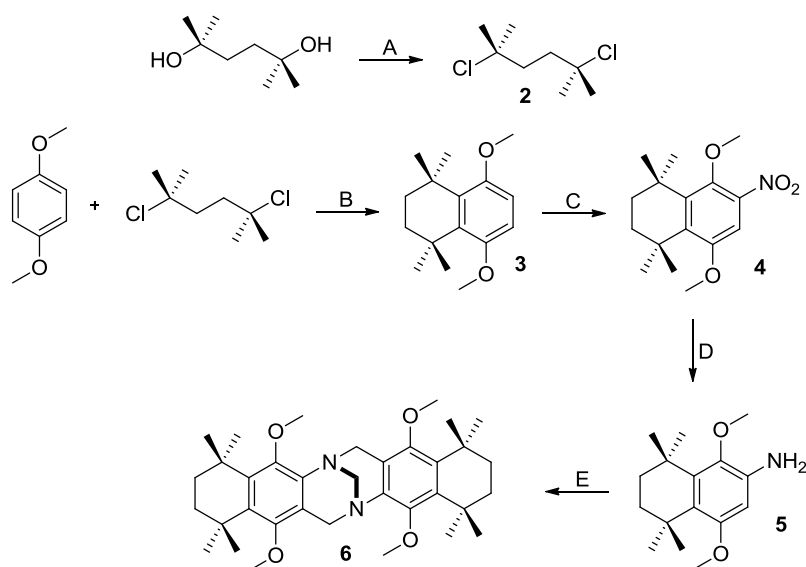
Table 2: A comparison between different methylene sources, showing reaction yield.

This study indicated that dimethoxymethane and paraformaldehyde would be the best reagents to use for the TB polymerisation, since only a highly efficient reaction would produce the high molecular polymer necessary for the formation of a polymer membrane. Furthermore, this study proved that the rate of reaction with these reagents is sufficiently fast to give a high yield of product after only 16 hours. This information proved essential in the development of the TB polymerisation reaction, but was initially used for the design and synthesis of novel TB dimers (i.e. model compounds for the desired polymers).

2.2 Design and synthesis of a novel TB derivative

It was desirable to design a model TB compound with bulky substituents to mimic the type of structural units likely to be used in making PIMs using the TB-forming reaction. The synthesis of such a compound began with the preparation of compound **2** from a simple nucleophilic substitution reaction between 2,5-dimethyl-2,5-hexanediol and concentrated hydrochloric acid, via a typical S_N1 mechanism (Scheme 15). The next step was the Friedel-Crafts alkylation of 1,4-dimethoxybenzene by compound **2**, in a reaction mediated by aluminium trichloride. A slight excess of compound **2** was used for this reaction in an attempt to maximise the yield of compound **3** from the reaction. This may explain the relatively moderate yield of the product from this reaction (66%), as it seems likely that some of the 1,4-methoxybenzene underwent a double Friedel-Crafts reaction, due to the activation of the benzene ring from the two methoxy substituents.

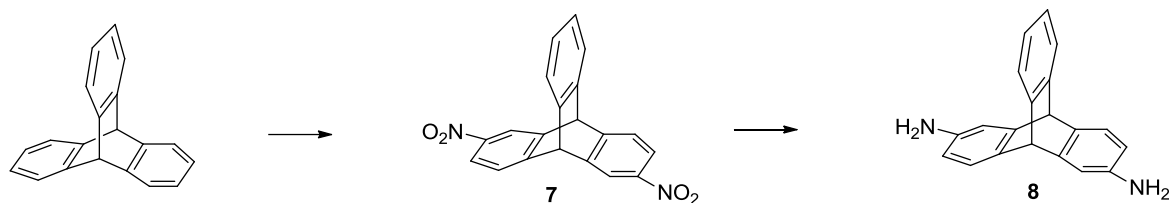
The nitration of compound **3** was performed using a mixture of concentrated nitric acid and glacial acetic acid at 0 °C, relatively mild conditions that were used to discourage the double nitration of the starting material. Compound **4** was then reduced using hydrazine monohydrate in THF, in a process catalysed by Raney nickel, giving the compound **5** in excellent yield (91%). This reaction has been found to be extremely efficient for a range of substrates¹²⁸⁻¹²⁹. Despite its toxicity, hydrazine is a useful reducing agent as the by-products from reaction are only nitrogen and water. Finally, compound **6** was produced in good yield (78%) by the reaction of compound **5** with dimethoxymethane in trifluoroacetic acid. Crystals were grown of compound **6** and analysed by single-crystal X-ray diffraction, details and discussion of which can be found in Appendix 1 (A1.1.2).



Scheme 15: The preparation of the TB model compound. *Reagents and conditions:* A. HCl, r.t., 16 hours. B. AlCl₃, CH₃NO₂, room temperature, 16 hours. C. HNO₃, Glacial acetic acid, 0 °C, 16 hours. D. Hydrazine monohydrate, Raney nickel, THF, N₂, 60 °C, 16 hours. E. Dimethoxymethane, TFA, 0 °C, 16 hours.

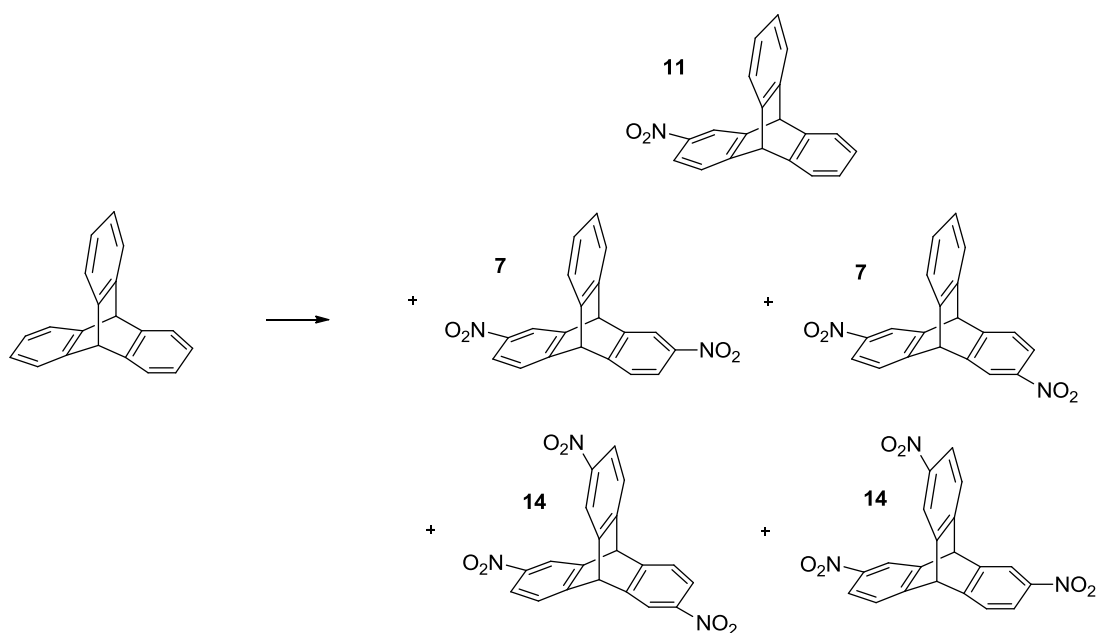
2.3 Triptycene chemistry

The first monomer chosen for the development of the TB polymerisation reaction was compound **8**, which is based around the triptycene unit, a proven building block for PIMs⁹², so it was expected that a triptycene based TB PIM would be highly microporous. Compound **8** is a mixture of 2,6-diaminotriptycene and 2,7-diaminotriptycene, which are the two possible structural isomers of the compound, but since they react similarly during the polymerisation reaction no attempt to separate the two isomers was made.



Scheme 16: The synthesis of 2,6(7)-diaminotriptycene (**8**).

The synthetic route chosen was to prepare compound **7**, from the nitration of triptycene, and then to prepare compound **8** via a reduction of the nitro groups (Scheme 16). Nitration using concentrated nitric acid is a simple reaction with numerous examples in literature¹³⁰⁻¹³¹, so was the first route considered to obtain compound **7**. Initially, 2 equivalents of nitric acid in a solution of acetic acid were used, but this reaction suffered problems due to the production of side products, identified as 2-mononitrotriptycene (**11**) and 2,6(7),14-trinitrotriptycene (**14**), arising from the single and triple nitration of the triptycene starting material (Scheme 17). As a result of this, compound **7** could only be obtained in relatively poor yield (35%), after difficult purification to remove the unwanted side products, which involved column chromatography. Purification was performed at this stage of the synthesis because it was anticipated that compound **8** would be less stable than compound **7**. The mixed-product problem arises from each ring of triptycene being reactive towards electrophilic attack¹³², despite every nitro group deactivating the next ring, due to its electron-withdrawing effect. In practice, it was found that there was an equal chance of a molecule of compound **7** being over-nitrated to form compound **14** as there is for a molecule of compound **11** being under-nitrated to form compound **7**, which results in a mixture of the three products being formed, as highlighted in Scheme 17.



Scheme 17: The nitration and over nitration of triptycene. *Reagents and conditions:* HNO_3 , CH_3COOH , 70°C , 48 hours.

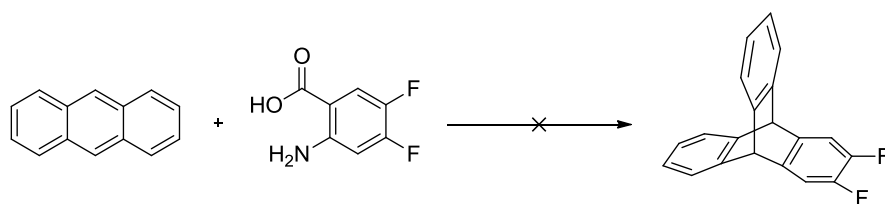
Purification of the mixture proved difficult so in an attempt to improve the yield of compound **7**, the experiment was performed with 2.5, 3, 4 and 5 equivalents of nitric acid, and the results analysed by integration of ^1H NMR peaks. The results shown in Table 3 clearly indicate that increasing the number of equivalents of nitric acid increases the yield of the desired compound, whilst decreasing the amount of compound **11** produced, but also increases the yield of compound **14**. This analysis showed that using 4 equivalents of nitric acid in the reaction gave the highest yield of compound **7**, whilst minimising the yield of the side products. At 5 equivalents there is actually a decrease in the yield of compound **7**, as more product is further nitrated to produce compound **14**. These yields are calculated using ^1H NMR data and rather than isolated yields.

Equivalents of nitric acid	Yield (%)		
	Mononitrotriptycene	Dinitrotriptycene	Trinitrotriptycene
2	40	58	2
2.5	35	60	5
3	32	63	10
4	4	79	17
5	1	67	32

Table 3: The yields of nitrated triptycenes produced when using different equivalents of concentrated nitric acid.

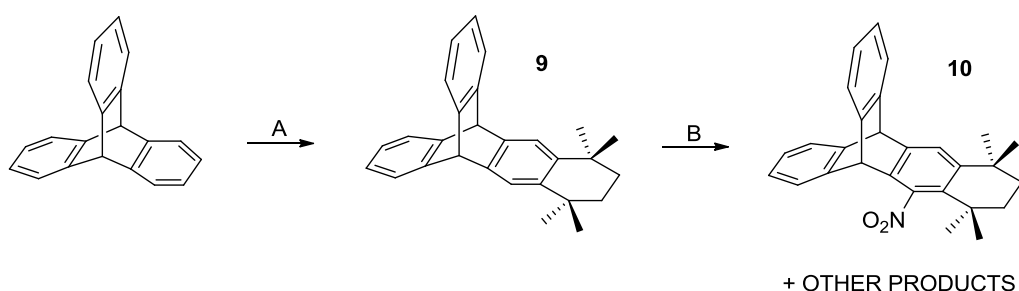
A slight modification of this nitration reaction, using a small quantity of sulphuric acid was then performed. Sulphuric acid acts as a catalyst by aiding the production of the nitronium ion (NO_2^+), which is the active species for nitration, thereby reducing the number of nitric acid equivalents required for the reaction. Under these conditions an improved yield of pure compound **7** was obtained after purification (41%), but the yield was still only moderate. To perform the polymerisation study a substantial amount of compound **7** was required, so an alternative and more efficient route was required, with two possible solutions. The first solution was to effectively block one of the triptycene rings from reacting, meaning that the original nitration reaction could be performed under harsher conditions giving an improved yield of the desired product. The second route was to perform a more selective nitration to maximise the yield of compound **7**.

The first option, to use blocking chemistry to control the nitration reaction was the first to be attempted. The idea was to synthesise 2,3-difluorotriptycene from the Diels-Alder reaction between anthracene and 4,5-difluoroanthranilic acid (Scheme 18). This anthranilic acid was chosen because 4,5-difluoroanthranilic was commercially available and it was predicted that the presence of the fluorine atoms in the final polymer would have a beneficial effect on gas separation properties. However, after numerous attempts at the reaction, no product was formed or detected by analysis and the idea was abandoned. It was thought that the electron withdrawing properties of the two highly electronegative fluorine atoms prevented the Diels-Alder reaction from occurring.



Scheme 18: The attempted preparation of 2,3-difluorotriptycene. *Reagents and conditions:* Isoamyl nitrite, Acetone, DCM, Reflux, 24 h.

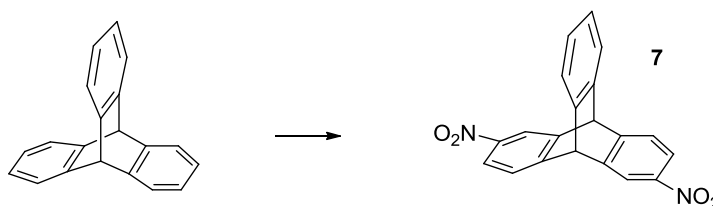
Another method for blocking substitution onto one of the triptycene benzene rings was to react triptycene with compound **2** (Scheme 19), a material easy to synthesise (Scheme 15). This reaction worked well and a high yield of compound **9** was obtained. However, problems were encountered during the subsequent nitration reaction, which produced a mixture of products that could not be separated from the desired product. Analysis indicated that the cause was the activation of the substituted ring by the electron donating alkyl ring system, which resulted in the ring becoming easily nitrated. Unfortunately, this meant that this synthetic pathway had to be ruled out, and the idea of blocking a triptycene ring from nitration was much more difficult than expected.



Scheme 19: The reaction of triptycene with 2,5-dichloro-2,5-dimethylhexane (**9**) and the subsequent nitration, highlighting the problem encountered. *Reagents and conditions:* A. **2**, AlCl₃, CH₃NO₂, Room temperature, 16 hours, B. HNO₃, CH₃COOH, Acetic anhydride, 0 °C, 24 hours.

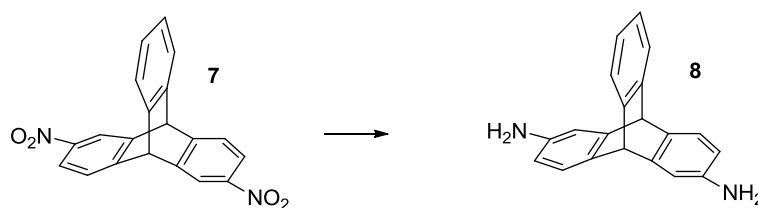
Instead, optimisation of the nitration of triptycene to give compound **7** proved successful after the discovery and development of a nitration reaction using potassium nitrate¹³³ (Scheme 20). Various solvents were trialled for the reaction before it was found that acetonitrile was able to dissolve both triptycene and potassium nitrate. Using this reaction, catalysed by trifluoroacetic anhydride, a high yield of pure compound **7** was obtained after purification (80%). Clearly this was a much improved route to compound **7**, with the best results achieved when just 2 equivalents of potassium nitrate were used, indicating a highly

efficient reaction. Using a greater number of equivalents of potassium nitrate gave more trinitrated product and correspondingly less compound **7**.



Scheme 20: The potassium nitrate reaction for producing 2,6(7)-dinitrotriptycene (**7**). *Reagents and conditions:* KNO₃, trifluoroacetic anhydride, CH₃CN, room temperature, 16 hours.

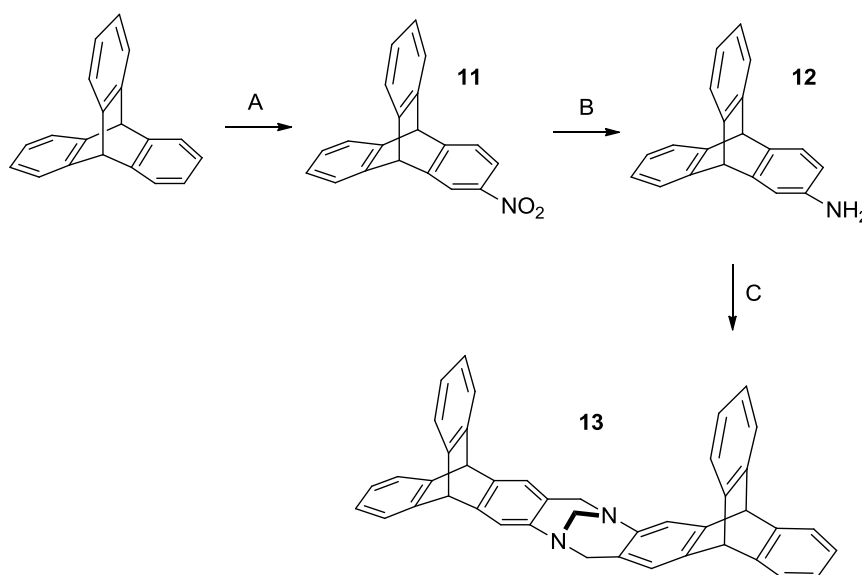
Using this reaction a sufficiently large quantity of compound **7** was produced, although the process was time consuming due to the difficulty of removing the side products. Nevertheless, with a good nitration procedure found, the last challenge in synthesising compound **8** was the efficient reduction of compound **7**. Several reduction procedures were trialled on a small scale, including palladium with hydrogen gas, tin with concentrated hydrochloric acid, and iron with hydrazine monohydrate. However, the best yield was achieved with using Raney nickel and hydrazine monohydrate in THF¹³⁴ (Scheme 21). Due to the expected sensitive nature of the monomer the reaction was performed under a nitrogen atmosphere. The polymerisation reaction using compound **8** are discussed in Chapter 3 (3.2 and 3.3.1).



Scheme 21: The reduction of 2,6(7)-dinitrotriptycene (**7**). *Reagents and conditions:* Raney nickel, hydrazine monohydrate, THF, N₂, 60 °C, 16 hours.

In order to better understand the structure and properties of the ladder polymer made by the TB polymerisation of compound **8** it was desirable to synthesise a TB model compound based around the triptycene unit. This involved the mononitration of triptycene, purification of the product and reduction to give compound **12**, from which compound **13** was generated in the typical TB formation reaction (Scheme 22). The nitration reaction was performed using a mixture of concentrated nitric acid in glacial acetic acid¹³⁵, which resulted in mild nitration conditions so that the product could be obtained in good yield

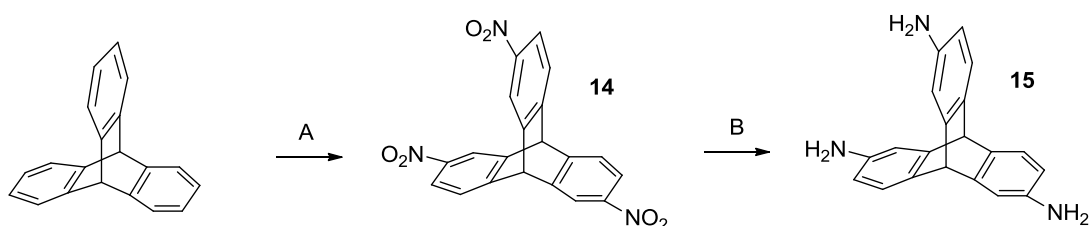
(73%). Nevertheless, this reaction produced unwanted products: compounds **7** and **14**, resulting from the over nitration of the starting material. Once pure, compound **11** was reduced using a mixture of hydrazine monohydrate and Raney nickel in THF to give compound **12**¹³⁵. Compound **13** was then produced from compound **12** using dimethoxymethane in trifluoroacetic acid, in a standard TB formation reaction. Due to the expected instability of the starting material a temperature of 0 °C was used at the start of the reaction, although the reaction mixture was slowly allowed to warm to room temperature. After some initial difficulties, crystals were grown of compound **13** and analysed by single-crystal X-ray diffraction, the details and discussion of this can be found in Appendix 1 (A1.1.3).



Scheme 22: The synthesis of TB triptycene model compound. *Reagents and conditions:* A. Concentrated HNO₃, glacial acetic acid, 75 °C, 16 hours. B. Raney nickel, hydrazine monohydrate, THF, N₂, 60 °C, 16 hours, N₂. C. Dimethoxymethane, TFA, 0 °C, 16 hours.

The synthesis of compound **15** was necessary for the preparation of a TB network PIM built around the triptycene build block. This synthesis proved relatively simple, involving the trinitration of triptycene to produce compound **14**, purification and then reduction to form the desired monomer (Scheme 23). The nitration reaction was performed under relatively harsh conditions using hot concentrated nitric acid and was catalysed by sulphuric acid¹³⁶. These conditions were used in order to maximise the yield of the trinitrated triptycene product, but small amounts of compounds **7** and **11** were also produced. The reduction reaction was performed by the using the Raney nickel and

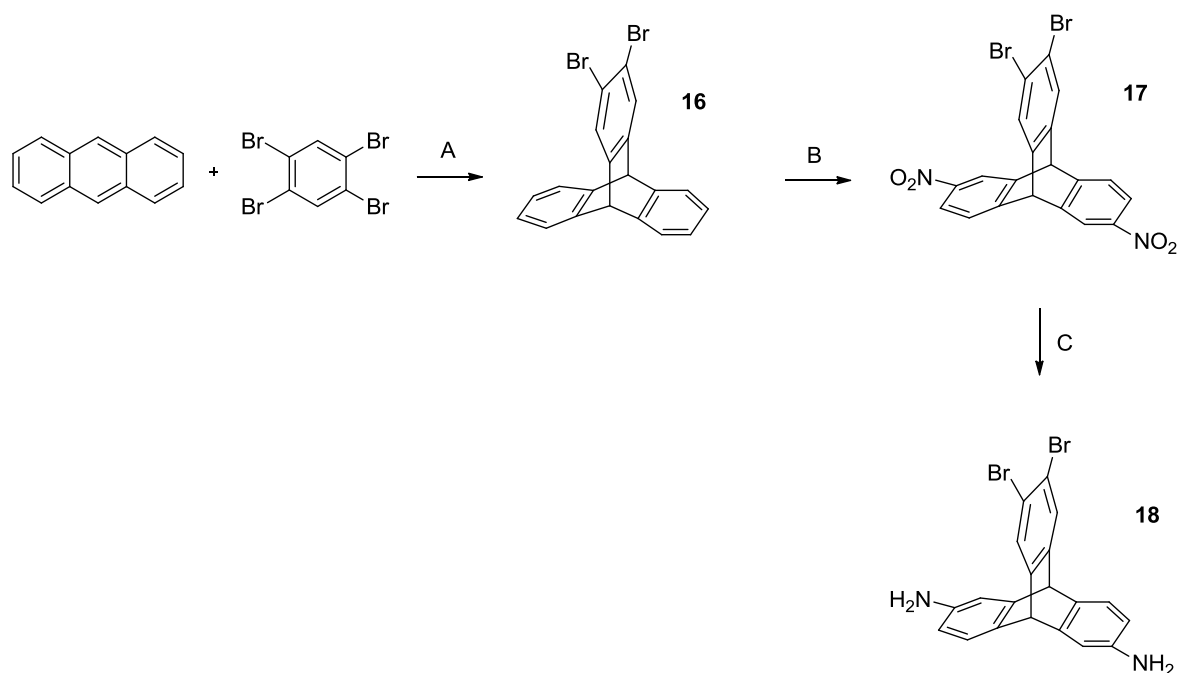
hydrazine monohydrate system in THF¹³⁶, obtaining the desired compound in excellent yield. The subsequent polymerisation reaction is described in Chapter 3 (3.3.3).



Scheme 23: The synthesis of 2,6(7),14-triaminotriptycene (**15**). *Reagents and conditions:* A. Concentrated HNO₃, concentrated H₂SO₄, 80 °C, 16 hours, 100 °C, 2 hours. B. Raney nickel, hydrazine monohydrate, THF, 60 °C, 16 hours, N₂.

2.4 Dibromotriptycene chemistry

Following the success of the TB triptycene derivatives an attempt was made to create a ladder polymer built around the triptycene framework, but featuring two bromine atoms, which it was hoped would have two effects. Firstly, it was anticipated that the presence of the bulky bromine atoms would effectively block one of the triptycene rings from being nitrated, resulting in an easier synthesis. Secondly, it was hoped that the presence of the bromine would help enhance the gas separation properties of the ladder polymer, in case it was possible to cast a self-standing membrane. The synthetic pathway involved the synthesis of compound **16**, since the compound was not commercially available, followed by the usual nitration and reduction reactions to produce the monomer, compound **18** (Scheme 24).

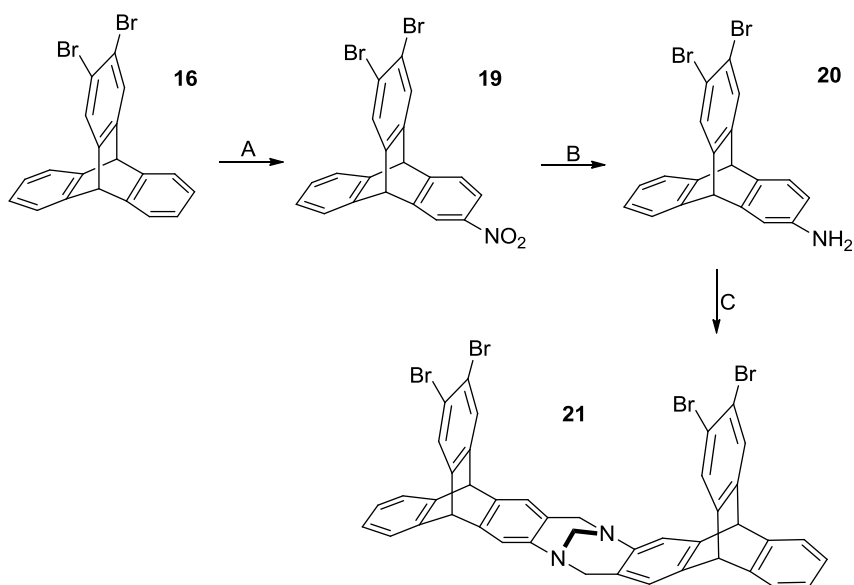


Scheme 24: The synthesis of 2,3-dibromo-6(7),14-diaminotriptycene (**18**). *Reagents and conditions:* A. BuLi, hexane, toluene, 0 °C, 16 hours. B. KNO₃, trifluoroacetic anhydride, CH₃CN, room temperature, 16 hours. C. Hydrazine monohydrate, Raney nickel, Et₂O, N₂, 30 °C, 16 hours.

Compound **16** was synthesised from the Diels-Alder reaction between anthracene and 1,2,4,5-tetrabromobenzene, initiated by butyl lithium¹³⁷. This reaction produced a mixture of products, but after purification by column chromatography the product was obtained in good yield (57%). The next stage of the synthesis involved the nitration of compound **16** using the potassium nitrate procedure, which produced compound **17** in excellent yield (99%). This was evidence that the two bromine atoms were indeed blocking the associated ring from reaction, whilst the excess of potassium nitrate ensured that the two other rings of each molecule were successfully nitrated. Finally, compound **18** was produced via a reduction reaction using Raney nickel and hydrazine monohydrate. The polymerisation of compound **18** is described in Chapter 3 (3.3.1).

To enable further understanding of the structure and properties of the TB ladder polymer built from the 2,3-dibromotriptycene unit it was desirable to synthesise the TB model compound built around the same compound. For this it was necessary to generate compound **20**, which was prepared from the nitration of compound **16**, producing compound **19**, which was subsequently reduced (Scheme 25). The nitration reaction was performed using the potassium nitrate procedure with just over one equivalent of potassium nitrate, to maximise the yield of the target product since over nitration was not

expected. The reaction produced a mixture of compounds **19** and **17**, but the unwanted material was easily removed by column chromatography. Compound **19** was then reduced using the Raney nickel and hydrazine monohydrate reaction, which gave compound **20** in the expected high yield. This compound underwent TB formation using dimethoxymethane and trifluoroacetic acid, giving compound **21**.



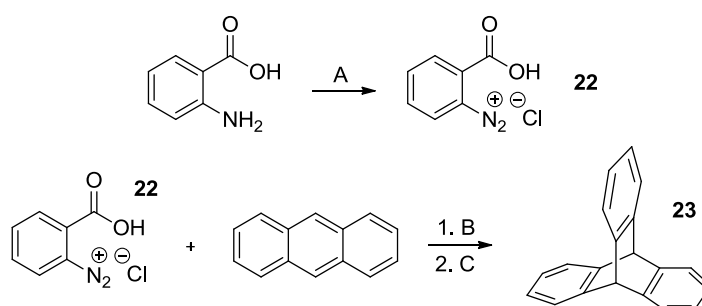
Scheme 25: The synthesis of the TB dibromotriptycene model compound (**21**). *Reagents and conditions:* A. KNO_3 , trifluoroacetic anhydride, CH_3CN , $50\text{ }^\circ\text{C}$, 16 hours. B. Raney nickel, hydrazine monohydrate, THF, $50\text{ }^\circ\text{C}$, N_2 , 16 hours. C. Dimethoxymethane, TFA, $0\text{ }^\circ\text{C}$, 16 hours.

2.5 Methyl substituted triptycenes

Another idea to improve the already successful of TB triptycene monomers was to add methyl groups to the triptycene unit, which have previously been proven to increase the surface area of PIMs, particularly if placed on the triptycene bridgehead carbons⁹².

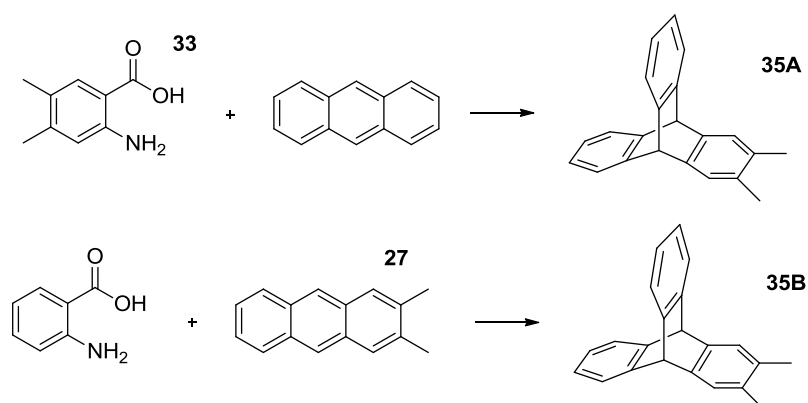
Triptycenes are typically generated via a Diels-Alder reaction between an anthracene derivative and an anthranilic acid derivative¹³⁸. The yield of such reactions can be enhanced by making the diazonium salt of the anthranilic acid derivative prior to reaction with the anthracene derivative, as this aids in the generation of the reactive benzyne intermediate¹³⁹. Before attempting the synthesis of the methyl substituted triptycenes the reaction was optimised for unsubstituted triptycene before the more expensive reagents were consumed.

Compound **23** was synthesised from the Diels-Alder reaction between anthracene and the diazonium salt of anthranilic acid, compound **22** (Scheme 26). The diazonium salt was produced by the reaction between anthranilic acid (2-aminobenzoic acid) and isoamyl nitrite. The Diels-Alder reaction was performed under a variety of conditions until the optimum yield was achieved in refluxing dichloroethane over 48 hours, giving compound **23** in good yield (62%). This reaction was also useful as compound **23** is an expensive commercial reagent and this synthesis avoids any time consuming purification whilst still producing pure material.



Scheme 26: The preparation of triptycene (**23**). *Reagents and conditions:* A. Concentrated HCl, isoamyl nitrite, EtOH, Et₂O, 0 °C, 30 minutes. B. 1,2-Epoxypropane, DCE, 85 °C, 48 hours. C. Maleic anhydride, o-xylene, 110 °C, 1 hour.

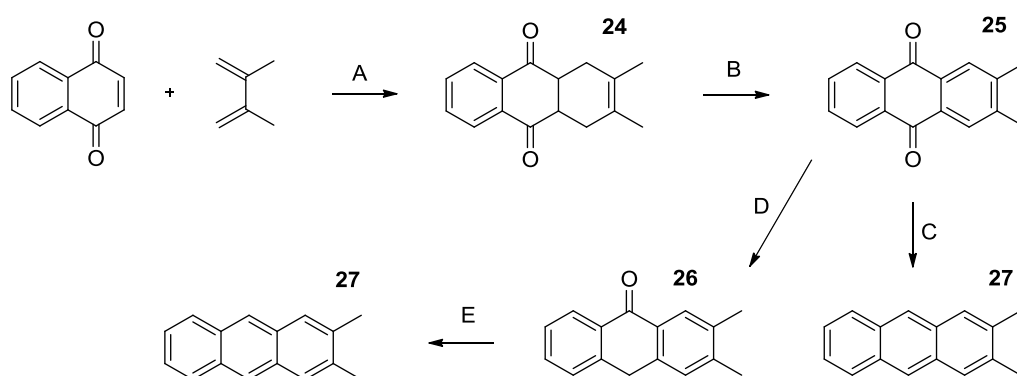
Two strategies were considered for the preparation of methyl substituted triptycenes: synthesis of the anthracene derivative with methyl substituents or synthesis of the anthranilic acid with methyl substituents, as proposed in Scheme 27. Both strategies were employed to produce 2,3-dimethyltriptycene on a sufficient scale.



Scheme 27: The two routes to 2,3-dimethyltriptycene.

The first approach (Scheme 28), involving the synthesis of compound **27** and started with the Diels-Alder reaction between 2,3-dimethyl-1,3-butadiene and α -naphthoquinone¹⁴⁰, producing compound **24**. This compound was then oxidised by exposure to air¹⁴⁰, a reaction activated by potassium hydroxide, which induces aromaticity in the second ring system, forming compound **25**. The reduction reaction causing the full aromatisation of compound **25** to form compound **27** proved challenging and two different reactions were tested before the compound was successfully synthesised.

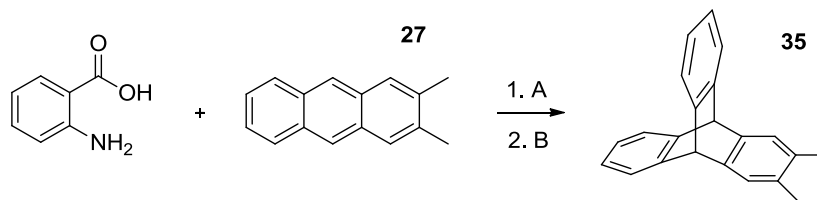
The first reduction reaction was performed using sodium hydroxide and zinc activated by treatment with acid¹⁴¹. This reaction produced a good yield of compound **27A** on a small scale (93%), but problems were encountered when reaction was performed at larger scales due to the large amount of zinc required. Attempts at reducing the amount of zinc gave a much lower yield, so this reaction was ruled out. The alternative reaction used hydroiodic acid in glacial acetic acid as the reducing agent¹⁴² and this encountered a similar problem. When performed on a small scale this reaction produced compound **27** in excellent yield (95%), but when performed on a larger scale compound **26** was instead produced in excellent yield (90%), suggesting that the reduction was not going to completion. Fortunately, this could be further reduced using sodium borohydride in a suspension of diglyme¹⁴³, which produced compound **27B** in excellent yield (91%) and worked on a large scale, allowing for a sufficient quantity of compound **27** to be produced.



Scheme 28: The synthesis of 2,3-dimethylantracene (**27**). *Reagents and conditions:* A. CH₃OH, 70 °C, 16 hours. B. EtOH, KOH, H₂O, room temperature, 72 hours. C. NaOH, H₂O, Zn, 100 °C, 48 hours. D. Glacial acetic acid, HI, 120 °C. E. NaBH₄, diglyme, MeOH, 16 hours.

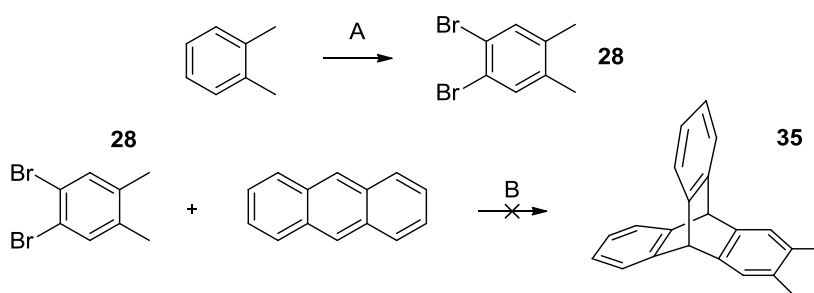
Compound **35** was then produced by the Diels-Alder reaction between compound **27** and 2-aminobenzoic acid in refluxing dichloromethane (Scheme 29), with the benzyne intermediate created *in-situ* by the reaction of anthranilic acid with amyl nitrite. After

reaction the unreacted anthracene was consumed by treatment with maleic anhydride before the reaction mixture was triturated in methanol, which gave compound **35A** in remarkably low yield (4%). This yield was too low to make this synthetic pathway worthwhile, especially since a large quantity of the triptycene was required for further synthesis.



Scheme 29: The preparation of 2,3-dimethyltriptycene (**35A**). *Reagents and conditions:* A. Amyl nitrite, DCM, 42 °C, 16 hours. B. Maleic anhydride, 110 °C, 2 hours.

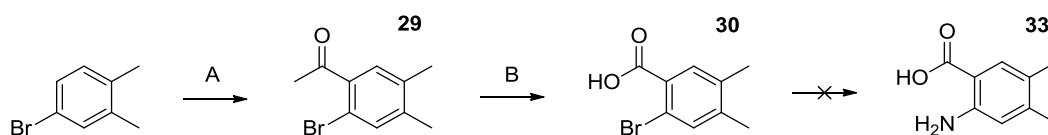
So alternate strategies to synthesising compound **35** were considered, the first of these explored involved the synthesis of compound **28** and its subsequent Diels-Alder reaction with anthracene (Scheme 30). The preparation of compound **28** was achieved by the bromination of *o*-xylene mediated by iodine¹⁴⁴. This procedure was performed on a large scale and gave compound **28** in modest yield (38%); perhaps due to the reaction mixture solidifying as the product is formed so the reactants cannot mix, resulting in a large quantity of unreacted starting material. However, the attempted Diels-Alder reaction between the benzyne generated from compound **28** and anthracene gave none of the desired product, even when using similar conditions used for the synthesis of compound **16**. So, after several failed attempts another pathway to compound **35** was sought.



Scheme 30: The proposed preparation of 2,3-dimethyltriptycene (**35**). *Reagents and conditions:* A. Br₂, I₂, room temperature, 24 hours; B. BuLi.

The alternate route (Scheme 31) involved the synthesis of dimethyl anthranilic acid **33**, as this reagent is not commercially available. The first attempted synthetic pathway to this

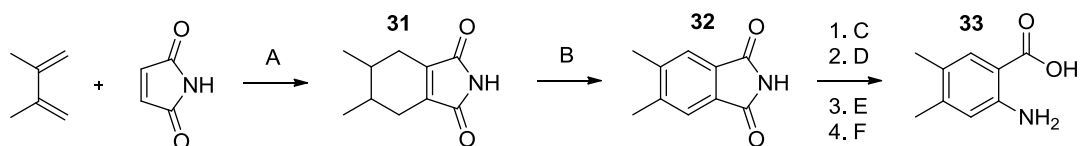
compound started with the commercially available 1-bromo-3,4-dimethylbenzene, which was acetylated with acetyl chloride in a typical Friedel-Crafts acylation reaction catalysed by aluminium trichloride¹⁴⁵, to give compound **29**. This was then oxidised by a mixture of sodium hydroxide in sodium hypochlorite solution, in a process mediated by sodium 1-dodecanesulphonate¹⁴⁵, which gave compound **30**. The final stage in the synthesis required the substitution of bromine with an amino group, but this is where the synthesis encountered problems. Several examples of similar copper catalysed reactions were identified from the literature¹⁴⁵⁻¹⁴⁷, but each one failed to produce the target product. This may have been caused by the need for hot aqueous ammonia and without the necessary pressurised reaction vessel the aqueous ammonia boiled-off before reaching a temperature sufficient for the reaction to occur, although a sealed reaction flask was used to avoid the loss of the ammonia from the reaction vessel. An alternative procedure that avoided the use of hot aqueous ammonia involved the use of sodium azide in a copper catalysed reaction¹⁴⁸, but this reaction was avoided due to the risk imposed by the high toxicity of sodium azide and an alternative route to the target product was investigated.



Scheme 31: The proposed synthesis of 4,5-dimethylantranilic acid (**33**) starting from 1-bromo-3,4-dimethylbenzene. *Reagents and conditions:* A. AcCl, CS₂, AlCl₃, 70 °C, 3 hours. B. NaOCl, NaOH, sodium 1-dodecanesulphonate, 75 °C, 16 hours.

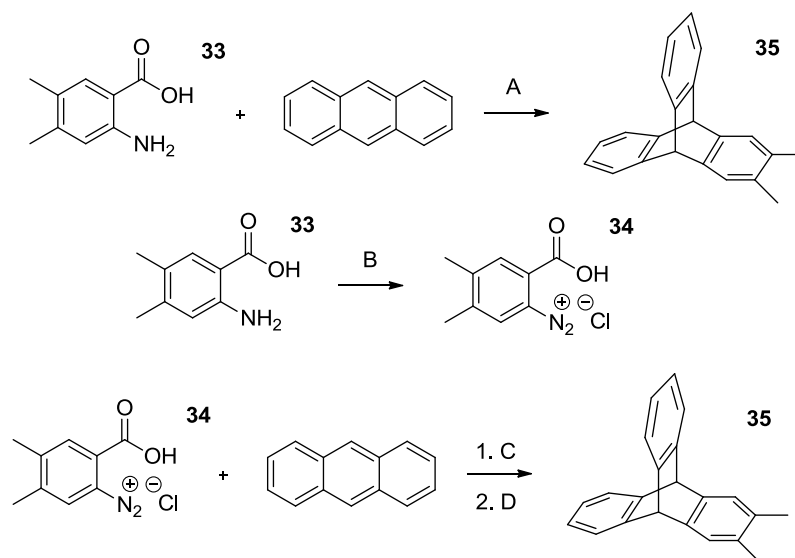
This alternative route to compound **33** started with the commercially available maleimide compound in a three-step synthesis¹⁴⁹ (Scheme 32). The first step was a Diels-Alder reaction between maleimide and 2,3-dimethyl-1,3-butadiene¹⁵⁰, which gave compound **31**. In the second step aromaticity was created in the partly saturated six-membered ring system via an oxidation reaction involving sulphur, iodine and diphenyl ether¹⁵⁰. High temperature was necessary to encourage production of the product, compound **32** (Scheme 30). The final stage was a multi-step Hoffmann rearrangement, involving the breaking of the five-membered ring system. Initially, only a moderate yield of compound **33** was obtained from this reaction (42%), when the procedure was performed using sodium hydroxide in sodium hypochlorite solution. However, this yield was greatly improved (70%) when the reaction was performed using sodium hypobromite, created from the reaction between sodium hydroxide and bromine¹⁵¹. This difference in yield can be

explained by bromine being a better leaving group than chlorine, since the Hoffmann rearrangement involves the loss of the halide from the nitrogen atom. This pathway allowed for the preparation of compound **33** on a sufficiently large scale for the subsequent synthesis.



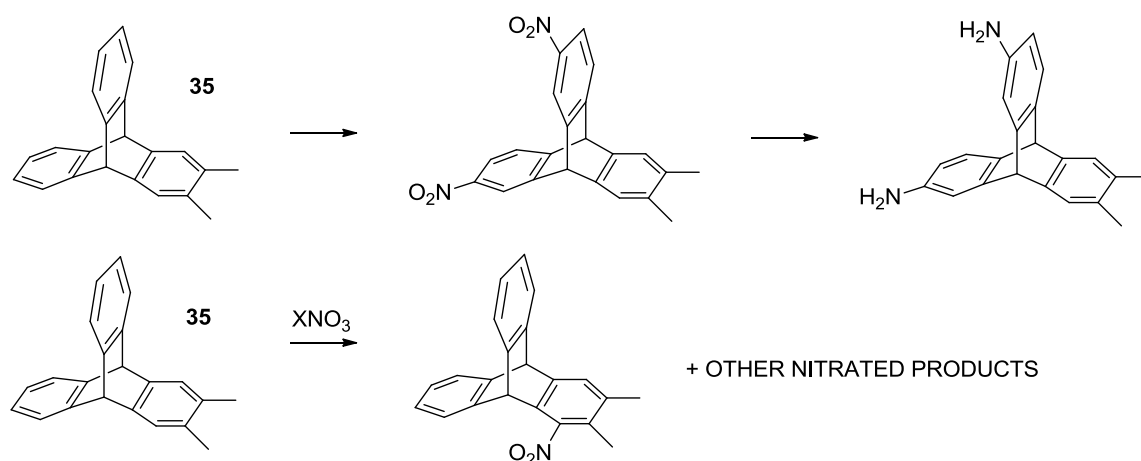
Scheme 32: The synthesis of 4,5-dimethylantranilic acid (**33**). *Reagents and conditions:* A. MeOH, 70 °C, 16 hours. B. S, I₂, Ph₂O, decalin, 190 °C, 24 hours. C. NaOH, H₂O, 0 °C. D. NaOH, Br₂, H₂O, 0 °C. E. 80 °C, 1 hour. F. HCl.

From this point the synthesis of compound **35** was relatively straightforward (Scheme 33). Initially, the Diels-Alder reaction between anthracene and compound **33** was performed in a refluxing mixture of acetone and dichloroethane, with the reactive benzyne intermediate formed *in-situ* by reaction of the anthranilic acid with amyl nitrite¹⁵². This procedure gave **35B** in low yield (26%), after trituration in methanol. Therefore, to improve the yield, the Diels-Alder the diazonium salt **34** was isolated following the reaction with isoamyl nitrite, catalysed by hydrochloric acid. The subsequent Diels-Alder reaction between **34** and anthracene in refluxing dichloroethane gave compound **35C** in a much improved yield (64%) after purification by column chromatography. The unreacted anthracene was consumed by reaction with maleic anhydride, which again aided purification.



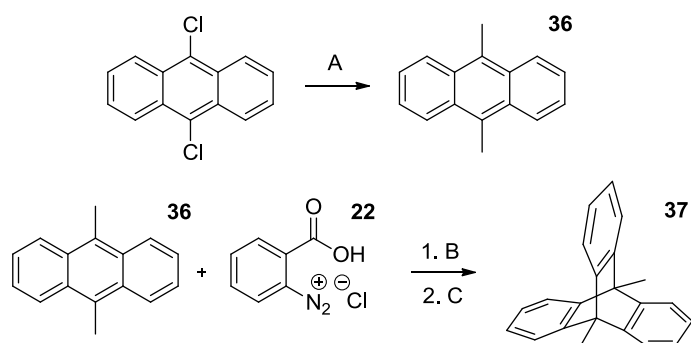
Scheme 33: The second synthetic pathway to 2,3-dimethyltritycene (**35**). *Reagents and conditions:* A. Acetone, amyl nitrite, dichloroethane, 85 °C, 16 hours. B. EtOH, HCl, isoamyl nitrite, Et₂O, 0 °C, 30 minutes. C. DCE, 1,2-epoxypropane, 85 °C, 48 hours. D. Maleic anhydride, o-xylene, 110 °C, 1 hour.

Once a sufficient quantity of 2,3-dimethyltritycene had been created the synthesis of the monomer, 2,3-dimethyl-6(7),14-diaminotriptycene was attempted. The proposed route to this compound involved the nitration of compound **35** (Scheme 34), but unfortunately this proved unsuccessful. Instead, the reaction was found to produce a mixture of products from either the potassium nitrate or nitric acid based procedures, which proved impossible to separate. Unexpectedly, ¹H NMR analysis suggested that one of these products was 2,3-dimethyl-4-mononitrotritycene (Scheme 34), this suggested that rather than blocking the ring system from further reaction the two methyl groups activated the adjacent position to nitration, which caused the reaction to produce the mixture of products observed. Due to these problems, this line of research was discarded.



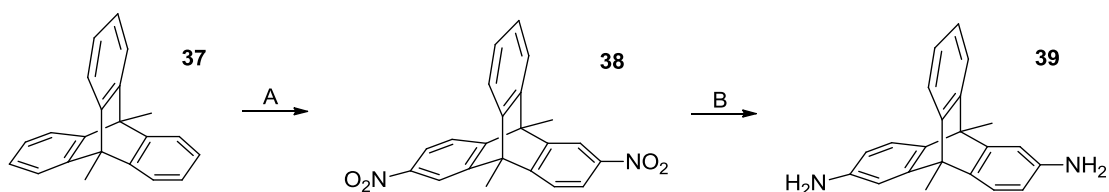
Scheme 34: The proposed synthesis of 2,3-dimethyl-6(7),14-diaminotriptycene, highlighting the problem encountered during the synthesis. X = K or H.

In order to investigate the effect of triptycene bridgehead methyl substituents on the properties of the ladder and network polymers built from the triptycene unit it was necessary to synthesise 9,10-dimethyltriptycene (compound **37**). This compound was created from the Diels-Alder reaction between the benzyne intermediate generated from anthranilic acid (2-aminobenzoic acid) and 9,10-dimethylantracene (compound **36**, Scheme 35). Fortunately, the synthesis of compound **36** proved relatively straightforward and was achieved by a Kumada-Corriu cross-coupling reaction between 9,10-dichloroanthracene and methyl magnesium bromide using the PEPPSI-IPr catalyst¹⁵³. The Diels-Alder reaction was performed using the optimised conditions for triptycene formation, refluxing dichloroethane with 1,2-epoxypropane using the *in-situ* preparation of the reactive benzyne species. After reaction the unreacted compound **36** was consumed by reaction with maleic anhydride, to aid purification of compound **37**, which was obtained in high yield (81%). The yield was significantly higher than for the previously discussed triptycenes, compounds **35** and **23**. This may be attributed to the directing effect of the methyl substituents of compound **36**, which encourage reaction on the central ring system due to their electron donating effect that creates an electron rich diene for Diels-Alder reactions.



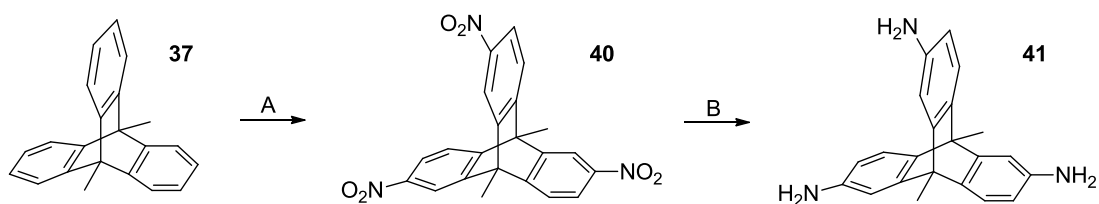
Scheme 35: The synthesis of 9,10-dimethyltritycene (**37**). *Reagents and conditions:* A. MeMgBr, PEPPSI-IPr catalyst, 1,4-dioxane, room temperature, 24 hours. B. 1,2-epoxypropane, DCE, 85 °C, 40 hours. C. Maleic anhydride, o-xylene, 110 °C, 1 hour.

The required diaminotriptycene monomer (compound **39**) was formed by the nitration of compound **37**, followed by reduction of compound **38** (Scheme 36). The nitration reaction was performed with potassium nitrate and trifluoroacetic acid, but due to the poor solubility of the triptycene in acetonitrile a small volume of dichloromethane was added to completely dissolve the starting material. This reaction also gave a small quantity of unwanted over- and under-nitrated side products: compounds **42** and **40** that were removed by column chromatography, which proved easier than for the nitration of triptycene bearing no methyl groups. Monomer **39** was then produced via the reduction reaction using hydrazine monohydrate, catalysed by Raney nickel. The polymerisation of this monomer is discussed in Chapter 3 (3.3.1).



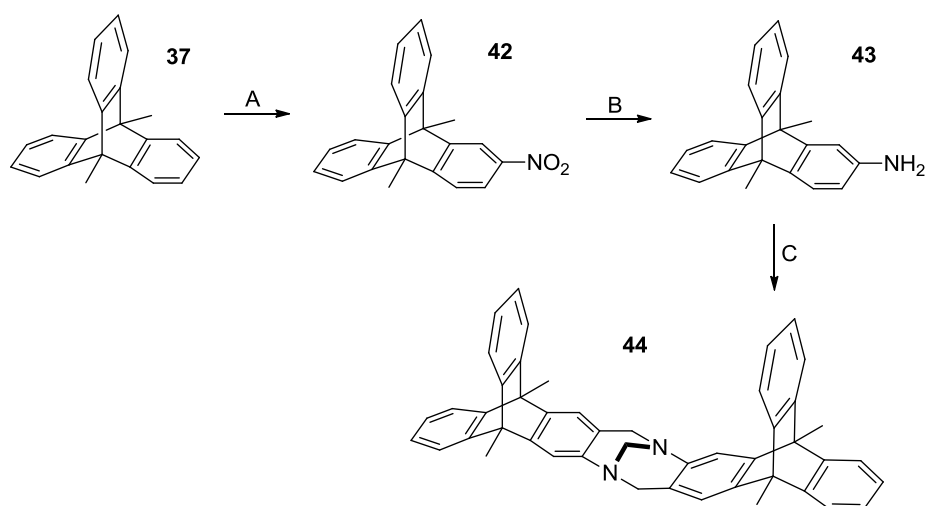
Scheme 36: The preparation of 2,6(7)-diamino-9,10-dimethyltritycene (**39**). *Reagents and conditions:* A. KNO₃, trifluoroacetic anhydride, DCM, CH₃CN, 50 °C, 48 hours. B. hydrazine monohydrate, Raney nickel, THF, 60 °C, N₂, 16 hours.

The triaminotriptycene monomer (compound **41**), required for network polymer formation was produced by the nitration of compound **37** and subsequent reduction of compound **40** (Scheme 37). The polymerisation of this compound is described in Chapter 3 (3.3.3).



Scheme 37: The preparation of 2,6(7),14-triamino-9,10-dimethyltritycene (**41**). *Reagents and conditions:* A. HNO_3 , H_2SO_4 , $80\text{ }^\circ\text{C}$, 40 hours. B. hydrazine monohydrate, Raney nickel, THF, $60\text{ }^\circ\text{C}$, N_2 , 16 hours.

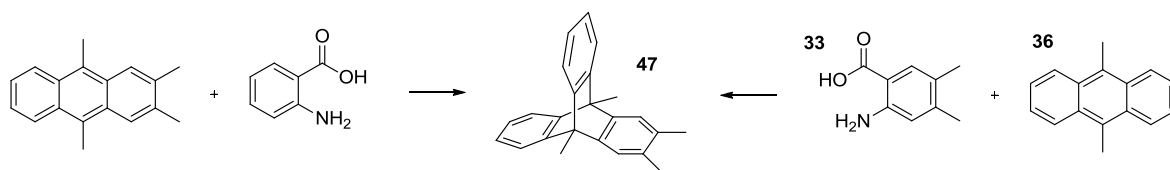
To allow for greater understanding of the structure and properties of the TB polymers built around the 9,10-dimethyltritycene unit, the related compound **44** was also prepared. This involved the synthesis of compound **43**, which was synthesised from the nitration and subsequent reduction of compound **37** (Scheme 38). The model compound was then formed by the typical TB reaction, producing compound **44** in good yield. Unfortunately, crystals could not be grown for this compound, preventing analysis by single-crystal X-ray diffraction.



Scheme 38: The preparation of the TB 9,10-dimethyltritycene model compound (**44**). *Reagents and conditions:* A. KNO_3 , trifluoroacetic anhydride, CH_3CN , DCM, $50\text{ }^\circ\text{C}$, 16 hours. B. hydrazine monohydrate, Raney nickel, THF, N_2 , $60\text{ }^\circ\text{C}$, 16 hours. C. Dimethoxymethane, TFA, $0\text{ }^\circ\text{C}$, 48 hours.

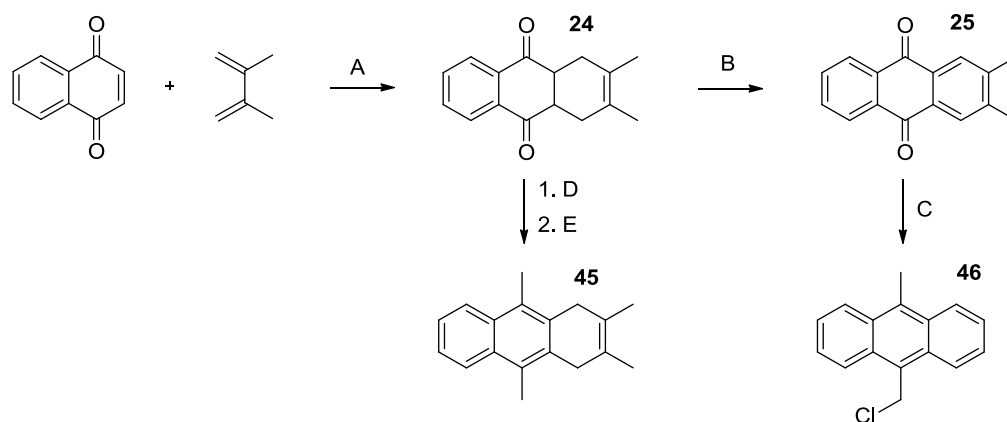
The final member in this series of methyl substituted triptycenes to be synthesised was compound **47**, possessing both bridgehead and ring methyl substituents, which it was hoped would enhance the properties of the corresponding polymers, whilst blocking the substituted ring from being nitrated. The synthesis of this triptycene required either the synthesis of 2,3,9,10-tetramethylantracene, which could then be reacted with 2-aminobenzoic acid, or a reaction between compounds **36** and **33** (Scheme 39). Once again,

both options were considered, with the synthesis via 2,3,9,10-tetramethylantracene originally deemed a faster route to the desired compound.



Scheme 39: The two proposed routes to 2,3,9,10-tetramethyriptycene (**47**).

The preparation of 2,3,9,10-tetramethylantracene (Scheme 40) started with the synthesis of compound **24** from 2,3-dimethyl-1,3-butadiene and α -naphthoquinone, which has been previously described (Scheme 28). At this stage two options existed, either to induce aromaticity in the second ring system before performing a Grignard reaction to replace the ketones with methyl groups, or to perform the Grignard reaction before inducing aromaticity. The former option was the first to be attempted, with the reaction between compound **24** and methylmagnesium bromide in THF¹⁵⁴, which gave compound **45** in poor yield (20%). After repeated failed attempts to improve the yield, this route was discarded, since a large quantity of 2,3,9,10-tetramethylantracene was required for subsequent steps.



Scheme 40: The attempted synthesis of 2,3,9,10-tetramethylantracene. *Reagents and conditions:* A. MeOH, 70 °C, 16 hours. B. EtOH, KOH, H₂O, room temperature, 72 hours. C. MeMgBr, THF, 0 °C, 16 hours. D. MeMgBr, THF, 0 °C, 16 hours. E. Glacial acetic acid, MeOH.

A new route began with the conversion of compound **24** to compound **25** using the procedure previously detailed (Scheme 28). The subsequent Grignard reaction of compound **25** with methylmagnesium bromide in THF¹⁵⁵ did not give 2,3,9,10-tetramethylantracene as expected, but instead gave compound **46** in moderate yield

(50%). This could be explained by occurrence of a competitive reaction outlined in Figure 21.

After the double attack of the Grignard reagent, the reaction was quenched with concentrated hydrochloric acid. One water molecule is lost immediately to form a stable carbocation. The elimination of the second water molecule leads to the formation of a conjugated double bond which contributes to the delocalization of the positive charge, forming the stable benz[*a*]anthracene carbocation, which is attacked by the chloride anion, present due to the acidic work up, which forms compound **46**.

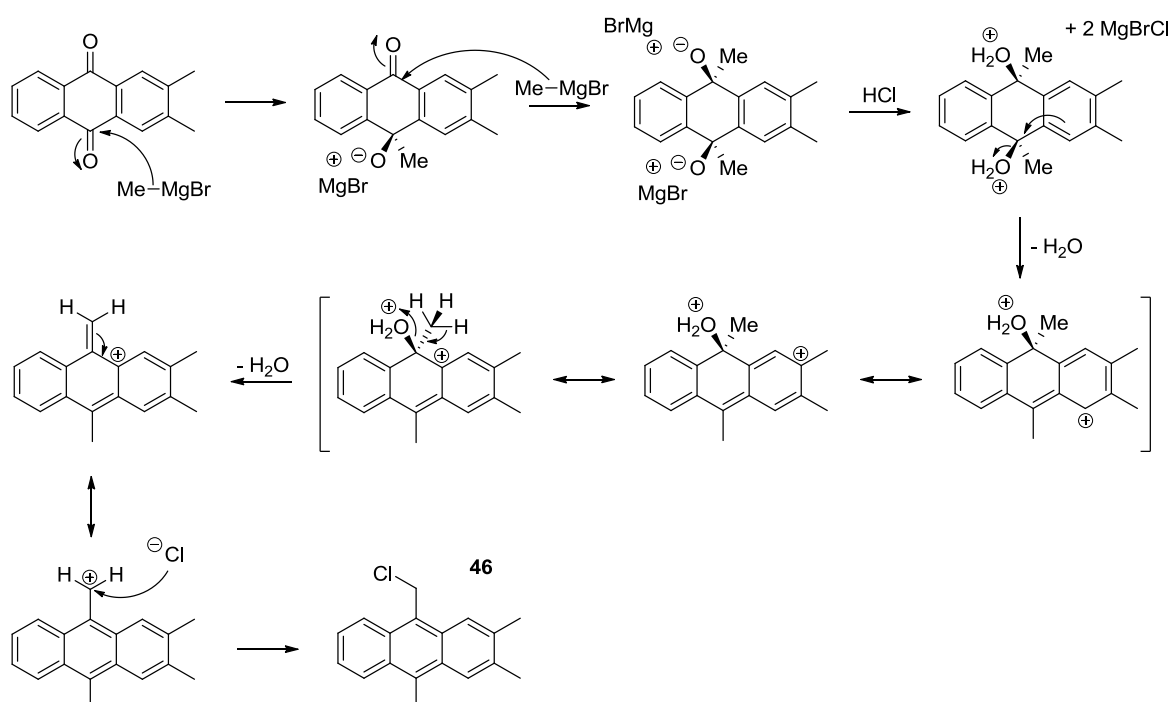
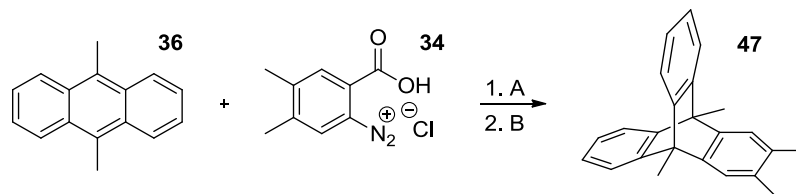


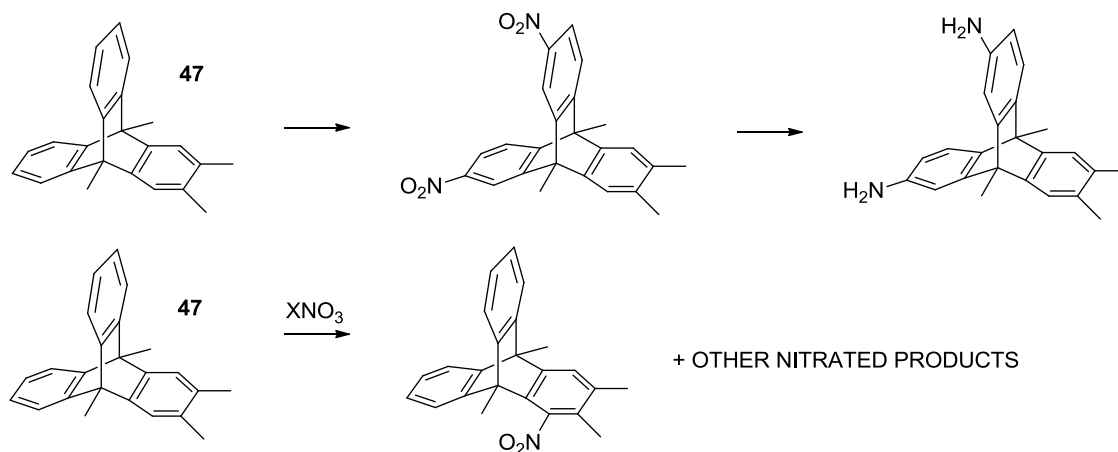
Figure 21: The mechanism for the formation of 2,3,9-trimethyl-10-chloromethylantracene (**46**).

Finally, the synthesis of compound **47** using the Diels-Alder reaction between compounds **36** and the benzyne generated from diazonium salt **34** was attempted (Scheme 41). The synthesis of these two starting materials has been previously discussed (Schemes 32 and 35). This reaction gave compound **47** in high yield (84%), which was achieved due to the optimised reaction conditions used and the beneficial effect of the methyl substituents on the central ring.



Scheme 41: The Diels-Alder reaction for the preparation of 2,3,9,10-tetramethyltritycene (**47**). *Reagents and conditions:* A. DCE, 1,2-epoxypropane, 85 °C, 40 hours. B. Maleic anhydride, o-xylene, 110 °C, 1 hour.

Following the successful synthesis of compound **47** attempts were made to synthesise 6(7),14-diamino-2,3,9,10-dimethyltritycene, which involved the synthesis of 6(7),14-dinitro-2,3,9,10-dimethyltritycene (Scheme 42). Various conditions for the nitration of compound **47**, using potassium nitrate or nitric acid were attempted, but each time a mixture of products was obtained. This mixture proved impossible to separate by column chromatography, but ^1H NMR analysis suggested that nitration had occurred unexpectedly on the ring with the two methyl substituents, similar to what had occurred during the nitration of 2,3-dimethyltritycene. Unfortunately, this meant that no further progress could be made on the synthesis of 6(7),14-diamino-2,3,9,10-dimethyltritycene monomer as the desired product could not be isolated.



Scheme 42: The proposed route to 6(7),14-diamino-2,3,9,10-dimethyltritycene, highlighting the problem encountered during the reaction. X = K or H.

This work concluded the synthesis of methyl substituted triptycene monomers, which despite all three target compounds being successfully synthesised, sufficient quantity of monomers for the preparation of ladder and network polymers could only be created from compound **37**.

2.6 Crown ether chemistry

Another potentially useful building block for TB PIM synthesis that was identified was the dibenzo-18-crown-6 compound (Figure 22). This compound possesses a flexible ring system between its two phenyl rings, and as a consequence the resulting polymer was expected to display low microporosity, as the polymer chains would be too flexible to avoid packing space efficiently. However, it was also hoped that the six oxygen atoms contained within the crown ether ring system would aid affinity of the polymer towards carbon dioxide so the compound could be interesting for incorporation into a polymer.

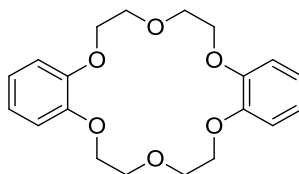
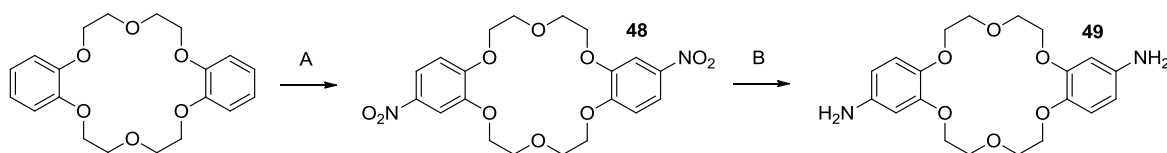


Figure 22: The structure of dibenzo-18-crown-6.

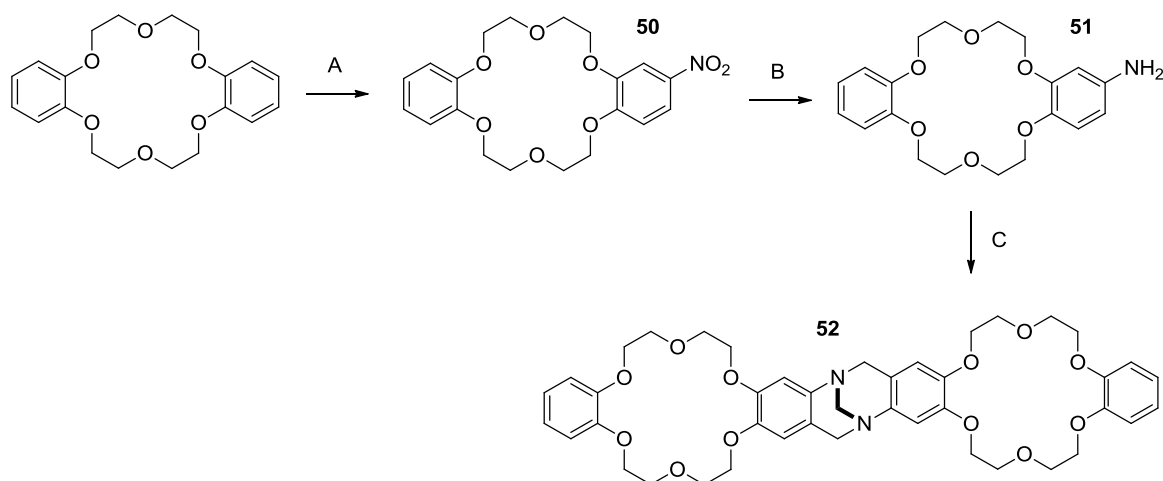
The preparation of a ladder polymer built from this unit required the synthesis of compound **49**, which involved the nitration of dibenzo-18-crown-6 (Scheme 43). The nitration reaction was performed using potassium nitrate and trifluoroacetic anhydride, which formed compound **48**, in high yield. Only two equivalents of potassium nitrate were used for the reaction indicating that the presence of the two oxygen atoms on each phenyl ring sufficiently activates it towards nitration. The reduction was performed with hydrazine monohydrate and Raney nickel, producing compound **49** in high yield. The polymerisation of this compound is covered in Chapter 3 (3.4.1).



Scheme 43: The synthesis of 2,13(14)-diaminodibenzo-18-crown-6 (**49**). *Reagents and conditions:* A. KNO_3 , trifluoroacetic anhydride, CH_3CN , 50°C , 16 hours. B. Hydrazine monohydrate, Raney nickel, EtOH , N_2 , 60°C , 16 hours.

The TB model compound **52** was synthesised by initial nitration of dibenzo-18-crown-6, and reduction of compound **50** before the TB reaction (Scheme 44). Once again the nitration was performed using potassium nitrate giving an excellent yield of compound **50**, which was then reduced using hydrazine monohydrate and Raney nickel to obtain

compound **51** in similarly excellent yield. Compound **52** was then synthesised via a TB formation reaction between compound **51** and paraformaldehyde in trifluoroacetic acid. Unfortunately, crystals could not be prepared for this compound, preventing analysis by single-crystal X-ray diffraction.



Scheme 44: The preparation of the crown-ether TB model compound (**52**). Reagents and conditions: A. KNO_3 , trifluoroacetic anhydride, CH_3CN , DCM, 50°C , 16 hours. B. Hydrazine monohydrate, Raney nickel, THF, N_2 , 60°C , 16 hours. C. Paraformaldehyde, TFA, -15°C , 16 hours.

2.7 Naphthalene chemistry

As well as synthesising new monomers suitable for TB polymerisation, several suitable commercially available compounds were investigated. One of these was 1,5-diaminonaphthalene (Figure 23), which was readily available. Despite its lack of a site of contortion and potential for π -stacking, it was hoped that the building block would prove useful for TB PIM synthesis because it was predicted that the TB unit would hinder π -stacking and provide sufficient non-linearity to enable the polymer to exhibit microporosity. The polymerisation of this compound is detailed in Chapter 3 (3.4.2).

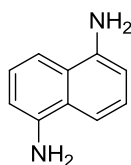
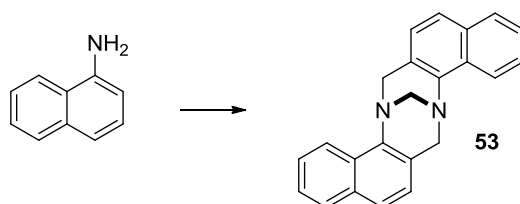


Figure 23: The structure of 1,5-diaminonaphthalene.

The model compound **53** was synthesised from a published procedure¹⁵⁶, using the starting material, 1-naphthylamine in a TB reaction with paraformaldehyde and trifluoroacetic acid (Scheme 45), giving a mixture of products that were purified by column chromatography. This gave compound **53** pure, but in relatively low yield (19%), suggesting that the TB formation reaction with 1-naphthylamine was inefficient. Crystals of compound **53** were grown and analysed by single crystal X-ray diffraction, the details and discussion of this can be found in Appendix 1 (A1.1.4).



Scheme 45: The synthesis of the TB naphthalene model compound (**53**). *Reagents and conditions:* Paraformaldehyde, TFA, -15 °C, 16 hours.

2.8 1,4-Dimethylbenzene chemistry

Another commercially available monomer identified for study was 2,5-dimethyl-1,4-phenylenediamine (Figure 24). This material was chosen for investigation due to its structure, with the monomer unit possessing two amino groups on a single phenyl ring with two para-methyl substituents, which means that the compound has a high content of nitrogen and is hindered from cross-linking during the polymerisation reaction. It was expected that the high nitrogen content would help enhance affinity for CO₂, which would be useful for gas separation applications. Discussion of the polymerisation reaction using this compound can be found in Chapter 3 (3.4.3).

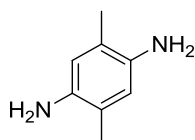
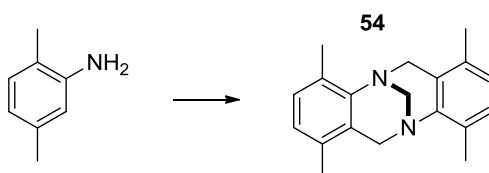


Figure 24: The structure of 2,5-dimethyl-1,4-phenylenediamine.

The TB model compound built around the 1,4-dimethylbenzene unit was synthesised to provide useful insights into the structure and properties of the corresponding ladder

polymer. The TB reaction (Scheme 46) was performed using a published procedure¹¹⁵ between commercial 2,5-dimethylaniline and paraformaldehyde in trifluoroacetic acid. This gave a mixture of products that was purified by column chromatography, from which the product was obtained pure in relatively low yield (23%), suggesting that the TB reaction with the starting material is inefficient. Crystals of compound **54** were grown and analysed by single-crystal X-ray diffraction, the details and discussion of this can be found in Appendix 1 (A1.1.5).



Scheme 46: The synthesis of the TB 1,4-dimethylbenzene model compound (**54**). *Reagents and conditions:* Paraformaldehyde, TFA, -15 °C, 16 hours.

2.9 1,4-Dimethoxybenzene chemistry

It was predicted that the presence of oxygen atoms on the monomer unit would enhanced the properties of the polymer towards the adsorption of CO₂. However, the monomer for this synthesis, compound **56** (Figure 25), was not commercially available and hence required synthesis.

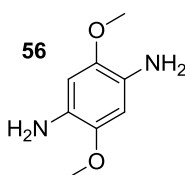
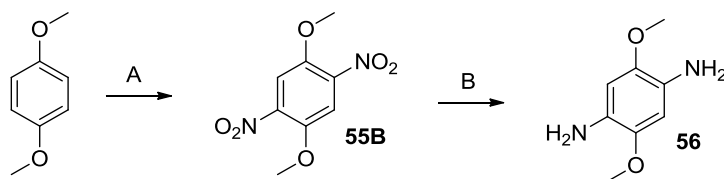


Figure 25: The structure of 2,5-dimethoxy-1,4-phenylenediamine.

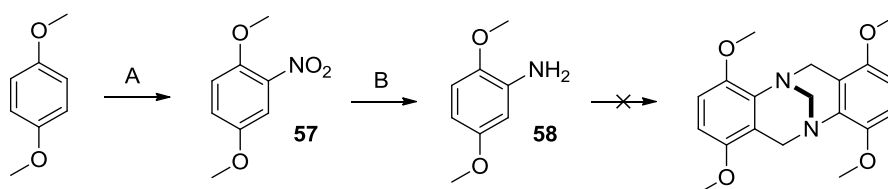
The starting point for this synthesis was 1,4-dimethoxybenzene, which was commercially available and cheap. It was assumed that this could be easily nitrated, due to the activating effect of the two methoxy substituents, before reduction to give compound **56** (Scheme 47). The first step, the nitration reaction, was performed using potassium nitrate and trifluoroacetic anhydride, but was not as simple as anticipated, due to the major product from the reaction being compound **55A** and not the desired compound **55B**. This can be

explained by the electronics of the starting material that favours the double nitration occurring on the same side of the ring¹⁵⁷. Despite the low yield of compound **55B** this reaction did prove adequate for the preparation of a sufficient quantity of the compound. The next step was the reduction of compound **55B** to give compound **56**, which was performed with hydrochloric acid and tin¹⁵⁸, this mixture creates tin chloride in situ, which is a strong reducing agent. A description of the polymerisation of compound **56** can found in Chapter 3 (3.4.4).



Scheme 47: The synthesis of 2,5-dimethoxy-1,4-phenylenediamine (**56**), showing the two products obtained from the nitration step. *Reagents and conditions:* A. KNO₃, TFAA, CH₃CN, 50 °C, 16 hours. B. HCl, Sn, EtOH, 120 °C, 16 hours.

The TB model compound based around the 1,4-dimethoxybenzene unit was wanted for investigation into the structure and properties of the related ladder polymer (Scheme 48). The first step in its synthesis was the mononitration of 1,4-dimethoxybenzene, which was achieved by the usual method with potassium nitrate. This gave compound **57** in excellent yield, due to the activating effect of the two methoxy substituents. This compound was then reduced by the usual hydrazine method, producing compound **58** in a highly efficient reaction. At this stage the synthesis encountered problems, as compound **58** did not form the desired model compound via TB reaction. Instead a mixture of products was formed, this was analysed by mass spectrometric analysis and found to be a mixture of unidentifiable low molecular weight material, without any indication that the correct product had been formed. Numerous attempts using a variety of conditions were made to generate the model compound, but each time none of the desired product was found by mass spectrometric analysis. It is believed that the starting material underwent a crosslinking reaction with the methylene precursor before the model compound could be formed, due to the activating effect of the two methoxy substituents that made the starting material too reactive under the reaction conditions. This did not happen for the TB dimer based upon 1,4-dimethylbenzene as methyl groups are much less activating than methoxy groups, since they lack the oxygen atoms that can donate electron density into the ring system. Unfortunately, this meant that the desired model compound could not be prepared.



Scheme 48: The proposed synthesis of the TB 1,4-dimethoxybenzene model compound. *Reagents and conditions:* A. KNO_3 , TFAA, CH_3CN , $50\text{ }^\circ\text{C}$, 16 hours. B. Hydrazine monohydrate, Raney nickel, EtOH, N_2 , $60\text{ }^\circ\text{C}$, 16 hours.

2.10 9,9'-Spirobisfluorene chemistry

9,9'-Spirobisfluorene (compound **59**), which consists of four benzene rings linked together by two five-membered rings (Figure 26), was identified as a potentially useful building block for PIM synthesis due to its spirocyclic site of contortion¹⁵⁹.

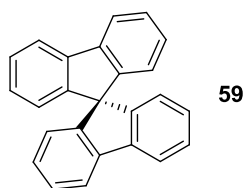
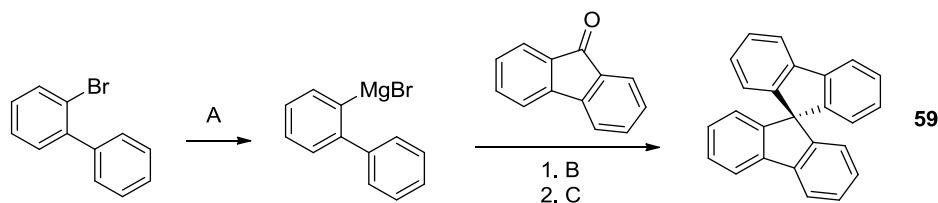


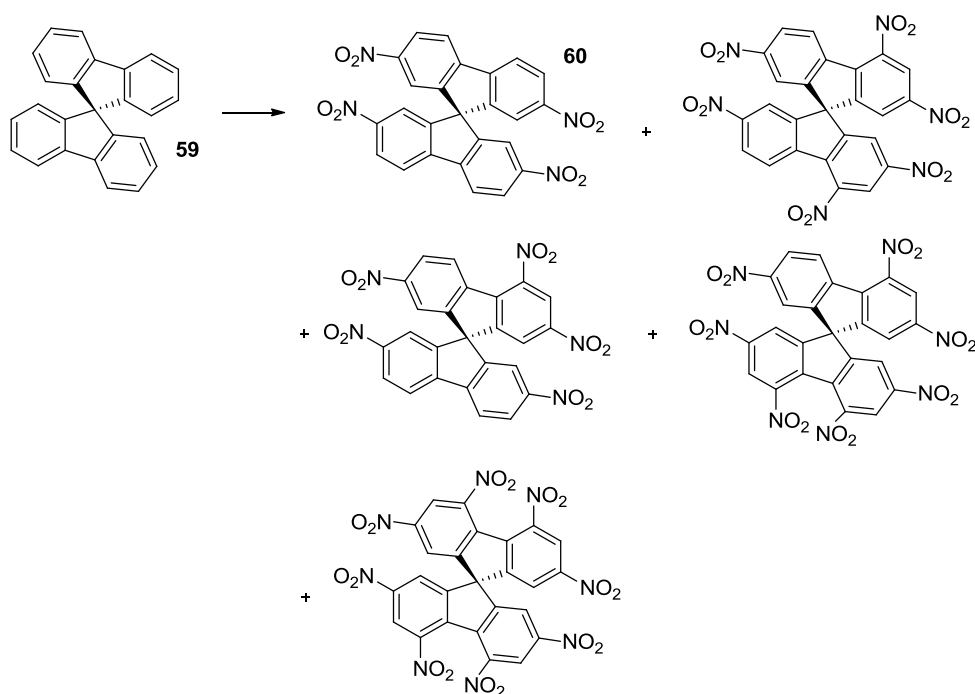
Figure 26: The structure of 9,9'-spirobisfluorene.

The synthesis of compound **59**¹⁶⁰ was achieved by a Grignard reaction between 9-fluorenone and 1,1'-biphenyl-2-magnesium bromide, which was synthesised *in-situ* from 2-bromo-1,1'-biphenyl due to its poor stability (Scheme 49). Following the addition of the Grignard reagent compound **59** was prepared by the treatment with glacial acetic acid and concentrated hydrochloric acid in good yield.



Scheme 49: The synthesis of 9,9'-spirobisfluorene (**59**). *Reagents and conditions:* A. Mg, THF, I_2 , N_2 , $85\text{ }^\circ\text{C}$, 1.5 hours. B. THF, $70\text{ }^\circ\text{C}$, 16 hours. C. AcOH, HCl, $120\text{ }^\circ\text{C}$, 2 hours.

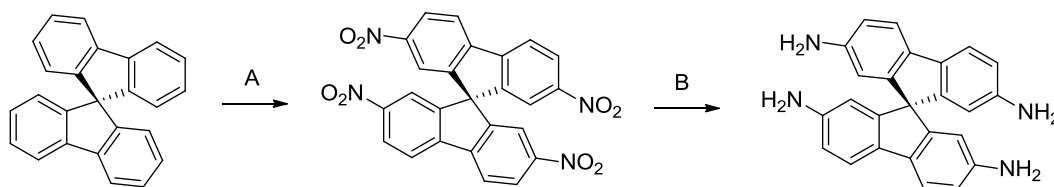
The synthesis of a ladder polymer based around this unit was avoided because of the activated nature of the biphenyl units of the spirobisfluorene which were anticipated to promote cross-linking. Instead, it was reasoned that the preparation of a network polymer based around the tetraamine **59** would prove simpler. In order to prepare the network polymer, compound **59** was tetra-nitrated to give compound **60**, which was reduced to give the monomer, compound **61** (Scheme 51). The nitration reaction was performed with a procedure found in literature¹⁶¹, using fuming nitric acid. However, after several failed reactions using the literature procedure it became clear that fuming nitric acid was too powerful a nitrating reagent at 0 °C as ¹H NMR and mass spectrometric analysis indicated that the nitration had occurred more than the desired four times required (Scheme 50).



Scheme 50: The multi-nitration of 9,9'-spirobisfluorene (**59**). *Reagents and conditions:* Fuming HNO₃, 0 °C, 1 hour.

After numerous attempts of the reaction the solution to this problem was found to be performing the reaction at a reduced temperature of -45 °C. This caused the nitration reaction to slow to a speed that could be monitored and hence the reaction was quenched once the product had formed, but before it became over-nitrated. This did not give the product pure, but the impurities were found to be soluble in a hot 1:1 mixture of THF and hexane, whilst the product remained insoluble. Using this modified procedure compound **60** was successfully isolated in good yield. This compound was then reduced via the

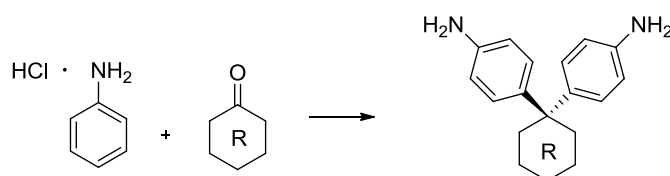
hydrochloric acid and tin method, which produced compound **61** in good yield. The polymerisation of compound **61** is detailed in Chapter 3 (3.4.5).



Scheme 51: The synthesis of 2,2',7,7'-tetraamino-9,9'-spirobisfluorene (**61**). *Reagents and conditions:* A. Fuming HNO₃, -45 °C, 20 minutes. B. HCl, Sn, 140 °C, 16 hours.

2.11 Bis-aniline chemistry

In an effort to prepare suitable yet simple monomers for TB polymerisation a series of related compounds were prepared using a simple HCl-catalysed condensation reaction between a ketone and either aniline¹⁶² or 2-methylaniline¹⁶³, which are cheap and readily available starting materials. The resulting products contain two amino substituted benzene rings linked together by a pendant group, making them ideal for use in the preparation of ladder polymers (Scheme 52). However, these monomers lack the fused ring skeleton normally used for the synthesis of PIMs, but possess a bulky pendant group that might hinder the efficient packing of the ladder polymers and result in microporosity. This type of compound has been previously used for the synthesis of high molecular weight and highly soluble polyimides, which was a direct consequence of the presence of bulky substituents¹⁶⁴.



Scheme 52: The preparation of the bis-aniline monomers. R = any alkyl ring system.

This condensation reaction between the aniline and ketone is carried out at high temperature, which is sufficient to melt all of the starting materials thus eliminating the need for a solvent. To avoid degradation of the bis-aniline product once formed, which could occur at the high temperature used, the reaction was performed under a nitrogen

atmosphere. This reaction is unusual since normally an amine would be expected to perform a nucleophilic attack upon a ketone, but the formation of a stable salt from reaction between the amine and hydrochloric acid prevents this from happening. The reaction proceeds with protonation of the ketone, which activates it towards attack by the electron rich phenyl ring. Aromaticity is then restored to the ring system by removal of a proton by a molecule of water or chlorine ion. This process repeats with another molecule of aniline and the loss of water to give the hydrochloride salt of the product, which when treated with aqueous ammonia gives the desired bis-aniline product (Figure 27).

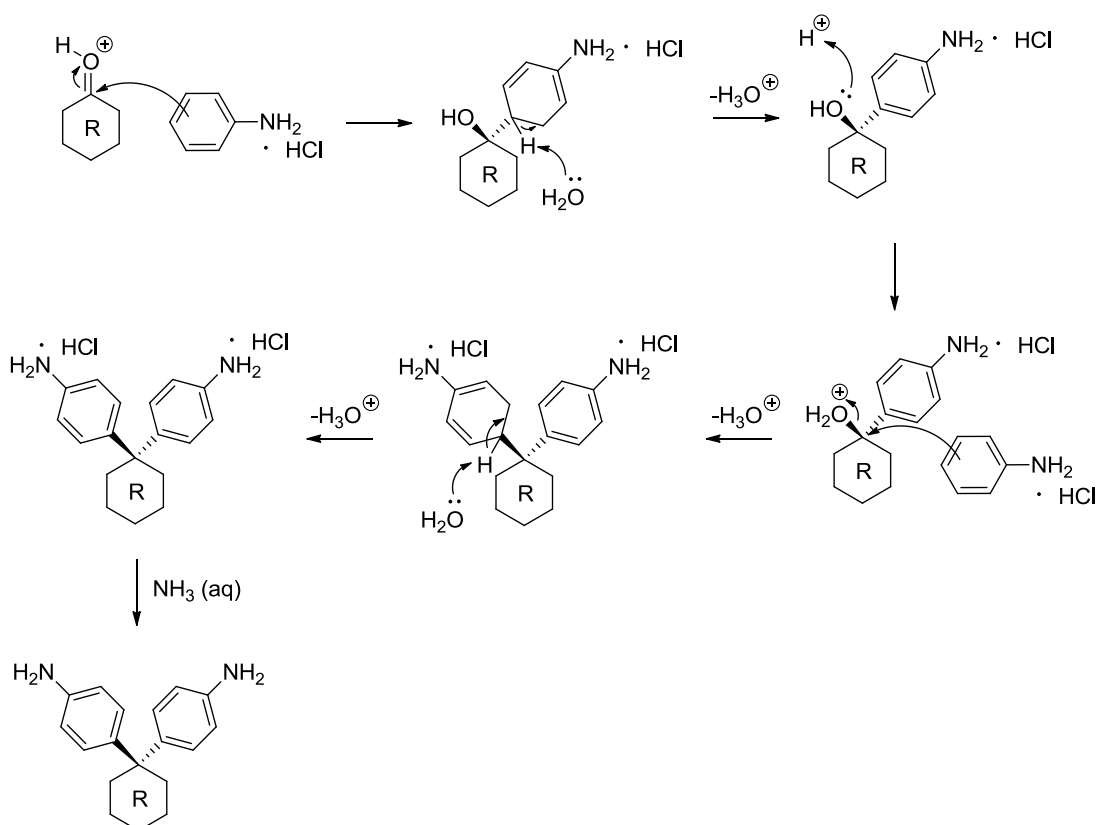
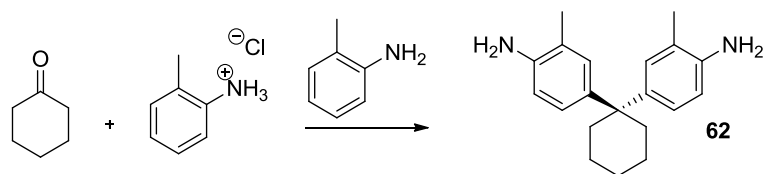


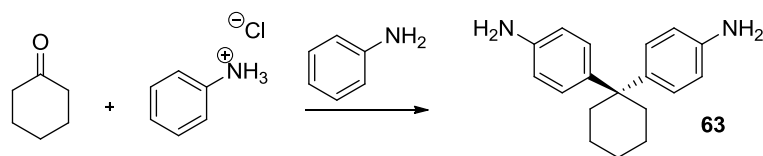
Figure 27: The mechanism of bis-aniline formation.

The first of this series to be prepared was obtained from cyclohexanone and 2-methylaniline hydrochloride in 2-methylaniline (Scheme 53). After treatment with aqueous ammonia the reaction gave a mixture of product, unreacted starting material and 2-methylaniline. Final purification was achieved by column chromatography, which gave compound **62** in good yield (70%). The polymerisation of this compound is discussed in Chapter 3 (3.5.1). Crystals of compound **62** were grown and analysed by single-crystal X-ray diffraction, details and discussion of this can be found in Appendix 1 (A1.2.1).



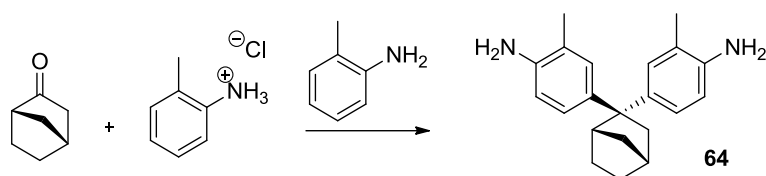
Scheme 53: The synthesis of 2,2-bis(3-methyl-4-aminophenyl)cyclohexane (**62**). *Reagents and conditions:* 150 °C, N₂, 20 hours.

The analogous bis-aniline **63** was prepared from the condensation between cyclohexanone and aniline hydrochloride in aniline (Scheme 54). After purification, compound **63** was obtained in moderate yield (49%). The difference in yield between the two analogous bis-anilines was significant and suggests that the presence of the methyl substituent on the phenyl ring improves the reaction yield by donating electron density into the ring system. A discussion of the polymerisation reaction using compound **63** can be found in Chapter 3 (3.5.1). Crystals of this compound could not be prepared, preventing analysis by single-crystal X-ray diffraction.



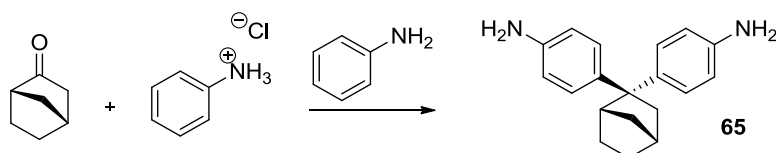
Scheme 54: The preparation of 2,2-bis(4-aminophenyl)cyclohexane (**63**). *Reagents and conditions:* 150 °C, N₂, 20 hours.

In order to investigate the effect of a bulkier pendant group on the properties of the final polymer compound **64** was synthesised from the condensation between norcamphor and 2-methylaniline hydrochloride in 2-methylaniline (Scheme 55) in poor yield (25%), which suggested that this ketone was not as good a starting material for this reaction as cyclohexanone, perhaps due to its bulkier nature. Discussion of the polymerisation reaction using this monomer can be found in Chapter 3 (3.5.1). Crystals of compound **64** were grown and analysed by single-crystal X-ray diffraction, discussion of this can be found in Appendix 1 (A1.2.2).



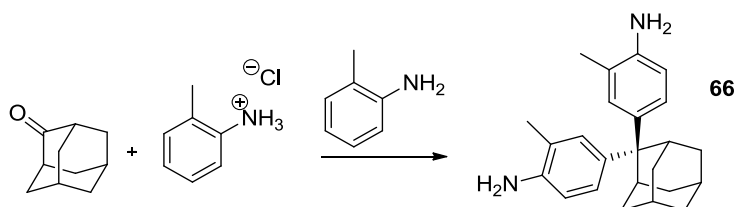
Scheme 55: The synthesis of 2,2-bis(3-methyl-4-aminophenyl)bicyclo[2.2.1]heptane (**64**). *Reagents and conditions:* 150 °C, N₂, 20 hours.

The analogous bis-aniline compound **65** was prepared in low yield (17%) from the condensation between norcamphor and aniline hydrochloride in aniline (Scheme 56). The subsequent polymerisation of this monomer is covered in Chapter 3 (3.5.1). Crystals of compound **65** were grown and resolved by single-crystal X-ray diffraction; details of this can be found in Appendix 1 (A1.2.3).



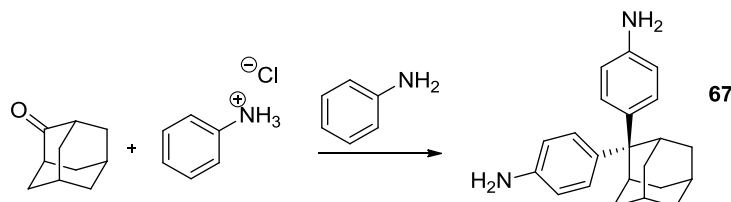
Scheme 56: The synthesis of 2,2-bis(4-aminophenyl)bicyclo[2.2.1]heptane (**65**). *Reagents and conditions:* 170 °C, N₂, 18 hours.

To further investigate the effect of using bulky pendant groups, compound **66** was synthesised in low yield (34%) from the condensation between 2-adamantanone and 2-methylaniline in 2-methylaniline (Scheme 57). This low yield suggests that the bulky nature of the ketone does have some effect on the yield of the reaction. A discussion of the TB polymerisation using compound **66** can be found in Chapter 3 (3.5.1). Crystals of this compound were grown and analysed by single-crystal X-ray diffraction, the discussion of this can be found in Appendix 1 (A1.2.4).



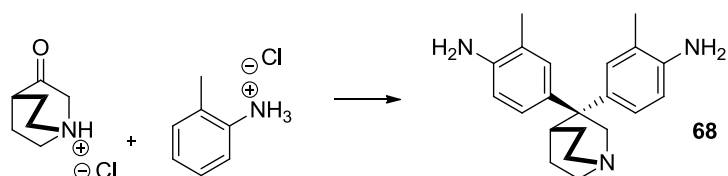
Scheme 57: The preparation of 2,2-bis(3-methyl-4-aminophenyl)adamantane (**66**). *Reagents and conditions:* 180 °C, N₂, 20 hours.

The analogous compound to compound **66** was prepared from the condensation between 2-adamantanone and aniline hydrochloride in aniline with low yield of 31% achieved (Scheme 58). The polymerisation of compound **67** is described in Chapter 3 (3.5.1). Crystals of this compound were grown and resolved by single crystal X-ray diffraction, the discussion of which can be found in Appendix 1 (A1.2.5).



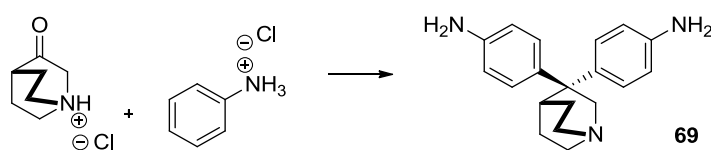
Scheme 58: The preparation of 2,2-bis(4-aminophenyl)adamantane (**67**). *Reagents and conditions:* 180 °C, N₂, 40 hours.

The bis-aniline with 3-quinuclidone as a pendant group, but lacking methyl substituents, has previously been used for the preparation of high molecular weight, highly soluble, thermally stable and highly basic polymers that were capable of forming robust membranes¹⁶⁵. Therefore, it was of interest to use this monomer for the generation of a TB polymer. Towards this goal the first bis-aniline featuring this pendant group was synthesised from the condensation between 3-quinuclidone and 2-methylaniline hydrochloride (Scheme 59). However, 3-quinuclidone is not stable under ambient conditions, so was purchased as a hydrochloride salt, which was treated with aqueous ammonia to give the free base. Isolation of the product from this reaction proved difficult. The solution to this problem was the distillation of the unreacted starting materials from the mixture, as the bis-aniline product had a substantially higher boiling point. Unfortunately, 2-methylaniline also has a high boiling point, even under reduced pressure, which meant that high temperature (180 – 220 °C) was needed for the distillation, which may have degraded the bis-aniline product, but spectrometric analysis showed that the product was pure, despite its dark colour that suggested degradation. Using this technique compound **68** was obtained in good yield (67%). The TB polymerisation reaction of this monomer is described in Chapter 3 (3.5.1). Unfortunately, crystal growth proved unsuccessful for compound **68**, preventing analysis by single-crystal X-ray diffraction.



Scheme 59: The production of 3,3-bis(3-methyl-4-aminophenyl)-1-azabicyclo[2,2,2]octane (**68**). *Reagents and conditions:* A. Aqueous NH_3 , H_2O , 1 minute. B. $170\text{ }^\circ\text{C}$, N_2 , 72 hours.

The bis-aniline monomer from the paper was also synthesised, from the condensation reaction between 3-quinuclidone and aniline hydrochloride (Scheme 60). Compound **69** was isolated by purification via distillation, and recovered in good yield.



Scheme 60: The production of 3,3-bis(4-aminophenyl)-1-azabicyclo[2,2,2]octane (**69**). *Reagents and conditions:* $170\text{ }^\circ\text{C}$, N_2 , 24 hours.

1,4-Bis(2-hydroxyisopropyl)benzene (Figure 28) is a cheap and commercially available compound that differs from the other bis-aniline starting materials as it possesses two hydroxyl groups rather than ketone functionality. This compound is very flexible and lacks both a site of contortion and any hindrance to flexibility, such as a fused ring skeleton, so it was predicted that the resulting polymer would show little or no microporosity. However, the analogous bis-aniline monomer without methyl substituents has previously been used for the production of highly soluble and high molecular weight polyimides suitable for robust film formation¹⁶⁶, making it an ideal candidate for TB polymerisation.

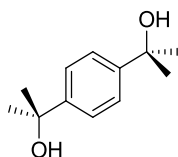
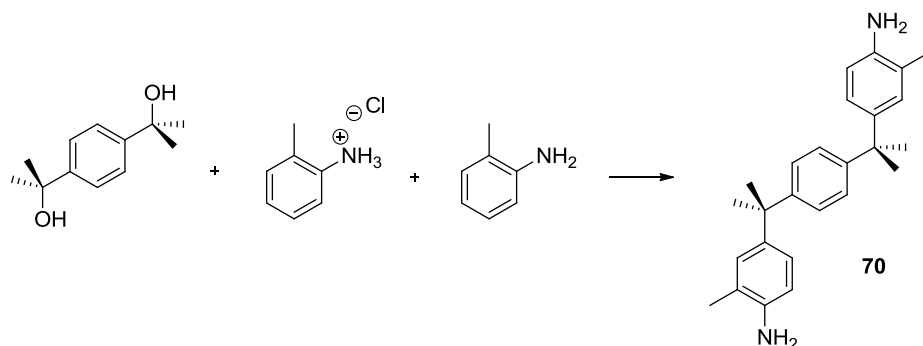


Figure 28: The structure of 1,4-bis(2-hydroxyisopropyl)benzene.

The condensation between 1,4-bis(2-hydroxyisopropyl)benzene and 2-methylaniline hydrochloride in 2-methylaniline (Scheme 61) produced compound **70**, which was obtained in good yield (76%). This reaction clearly showed that diol based starting materials work efficiently in the production of bis-aniline monomer using the condensation

reaction. The polymerisation reaction using this monomer is described in Chapter 3 (3.5.1). Crystals of this compound were grown and resolved by single-crystal X-ray diffraction, the description and discussion of this can be found in Appendix 1 (A1.2.6).



Scheme 61: The preparation of 1,1',4,4'-tetramethyl-1,4-(3-methyl-4-aminophenyl)benzene (**70**). *Reagents and conditions:* 170 °C, N₂, 72 hours.

Another compound that was identified as a potentially useful pendant group for bis-aniline synthesis and polymerisation was 9-fluorenone (Figure 29). This compound offered the opportunity to include useful substituents, such as bromine atoms or methyl groups, into the bis-aniline monomer and resulting polymer. Furthermore, it was anticipated that the bulky nature of the compound would hinder flexibility and encourage inefficient packing of the final polymer, ensuring microporosity. Finally, this compound was commercially available and inexpensive, which helped to simplify the bis-aniline monomer synthesis.

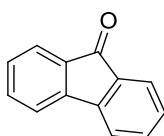
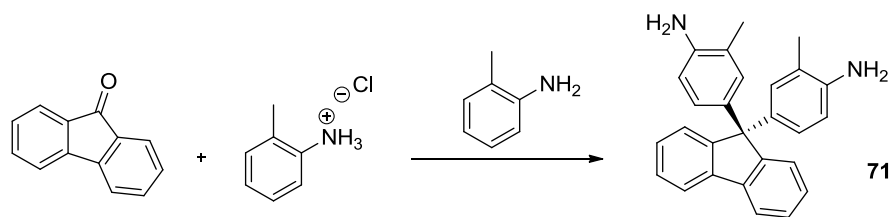


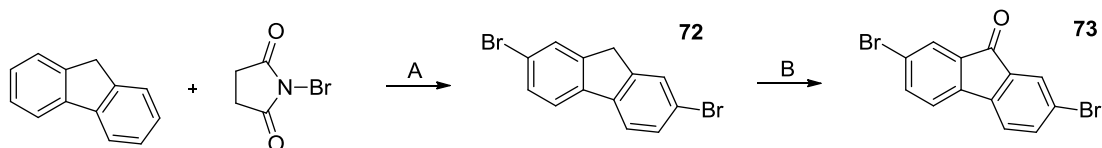
Figure 29: The structure of 9-fluorenone.

The reaction between 9-fluorenone and 2-methylaniline hydrochloride (Scheme 62) produced compound **71** in good yield. The polymerisation of compound **71** is detailed in Chapter 3 (3.5.1). Crystals of this monomer were grown and analysed by single-crystal X-ray diffraction, the discussion of this can be found in Appendix 1 (A1.2.7).



Scheme 62: The synthesis of 9,9'-(3-methyl-4-aminophenyl)-fluorene (**71**). *Reagents and conditions:* 170 °C, N₂, 48 hours.

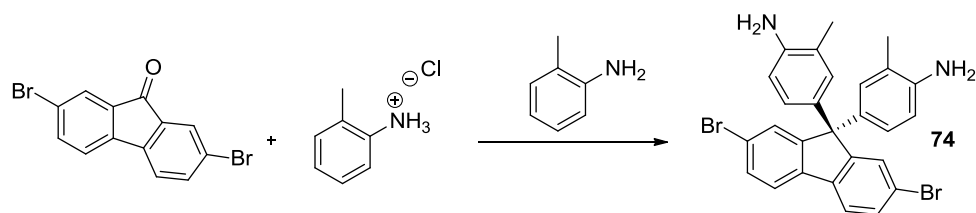
Bromine substitution in the pendant group of compound **71** was expected to enhance the properties of the polymer towards gas separation, if a membrane could be successfully prepared. A simple method¹⁶⁷ for preparing the precursor 5,7-dibromofluorenone (compound **73**) was researched and used (Scheme 63).



Scheme 63: The preparation of 2,7-dibromo-9-fluorenone (**73**). *Reagents and conditions:* A. Propylene carbonate, 245 °C, 4 hours. B. CrO₃, acetic anhydride, 0 °C, 7 hours.

The bromination between fluorenone and *n*-bromosuccinimide was performed in propylene carbonate, which is a useful polar and aprotic solvent for such reactions. *N*-bromosuccinimide was used as the bromine source to enable fine control over the stoichiometry of the reaction. This produced compound **72** in modest yield, which was then oxidised with chromium trioxide, a powerful oxidising reagent¹⁶⁸. To control the exothermic reaction an initial temperature of 0 °C was used. After purification compound **73** was obtained in high yield.

The preparation of the bis-aniline monomer was then achieved by the condensation reaction between compound **73** and 2-methylaniline hydrochloride in 2-methylaniline (Scheme 64), after purification the product, compound **74**, was isolated in high yield. The synthesis of the TB polymer from this monomer is discussed in Chapter 3 (3.5.1). This compound proved suitable for the growth of crystals, which were analysed by single-crystal X-ray diffraction, the discussion of this can be found in Appendix 1 (A1.2.8).



Scheme 64: The preparation of 2,7-dibromo-9,9'-(3-methyl-4-aminophenyl)-fluorene (**74**). Reagents and conditions: 170 °C, N₂, 48 hours.

Even after substantial research into the synthesis of the methyl substituted bis-aniline analogue no simple method for its synthesis was found, so rather than attempt a potentially time consuming synthesis the idea was scrapped. This concludes the synthesis of the bis-aniline monomers.

2.12 Coumaron chemistry

The coumaron unit (Figure 30) was identified as a potentially useful building block for PIMs, due to the rigidity imposed by its unique structure. The unit consists of a central fused ring component, featuring two phenyl rings linked together by two fused five-membered heterocyclic rings, and two axial phenyl rings. The four benzene rings contained in the structure offer significant synthetic freedom, allowing the design and preparation of a wide range of compounds based on the structure.

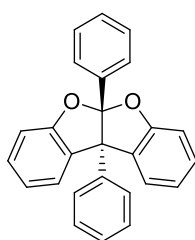
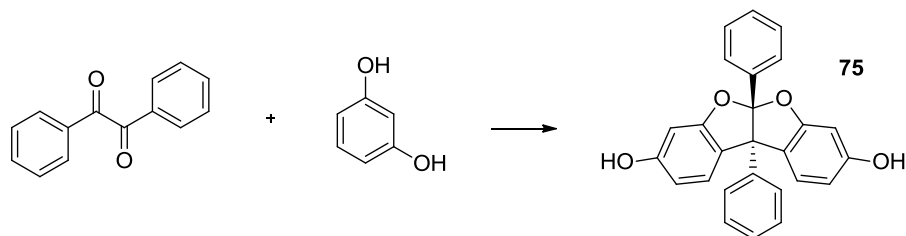


Figure 30: The coumaron building block.

The coumaron structure was first synthesised in 1941 when Joseph Niederal and Richard Nagel performed a condensation reaction between resorcinol (1,3-dihydroxybenzene) and benzil from which they isolated a compound with molecular formula C₂₆H₁₈O₄. They gave this compound the incorrect name 2,8-dihydroxy-4b,9b-diphenylcoumarano-3',2',2,3-coumaron but did not solve its structure¹⁶⁹. The structure was not correctly assigned until 1968 when J. C. McGowan and co-workers used NMR analysis to show that the

condensation reaction between resorcinol and benzil in a mixture of acetic acid and sulphuric acid gave 3,8-dihydroxy-5a,10b-diphenylcoumarano-2',3',2,3-coumaron¹⁷⁰ (compound **75**, Scheme 65). Since that time little investigation has been performed on this interesting structural unit.



Scheme 65: McGowan's procedure for the preparation of 3,8-dihydroxy-5a,10b -diphenylcoumarano-2',3',2,3-coumaron. *Reagents and conditions:* Acetic acid, H₂SO₄, 0 °C, 3 days.

Compound **75** is formed from the acid catalysed condensation reaction between resorcinol and benzil (Figure 31). The mechanism for the formation of this compound is not known, but a potential mechanism is shown below.

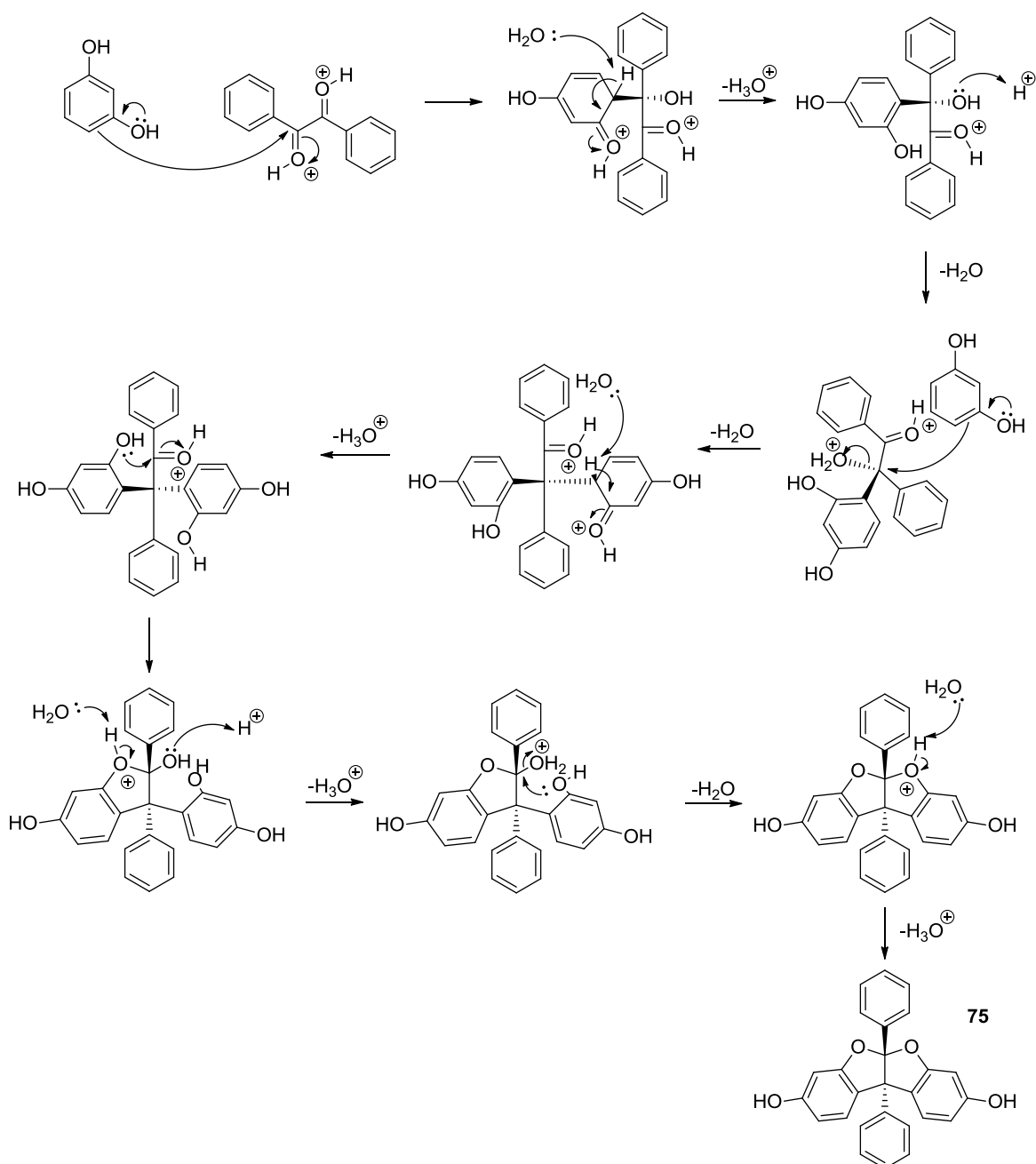


Figure 31: The mechanism of formation for 3,8-dihydroxy-5a,10b -diphenylcoumarano-2',3',2,3-coumaron (**75**).

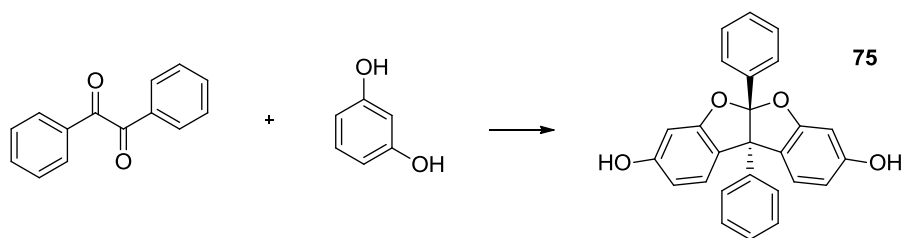
The procedure for the coumaron condensation reaction between resorcinol and benzil detailed by McGowan in his paper gave a product yield of 30%. This reaction used a mixture of acetic acid (95%) and concentrated sulphuric acid (5%) to catalyse the process, which was carried out at room temperature for 120 hours. After performing this reaction it was noticed that compound **75** could be isolated by boiling the reaction mixture in chloroform, within which the unreacted starting materials were soluble, but the product was not. This procedure gave a meagre yield despite its long reaction time, which is why

work started with improving the process until a much higher yield was obtained. The optimisation of this reaction was performed by varying the reaction parameters, temperature, duration, ratio of reactants and acid catalyst, and assessing how these affected the yield (Table 4).

Acid/Solvent mixture	Temperature	Duration (hours)	Ratio	Yield
95% Acetic acid, 5% Sulphuric acid	Room	120	2:1	30%
95% Acetic acid, 5% Trifluoroacetic acid	Room	168	2:1	< 5%
95% Acetic acid, 5% Hydrochloric acid	Room	72	2:1	30%
95% Acetic acid, 5% Sulphuric acid	60 °C	120	2:1	40%
95% Acetic acid, 5% Trifluoroacetic acid	60 °C	120	2:1	9%
95% Acetic acid, 5% Hydrochloric acid	60 °C	72	2:1	68%
95% Acetic acid, 5% Methanesulphonic acid	60 °C	72	2:1	47%
66% Chloroform, 17% Acetic acid, 17% Hydrochloric acid	60 °C	48	2:1	75%
66% Chloroform, 17% Acetic acid, 17% Hydrochloric acid	60 °C	48	4:1	85%
66% Chloroform, 17% Acetic acid, 17% Sulphuric acid	60 °C	72	4:1	65%

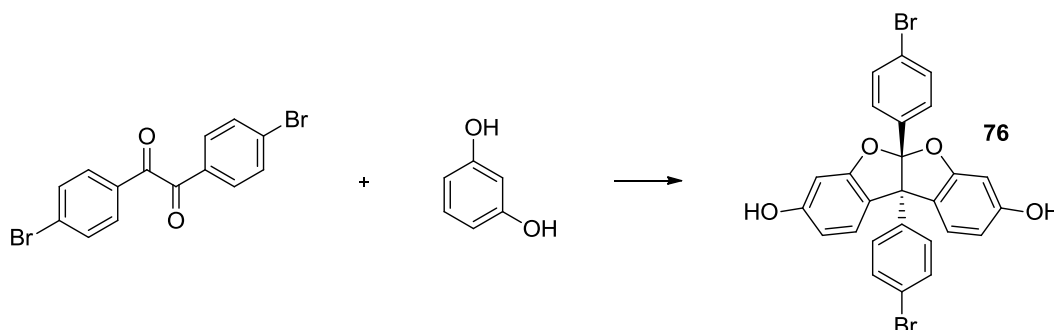
Table 4: The optimisation of the coumaron forming reaction.

The systematic variation of the conditions allowed for the optimisation of the reaction procedure, producing the desired compound **75** in much improved yield over the original procedure, 85% compared to 30%, and a significantly shorter reaction time, 48 hours compared to 120 hours (Scheme 66). Crystals of **75** were grown and analysed by single-crystal X-ray diffraction to enable better understanding of the unique coumaron structure, the discussion of this can be found in Appendix 1 (A1.3.1).



Scheme 66: The optimised procedure for the preparation of 3,8-dihydroxy-5a,10b-diphenylcoumarano-2,2',3,3'-coumaron (**75**). *Reagents and conditions:* Acetic acid, HCl, CHCl₃, 62 °C, 48 hours.

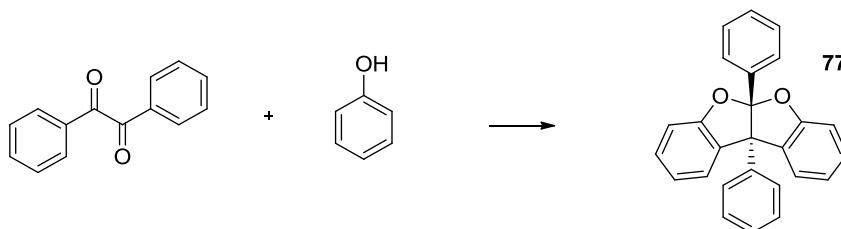
After the successful optimisation of the condensation reaction, the procedure was used for the preparation of a range of coumaron compounds. The first of these was created by the condensation between resorcinol and 4,4'-dibromobenzil (Scheme 67). This reaction gave an excellent yield of compound **76**. It was thought that this was caused by the presence of the bromine atoms on the benzil compound, which pull electron density away from the phenyl rings, resulting in the ketone carbons having less electron density and becoming slightly more positive, activating them towards nucleophilic attack by the phenyl ring of resorcinol. Crystals were also grown for compound **76** and were analysed by single-crystal X-ray diffraction, the discussion of this can be found in Appendix 1 (A1.3.2).



Scheme 67: The preparation of 3,8-dihydroxy-(4,4'-dibromo)-5a,10b-diphenylcoumarano-2,2',3,3'-coumaron (**76**). *Reagents and conditions:* Acetic acid, HCl, CHCl₃, 62 °C, 96 hours.

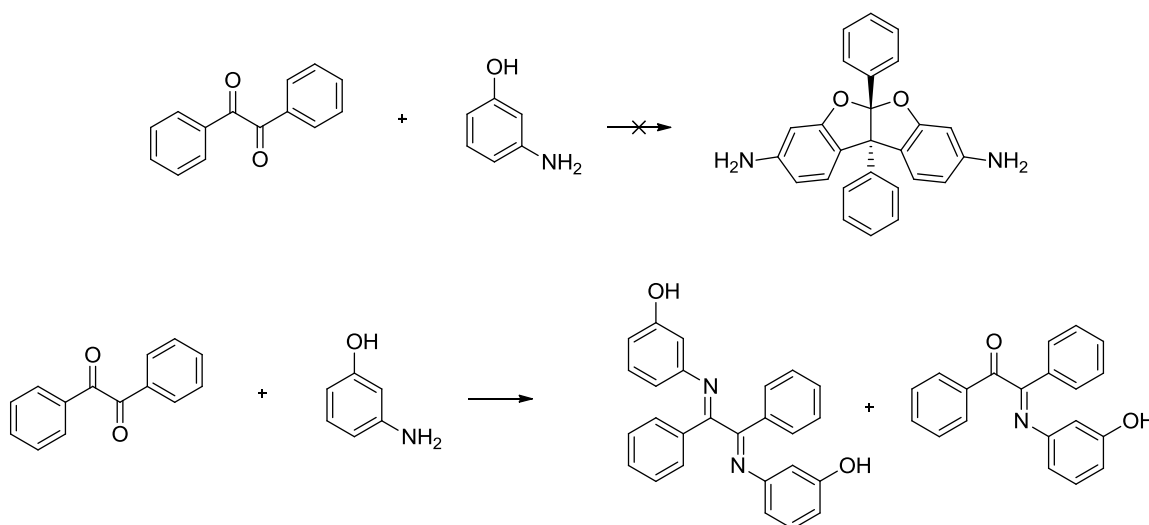
In an attempt to generate the coumaron framework without hydroxyl substituents, which would allow greater synthetic freedom in subsequent reactions, the condensation reaction was performed between phenol and benzil (Scheme 68). The reaction was successful, but unlike the previous coumarons the product proved soluble in chloroform, which meant it could not be purified in the same manner. Instead column chromatography gave the product, compound **77**, in low yield (19%); significantly lower than for the hydroxyl substituted coumarons. This difference can be explained by the lack of a second hydroxyl

group on phenol, which in resorcinol activates the phenyl ring towards nucleophilic attack on the ketone carbon of benzil by donating electron density. Clearly, phenol is a less powerful reagent for this reaction than resorcinol, but is still capable of forming the coumaron.



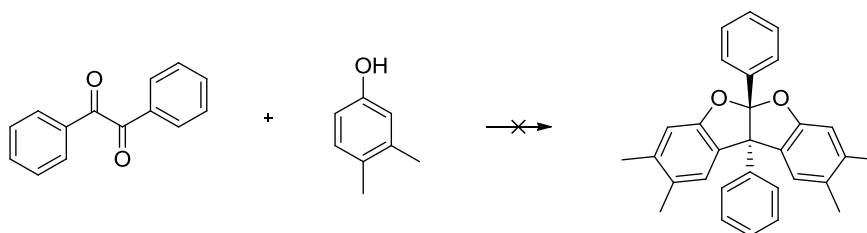
Scheme 68: The synthesis of 5a,10b-diphenylcoumarano-2,2',3,3'-coumaron (**77**). *Reagents and conditions:* Acetic acid, HCl, CHCl₃, 62 °C, 48 hours.

Another potentially useful coumaron-based compound that was identified was 3,8-diamino-5a,10b-diphenylcoumarano-2',3',2,3-coumaron, which was a suitable monomer for TB polymerisation and it was thought could be formed from the condensation reaction between 3-aminophenol and benzil (Scheme 69). This reaction was performed several times and none of the desired product could be extracted from the complex product mixture, but mass spectrometric analysis suggested that it had been formed. It is thought that instead of forming the desired product the amino group of 3-aminophenol attacked the ketone carbon to form an imine, in a typical competitive nucleophilic substitution reaction. Mass spectrometric analysis indicated the presence of two imines compounds, which gave evidence towards this theory.



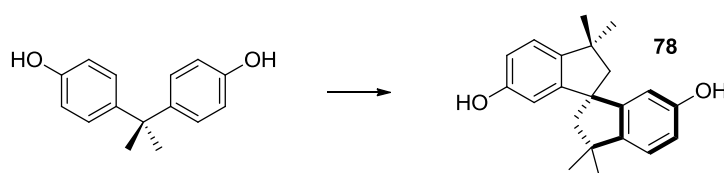
Scheme 69: The proposed synthesis of 3,8-diamino-5a,10b-diphenylcoumarano-2',3',2,3-coumaron.

Another coumaron-based compound for which synthesis was unsuccessful was 2,3,8,9-tetramethyl-5a,10b-diphenylcoumarano-2',3',2,3-coumaron, which was anticipated to be the product from the condensation reaction between 3,4-dimethylphenol and benzil (Scheme 70). The product mixture was analysed using mass spectrometry, which indicated the presence of the coumaron, but purification by column chromatography proved unsuccessful.



Scheme 70: The proposed synthesis of 2,3,8,9-tetramethyl-5a,10b -diphenylcoumarano-2',3',2,3-coumaron.

It was of interest to assess whether the coumaron condensation reaction would work between benzil and a more complex hydroxylphenyl possessing compound, as this would allow the generation of a wider range of coumaron-possessing compounds. Spirobisindane-based compound **78** was chosen as a suitable candidate to test because it features a spirocyclic site of contortion that makes it useful for incorporation in PIMs whilst being relatively simple to synthesise. For this reason this compound has been used in the preparation of highly stable, soluble and high molecular weight PIM-polyimides suitable for robust membrane formation⁹⁸. The preparation of compound **78** was achieved in excellent yield (90%) by the acid catalysed reaction of bisphenol A, 4,4'-(propane-2,2-diyl)diphenol (Scheme 71) in methanesulphonic acid⁹⁹.

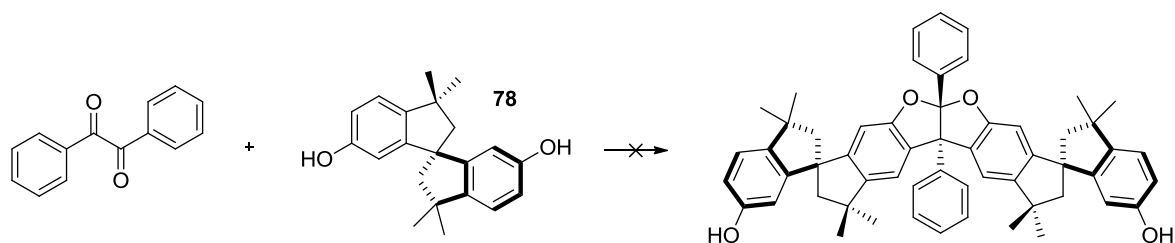


Scheme 71: The synthesis of 3,3,3',3'-tetramethyl-2,2',3,3'-tetrahydro-1,1'-spirobi[indene]-6,6'-diol (**78**).

Reagents and conditions: Methanesulphonic acid, 25 °C, N₂, 72 hours.

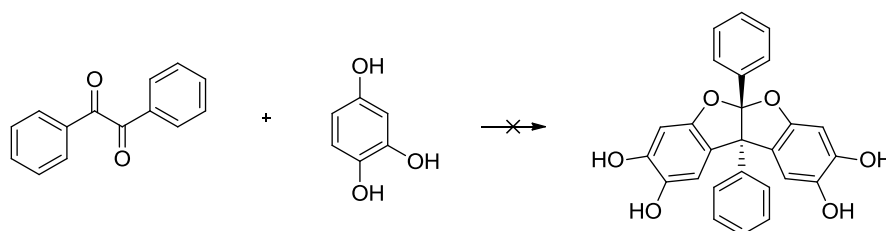
A coumaron-type condensation reaction was then attempted between compound **78** and benzil, with the aim being to synthesise a coumaron structure made from two molecules of compound **78** (Scheme 72). Despite several attempts at this reaction, using the optimised

condensation reaction conditions, none of the desired product was formed and both of the starting materials were recovered in full so this idea was abandoned.



Scheme 72: The proposed synthesis of the coumaron compound built using 3,3,3',3'-tetramethyl-2,2',3,3'-tetrahydro-1,1'-spirobisindane.

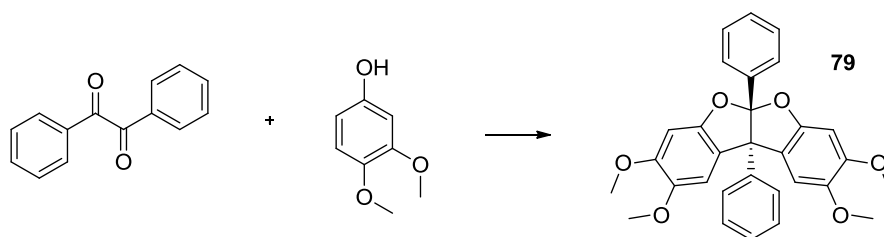
It was surmised that the coumaron condensation reaction might be more efficient when strongly electron donating substituents were present on the phenol derivative. Therefore the reaction between benzil and 1,3,4-trihydroxybenzene was attempted, which was hoped would generate a suitable monomer for dibenzodioxane PIM synthesis, possessing two pairs of hydroxyl groups (Scheme 73). However it soon became clear that 1,3,4-trihydroxybenzene was insufficiently stable in warm acid, so no useful material was created. An alternative strategy to the desired monomer was then devised.



Scheme 73: The proposed synthesis of 2,3,8,9-tetrahydroxy-5a,10b -diphenylcoumarano-2',3',2,3-coumaron.

This alternate strategy was to make a coumaron from the more stable 3,4-dimethoxyphenol rather than 1,3,4-trihydroxybenzene and then perform a simple demethylation to obtain the hydroxyl groups, which are necessary for PIM synthesis. The condensation reaction between 3,4-dimethoxyphenol and benzil was performed using the previously optimised conditions for coumaron synthesis (Scheme 74). The reaction mixture proved to be completely soluble in chloroform, which ruled out the usual technique for product purification, fortunately, the product was found to be insoluble in methanol, whilst the starting materials were soluble. So purification of compound **79** was achieved by stirring the reaction mixture in boiling methanol, which gave the product in moderate yield (58%).

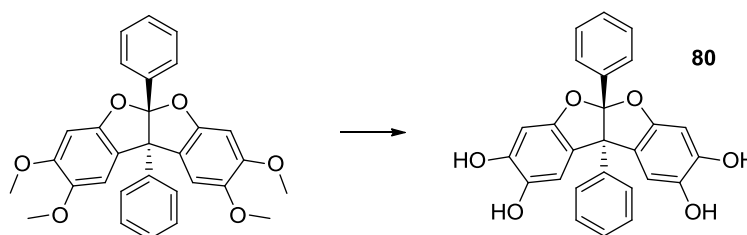
Crystals of this compound were grown and analysed by single-crystal X-ray diffraction, the discussion of this can be found in Appendix 1 (A1.3.3).



Scheme 74: The preparation of 2,3,8,9-tetramethoxy-5a,10b-diphenylcoumarano-2,2',3,3'-coumaron (**79**).

Reagents and conditions: Acetic acid, HCl, CHCl₃, 60 °C, N₂, 96 hours.

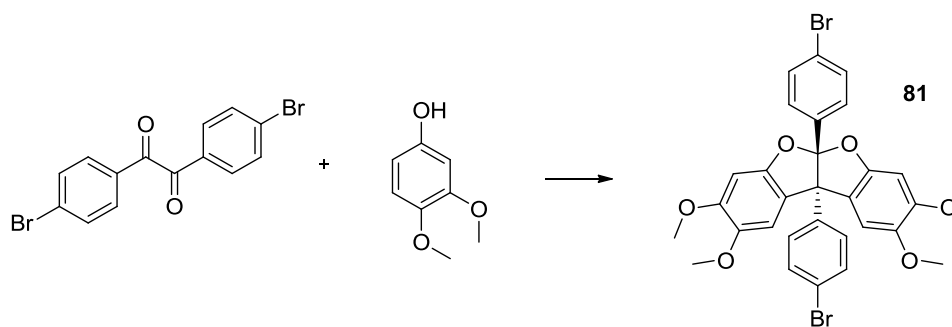
The demethylation of **79** was performed with boron tribromide in dichloromethane, a highly useful and generally reliable procedure¹⁷¹ (Scheme 75). Initially, problems were encountered with this reaction as during the work up stage the product was found to decompose. In an effort to avoid product degradation anhydrous dichloromethane and a much lower temperature were used for the reaction. During the reaction work up the product appeared to decompose once again as, upon addition of water to quench the reaction, the product immediately blackened but, despite this, compound **80** was successfully isolated, albeit in low yield (32%). Following the preparation of this compound it was immediately used for a polymerisation reaction, which is described in Chapter 3 (3.6.2).



Scheme 75: The preparation of 2,3,8,9-tetrahydroxy-5a,10b-diphenylcoumarano-2,2',3,3'-coumaron (**80**) by demethylation. *Reagents and conditions:* BBr₃, anhydrous DCM, -78 °C, N₂, 4 hours.

The final coumaron compound to be produced was from the condensation reaction between 4,4'-dibromobenzil and 3,4-dimethoxyphenol (Scheme 76). After initially performing the reaction under the standard conditions it was noticed that 4,4'-dibromobenzil was very poorly soluble in the acid chloroform mixture, and consequently none of the product could be isolated, although mass spectrometric analysis confirmed its presence. So the reaction

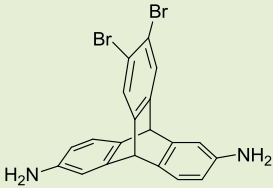
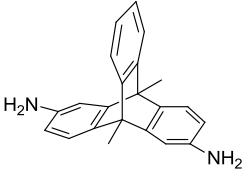
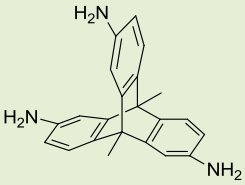
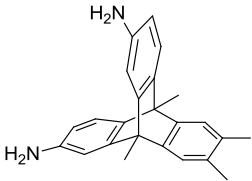
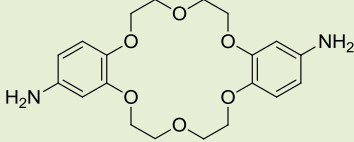
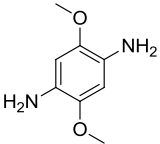
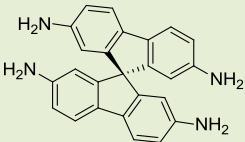
was performed with *o*-dichlorobenzene instead of chloroform, as the former has a significantly higher boiling point so that a higher temperature could be used to aid the solubility of 4,4'-dibromobenzil. Performing the reaction under these conditions gave a higher yield of compound **81**, but this still too low for subsequent polymer synthesis. However, crystals of this novel compound were grown and studied by single-crystal X-ray diffraction; the discussion of this can be found in Appendix 1 (A1.3.4).

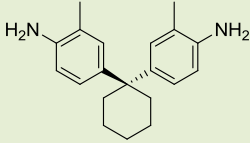
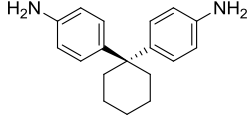
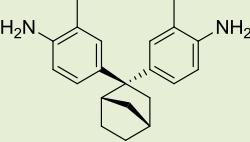
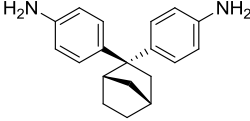
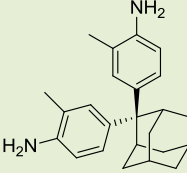
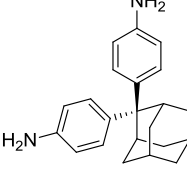
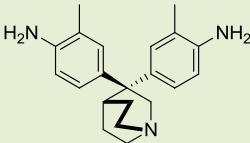


Scheme 76: The synthesis of 2,3,8,9-Tetramethoxy-(4,4'-dibromo)-5a,10b-diphenylcoumarano-2,2',3,3'-coumaron (compound **81**). *Reagents and conditions:* Acetic acid, HCl, *o*-dichlorobenzene, 120 °C, 48 hours.

2.13 Summary of monomer yields

Monomer	N°	Yield (%)	Notes
	8	99.6	<ul style="list-style-type: none"> Very efficient reduction reaction. Difficult to purify dinitro-precursor (7). Relatively stable in air.
	-	-	<ul style="list-style-type: none"> Attempts to form dinitro-precursor failed due to ring activation by methyl groups thus monomer could not be prepared.
	15	98.8	<ul style="list-style-type: none"> Very efficient reduction reaction. Difficult to purify trinitro-precursor (14). Less stable in air than 8.

Monomer	N°	Yield (%)	Notes
	18	99.0	<ul style="list-style-type: none"> • Very efficient reduction reaction. • However, low overall yield due to necessity of preparing initial triptycene precursor 16. • Poor solubility.
	39	97.0	<ul style="list-style-type: none"> • Very efficient reduction reaction. • Multi-step synthesis required to produce initial triptycene precursor (37). • Improved solubility vs. 8. • Relatively stable in air.
	41	96.5	<ul style="list-style-type: none"> • Very efficient reduction reaction. • Multi-step synthesis required to produce initial triptycene precursor (37). • Improved solubility vs. 15. • Less stable than 39.
	-	-	<ul style="list-style-type: none"> • Attempts to form dinitro-precursor failed due to ring activation by methyl groups thus monomer could not be prepared.
	49	82.1	<ul style="list-style-type: none"> • Highly efficient reduction reaction. • The dinitro-precursor 48 was simple to prepare and purify. • Relatively poor solubility.
	56	61.6	<ul style="list-style-type: none"> • The directing nature of the methoxy substituents made the preparation of the dinitro-precursor more complicated than expected. • Relatively poor stability.
	61	67.1	<ul style="list-style-type: none"> • Efficient acid-catalysed reduction reaction. • Required challenging multi-step synthesis to prepare the necessary tetranitro-precursor (60). • Poor stability and solubility.

Monomer	N°	Yield (%)	Notes
	62	70.1	<ul style="list-style-type: none"> Commercially available starting materials. Efficient acid-catalysed condensation reaction. Relatively simple, but time-consuming to purify. Highly soluble and relatively stable in air.
	63	49.1	<ul style="list-style-type: none"> Cheap and commercially available starting materials. Lower yield than expected vs. 62. Relatively simple, but time-consuming to purify. Lower solubility vs. 62, but similar stability.
	64	25.4	<ul style="list-style-type: none"> Commercially available starting materials. Lower yield than expected vs. 62, despite chemical similarity. Relatively simple, but time-consuming to purify. Highly soluble and relatively stable in air.
	65	17.6	<ul style="list-style-type: none"> Cheap and commercially available starting materials. Lower yield than expected vs. 64. Relatively simple, but time-consuming to purify. Lower solubility vs. 64, but similar stability.
	66	34.9	<ul style="list-style-type: none"> Commercially available starting materials. Low yield despite varying reaction conditions. Relatively simple, but time-consuming to purify. Highly soluble and relatively stable in air.
	67	31.1	<ul style="list-style-type: none"> Cheap and commercially available starting materials. Similarly low yield to 66. Relatively simple, but time-consuming to purify. Lower solubility vs. 66, but similar stability.
	68	67.2	<ul style="list-style-type: none"> Commercially available starting materials. Challenging both to synthesise and purify. Relatively poor stability. Relatively high solubility.

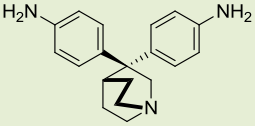
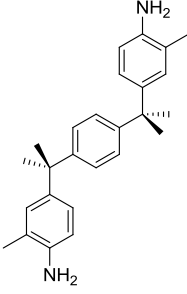
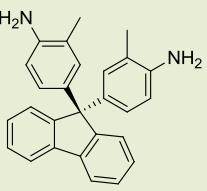
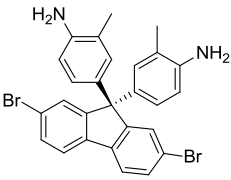
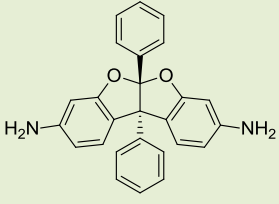
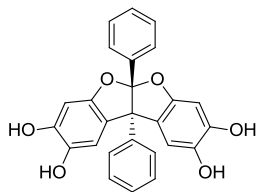
Monomer	N°	Yield (%)	Notes
	69	70.5	<ul style="list-style-type: none"> Commercially available starting materials. Challenging both to synthesise and purify. Relatively poor stability. Similar solubility to 68.
	70	76.2	<ul style="list-style-type: none"> Commercially available starting materials. Efficient acid-catalysed condensation reaction. Relatively simple, but time-consuming to purify. Highly soluble and relatively stable in air.
	71	67.6	<ul style="list-style-type: none"> Commercially available starting materials. Highly efficient acid-catalysed condensation reaction. Relatively simple, but time-consuming to purify. Highly soluble and relatively stable in air.
	74	86.7	<ul style="list-style-type: none"> Highly efficient acid-catalysed condensation reaction. Requires a multi-step synthesis. Relatively simple, but time-consuming to purify. Highly soluble and relatively stable in air.
	-	-	<ul style="list-style-type: none"> Attempts to prepare this monomer failed due to a competitive reaction between the amine substituents of one of the starting materials with ketone substituents of the other reagent.
	80	32.9	<ul style="list-style-type: none"> Cheap and commercially available starting materials. Challenging two-part synthesis. Highly unstable.

Table 5: A summary of the results of the monomer forming reactions detailed above together with a discussion of the properties of the successfully prepared monomers.

Chapter 3: Polymer synthesis

3.1 PIM polymerisation reactions

PIMs are generally composed of fused-ring components to provide rigidity and prohibit rotation within the polymer chain that would result in efficient packing in the solid state. Previously PIMs have been synthesised from a double nucleophilic aromatic substitution reaction between suitable tetrahydroxy and tetrafluoro monomers (Figure 32) that provides a fused-ring dioxan linking group. This reaction proceeds via a two-step substitution process in which a hydroxyl group displaces a fluorine atom from an activated aryl-halide system (S_NAr)¹⁷². The fluorine atoms pull electron density away from the phenyl ring activating it towards nucleophilic attack by the deprotonated hydroxyl group of the other monomer. This produces a negatively charged species called a Meisenheimer complex, from which fluoride is eliminated to give an ether-link between the two monomers. The two-step addition-elimination process then repeats until all of the tetrafluorinated monomer has been consumed by the substitution of the fluorine atoms, forming a polymer.

This is an efficient and useful reaction that can be further enhanced by the presence of strongly electron-withdrawing substituents, such as nitrile, sulphone or ketone, on the tetrafluorinated monomer, these substituents serve two purposes: to make the phenyl ring further electron deficient and to lower the activation energy of the reaction by stabilising the Meisenheimer intermediate. This reaction has also been found to work with the aryl-chlorides¹⁷³, although the yield of such reactions is significantly lower as chlorine is not as electronegative as fluorine and hence, less activating.

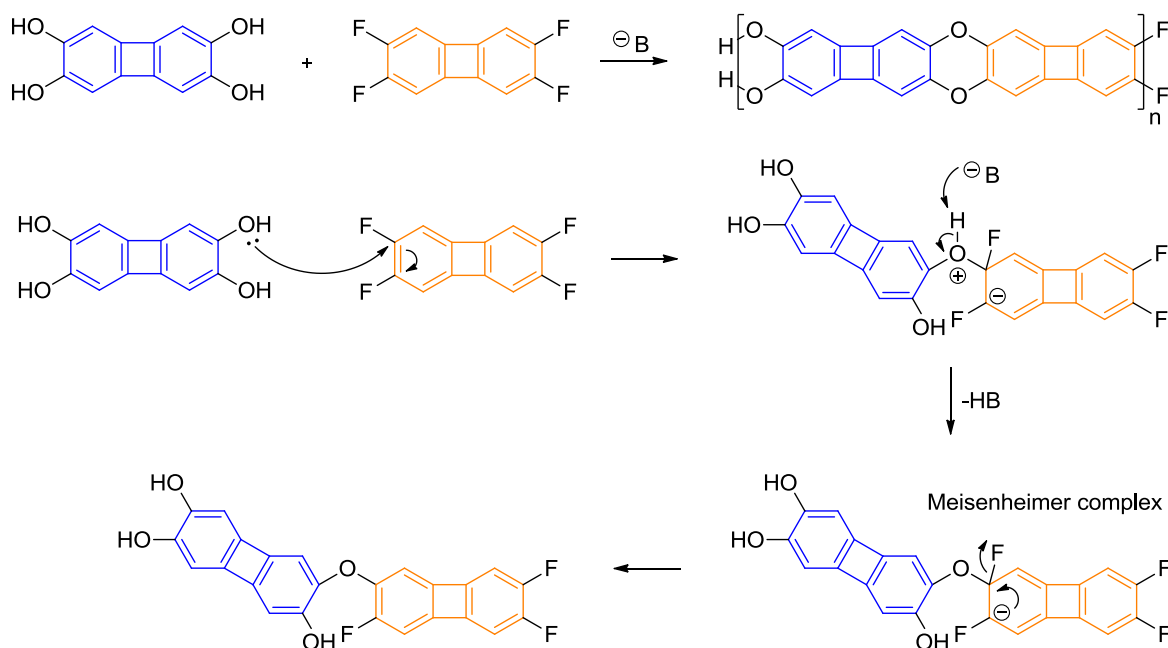


Figure 32: The mechanism for PIM polymerisation.

The primary objective of the research project described in this thesis is the exploitation of the efficient reaction used to form Tröger's base (TB) as the polymerisation reaction to prepared fused-ring PIMs. This reaction has several key differences when compared to that of the conventional dioxan-based PIM-polymerisation. For example, only a single type of synthetic monomer (featuring two or more amino groups) is required with the linking group formed from a "methylene" source, usually paraformaldehyde or its proxy dimethoxymethane. The reaction proceeds via a series of Friedel-Crafts alkylation reactions resulting in the formation of a TB link between two monomer units (Figure 33).

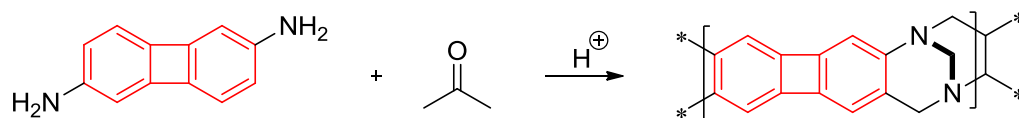


Figure 33: The TB polymerisation reaction.

These PIM polymerisation reactions are both examples of step-growth polymerisation, a type of polymerisation in which the polymer chain builds up slowly starting with the formation of dimers, which link together to form first oligomers and then long polymer chains. Hence, in order to prepare high molecular weight polymer an extremely efficient polymerisation reaction is required. Step-growth polymerisation was first studied by American scientists Wallace Hume Carothers and Paul John Flory in the 1930s for the

optimisation of polyester production whilst they worked for the chemical company DuPont¹⁷⁴. They were part of the team that performed the first polymerisation reaction designed to create high molecular weight polymer and who developed a method for the prediction of results from step-growth polymerisation. Carothers is credited with the invention of Nylon and Neoprene, as well as the development of scientific theories useful for understanding aspects of step-growth polymerisation including kinetics, stoichiometry, molecular weight distribution and average degree of polymerisation.

The method for relating the average degree of polymerisation to the fractional conversion of monomer into polymer is often called ‘The Carothers equation’. This equation describes the relationship between the degree of polymerisation and the fractional monomer conversion. There are two main scenarios for linear polymerisation using this equation, where both monomers are present in equimolar amounts or where one monomer is in excess to the other.

For the simpler scenario, where both monomers are present in the same quantity the average polymer chain length or degree of polymerisation can be derived by dividing the number of molecules originally present in the reaction by the number present after a certain time period. This can be expressed as follows:

$$\bar{X}_n = \frac{[M]}{[M]_o} \quad \text{Equation 1}$$

Figure 34: The relationship between the degree of polymerisation and number of molecules. \bar{X}_n is the degree of polymerisation, representing the number of repeat units in the polymer chain. $[M]_o$ is the original number of molecules and $[M]$ is the number of molecules after a certain time period.

There also exists a relationship between the original number of molecules and number of molecules after a particular time period, since whenever a monomer adds to the polymer chain there is one fewer molecule in the reaction mixture:

$$[M] = [M]_o(1 - p) \quad \text{Equation 2}$$

Figure 35: The relationship between the original number of molecules and the number of molecules after a particular time period. p is the extent of reaction, representing how much monomer has been converted into polymer.

Substituting equation 2 into equation 1 gives the relationship between the degree of polymerisation and the fractional monomer conversion, expressed as the following equation:

$$\bar{X}_n = \frac{1}{1 - p}$$

Figure 36: The Carothers equation for two monomers in equimolar quantities. \bar{X}_n is the degree of polymerisation, p is the extent of reaction.

The equation indicates that high molecular weight polymer chains only form at a very high extent of reaction (Figure 37). For example, when p is 0.80 (80% of monomer converted to polymer) the degree of polymerisation is only 5, whilst when p is 0.99 the degree is polymerisation is 100.

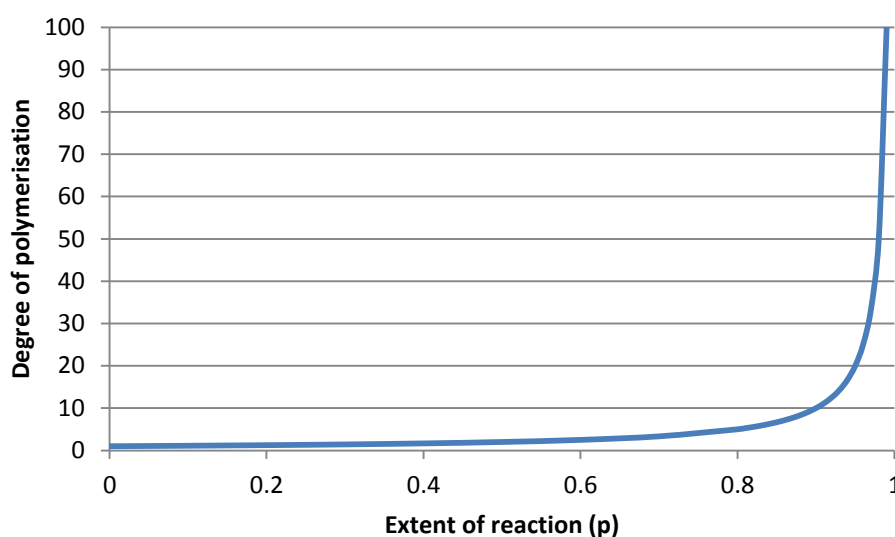


Figure 37: A graphical representation of the Carothers equation.

The Carothers equation requires modification for the second and more complex scenario, where one of the monomer is in excess compared to the other. In this case the polymer chain length is limited by the ratio of the two monomers (Figure 38), as the monomer in excess will generally only be able to react with an equal amount of the other monomer, so the excess material will be wasted. The reactant ratio can be expressed as:

$$r = \frac{f_a}{f_b}$$

Figure 38: The ratio of monomers. f_a is the quantity of the limiting monomer, f_b is the quantity of the monomer in excess.

Hence, r cannot be greater than 1 and has an influencing effect on the Carothers equation, which becomes:

$$\bar{X}_n = \frac{1 + r}{1 + r - 2rp}$$

Figure 39: The modified Carothers equation. \bar{X}_n is the degree of polymerisation, r is the monomer ratio and p is the extent of reaction.

When nearly all of the monomer has been consumed by conversion into polymer (p approaches 1) the equation can be simplified to:

$$\bar{X}_n = \frac{1 + r}{1 - r}$$

Figure 40: The modified Carothers equation. \bar{X}_n is the degree of polymerisation, r is the monomer ratio and p is the extent of reaction.

Quite clearly the ratio of monomers has a big effect on the degree of polymerisation (Figure 41). For example, when p is 0.99 and there is an excess of 2% of one monomer compared to the other, r is 0.98 and the degree of polymerisation is limited to 49.5, whilst for the equimolar scenario the degree of polymerisation is 100. Thus, using an excess of one monomer is a method for controlling the molecular weight of the polymer. This can be a useful trick for controlling the properties of a polymer, such as melting point and solution viscosity, which increase with molecular weight. However, it can also result in low molecular weight polymer being formed unintentionally when at least one of the monomers contains impurities.

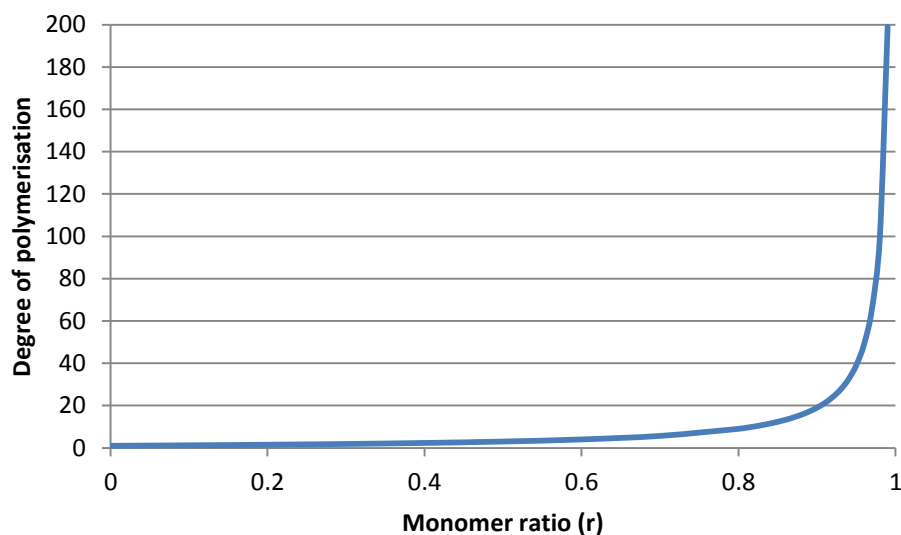
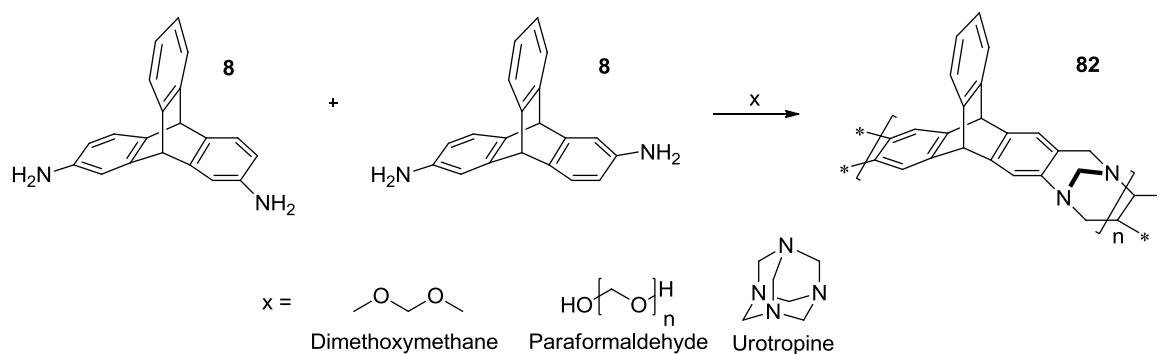


Figure 41: A graphical representation of the modified Carothers equation, assuming that $p = 1$.

3.2 The development and optimisation of TB polymerisation

Following the successful optimisation of the reaction used for TB formation and the preparation of diamine monomer **8**, an investigation was performed to assess the viability of creating PIMs using the TB-forming reaction (Scheme 77). Firstly, it was important to establish the best source of formaldehyde proxy for the methylene precursor between dimethoxymethane, paraformaldehyde or urotropine. This was done by performing the polymerisation reaction under similar conditions, 1 gram of monomer in 10 ml of trifluoroacetic acid with 5 equivalents of each of the precursors. After the reaction was completed the mixture was worked up and the polymer was purified by solvent reflux to remove low molecular weight material. Reprecipitation was then performed to remove oligomeric material and narrow the polydispersity of the polymer sample.

The molecular weight of each sample was determined by GPC (Gel Permeation Chromatography) analysis, which compared the polymer samples to polystyrene standards. As PIMs are a lot less flexible than polystyrene over-estimation of molecular weight may have occurred since a PIM of a particular molecular weight may spend less time in the porous beads of the column and elute faster than polystyrene with the same or similar molecular weight. The optimised synthesis of this polymer is discussed in the next section (3.3.1).



Scheme 77: The TB polymerisation of **8**. *Reagents and conditions:* x (5 equiv.), TFA (10 ml), 0 °C, 48 hours.

The study found that each reaction had successfully formed polymer **82**, but dimethoxymethane was the best of the three reagents (Table 6), as it gave the polymer with the highest molecular weight. Paraformaldehyde was the second best, but the polymer had a significantly lower molecular weight. Finally, using urotropine as the precursor gave the triptycene polymer with the lowest molecular weight, confirming that it was not an efficient reagent for the reaction. The yield of polymer from each reaction was high (around 80%), despite the difference in molecular weight.

What was strange about the three batches of polymer **82** was that the surface area, measured by BET nitrogen adsorption, of each was very similar, suggesting that the polymer is capable of forming a microporous material even with a very low degree of polymerisation. Indeed, the batch of polymer **82** with the lowest molecular weight had the highest observed surface area by $80 \text{ m}^2\text{g}^{-1}$, which even after acknowledgement of the errors associated with nitrogen adsorption analysis is still a significant difference. It is possible that this difference is related to the higher molecular weight batch of polymer **82** having a less-accessible microporous structure due to the packing of the longer polymer chains.

The polydispersity index (M_w/M_n) was below 1.8 for each of the three samples, indicating efficient removal of oligomeric material by reprecipitation. It is important to note that the batch of polymer **82** created using dimethoxymethane had a higher polydispersity index than the other two samples. This is likely to be a direct consequence of the higher molecular weight of this sample, meaning that polymer chains with a wider range of lengths could be created.

Methylene source (x)	Molecular weight $M_w(\text{g mol}^{-1})^*$	Polydispersity Index $(M_w/M_n)^*$	BET surface area (m^2/g)
Dimethoxymethane	34,000	1.78	900
Paraformaldehyde	10,500	1.54	900
Hexamine	7,000	1.53	980

Table 6: A comparison of methylene precursors for the preparation of polymer **82**, showing the molecular weight (M_w) and BET surface area of the resulting polymers. *These numbers have been rounded.

Following the identification of dimethoxymethane as the best methylene precursor of those tested a study was performed to identify the optimal number of equivalents to use for the polymerisation reaction. The TB polymerisation reaction between compound **8** and dimethoxymethane was performed using the same reaction conditions, but from 3 to 6 equivalents of dimethoxymethane and the molecular weight of each batch of polymer **82** was analysed by GPC (Figure 42). The reaction formally requires 3 equivalents of dimethoxymethane for each compound **8**, but it was expected that a slight excess of dimethoxymethane would not adversely affect the reaction.

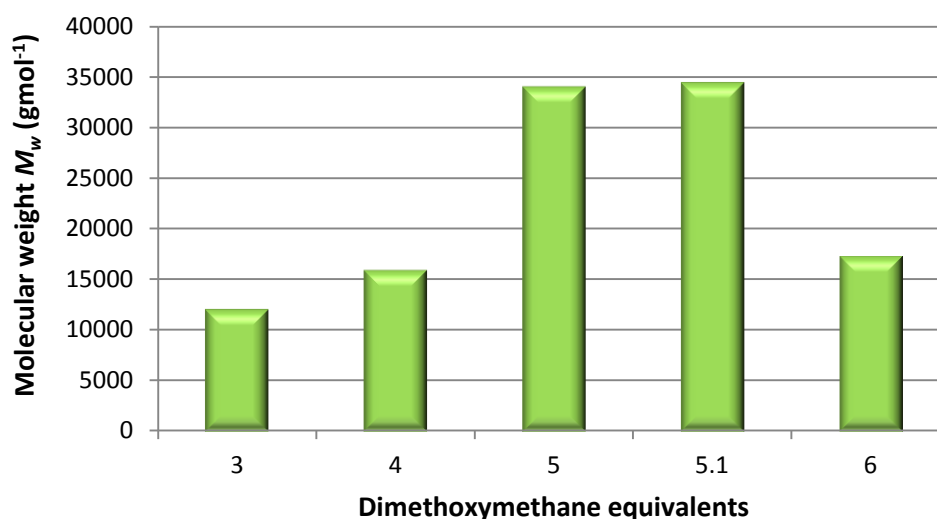


Figure 42: A chart showing the effect of using different equivalents of dimethoxymethane on the molecular weight (M_w) of polymer **82**.

The study found a linear trend linking the number of dimethoxymethane equivalents and molecular weight (M_w) of polymer **82** obtained between 3 and 5 equivalents, with a

significant increase in molecular weight between 4 and 5 equivalents, 15,500 gmol^{-1} to 34,000 gmol^{-1} . Using 5.1 equivalents of dimethoxymethane gave the highest molecular weight polymer, 34,500 gmol^{-1} , but the difference between the molecular weight achieved when using 5.1 and 5 equivalents was insignificant and within the error margins of the GPC instrument. Additionally, the study found that when the reaction was performed using 6 equivalents of dimethoxymethane a significantly lower molecular weight was achieved for polymer **82**, 17,500 gmol^{-1} . This indicated that the optimal number of equivalents of dimethoxymethane to use for the polymerisation reaction was 5, since somewhere between 5.1 and 6 equivalents the reaction became less efficient.

An investigation was then performed to discover how much time was required to achieve a polymer of high molar mass. For this analysis a large scale polymerisation of compound **8** was conducted, with small samples taken out at regular intervals: every hour for the first 7 hours, then after 24 hours, 36 hours, 48 hours and 72 hours until the reaction was worked up after 144 hours. Each sample was treated independently and analysed by GPC analysis (Figure 43). The study showed that the polymerisation reaction between compound **8** and dimethoxymethane had reached completion after approximately 24 hours, since the molecular weight (M_w) of each sample of polymer **82** after this point was found to be relatively constant, around 30,000 gmol^{-1} . In fact the molecular weight of each sample after 24 hours was found to slightly decrease, so that a downwards linear trend was observed, but the overall difference was small enough that this could be attributed to instrument error, especially since TB has been proven to be stable in a variety of conditions, including strong reducing and oxidising agents¹⁷⁵, meaning that it was unlikely that the polymer chain was breaking down in the reaction mixture.

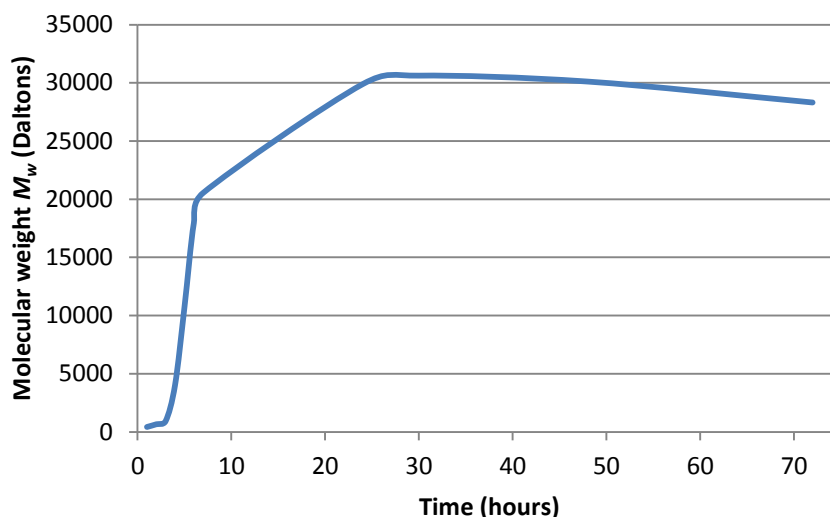


Figure 43: A graph showing how the molecular weight (M_w) for polymer **82** grows over time.

Another property of the reaction that was investigated was the importance of solution concentration on the molecular weight of polymer **82**. This is an important parameter for step-growth polymerisation reactions because if the solution is too dilute then the rate of chain growth becomes too slow and cyclic oligomers predominate resulting in low molecular weight polymer. However, if the solution is too concentrated unwanted cross-linking may occur due to side reactions happening during polymer chain growth, resulting in covalent bonds being forming between polymer chains. These cross-links can be formed directly between neighbouring chains or the link may be formed between two chains through a third common molecule. This will result in the polymer becoming insoluble as solvent molecules cannot disrupt the strong bonds between polymer chains. For this reason cross-linking must be avoided if a solution-processable polymer is desired, such as for the preparation of polymer membranes.

Initially, this study was undertaken by using a reduced volume of trifluoroacetic acid for the polymerisation reaction. The reaction was performed using 1 gram of compound **8** with 5 equivalents of dimethoxymethane and 5 ml of trifluoroacetic acid. After only a few hours the reaction mixture was observed to become more viscous and eventually became too thick so that the stirring stopped after around 24 hours, which it was thought, was a sign of unwanted cross-linking (gelation). The reaction was worked up and the batch of polymer **82** tested for solubility, which discovered that only a small amount of the material was soluble in common organic solvents, such as chloroform and THF. The molecular weight

(M_w) of the soluble portion was measured by GPC analysis, which found that the polymer had significantly lower molecular weight (M_w) compared to the material produced when 10 ml of trifluoroacetic acid was used for the reaction (Table 7), 21,500 gmol^{-1} and 34,500 gmol^{-1} , respectively. Hence, it can be inferred that using less than 10 ml of trifluoroacetic acid per gram of monomer was detrimental to the reaction.

Furthermore, testing was conducted to discover the effect of making the reaction mixture less concentrated. It was decided that using a co-solvent for the reaction would prove a more interesting comparison, as the acid would be diluted, not just the concentration of the monomer. The monomer proved readily soluble in a range of common organic solvents, including chloroform, DCM and THF. Chloroform was chosen as the co-solvent for the reaction as it was itself slightly acidic and most importantly was completely miscible with trifluoroacetic acid.

Solvent system	Molecular weight		
	M_n (gmol^{-1})	M_w (gmol^{-1})	M_z (gmol^{-1})
5 ml Trifluoroacetic acid	7,500	21,500	45,000
10 ml Trifluoroacetic acid	14,000	34,500	63,000
10 ml Trifluoroacetic acid and 10 ml Chloroform	17,500	34,500	47,000

Table 7: The molecular weight of polymer **82** formed when using different solution concentrations. The numbers have been rounded.

The reaction of compound **8** with 5 equivalents of dimethoxymethane was performed using a 1:1 mixture of trifluoroacetic acid and chloroform (10 ml:10 ml). During the reaction no apparent change in the solution viscosity was observed, but this batch of polymer **82** was found to have a similar molecular weight (M_w) to that produced when no co-solvent was used for the reaction (Table 7). However, its molecular weight was found to have a lower maximum (M_z), suggesting that whilst the chloroform aided the solubility of the monomer and the generation of polymer at the start of the reaction, the dilution of the reaction mixture had an adverse effect on the generation of the longest molecular weight polymer chains, possibly by decreasing branching and cross-linking reactions.

This investigative work allowed the development of a general method for the preparation of TB PIMs. The basic general procedure for the reaction is to dissolve the monomer in trifluoroacetic acid, using 10 ml of the acid solvent for every gram of monomer. This is done at 0 °C to prevent the degradation of the monomer in the strong acid prior to polymerisation. Once dissolved, 5 equivalents of dimethoxymethane are slowly added to the solution over a few minutes. The reaction vessel is then covered to prevent dust or other impurities from disturbing the reaction mixture, which is allowed to slowly warm to room temperature before being left stirring for 48 hours. After this time the reaction is quenched by addition of aqueous sodium hydroxide or 1:1 mixture of water and aqueous ammonia, to raise the pH of the mixture to at least 10 and precipitates the polymeric material out of solution by deprotonation of the basic TB units. The polymer is collected by filtration and washed with water and acetone before refluxing in acetone for a few hours to remove any soluble impurities. The polymer is then tested for its solubility in common low boiling point organic solvents, such as chloroform and THF, and the subsequent purification technique depends on the solubility of the polymer.

If the polymer is found to be completely soluble in low boiling point solvents, then the material is purified by dissolving it in a suitable solvent before adding just enough hexane to reprecipitate the first portion of the polymer from solution. This separates the low molecular weight material, which stays in solution, and the higher molecular weight material which precipitates from the solution as a solid. This process is repeated at least twice more, prior to refluxing the polymer in methanol to remove any traces of other solvents. If the polymer is found to be insoluble then it is purified by refluxing in THF, chloroform and finally methanol. This removes any soluble low molecular weight material from the polymer product, before the methanol reflux which removes any traces of the other solvents. Following either technique the polymer is dried in a vacuum oven at 120 °C under reduced pressure to ensure that the material is thoroughly dry prior to analysis.

Some of the synthesised polymers were found to be soluble in high boiling point solvents, such as quinoline and N-methyl-2-pyrrolidone (NMP), but these solvents were avoided for purification due to the great difficulty encountered when trying to completely remove them from polymer samples, which is necessary for reliable analysis. In these cases the polymer was purified as though it was insoluble.

The development of the TB polymerisation reaction of compound **8** was successful in discovering the optimal conditions for making TB PIMs. Following the synthesis of polymer **82** (a ladder polymer based on the triptycene building block) the same method was used for generation of TB polymers from a variety of different monomers. During this work several subtle observations were made on how to alter the TB polymerisation reaction to best allow the generation of higher molecular weight polymer. For example, the polymerisation reaction was found to give the highest molecular weight material when the diamine monomer was mixed with dimethoxymethane before trifluoroacetic acid was added slowly to the reaction mixture. Another empirical observation was that the quenching of the polymer reaction mixture is easier with aqueous ammonia rather than aqueous sodium hydroxide is used. Unfortunately, it took time to optimise the polymerisation and time-constraints meant that it was impossible to repeat the synthesis of all of the polymers discussed in this chapter using the optimised procedures. The best analytical results from each polymer are described, but the synthesis and results of each were repeated at least once to ensure reliability and accuracy.

3.3 TB PIMs based on the triptycene unit

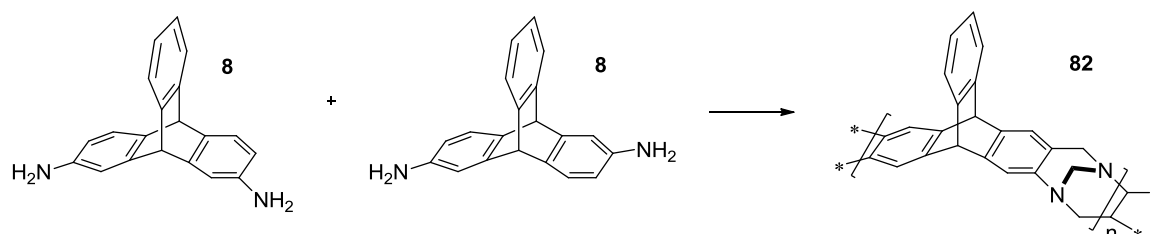
This section of the chapter details the synthesis of the TB polymers based around triptycene, which proved to be a highly useful and versatile building block. This discussion will be divided into two sections: discussion of the synthesis of the ladder polymers and then discussion of the synthesis of the network polymers. The analysis of each polymer is described in the next chapter.

3.3.1 TB triptycene ladder polymers (82 - 84)

The polymerisation reaction between compound **8** and dimethoxymethane was performed numerous times in an attempt to optimise the reaction, but each time the molecular weight (M_w) of polymer **82** was consistently found to be around 35,000 g mol^{-1} . Although demonstrating the viability of the reaction, this molecular weight proved insufficient for the preparation of a robust membrane. Each attempt at film formation resulted in only large fragments of film due to extensive cracking. Otherwise polymer **82** showed promising

microporosity (up to 900 m²/g) and excellent solubility in a range of solvents. Therefore, towards the end of the project the synthesis was repeated using the ‘tricks’ that had been learned from the synthesis of other polymers in the hope of achieving a higher molecular weight for the polymer.

The polymerisation reaction (Scheme 78) was performed by dissolving compound **8** in a mixture of dimethoxymethane and dichloromethane (5:3), which was added to aid the solubility of compound **8** in dimethoxymethane. Trifluoroacetic acid was then added slowly over two hours before the reaction mixture was left stirring for 168 hours, during which time it was observed to become increasingly viscous, but did not become so viscous that it stopped stirring. After quenching the reaction polymer **82** crashed out of solution as long and thin fibres – a good indication that high molecular weight polymer had formed.

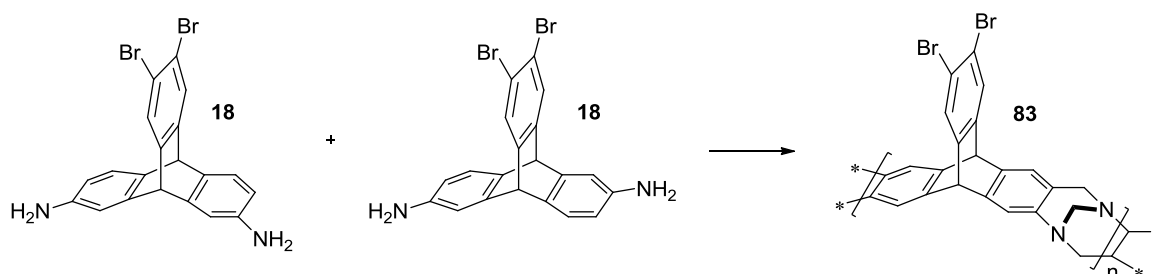


Scheme 78: The TB polymerisation of **8**. *Reagents and conditions:* Dimethoxymethane, DCM, TFA, 0 °C, 168 hours.

From this reaction polymer **82** was isolated in high yield and once again demonstrated excellent solubility in a range of solvents (Table 8), particularly chloroform, dichloromethane and the higher boiling point solvents. The complete solubility of polymer **82** in chloroform allowed NMR analysis to be performed, with the ¹H NMR showing a spectrum with the peaks substantially broadened, typical of a polymeric material, caused by restricted tumbling of the large rigid macromolecule. The ¹³C NMR spectrum provided little information, as each peak was relatively weak, so a sample of polymer **82** was sent away for solid-state analysis, which provided more information and showed the broad peaks typical of solid-state ¹³C NMR. GPC analysis performed on this batch of polymer **82** showed significant improvement in molecular weight compared to previous batches of the polymer, with *M_n* of 21,000 gmol⁻¹ and *M_w* of 51,000 gmol⁻¹.

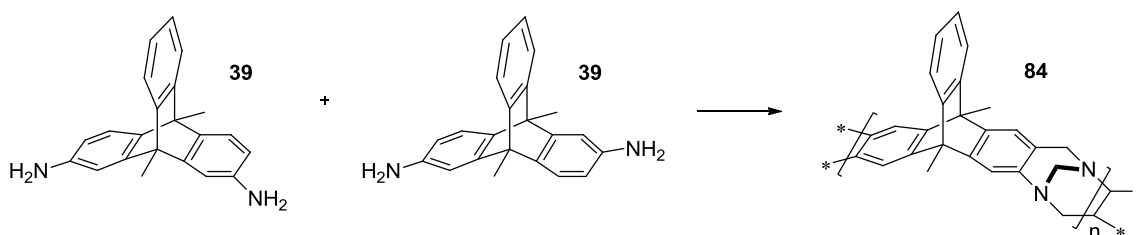
Similarly to the preparation of polymer **82**, polymer **83** was produced from the polymerisation reaction between compound **18** and dimethoxymethane (Scheme 79). The solubility of compound **18** in TFA was found to be poor, which may have hindered the

generation of high molecular polymer and is especially likely considering the relatively poor yield (35%) of polymer **83** meaning that a significant portion of the material was removed during purification. Polymer **83** demonstrated poor solubility in chloroform and only partial solubility in THF, but proved completely soluble in DMAc, NMP and quinoline (Table 8). This meant that whilst GPC analysis was not possible, ^1H NMR analysis was achieved by using d_6 -DMSO as the solvent, the spectrum obtained showed the expected peak broadening typical of polymeric materials. The poor solubility exhibited by polymer **83** can be explained by the presence of the bulky bromine atoms along the polymer chain, these atoms hinder interaction between the solvent molecules and polymer chain.



Scheme 79: The polymerisation of **18**. *Reagents and conditions:* Dimethoxymethane, TFA, 0 °C, N_2 , 72 hours.

The final ladder polymer in this series to be generated was polymer **84**, which was formed from the TB polymerisation reaction between compound **39** and dimethoxymethane (Scheme 80). This polymer displayed excellent solubility in a range of solvents, including THF and chloroform (Table 8). ^1H NMR analysis gave a well-defined spectrum with the broad peaks expected for a polymer.

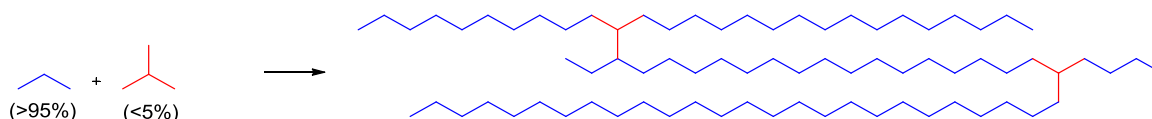


Scheme 80: The polymerisation of **39**. *Reagents and conditions:* Dimethoxymethane, TFA, 0 °C, N_2 , 96 hours.

Polymer **84** was successfully isolated in high yield and its high solubility allowed the molecular weight to be measured by GPC analysis. Unfortunately, this showed that this batch of polymer **84** possessed only low molecular weight, $M_n = 6,000 \text{ gmol}^{-1}$ and $M_w =$

13,600 g mol^{-1} . Despite repeating the polymerisation reaction numerous times and for prolonged periods, a batch of polymer **84** with an improved molecular weight could not be generated.

In an attempt to improve upon the molecular weight of polymer **84** an experiment was undertaken to dose diamine compound **39** with triamine compound **15** prior to the polymerisation reaction. It was hoped that this would induce a small amount of branching between polymer chains (Scheme 81), so that whilst each individual chain may be small the connection of several such chains could generate polymer **84** with sufficient molecular weight for the preparation of a robust membrane. However, there was a risk that if too much of compound **15** were used there would be too much branching induced between polymer chains resulting in cross-linking and an insoluble polymer sample.



Scheme 81: A representation of the branching experiment.

The investigation was undertaken by performing a series of experiments where the polymerisation reaction between compound **39** and dimethoxymethane was dosed with a small quantity of compound **15** (between 1 and 6 % of the total monomer weight). A control experiment was conducted to perform a basis for comparison. Each experiment was performed on a small half-gram scale and worked-up independently prior to purification and molecular weight determination by GPC analysis. The results of this investigation showed that using compound **15** did appear to increase the molecular weight of polymer **84** (Figure 44).

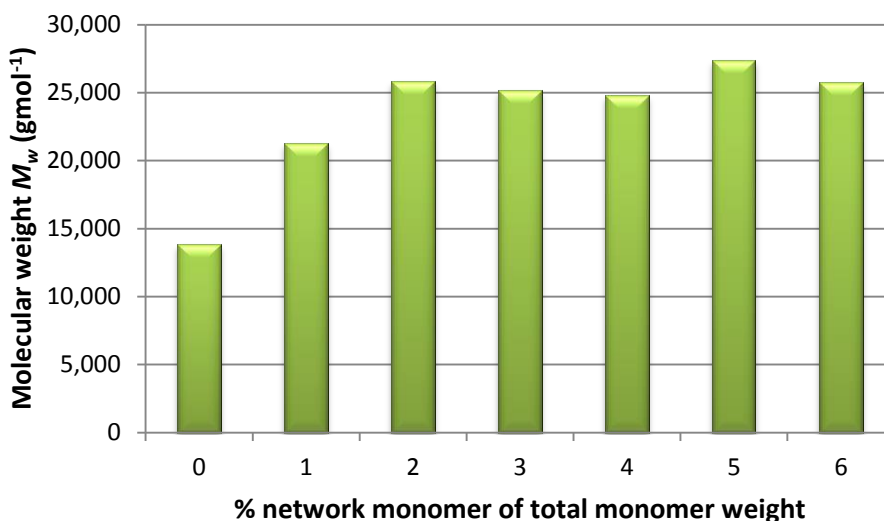


Figure 44: A graph showing the change in molecular weight (M_w) of polymer **84** with increasing quantity of compound **15**.

There was a significant increase in the molecular weight of polymer **84** between the control experiment and the experiment where 1% of compound **15** was used, from $M_w = 14,000 \text{ gmol}^{-1}$ to $21,000 \text{ gmol}^{-1}$, an increase of 50%. This indicated that the presence of compound **15** was aiding in the generation of higher molecular weight polymer by linking together polymer chains. There was an increase of 24% between the experiments using 1 and 2% of compound **15**, showing that using extra compound **15** caused an improvement in molecular weight by inducing further connections between polymer chains. After this point using increasing quantities of compound **15** had little effect on the molecular weight of the polymer, as the molecular weight of polymer **84** produced from the experiments using 2% to 6% of compound **15** remained reasonably constant at around $25,000 \text{ gmol}^{-1}$. However, the experiment using 6% of compound **15** produced a batch of polymer **84** that was not completely soluble in chloroform, suggesting that too much branching had occurred between the polymer chains, resulting in a cross-linked sample. Thus the limit to maintain the solubility of polymer **84** appeared to be 5% of compound **15**. Finally, despite the improvement in molecular weight for polymer **84** it was still deemed insufficient to allow the preparation of a polymer membrane.

3.3.2 Discussion of solubility properties

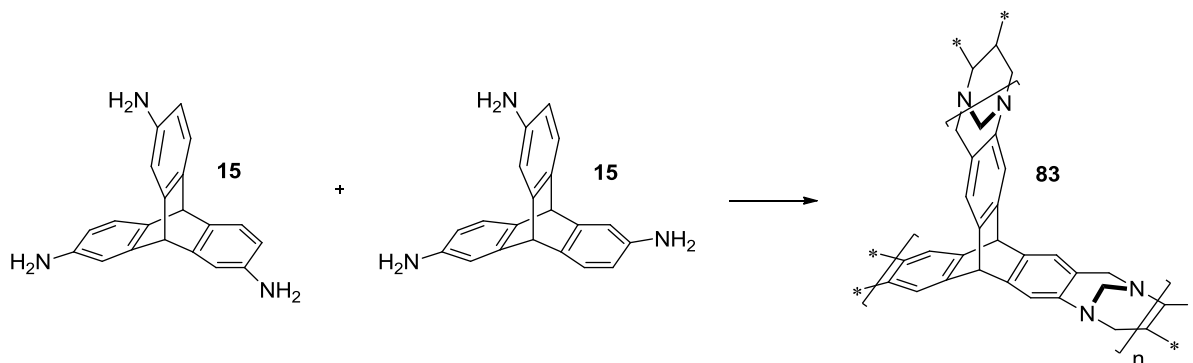
A solubility study was performed by thoroughly mixing 50 mg of polymer sample with 2 ml of solvent and assessing how much of the polymer had dissolved after 30 minutes. The solubility of ladder polymers **82** - **84** varied greatly (Table 8). Polymer **83** demonstrated poor solubility in the halogen-based solvents, but complete solubility in THF and the higher boiling point solvents. The other two ladder polymers (**82** and **84**) show excellent solubility in nearly all of the solvents tested. This can perhaps be explained by the high microporosity of these polymers, with large voids between the polymer chains arising from inefficient packing. Solvent molecules can easily enter these voids, which allows for stronger polymer-solvent interaction and faster dissolution.

Polymer	Solvent									
	THF	DCM	CHCl ₃	DMF	Ph-Cl	DMAc	NMP	Quinoline	MeOH	Acetone
82	++	+++	+++	+++	++	+++	+++	+++	-	-
83	++	-	+	++	-	+++	+++	+++	+	-
84	+++	+++	+++	+++	++	+++	+++	+++	-	-

Table 8: Table summarising the solubility of polymers **82**, **84** and **85** in a range of solvents. +++ = completely soluble, ++ = mostly soluble, + = partially soluble, - = insoluble.

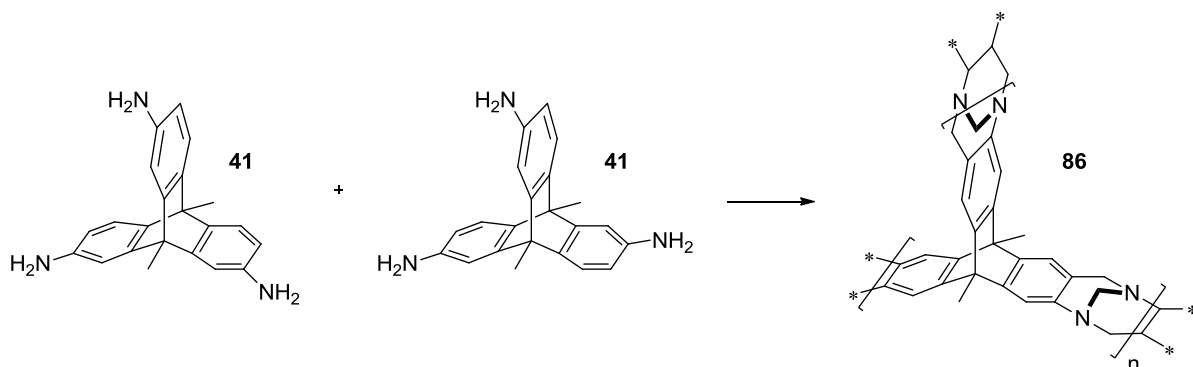
3.3.3 TB triptycene network polymers (85 - 86)

Polymer **85** was synthesised from the TB polymerisation reaction between compound **15** and dimethoxymethane (Scheme 82). It was found to be insoluble, which confirmed that the polymer had the desired network structure, but meant that solution ¹H NMR and GPC analysis was not possible.



Scheme 82: The polymerisation of **15**. *Reagents and conditions:* Dimethoxymethane, TFA, 0 °C, 48 hours.

In a similar manner polymer **86** was synthesised from compound **41** and dimethoxymethane (Scheme 83). As expected it also proved to be insoluble, which confirmed its network structure, but prevented characterisation by ^1H NMR or GPC analysis.



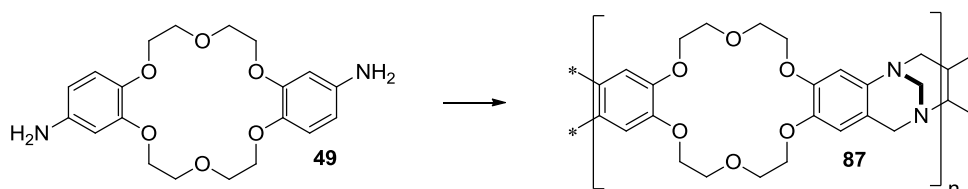
Scheme 83: The polymerisation of **41**. *Reagents and conditions:* Dimethoxymethane, TFA, 0 °C, N_2 , 72 hours.

3.4 Other TB polymers (87 – 92)

This section of the chapter covers the synthesis and structural properties of the TB polymers that are not based around triptycene. This includes polymers based upon dibenzo-18-crown-6, naphthalene, 1,4-dimethylbenzene, 1,4-dimethoxybenzene, and spirobisfluorene components. The grouping of these polymers allows a comparison of the various building blocks to be made that would otherwise not be possible. Discussion of the analysis of these polymers can be found in the next chapter.

3.4.1 TB dibenzo-18-crown-6 ladder polymer (87)

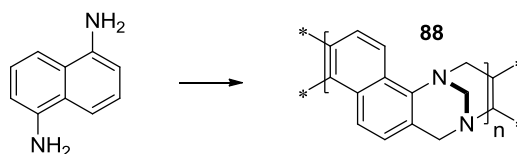
Polymer **87** was synthesised from the polymerisation reaction between compound **49** and dimethoxymethane (Scheme 84). From this reaction polymer **87** was isolated, but the material proved to be insoluble in THF, partially soluble in chloroform and dichloromethane and only completely soluble in DMF, NMP and methanol (Table 9). The solubility of polymer **87** in methanol was surprising since PIMs are generally insoluble in methanol and meant that purification of the material was achieved solely by refluxing in acetone. The modest solubility of polymer **87** in chloroform made molecular weight determination by GPC analysis impossible, but proved sufficient for ^1H NMR analysis, the spectrum from which showed the expected broad peaks for a polymer.



Scheme 84: The polymerisation of **49**. *Reagents and conditions:* Dimethoxymethane, TFA, 0 °C, 72 hours.

3.4.2 TB naphthalene ladder polymer (88) and its derivatives (89 – 90)

Polymer **88** was created from the polymerisation reaction between purified 1,5-diaminonaphthalene and dimethoxymethane (Scheme 85). It was found to be only sparingly soluble in all of the solvents tested (Table 9). This poor solubility might be attributed to some cross-linking due to the activating nature of naphthalene towards aromatic electrophilic substitution. Hence, the molecular weight of polymer **88** could not be determined, but it was found to be sufficiently soluble in chloroform to allow characterisation by ^1H NMR, which showed the anticipated broad peaks of a polymer.



Scheme 85: The polymerisation of 1,5-diaminonaphthalene. *Reagents and conditions:* Dimethoxymethane, TFA, 0 °C, 72 hours.

The cheap and commercial availability of the monomer, albeit in an impure form that required purification, made polymer **88** a suitable starting material for the preparation of a material possessing quaternary amine functionality using a suitable alkyl-based reagent possessing a good leaving group¹⁷⁶. This S_N2 substitution reaction (Figure 45) proceeds with the nucleophilic attack by a nitrogen lone pair on the alkyl halide resulting in the formation of a quaternary amine, stabilised by the anion of the leaving group.

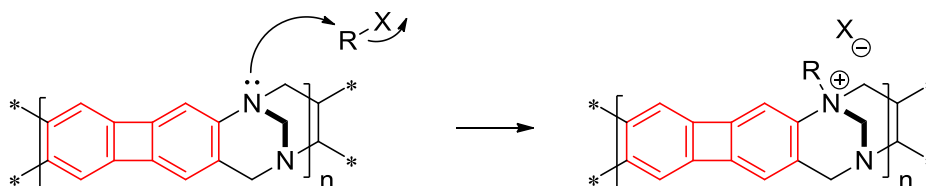


Figure 45: The mechanism for the preparation of a TB polymer with quaternary amine functionality. X = a good leaving group, such as iodine.

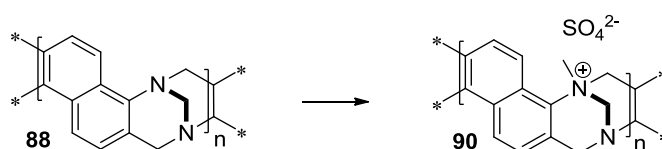
This process is relatively simple to perform on TB, only requiring a mixture of the alkyl-based reagent and a suitable solvent and producing the quaternary-TB product in excellent yield¹⁷⁷. In contrast, bis-alkyl substitution of the same TB unit is difficult, requiring harsh conditions, since this creates a species with two positive charges in close proximity. None of the bis-quaternary TB product is generated from the reaction, even when a large excess of the alkyl-based reagent is used¹⁷⁸. It was hoped that a polymer possessing this functionality would have increased affinity towards carbon dioxide, since in the presence of water carbon dioxide reacts to form carbonic acid (H₂CO₃), which can further reversibly react with water to form the bicarbonate anion (HCO₃⁻)¹⁷⁹. This anion will have a stronger interaction with a nitrogen cation, due to charge attraction, thereby enhancing its gas separation properties.

Quaternisation was achieved by stirring polymer **88** in a mixture of DMSO and a large excess of methyl iodide (Scheme 86). ¹H and solid-state ¹³C NMR analysis showed the presence of the added methyl groups, indicating that polymer **89** had undergone an efficient reaction. However, the material was found to be only partially soluble in THF or chloroform, which once again prevented molecular weight determination by GPC analysis.



Scheme 86: The synthesis of polymer **89**. *Reagents and conditions:* MeI, DMSO, 72 hours.

A second quaternary TB polymer was also created from polymer **88**, but in this case dimethyl sulphate was used. The sulphate counter ion was chosen since it possesses a -2 charge, which it was predicted could be shared between two quaternary amines and would therefore take up less space than two bulky iodine atoms, which each possess a -1 charge. The reaction was performed by stirring polymer **88** in a mixture of DMSO and dimethyl sulphate (Scheme 87). A large excess of dimethyl sulphate was used to encourage the reaction to go to completion.

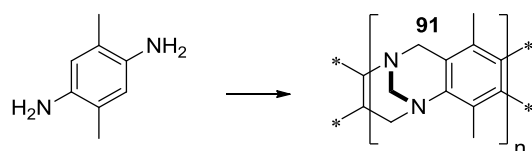


Scheme 87: The synthesis of polymer **90**. *Reagents and conditions:* Me₂SO₄, DMSO, 72 hours.

Similarly to polymer **89**, polymer **90** was found to be insoluble in methanol and only partially soluble in chloroform and THF. Unfortunately, this meant that GPC analysis was not possible, but ¹H and solid-state ¹³C NMR were performed on polymer **90**, indicating the presence of the expected methyl groups.

3.4.3 TB 1,4-dimethylbenzene ladder polymer (**91**)

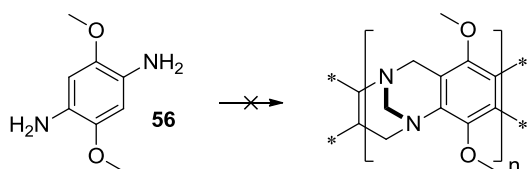
The polymerisation of 2,5-dimethyl-1,4-phenylenediamine with dimethoxymethane provided polymer **91** (Scheme 88). It demonstrated poor or only partial solubility in most of the solvents tested (Table 9), but proved completely soluble in chloroform. This allowed for the material to be characterised by ¹H NMR and GPC analysis, which determined that its molecular weight was extremely low, $M_n = 600 \text{ gmol}^{-1}$ and $M_w = 3,300 \text{ gmol}^{-1}$.



Scheme 88: The preparation of polymer **91**. *Reagents and conditions:* Dimethoxymethane, TFA, 0 °C, 48 hours.

3.4.4 Attempted preparation of TB 1,4-dimethoxybenzene ladder polymer

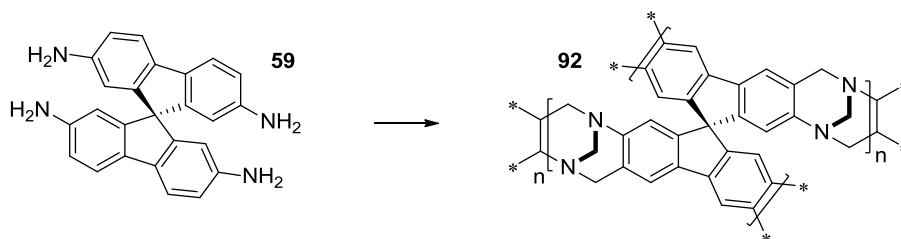
Following the successful synthesis of polymer **91** attempts were made to prepare the analogous polymer with methoxy substituents from the TB polymerisation reaction between compound **56** and dimethoxymethane (Scheme 89). However, the product from this reaction was found to be soluble in all common solvents, including methanol and acetone, which suggested that the product was not polymeric since PIMs are generally not soluble in these two solvents. ^1H NMR analysis showed that the material was a mixture of products, with many peaks appearing in the spectrum, none of which could be identified as belonging to the desired product or starting material. Indeed, the ^1H NMR spectrum showed none of the expected peak broadening expected for a polymer product, instead the peaks were well-defined. Mass spectrometric analysis was then performed on the material, but showed no evidence of the desired product, especially since the highest molecular weight peak was a meagre 300 gmol^{-1} . From this evidence it was clear that the polymerisation reaction had not occurred, but also that none of the monomer was present after reaction. It can be assumed that the monomer broke down in the reaction mixture due to its instability, a problem caused by the activating effect of the methoxy substituents that makes the phenyl ring system very reactive towards oxidation. This polymerisation reaction was repeated a few times, but with consistent results.



Scheme 89: The attempted polymerisation of **56**.

3.4.5 TB spirobisfluorene network polymer (92)

Equally disappointing was the TB polymerisation reaction between compound **59** and dimethoxymethane (Scheme 90). Despite an initial colour change from yellow to dark red, indicative of monomer degradation, the reaction proceeded as expected with the reaction mixture turning solid after 24 hours, as normal for a network polymer. The resulting polymer **92** was found to be insoluble in all of the solvents tested and solid-state ^{13}C NMR analysis gave a spectrum with the expected peaks, indicating that the reaction had successfully occurred. However, the polymer remained a dark colour even after purification, suggesting that the polymer had not properly formed, which is likely due to the oxidation of compound **59** prior to reaction. The reaction was repeated under strictly controlled conditions in an effort to prevent oxidation, but once again the monomer degraded prior to polymerisation.



Scheme 90: The preparation of polymer **92**. *Reagents and conditions:* Dimethoxymethane, TFA, 0 °C, N₂, 24 hours.

3.4.6 Discussion of solubility properties

Once again, a solubility study was performed by thoroughly mixing 50 mg of polymer sample with 2 ml of solvent and assessing how much of the polymer had dissolved after 30 minutes. The solubility of the three ladder polymers (**87**, **88** and **91**) varied greatly owing to their dissimilar structures (Table 9). Polymer **87** exhibited poor or only partial solubility in most of the tested solvents, except for DMF and methanol. Polymer **88** showed similarly poor solubility, but this could be attributed to either π -stacking or cross-linking between polymer chains hindering solvent-polymer interactions. Polymer **91** was found to be only completely soluble in chloroform, which was unexpected considering the small size of each monomer unit that should have allowed for stronger solvent-polymer interactions.

Polymer	Solvent									
	THF	DCM	CHCl ₃	DMF	Ph-Cl	DMAc	NMP	Quinoline	MeOH	Acetone
87	-	++	++	+++	+	++	+++	++	+++	-
88	+	+	+	++	+	++	++	++	-	-
91	+	++	+++	++	+	++	+	++	-	-

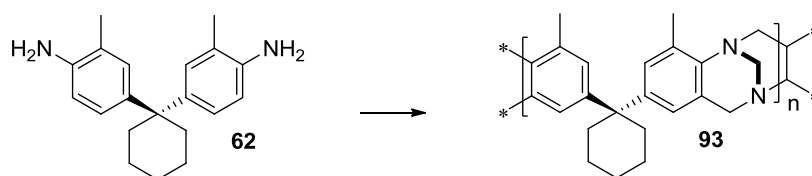
Table 9: Table summarising the solubility of polymers **87** - **92** in a range of solvents. +++ = completely soluble, ++ = mostly soluble, + = partially soluble, - = insoluble.

3.5 Bis-aniline TB polymers (93 – 103)

This section of the chapter describes the synthesis of the TB polymers built from the bis-aniline series of monomers, which share many structural features and were synthesised using the same condensation reaction. The analysis of each polymer is detailed in the next chapter.

3.5.1 Synthesis of polymers 93 - 103

Polymer **93** was generated from the polymerisation reaction between compound **62** and dimethoxymethane (Scheme 91). The material demonstrated excellent solubility in most of the solvents tested, including chloroform, DCM and THF (Table 10). This allowed for complete characterisation of the material, including GPC and NMR analysis, which showed that polymer **93** had the expected structure. GPC analysis against polystyrene standards showed that the material possessed high molecular weight, $M_n = 44,300 \text{ gmol}^{-1}$ and $M_w = 118,400 \text{ gmol}^{-1}$.



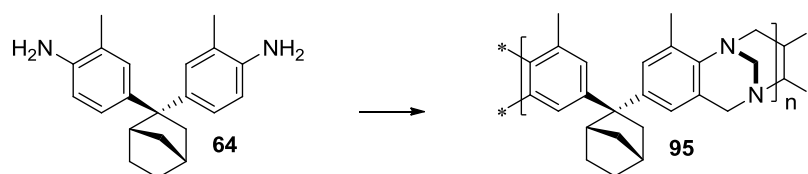
Scheme 91: The polymerisation of **62**. *Reagents and conditions:* Dimethoxymethane, TFA, 0 °C, N₂, 72 hours.

Polymer **94** was designed to be analogous to polymer **93**, but without methyl substituents on the phenyl rings so that their importance could be assessed. The polymerisation reaction was performed between compound **63** and dimethoxymethane (Scheme 92), during which the reaction mixture was observed to get noticeably more viscous. After purification polymer **94** was found to be almost insoluble in all of the solvents tested (Table 10), suggesting that the material had undergone cross-linking between polymer chains during formation. The soluble impurities were analysed by GPC and found to consist of low to moderate molecular weight material, $M_n = 5,800 \text{ g mol}^{-1}$ and $M_w = 35,300 \text{ g mol}^{-1}$, unfortunately, this accounted for a only tiny fraction of the material generated from the reaction, indicating that the polymer chains had reached only moderate molecular weight before cross-linking had occurred. The insolubility of polymer **94** prevented characterisation by ¹H NMR analysis.



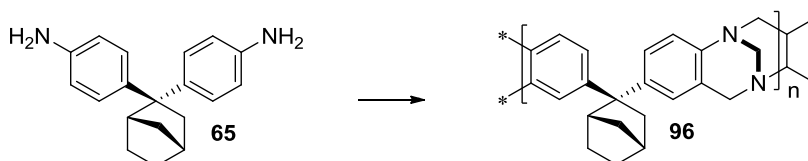
Scheme 92: The polymerisation of **63**. *Reagents and conditions:* Dimethoxymethane, TFA, 0 °C, N₂, 40 hours.

The polymerisation reaction between compound **64** and dimethoxymethane produced polymer **95** (Scheme 93). It displayed excellent solubility in most of the solvent range tested, including chloroform, DCM and THF (Table 10). The high solubility of polymer **95** allowed analysis by GPC, which showed that it consisted of moderate length polymer chains, $M_n = 13,900 \text{ g mol}^{-1}$ and $M_w = 31,600 \text{ g mol}^{-1}$. The difference in the molecular weight for polymers **93** and **95** was peculiar given their similar structures, and could not be explained.



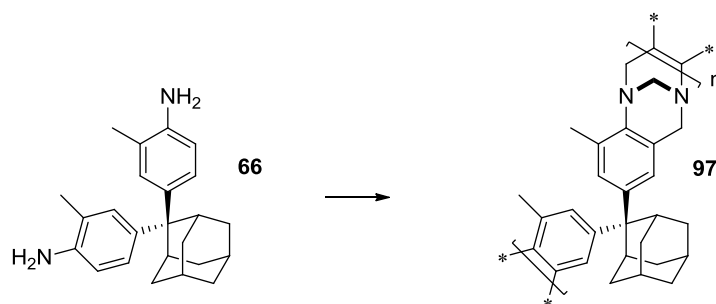
Scheme 93: The polymerisation of **64**. *Reagents and conditions:* Dimethoxymethane, TFA, 0 °C, N₂, 72 hours.

Polymer **96** was designed to be analogous to polymer **95**, but once again lacked methyl substituents on the phenyl rings so that the importance of these groups could be assessed. Polymer **96** was synthesised from the reaction between compound **65** and dimethoxymethane (Scheme 94). The material demonstrated good solubility in the range of solvents tested, but was less soluble than its analogous partner polymer **95** (Table 10). Despite broad peaks being observed in the ¹H NMR spectrum of polymer **96**, GPC analysis showed that it consisted of only very low molecular weight material, $M_n = 1,700 \text{ gmol}^{-1}$ and $M_w = 4,500 \text{ gmol}^{-1}$. This reaction was repeated, but there failed to be any improvement in molecular weight.



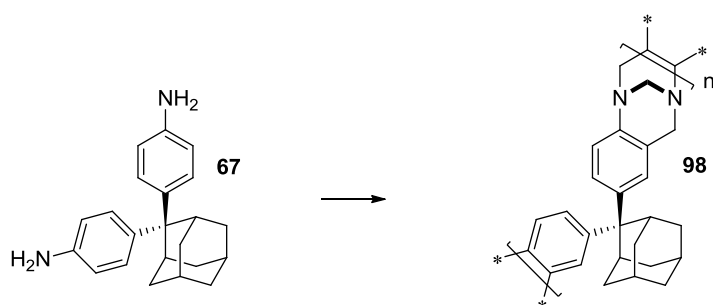
Scheme 94: The polymerisation of **65**. *Reagents and conditions:* Dimethoxymethane, TFA, 0 °C, N₂, 40 hours.

Compound **66** possessed a larger pendant group than the previous monomers (**62** – **65**) and consequently it was predicted that the resulting polymer would exhibit increased microporosity, since the packing of the polymer chains would be hindered by this bulkier group. The polymerisation of compound **66** (Scheme 95) was performed using the new optimised procedure and produced polymer **97**. The material demonstrated excellent solubility in most of the solvent range, but unlike polymers **93**, **95** and **96** displayed poor solubility in DMAc and NMP, which was presumably caused by the bulkier pendant group (Table 10). The molecular weight was determined from GPC analysis and this found that polymer **97** had a very broad, but generally high distribution of molecular weights, $M_n = 31,200 \text{ gmol}^{-1}$ and $M_w = 113,000 \text{ gmol}^{-1}$.



Scheme 95: The polymerisation of **66**. *Reagents and conditions:* Dimethoxymethane, TFA, 0 °C, N₂, 72 hours.

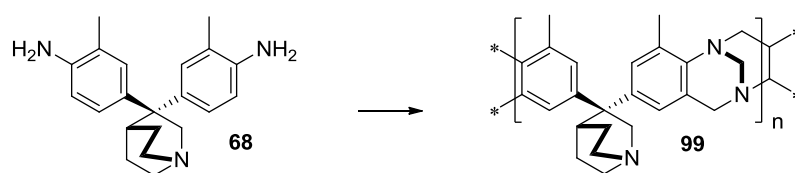
Polymer **98**, designed to be analogous to polymer **97**, was another polymer to be synthesised without methyl substituents on its phenyl rings so that their importance could be assessed. The material was generated from the polymerisation reaction between compound **67** and dimethoxymethane (Scheme 96). After just 16 hours the reaction mixture became so viscous that it could not be stirred, so was quenched. Unfortunately, the resulting material was found to be insoluble in all of the solvents tested (Table 10), indicating that once again cross-linking had occurred between the polymer chains, and prevented characterisation of polymer **98** by GPC or ¹H NMR. The soluble impurities were analysed by GPC, and showed the presence of only low molecular weight material, $M_n = 4,200 \text{ gmol}^{-1}$ and $M_w = 14,800 \text{ gmol}^{-1}$.



Scheme 96: The polymerisation of **67**. *Reagents and conditions:* Dimethoxymethane, TFA, 0 °C, N₂, 16 hours.

In an effort to prepare a TB PIM possessing a third nitrogen per repeat unit compound **68** was reacted with dimethoxymethane using the general procedure for TB polymerisation (Scheme 97). It was predicted that the presence of this third tertiary nitrogen would enhance the affinity of the material for carbon dioxide. Unlike the other bis-aniline monomers, compound **68** took a considerable amount of time to dissolve in trifluoroacetic

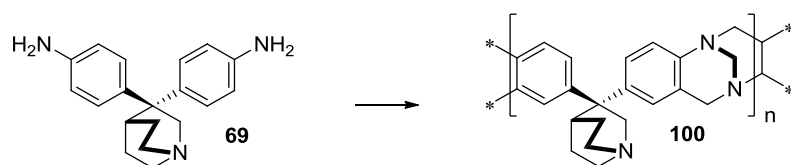
acid, suggesting poor solubility, but eventually became completely dissolved allowing the reaction to be performed.



Scheme 97: The polymerisation of **68**. *Reagents and conditions:* Dimethoxymethane, TFA, 0 °C, N₂, 120 hours.

The product from the reaction (polymer **99**) displayed good solubility in most of the solvent range tested, particularly chloroform, NMP and quinolone (Table 10). Unfortunately, molecular weight determination by GPC analysis showed that the polymer was in fact only oligomers, $M_n = 890 \text{ gmol}^{-1}$ and $M_w = 910 \text{ gmol}^{-1}$. This indicated that the polymerisation reaction had not been successful, terminating before the production of even modest molecular weight polymer. There are three possible explanations for this behaviour: the monomer may have degraded during the harsh conditions necessary for its purification, the oligomers may have crashed out of solution shortly after their production due to poor solubility or the monomer may have degraded quickly in trifluoroacetic acid due to its poor stability. The reaction was repeated using strictly controlled conditions, but no improvement in the quality of the product was made.

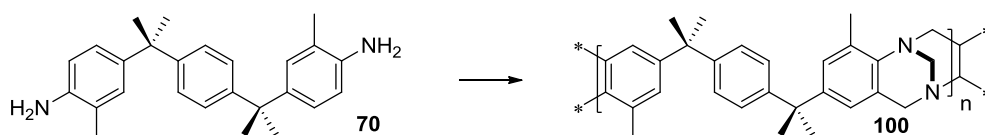
Yielding equally disappointing results was the polymerisation reaction of compound **69** with dimethoxymethane (Scheme 98) to give polymer **100**. This material was found to demonstrate lower solubility than the analogous polymer **99**, but was found to be completely soluble in chloroform, DMF, DMAc, NMP and quinolone (Table 10). Unfortunately, GPC analysis showed that the molecular weight of polymer **100** was as poor as for polymer **99**, $M_n = 900 \text{ gmol}^{-1}$ and $M_w = 930 \text{ gmol}^{-1}$. This may be explained either by the degradation of compound **69** during purification, its instability in trifluoroacetic acid or the poor solubility of the oligomers in trifluoroacetic acid. Once again, the reaction was repeated using strictly controlled conditions, but no improvement in the quality of the product was made. The poor properties of polymers **99** and **100** indicated that neither monomer was suitable for generating high molecular weight material, so work instead focussed on more promising monomers.



Scheme 98: The polymerisation of **69**. *Reagents and conditions:* Dimethoxymethane, TFA, 0 °C, N₂, 120 hours.

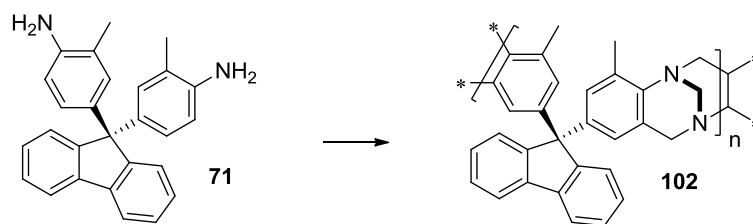
At this point it is worth mentioning that compounds **63**, **65**, **67** and **69**, which lack methyl substituents on the phenyl rings, appear to either undergo cross-linking during polymerisation or fail to achieve even moderate molecular weight. Therefore, for the remainder of the project work focussed on preparing monomers with these important methyl substituents, from which TB PIMs with useful and interesting properties were generated.

Polymer **101** has a structure possessing considerable flexibility and consequently was predicted to be non-microporous, but it was hoped that this flexibility would also result in excellent solubility behaviour and high molecular weight. The material was synthesised from the polymerisation reaction between compound **70** and dimethoxymethane (Scheme 99). It displayed excellent solubility in all of the solvents tested, except for DMF and DMAc (Table 10). This allowed GPC analysis to be performed, which determined that the material consisted of high molecular weight polymer, $M_n = 51,900 \text{ gmol}^{-1}$ and $M_w = 99,600 \text{ gmol}^{-1}$.



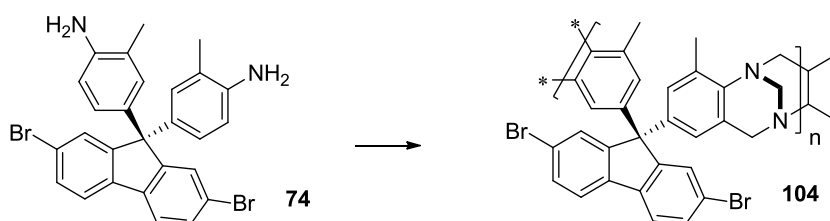
Scheme 99: The polymerisation of **70**. *Reagents and conditions:* Dimethoxymethane, TFA, 0 °C, 72 hours.

The polymerisation reaction between compound **71** and dimethoxymethane produced polymer **102** (Scheme 100). The material displayed excellent solubility in DCM, chloroform, NMP and quinoline, but showed only partial solubility in the remainder of the solvents tested (Table 10). GPC analysis showed that the material consisted of only moderate molecular weight polymer chains, $M_n = 13,800 \text{ gmol}^{-1}$ and $M_w = 33,600 \text{ gmol}^{-1}$. Despite repeating the reaction no improvement in molecular weight was made.



Scheme 100: The polymerisation of **71**. *Reagents and conditions:* Dimethoxymethane, TFA, 0 °C, N₂, 96 hours.

The final member in this series, polymer **103**, was synthesised from the reaction between **74** and dimethoxymethane (Scheme 101). It demonstrated quite different solubility behaviour compared to that of the analogous polymer **102**, with increased solubility in most of the solvents tested, but strangely, only partial solubility in dichloromethane (Table 10). The increased solubility appears to be a direct consequence of the presence of bromine substituents within the structure of the polymer, but this could also have caused a significant drop of solubility in dichloromethane. Following GPC analysis it was clear that the material consisted of only moderate molecular weight polymer chains, $M_n = 20,400 \text{ gmol}^{-1}$ and $M_w = 43,300 \text{ gmol}^{-1}$. This was another polymer whose synthesis was repeated, but unfortunately, no improvement in molecular weight was achieved.



Scheme 101: The polymerisation of **74**. *Reagents and conditions:* Dimethoxymethane, TFA, 0 °C, N₂, 72 hours.

3.5.2 Discussion of solubility properties

Once again, a solubility study was performed by thoroughly mixing 50 mg of polymer sample with 2 ml of solvent and assessing how much of the polymer had dissolved after 30 minutes. Almost all of the polymers showed excellent solubility properties in most of the solvent range tested (Table 10). The two exceptions to this were polymers **94** and **98**, which underwent cross-linking during the polymerisation reaction, appearing to be a

consequence of a lack of methyl substituents adjacent to the amine group. Even polymers **99** and **100** showed complete solubility in most of the tested solvents, but their extremely poor molecular weight may have been an influencing factor. Molecular weight and relative bulkiness of the pendant group seemed to have little effect on the solubility properties of the polymers, which may be a direct result of the comparative flexibility of each polymer compared to traditional PIMs. This flexibility helps the polymer chains adopt a structural conformation that enhances solvent-polymer interactions, and thus results in excellent solubility properties.

Polymer	Solvent									
	THF	DCM	CHCl ₃	DMF	Ph-Cl	DMAc	NMP	Quinoline	MeOH	Acetone
93	+++	+++	+++	-	+++	++	+++	+++	-	-
94	-	-	-	-	-	-	-	-	-	-
95	+++	+++	+++	-	+++	+++	+++	+++	-	-
96	++	+++	+++	-	++	+++	+++	+++	-	-
97	+++	+++	+++	-	+++	-	+	+++	-	-
98	-	-	-	-	-	-	-	-	-	-
99	+	+	+++	+++	+	+++	+++	+++	+	-
100	-	++	+++	+++	-	+++	+++	+++	-	-
101	+++	+++	+++	+	+++	+	+++	+++	-	-
102	++	+++	+++	+	+	+	+++	+++	-	-
103	+++	+	+++	++	++	++	+++	+++	-	-

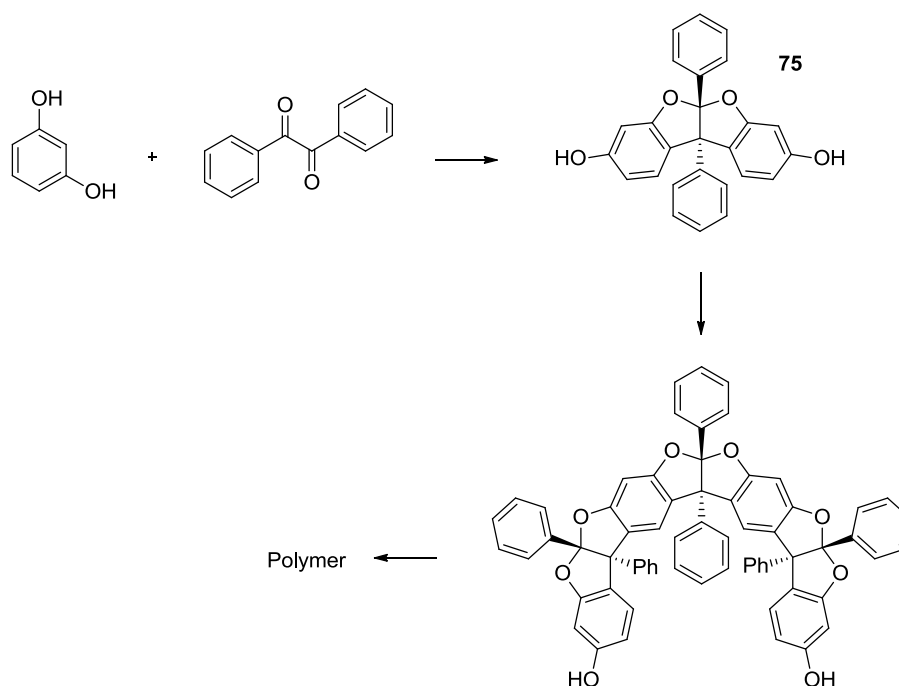
Table 10: A comparison of the solubility properties for polymers **93** - **103** for a variety of solvents. +++ = completely soluble, ++ = mostly soluble, + = partially soluble, - = insoluble.

3.6 Polymerisation of coumaron derivatives

Two strategies were devised for the synthesis of coumaron-based polymers; the first was to alter the stoichiometry of the coumaron forming condensation reaction so that additional benzil and resorcinol molecules were added to the coumaron framework, thus building a polymer via step-growth polymerisation. The second approach involved the preparation of compound **80**, which could be polymerised with tetrafluoroterephthalonitrile using the conventional dibenzodioxane-forming reaction to generate a coumaron-based PIM. It was believed that either approach would produce a material with useful properties, owing to the rigid coumaron building block, which would ensure high microporosity in the resulting polymer. Unfortunately, for different reasons neither strategy was successful.

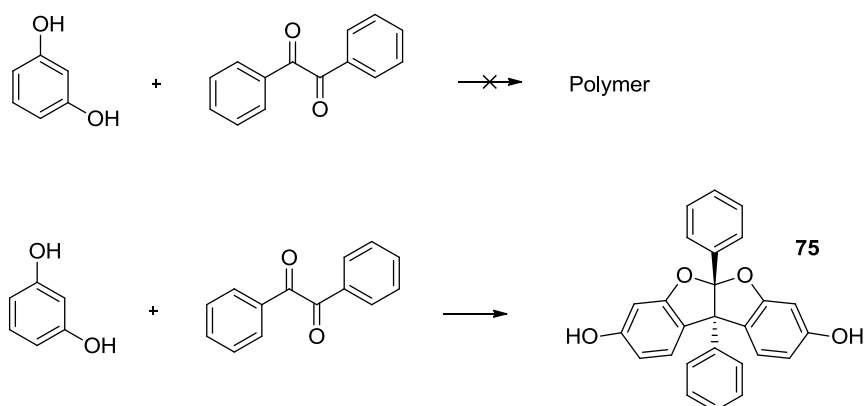
3.6.1 Attempted preparation of a polymer using a coumaron-forming condensation reaction

Following the successful optimisation of the condensation reaction used for the preparation of coumaron, an investigation was conducted to assess whether the reaction would continue if the stoichiometry was altered, resulting in the preparation of a polymer. This was thought possible because using the optimised procedure between resorcinol and benzil it is possible to generate compound **75** in excellent yield (> 85%), indicating a highly efficient reaction, which is necessary for step-growth polymerisation. Furthermore, it was believed that since compound **75** possessed two hydroxyl groups it would be able to react further with benzil, (Scheme 102).



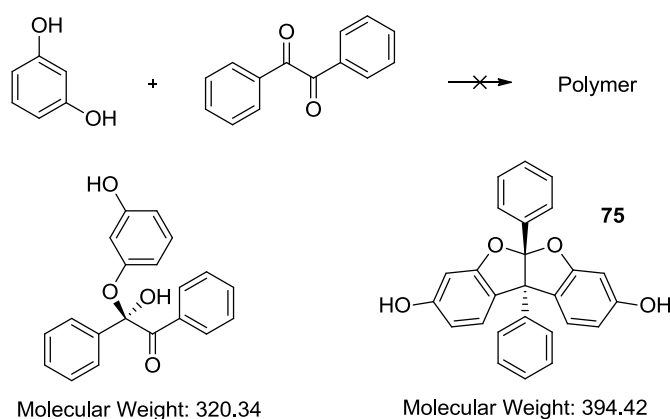
Scheme 102: The proposed preparation of coumaron-based polymers.

Polymerisation was initially attempted using the conditions for optimised coumaron formation, but with a 1:1 stoichiometry of benzil to resorcinol. However, after 96 hours of stirring the only product from the reaction was found to be compound **75** (Scheme 103). This was isolated in relatively low yield (28%) from the reaction mixture, the remainder of which was found to be starting material, indicating that whilst the condensation had occurred, it had done so inefficiently due to the reaction stoichiometry. The reaction was repeated, but when this also failed to produce any product other than compound **75** it became clear that different conditions were required.



Scheme 103: The attempted synthesis of a coumaron-polymer, highlighting what was produced from the reaction. *Reagents and conditions:* Chloroform, HCl, acetic acid, 60 °C, 96 hours.

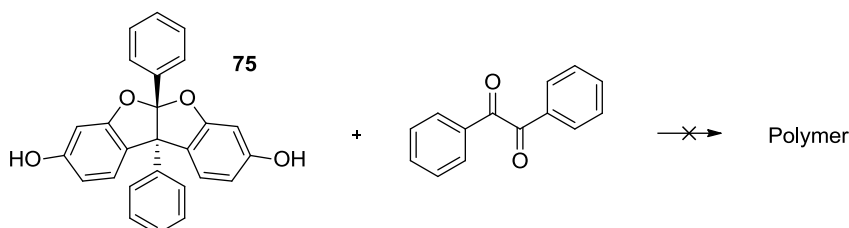
After consideration of the results from the previous reaction it appeared that harsher conditions were required to make the reaction more efficient. So the reaction was repeated, but at an elevated temperature. The temperature chosen was the boiling point of acetic acid, since resorcinol and benzil had previously been found to be completely soluble in hot acetic acid, but unfortunately this precluded the use of chloroform as co-solvent. Therefore the reaction was performed using only a refluxing mixture of glacial acetic acid and concentrated hydrochloric acid (Scheme 104). After a long reaction duration the reaction mixture was analysed by ^1H NMR and mass spectrometry, which showed that the major component of the mixture was benzil, but also indicated the presence of slightly higher molecular weight material. Unfortunately, no structure could be assigned to most of the peaks found by mass spectrometry, suggesting that they were fragments from larger molecules. One of the peaks that could be assigned belonged to the product of nucleophilic attack from resorcinol on benzil (320 gmol^{-1}), whilst the other belonged to compound **75** (394 gmol^{-1}), but there was no evidence to suggest that it had undergone further reaction.



Scheme 104: The second attempted synthesis of a coumaron-polymer, highlighting what was produced from the reaction. *Reagents and conditions:* Chloroform, HCl, acetic acid, 120 °C, 96 hours.

In an attempt to avoid any unwanted products from side-reactions and boost the efficiency of the reaction to produce polymer the procedure was altered. Instead of using a 1:1 mixture of resorcinol and benzil the reaction was performed using a 1:1 mixture of compound **75** and benzil (Scheme 105), which was thought would simplify the preparation of polymer whilst limiting the number of possible side-reactions. To further help to avoid unwanted side-reactions the original milder conditions were used for this reaction, since it was believed that if these conditions did not prove sufficient for the preparation of polymer the reaction would at least produce some oligomeric material. Frustratingly, this was not

the case and after analysis of the reaction mixture by ^1H NMR and mass spectrometry it became clear that no reaction had occurred, since both starting materials were recovered in full. The reaction was not repeated under harder conditions, as it believed that this would have only helped if any reaction had occurred, instead as no reaction happened it appeared that something was fundamentally wrong with the chemistry.



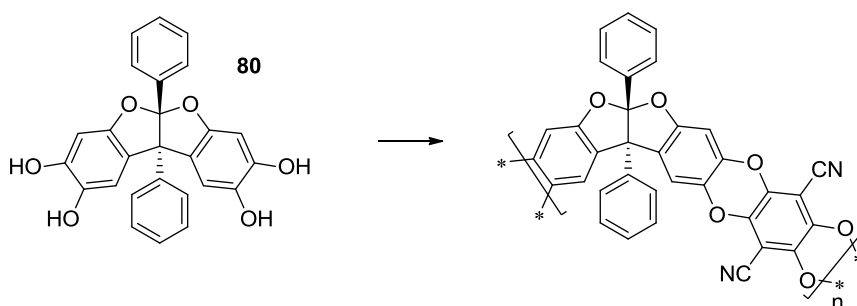
Scheme 105: The third attempted synthesis of a coumaron-polymer. *Reagents and conditions:* Chloroform, HCl, acetic acid, 120 °C, 48 hours.

This completes the discussion of this polymerisation strategy, which failed to produce any polymer. After careful analysis of the results it appears that this failure can be explained by the poor reactivity of compound **75** to further reactions, which is caused by the rigidity and bulkiness of the compound. This causes steric hindrance preventing the necessary nucleophilic attack from the hydroxyl group of compound **75** on a protonated ketone of benzil. Resorcinol can perform this nucleophilic attack on a protonated ketone of benzil since it is significantly smaller than **75** and therefore does not suffer from the same steric hindrance. Thus this strategy does not seem suitable for the preparation of a coumaron-based polymer, at least under the conditions trialled.

3.6.2 Attempted polymerisation of 2,3,8,9-tetrahydroxy-5a,10b-diphenylcoumarano-2,2',3,3'-coumaron

The second and simpler strategy for the preparation of a coumaron-based polymer was the dibenzodioxane polymerisation of compound **80** with tetrafluoroterephthalonitrile (Scheme 106), using the procedure previously optimised for PIM synthesis⁸¹. Despite the challenges that had been encountered whilst preparing compound **80**, ^1H NMR and mass spectrometric analysis had found it to be pure so it was believed that the polymerisation reaction would occur without any significant problems. Shortly after the addition of potassium carbonate the reaction mixture was observed to be a bright yellow suspension,

typical for a successful PIM polymerisation, so it was assumed that the reaction was proceeding well. However, after stirring for 96 hours and following work-up, the material isolated from the reaction was found to be soluble in acetone and methanol, suggesting that it consisted of only oligomers, since PIMs are generally not soluble in either of these solvents. This was confirmed by ^1H NMR analysis, which showed that the product from the reaction was a mixture of compounds, none of which was compound **80**, and lacked any signs of peak broadening, usually observed for polymers. It was concluded from this evidence, that the polymerisation reaction did not occur and instead compound **80** underwent oxidation in the presence of hot base, since it had previously shown signs of poor stability only at room temperature. Thus, this strategy also failed to produce any polymer.



Scheme 106: The dibenzodioxane polymerisation of 2,3,8,9-tetrahydroxy-5a,10b-diphenylcoumarano-2,2',3,3'-coumaron. *Reagents and conditions:* Tetrafluoroterephthalonitrile, DMF, K_2CO_3 , N_2 , 65°C , 96 hours.

At this late stage in the project no further time remained for attempting an alternative route for a coumaron-based PIM, so it could not be established whether the coumaron-framework would prove, as predicted, to be a useful building block for PIM synthesis.

Chapter 4: Discussion of polymer properties

This chapter details the properties of each of the polymers described in Chapter 3, which were carefully analysed by various methods in order to gain a better understanding of the suitability of each polymer as carbon dioxide capture materials. To be useful for carbon dioxide capture a TB polymer must be highly microporous, thermally stable and capable of forming a robust membrane, whilst possessing high capacity and permeability towards carbon dioxide. Network polymers were also assessed briefly for catalytic activity.

4.1 Microporosity

Analysis of the microporosity for each polymer was performed by measuring the nitrogen adsorption isotherm, from which the BET apparent surface area and pore volume was calculated. As predicted, the polymers generated during this project showed considerable variation in their microporous behaviour (Table 11), which can be explained given the diverse range of monomer building blocks. Nevertheless, this comparison highlights several useful trends in the structural requirements necessary for high microporosity. For example, all but one of the polymers built around the triptycene unit (polymers **82 – 86**) exhibited high microporosity, indicating that as predicted the rigid non-planar structure of triptycene hinders the polymer chains from packing space efficiently. It is also apparent from the data that the presence of large atoms, such as bromine or iodine, in the polymer structure (polymers **83, 89** and **90**) results in poor microporosity as the large atoms effectively fill the pores. Those polymers possessing great flexibility in their structures (polymers **87, 93** and **101**) demonstrate poor microporosity as the polymer chains are able to adopt a conformation to allow space efficient packing.

Polymer	Type	Number	Surface area (m ² /g)	Pore Volume (ml g ⁻¹)
TB Triptycene	Ladder	82	725	0.51
TB 2,3-Dibromotriptycene	Ladder	83	10	0.01
TB 9,10-Dimethyltriptycene	Ladder	84	775	0.57
TB Triptycene	Network	85	1035	0.63
TB 9,10-Dimethyltriptycene	Network	86	750	0.48
TB Dibenzo-18-crown-6	Ladder	87	3	0.02
TB Naphthalene	Ladder	88	700	0.32
Iodine stabilised quaternary TB naphthalene	Ladder	89	3	0.03
Sulphate stabilised quaternary TB naphthalene	Ladder	90	0	0.01
TB 1,4-Dimethylbenzene	Ladder	91	430	0.35
TB Spirobisfluorene	Network	92	0	0.00
TB Cyclohexane bis-methylaniline	Ladder	93	30	0.09
TB Cyclohexane bis-aniline	Ladder	94	50	0.21
TB Norcamphor bis-methylaniline	Ladder	95	70	0.37
TB Norcamphor bis-aniline	Ladder	96	4	0.03
TB Adamantane bis-methylaniline	Ladder	97	615	0.41
TB Adamantane bis-aniline	Ladder	98	50	0.25
TB Quinuclidinone bis-methylaniline	Ladder	99	55	0.21
TB Quinuclidinone bis-aniline	Ladder	100	10	0.05
TB Bis(hydroxyisopropyl)benzene bis-methylaniline	Ladder	101	6	0.02
TB Fluorene	Ladder	102	400	0.47
TB Dibromofluorene	Ladder	103	390	0.44

Table 11: Comparison of the BET surface areas for polymers **82** - **103**.

All of the triptycene based polymers, except for polymer **83**, displayed high surface areas with type I isotherms, showing considerable adsorption of nitrogen prior to $p/p_o = 0.01$ (Figure 46). This batch of polymer **82** was made using the newly optimised procedure and continued the trend seen for other batches of the material, whereby a lower microporosity was observed with an increase in molecular weight. The poor surface area exhibited by polymer **83** suggests that the bromine atoms effectively fill the pore volume that would

otherwise be available for adsorption. The similarity in the isotherms and surface areas between polymers **82** and **84** indicates that the presence of the methyl bridgehead substituents has very little effect on the microporosity of the polymer, which is contrary to that observed for previously prepared triptycene-based PIMs⁹². It is clear from the comparison that polymer **85** has the largest surface area, which was expected due to its 3D rigid framework structure. However, it was unexpected that the analogous polymer **86** would exhibit a significantly lower surface area; this may be caused by the bridgehead methyl substituents partially filling the available pore volume.

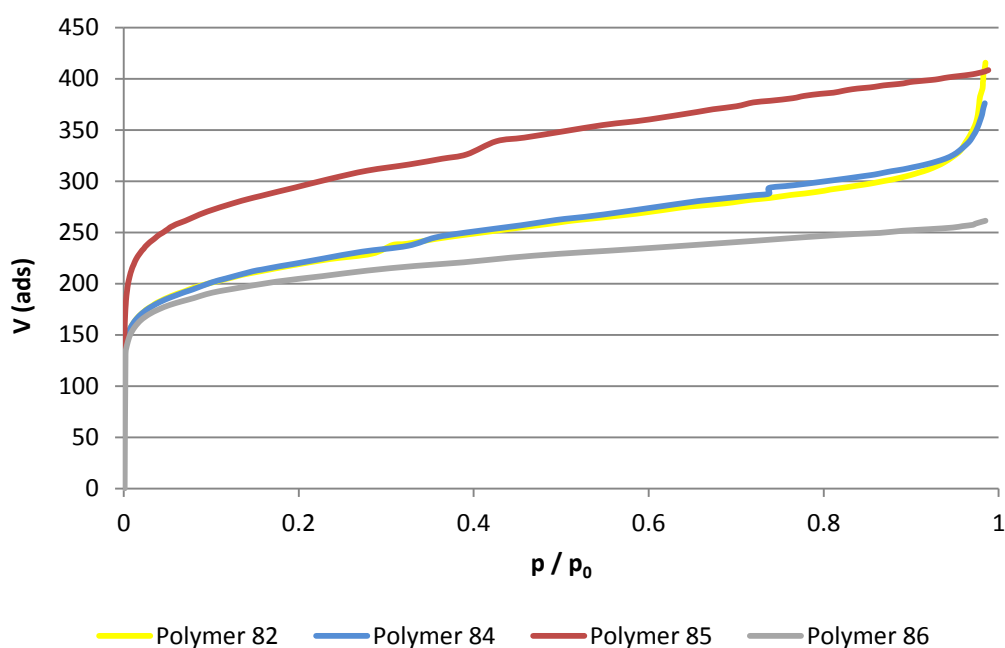


Figure 46: A comparison of the nitrogen adsorption isotherms for polymers **82** – **86**. Polymer **83** has been omitted because the polymer was found to be non-porous.

Polymers **87**, **89**, **90** and **92** were found to be non-porous, whilst polymers **88** and **91** displayed moderate to high microporosity with type I isotherms (Figure 47). Polymer **87** was non-porous as its flexible structure allowed the polymer chains too much flexibility, resulting in space efficient packing. Polymers **88** and **91** display more microporosity than had predicted since its monomer lacked a site of contortion, but this result proves that TB links provide sufficient contortion to hinder space efficient packing. The surface area of polymer **88** was found to be drastically reduced after conversion to the quaternary amine polymers (**89** – **90**), suggesting that the counter ions fill the pore space, effectively making the polymers non-porous. This significant loss of microporosity raised doubts over how useful the quaternary process was and meant that no further work in this area was

performed for the remainder of the project, which instead focussed on the synthesis of TB polymers from different building blocks. Polymer **92** was found to be non-porous, which was surprising considering that the monomer (compound **59**) possesses a well-defined site of contortion, but this can be explained by the poor stability of the monomer, which hindered the formation of the network polymer.

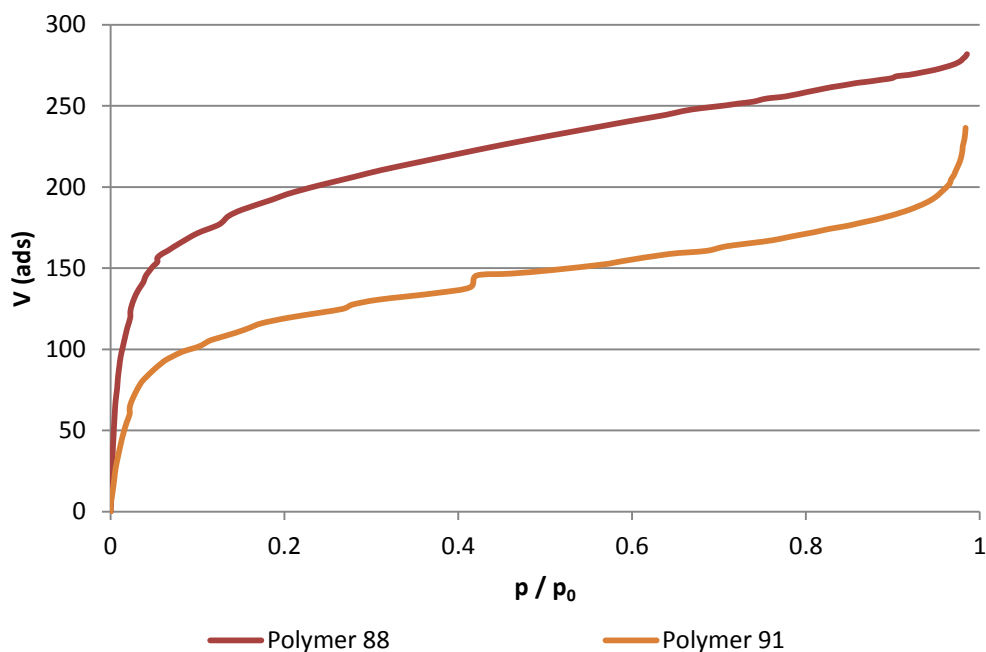


Figure 47: A comparison of the nitrogen adsorption isotherms for polymers **88** and **91**. Polymers **89**, **90** and **92** have been omitted because they were found to be non-porous.

The microporosity of the bis-aniline family of polymers was spread over a wide range; with polymers **93** – **96** and polymers **98** – **101** displaying little or no microporosity, whilst polymers **97**, **102** and **103** demonstrated moderate to high microporosity with type I isotherms (Figure 48). The size of the group between the two phenyl rings seems to play an important role in the microporosity of the resulting polymer, with the polymers formed from monomers with bulkier groups exhibiting larger microporosity as a consequence of hindered rotation within the monomeric unit. Polymers **93** and **101** possessed the smallest pendant groups and hence showed the least microporosity of the series whereas polymers **97**, **102** and **103**, with the bulkier pendant groups displayed the greatest microporosity.

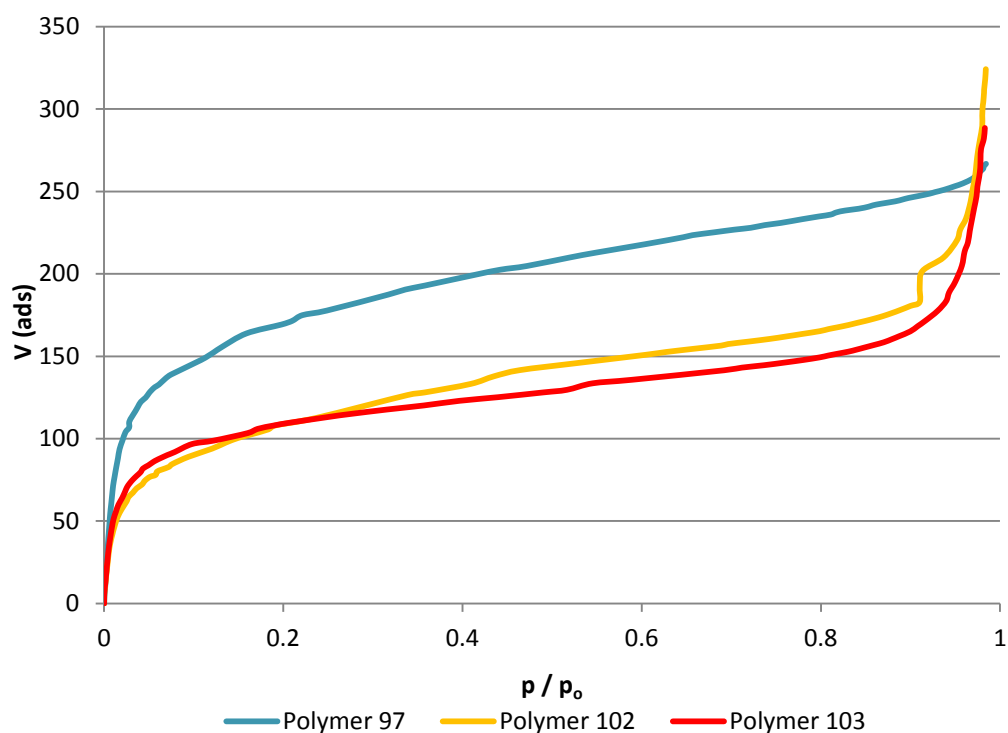


Figure 48: A comparison of the nitrogen adsorption isotherms for polymers **97**, **102** and **103**. Polymers **98** – **101** have been omitted because the polymers were found to exhibit low microporosity or to be non-porous.

Polymer **93** was found to be almost non-porous, which was expected considering that it possesses considerable flexibility since it lacks a fused ring skeleton, so the polymer chains can pack space efficiently. The analogous material, polymer **94** was found to be slightly more microporous, which may have been a result of the cross-linking between polymer chains that produced a network and hindered the mobility of the polymer chains, limiting efficient packing in the solid state.

Polymer **95** was found to be slightly porous, suggesting that the methyl bridge hindered the flexibility of the polymer chains, resulting in less efficient packing and consequently, higher microporous than observed for polymer **93**. The analogous polymer **96**, which lacked phenolic methyl substituents, was found to be almost non-porous due to the increased flexibility of the phenyl groups around the pendant group. Polymer **97** possesses a relatively bulky pendant group, and consequently exhibited high microporosity as the flexibility and packing of the polymer chains was hindered. However, the analogous polymer **98** was found to have substantially lower microporosity than polymer **97**, which may have been caused by the low molecular weight of the material and the cross-linking that it underwent during formation.

Polymers **99** and **100** both demonstrated poor microporosity as a direct result of their low molecular weight, although that either demonstrated any microporosity suggests that if their molecular weight could be improved substantially then the materials would likely be highly microporous. Unfortunately, this is unlikely due to the problems discussed previously. Polymer **101** exhibited low microporosity, which was predicted since the polymer chains possess considerable flexibility that allow them to pack space efficiently, thereby eliminating voids between chains. Polymers **102** and **103** both possess the bulky fluorene pendant group, which hinders the flexibility of the polymer chains, resulting in poor packing in solid-state and thus, moderate microporosity. It is interesting to note that both polymers have remarkably similar surface areas as it was anticipated that the two bulky bromine substituents on the fluorene pendant group of polymer **103** would occupy much of the available pore space, as seen in polymer **83**, reducing the microporosity of the material. Therefore, it may be that the bromine atoms are helping to maintain microporosity by forcing the polymer chains further apart.

4.2 Thermal stability

Thermal stability is a particularly important property for a material to possess. For the materials discussed in this thesis thermal stability was measured by slowly heating a small sample of the material up to 1000 °C using Thermogravimetric analysis and recording the temperature at which polymer degradation started to occur (T_{onset}) together with the total weight lost by the material from the process after T_{onset} . The best materials will be those with a high T_{onset} and small weight loss, indicating a thermally stable material. Each of the polymers showed minor loss of weight, <5%, prior to 150 °C, resulting from the loss of residual solvent molecules. The results from this thermal analysis are discussed and compared below (Table 12).

Each of the triptycene-based polymers (**82** – **86**) demonstrated excellent thermal stability, with a T_{onset} of at least 290 °C, but for most of the materials this was greater than 350 °C. The thermal analysis showed that each polymer only lost between 21 and 41% of its weight, indicating that the polymers make good precursors for carbonised materials. The network polymers lost the least weight during the analysis, due to their strong and rigid framework structure that proved more resistant to degradation than the related ladder

polymers. Polymer **83** lost the greatest weight from the thermal analysis (41%), which is likely to be caused by the carbon-bromine bonds breaking at elevated temperatures, causing a significant loss of weight. Polymer **86** had the lowest T_{onset} of the group (294 °C), possibly due to the methyl groups facilitating the retro Diels-Alder reaction at a lower temperature.

Polymer **87** had an early T_{onset} (201 °C) and lost a considerable amount of weight from the thermal analysis (55%), suggesting that the material was not particularly stable at elevated temperatures. This can be explained by the large crown ether system contained in the polymer structure, which would not be resistant to heat. Polymer **88** had a significantly higher T_{onset} , but lost the greatest weight of any of the studied polymers (71%) from the analysis, indicating that the polymer is thermally stable up to T_{onset} , but quickly degrades after that point.

Polymer	Type	T _{onset} (°C)	Weight loss after T _{onset} (%)
82	Ladder	400	31
83	Ladder	350	41
84	Ladder	376	33
85	Network	423	21
86	Network	294	29
87	Ladder	201	55
88	Ladder	400	71
89	Ladder	201	52
90	Ladder	184	34
91	Ladder	304	38
92	Network	34	29
93	Ladder	332	59
95	Ladder	350	59
97	Ladder	470	*
98	Ladder	349	58
99	Ladder	368	59
100	Ladder	393	52
102	Ladder	376	41
103	Ladder	350	59

Table 12: A comparison of the thermogravimetric analysis results for polymers **82 - 103**. Due to equipment failure polymers **94, 96, 98** and **101** were not tested.

Polymers **89** and **90** had significantly lower T_{onset} values than their precursor (polymer **88**), which may be explained by the relatively easy loss of methyl groups from the quaternary nitrogens. The T_{onset} of polymer **90** was particularly low (35 °C) and the polymer continued to degrade after this temperature, losing approximately 35% of its weight by 400 °C. Polymer **91** showed good thermal stability, with a high T_{onset} and low weight loss after the analysis, highlighting the strength of the TB links, even when the polymer possesses only low molecular weight. Polymer **92** was found to have a low T_{onset}, but lost only 29% of its

weight after the analysis, suggesting that despite its low microporosity the material did possess a stable network framework.

Unfortunately, due to equipment failure, the thermal stability of some of the bis-aniline family of polymers (**94**, **96**, **98** and **101**) could not be measured. Those from this series that were tested demonstrated excellent thermal stability, with T_{onset} values between 332 and 470 °C, although only polymer **97** exceeded 400 °C. Polymer **93** showed the least thermal stability, which was peculiar as it possessed the highest molecular weight. An interesting result was observed for polymer **97**, which was found to degrade violently after the T_{onset} and upset the finely tuned balance, thus preventing calculation of the weight lost after heating to 1000 °C. The other polymers were found to lose between 41 and 59% of their weight during the thermal analysis, although only polymer **103** had lost less than 52% of its weight after the analysis. This can be explained by the presence of the bromine atoms in the structure of **103**, which add significant weight to the polymer and thus skew the percentage weight loss.

In summary, the TB polymers generally showed excellent thermal stability, with only a few notable exceptions. The low mass loss at high temperature suggests application for some of these polymers as carbon precursors.

4.3 Film formation

As previously stated, the aim of this project was to create highly microporous nitrogen-containing polymers suitable for carbon dioxide capture, but it was desirable for the ladder polymers to also be highly soluble and capable of forming robust self-standing membranes. For those polymers found to be soluble in chloroform useful information indicating the likelihood of robust film-formation was obtained from GPC analysis, which measures molecular weight against polystyrene standards. Materials with high molecular weight are more likely to successfully form robust films because the long polymer chains can entangle. In order to investigate the film-forming properties of the TB polymers, an attempt was made to form a membrane from every polymer with a molecular weight (M_w) greater than 30,000 g mol^{-1} and those polymers which proved insoluble in chloroform, but soluble in other organic solvents.

Membrane preparation was performed by dissolving a sample of the polymer (approximately 600 mg) in a small volume of a suitable solvent (approximately 20 ml). Once the polymer was completely dissolved, the solution was filtered through cotton wool and transferred to a Teflon dish with a glass cover. The solvent was then allowed to slowly evaporate, eventually leaving behind the polymer either as a whole film or, if unsuccessful, brittle fragments of film. Higher boiling points solvents obviously take longer to evaporate, often needing the application of heat to achieve full evaporation. The results from the membrane preparation for each of the suitable polymers are given below in Table 13. In each case the strength of each membrane was assessed by seeing if it was sufficiently robust to survive bending, those membranes that survived intact without breaking were deemed successful.

Polymer	Type	Molecular weight M_w (g mol ⁻¹)	Solvent	Film forming?
82	Ladder	51,000	Chloroform	Yes
83	Ladder	-	NMP	No
87	Ladder	-	NMP	No
93	Ladder	118,400	Chloroform	Yes
95	Ladder	31,600	Chloroform	No
97	Ladder	113,000	Chloroform	Yes
101	Ladder	99,600	Chloroform	Yes
102	Ladder	33,600	Chloroform	No
103	Ladder	43,300	Chloroform	No

Table 13: The membrane forming properties of the most appropriate polymers, the polymers omitted were either insoluble or were found to have insufficient molecular weight to warrant an attempt at membrane formation.

This data seems to indicate that for a TB polymer to successfully form a strong membrane a molecular weight (M_w) of at least 50,000 g mol⁻¹ is necessary. This threshold is apparent from a comparison of polymers **82** and **103**, which had similar molecular weights (M_w) of 51,000 and 43,000 g mol⁻¹, respectively, but different results from the film preparation process. Rather than a strong membrane polymer **103** produced a membrane that cracked into large fragments when bent, indicating that if the molecular weight could be even slightly improved the membrane would be sufficiently strong, unfortunately this was not

achieved during the project. Those polymers with a lower molecular weight (M_w) less than 50,000 g mol^{-1} failed to produce a robust membrane, whilst those with a higher molecular weight (M_w) produced strong and self-standing membranes capable of withstanding bending. Polymers **83** and **87** failed to produce more than small fragments of polymer membrane, indicating that their molecular weight was insufficient for membrane formation. Of these materials, only the synthesis of polymers **82** and **97** was repeated using the new optimised procedure, so it is likely that if the synthesis of the other polymers was repeated under these conditions higher molecular weight polymer could be generated allowing the preparation of several new and interesting polymer membranes.

4.4 Gas permeation properties

Each polymer membrane that proved sufficiently strong to withstand bending without cracking was sent to Dr. John Jansen of the Institute on Membrane Technology (ITM) Italy for single-gas permeation measurements. This analysis provided useful and important data on the selectivity and permeability of each membrane towards select gases, indicating the usefulness of each polymer towards the separation of particular gas pairs. In order to gain better understanding of these results and draw insightful conclusions a comparison has been made between these TB membranes, a TB polymer based on ethanoanthracene (TB Ethanoanthracene) and PIM-1. TB Ethanoanthracene is a recently published TB ladder polymer¹²³ synthesised by another member of the research group, Mr Richard Malpass-Evans, using similar techniques to those described in this thesis. It has a rigid structure similar to the TB triptycene polymers, but instead of a bridging phenyl ring has only an ethyl bridge (Figure 49). It is highly microporous, with a BET surface area of 1030 m^2/g , the highest recorded for any ladder PIM.

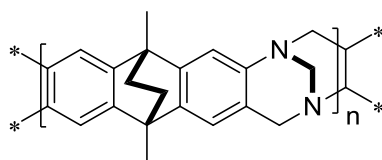


Figure 49: The structure of TB Ethanoanthracene.

As previously discussed PIM-1 is the most studied PIM for membrane application⁹³ and provides a useful standard for comparison. In practice for a membrane to be useful for CO₂ capture it must possess better selectivity than that offered by PIM-1⁹⁴.

Before discussion of the gas permeation results it is important to look at the variety in microporosity between the six film-forming polymers (Table 14), as those with higher microporosity will generally have higher permeability to aid gas transport through the polymer membrane. Hence, TB Ethanoanthracene and PIM-1 should exhibit the highest permeabilities, whilst polymers **93** and **101** should exhibit the lowest.

Polymer	BET Surface area (m ² /g)
PIM-1	850
TB Ethanoanthracene	1030
Polymer 82	725
Polymer 97	615
Polymer 93	30
Polymer 101	6

Table 14: A comparison of the BET surface areas for the six polymers.

The remaining commentary is divided into two sections, comparison of the membrane properties prior to treatment with methanol (Table 15), followed by comparison of membrane properties after methanol treatment, where such information exists (Table 16). This allows for a fair comparison between the polymers to be made, especially for those polymers where membrane properties have not been measured after treatment with methanol to purge any residual chloroform.

Polymer		O ₂	N ₂	He	H ₂	CO ₂	CH ₄
PIM-1	Selectivity (PX/N ₂)	3.97	1.00	6.20	13.25	22.95	1.38
	Average permeability (Barrer)	600	151	936	2001	3465	208
TB Ethanoanthracene	Selectivity (PX/N ₂)	3.25	1.00	3.48	8.21	16.22	2.08
	Average permeability (Barrer)	205	63	219	517	1022	131
82	Selectivity (PX/N ₂)	3.33	1.00	3.54	8.20	17.63	2.24
	Average permeability (Barrer)	153	46	163	377	811	103
93	Selectivity (PX/N ₂)	6.25	1.00	54.01	68.40	26.57	1.07
	Average permeability (Barrer)	2	1	21	26	10	1
97	Selectivity (PX/N ₂)	4.88	1.00	10.49	19.63	24.39	2.04
	Average permeability (Barrer)	40	8.2	86	161	200	16.7
101	Selectivity (PX/N ₂)	6.63	1.00	42.70	52.20	26.37	1.54
	Average permeability (Barrer)	3.58	0.54	23.06	28.20	14.24	0.83

Table 15: A comparison of gas separation for polymers **82**, **93**, **101**, TB Ethanoanthracene¹²³ and PIM-1⁹⁴.

Results are prior to treatment with methanol to purge residual chloroform.

Prior to methanol treatment PIM-1 shows greater selectivity and permeability properties than all TB-based polymers. This may be due to a greater amount of solvent residue from the casting process.

Polymers **93**, **97** and **101** show the highest selectivity properties of the six polymers, which suggests a relationship between the flexibility of the polymer chains and selectivity, where polymers with the highest flexibility display the greatest selectivity properties. This is contrary to what seems logical, as flexible polymers should demonstrate the least well-defined pore structures and channels. Whilst this may be a consequence of the presence of residual chloroform in the membrane, these results indicate that these polymers would be suitable materials for helium and hydrogen purification and carbon dioxide capture.

These three polymers demonstrated significantly lower permeability properties than PIM-1, TB Ethanoanthracene and polymer **82**. Polymer **97** did show enhanced permeability compared to polymers **93** and **101**, but this was still comparatively low. Whilst this may be explained by the almost non-porous nature of polymers **93** and **101**, it cannot be so easily explained for polymer **97**. In this case the polymer possesses considerable microporosity, so the low permeability properties must either be linked to considerable residual chloroform present in the membrane or pore channels that somehow hinder the transport of gas.

It would be interesting to discover if polymers **93** and **101** keep their impressive gas separation properties after treatment with methanol, as they are both relatively straightforward to synthesise so could make useful materials. Quite clearly the properties of membranes are heavily influenced by the microporosity of the polymer, but low microporosity does not necessarily result in poor gas separation properties. Whilst TB Ethanoanthracene and polymer **82** have reduced selectivity and permeability properties compared to PIM-1, polymers **93**, **97** and **101** show similar to better properties to PIM-1, which is promising for the development of TB PIMs as materials for gas capture. In particular the five TB polymers showed excellent selectivity for CO₂/N₂, which was similar or exceeded that displayed by PIM-1, suggesting that as predicted TB functionality in a PIM does indeed lead to strong CO₂-polymer interactions.

Polymer		O ₂	N ₂	He	H ₂	CO ₂	CH ₄
PIM-1	Selectivity after methanol treatment (PX/N ₂)	2.50	1.00	2.16	5.40	18.80	1.90
	Permeability after treatment with methanol (Barrer)	1530	610	1320	3300	11200	1160
TB Ethanoanthracene	Selectivity after methanol treatment (PX/N ₂)	4.09	1.00	4.90	14.78	13.60	1.33
	Permeability after treatment with methanol (Barrer)	2146	525	2574	7760	7142	699
82	Selectivity after methanol treatment (PX/N ₂)	4.32	1.00	3.97	12.78	15.44	1.44
	Permeability after treatment with methanol (Barrer)	2718	629	2500	8039	9709	905
97	Selectivity after methanol treatment (PX/N ₂)	3.61	1.00	5.20	14.84	15.04	1.34
	Permeability after treatment with methanol (Barrer)	437	121	629	1796	1820	162

Table 16: A comparison of gas separation performance for PIM-1⁹⁴, TB Ethanoanthracene¹²³, polymer **82** and polymer **97** after treatment with methanol.

A more informative comparison of gas permeation properties can be made from the results of membrane analysis after treatment with methanol, which removes any residual chloroform. This substantially increases the permeability performance of a membrane, as the pore channels are cleaned, allowing for easier gas transport. Importantly, it also ensures that the results are solely due to the performance of the material, rather than a combination of chloroform and material.

In contrast to the trend observed for PIM-1, TB Ethanoanthracene and polymer **82** were found to have improved selectivity after treatment, suggesting that the presence of chloroform had a negative effect also on the gas selectivity of the material. It is interesting to note that despite polymer **82** being less microporous than TB Ethanoanthracene it was found to possess greater permeability for all of the gases tested.

Polymer **97** was found to have an associated decrease in selectivity performance together with enhanced permeability performance after treatment. In addition, polymer **97** was found to be the least permeable of all of the four polymers treated by methanol. This can be explained by polymer **97** possessing the least microporosity of the four polymers due to the greater inherent flexibility in the polymer structure resulting in less well-defined pores.

Clearly, for the target gas pair of CO₂/N₂ of the four polymers PIM-1 is both the most permeable and most selective to carbon dioxide, but the selectivity of CO₂/N₂ for the three TB polymers were only moderate. It is possible that PIM-1 is more suitable for carbon dioxide purification because it possesses more heteroatoms than the TB polymers, which increase affinity towards carbon dioxide, or perhaps the chemical structure of PIM-1 results in pores more selective for carbon dioxide.

The permeability and selectivity of polymer **82** towards carbon dioxide was found to be the highest for the three TB polymers and these values are quite impressive (see below). In addition, Polymer **82** and TB Ethanoanthracene are both highly permeable to all gases and demonstrate remarkable selectivity for O₂/N₂, He/N₂ and H₂/N₂ gas pairs making them very useful membrane materials for the enrichment of oxygen or nitrogen from air, or the recovery of hydrogen from ammonia. Unfortunately, whilst polymer **97** was found to have excellent selectivity for many gas pairs the low permeability performance of the material makes it a less competitive material.

As previously stated, for a material to be competitive for gas separation it must possess both high selectivity and permeability towards a particular gas. On a Robeson plot, which plots permeability against selectivity, promising materials can be judged by their proximity to the Upper Bound. Robeson plots are presented from the gas permeation data for the four treated polymer membranes for CO₂/N₂, O₂/N₂, H₂/N₂ and He/N₂ (Figures 50 – 53).

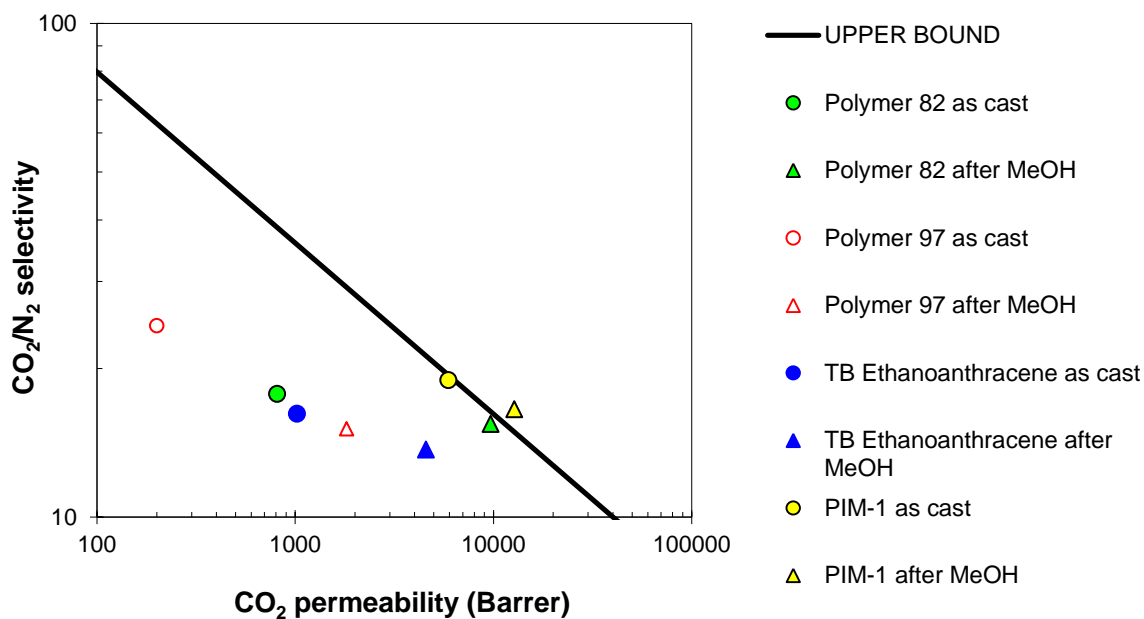


Figure 50: A Robeson plot showing CO₂ selectivity and permeability for PIM-1, TB Ethanoanthracene, polymer **82** and polymer **97**.

For the CO₂/N₂ Robeson plot (Figure 50) – of particular relevance to post combustion carbon capture – only PIM-1 lies above the Upper Bound, so is an excellent and competitive material for carbon dioxide capture. Each of the treated TB polymers lay below the Upper Bound, with polymer **82** displaying the best overall properties.

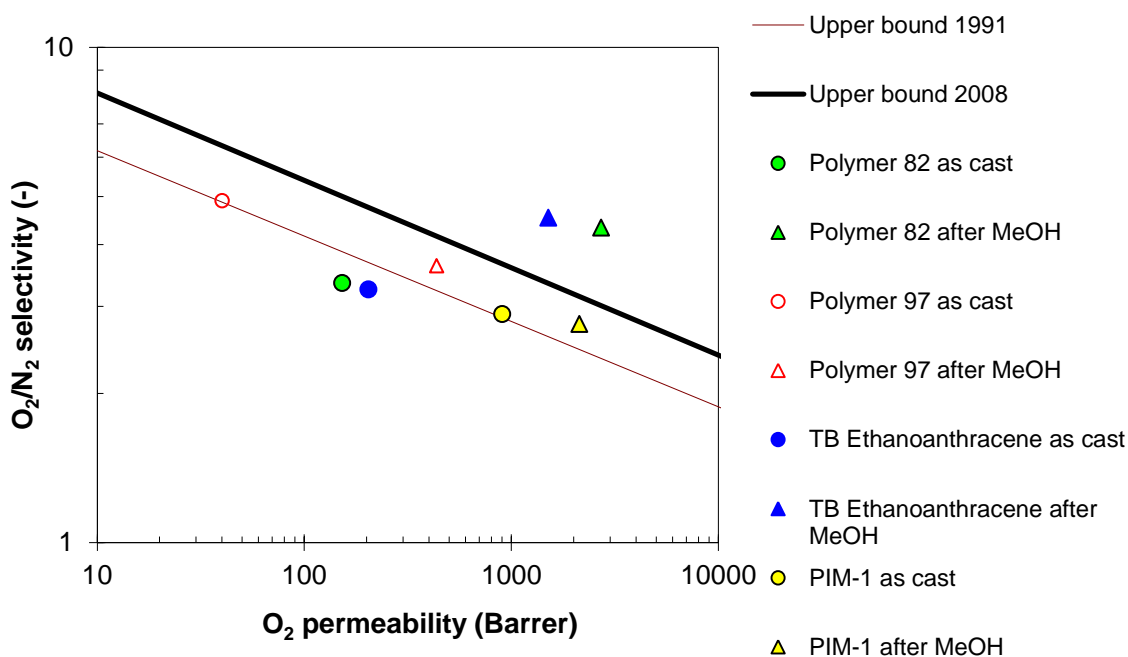


Figure 51: A Robeson plot showing O₂ selectivity and permeability for PIM-1, TB Ethanoanthracene, polymer **82** and polymer **97**.

Figure 51 is the Robeson Plot for O₂/N₂. Interestingly, methanol treated TB Ethanoanthracene and polymer **82** both lay significantly above the 2008 Upper Bound, which makes both materials ideally suited and highly competitive materials for oxygen purification or nitrogen enrichment of air. Polymer **82** shows an enhanced permeability relative to TB Ethanoanthracene and is slightly higher above the upper bound. Polymer **97** and PIM-1 are situated where most PIMs lie - between the 2008 and 1991 Upper Bounds.

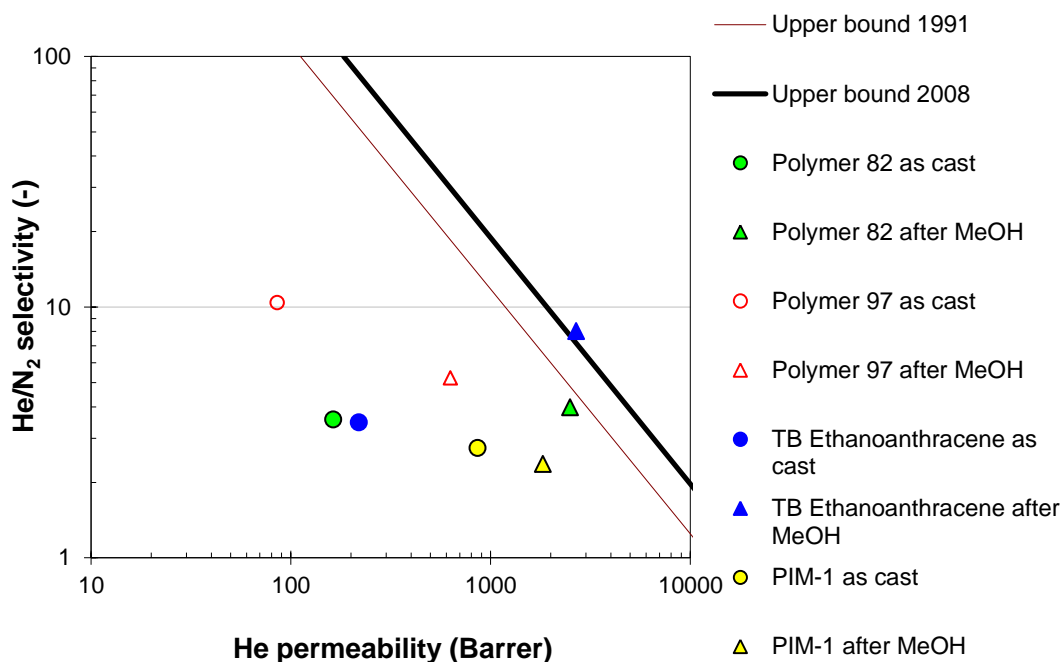


Figure 52: A Robeson plot showing He selectivity and permeability for PIM-1, TB Ethanoanthracene, polymer **82** and polymer **97**.

Figure 52 is the Robeson plot for He/N₂ and shows that only TB Ethanoanthracene lies above the 2008 Upper Bound, making it the most useful out of the four polymers for helium purification. PIM-1, polymer **82** and polymer **97** all lay beneath the 1991 Upper Bound.

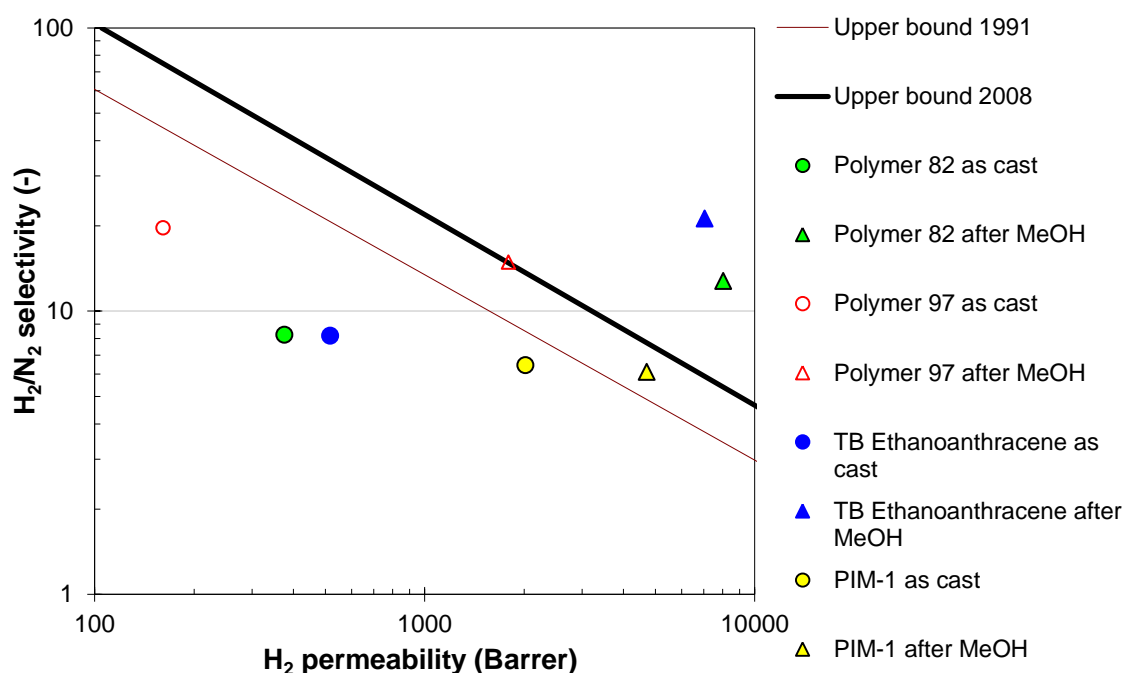


Figure 53: A Robeson plot showing H₂ selectivity and permeability for PIM-1, TB Ethanoanthracene, polymer **82** and polymer **97**.

Finally, Figure 53 shows that TB Ethanoanthracene, polymer **82** and polymer **97** all lay on or above the 2008 Upper Bound. Polymer **97** shows a good balance between selectivity and permeability, with a slightly higher selectivity than polymer **82** but with a far lower permeability, nevertheless it lies on the 2008 Upper Bound, indicating that the material would be most useful for hydrogen purification. PIM-1 lies between the 1991 and 2008 Upper Bounds, suffering an imbalance with a high permeability and a low selectivity.

In conclusion, the results of gas permeability analysis indicate that TB functionality is not only useful for CO₂ capture, but for other important gas separation. Thus the future of TB PIMs is promising, since two of the earliest examples possess gas separation properties that exceed those found for PIM-1, although disappointingly CO₂/N₂ selectivity is not among these.

4.5 Carbon dioxide capacity

This project was part of a research collaboration led by the Brandani group at the University of Edinburgh, who measure CO₂ uptake by microporous material using the zero-length column (zlc) system, which has previously been used to measure intracrystalline or intraparticle diffusion¹⁸⁰ or adsorption equilibria¹⁸¹. The zlc system is essentially a chromatographic method that works by exposing a small sample of microporous adsorbent to a particular adsorbate gas at known partial pressure and analysing the desorption behaviour of the adsorbate when the sample is purged. This can be used to provide useful information on the adsorption properties of the adsorbent towards a particular adsorbate gas, including kinetics and capacity. Furthermore, the system only requires a small amount of sample (5 – 15 mg) and allows for the rapid screening of materials since the analysis time of each sample is short.

Several of the polymers previously described in this thesis were analysed for carbon dioxide capacity using the zlc system, the results from this were varied and interesting, but ultimately low compared to that observed for other competitive materials (Figure 54). It is worth mentioning that since the time scale of the zero length column method is short and carbon dioxide adsorption into PIMs can be a slow process, the capacity measured by the zlc method may be significantly lower than the actual capacity of the material. It would require a much longer analysis time to obtain accurate and reliable capacity measurements for PIM-based materials.

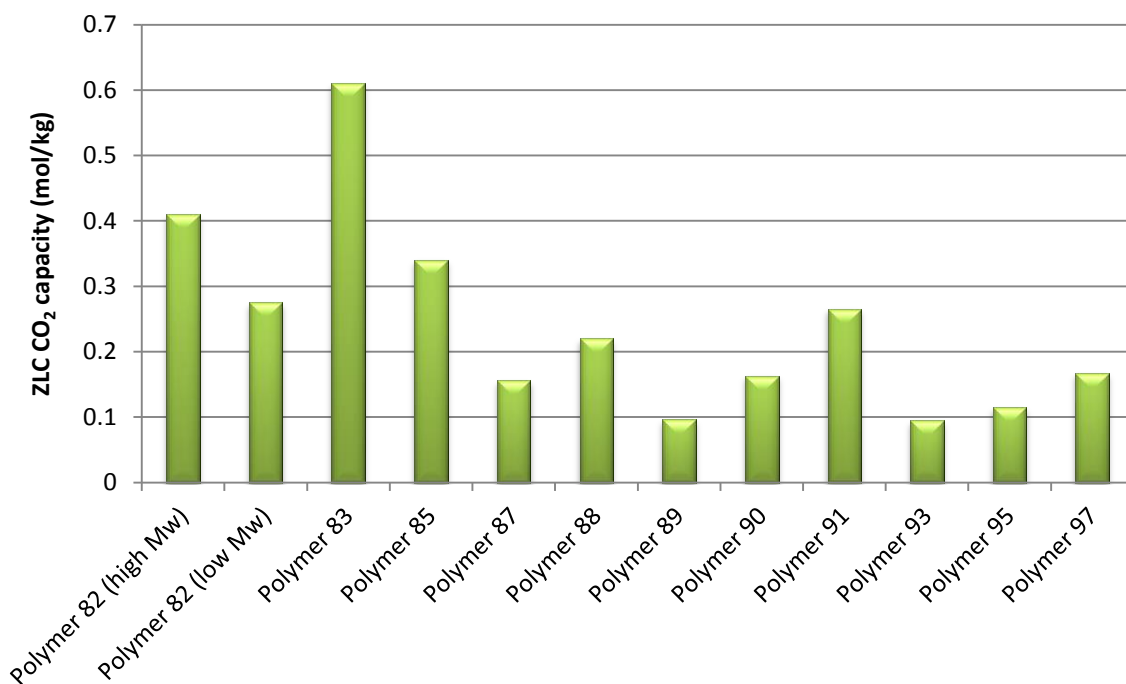


Figure 54: The carbon dioxide capacity measurements for several polymers, found by zero length column analysis.

Polymer **82** performed well compared to the other polymers tested, which can be explained by the high microporosity of the material, allowing for more CO₂ adsorption. There was a significant jump in measured capacity between high and low molecular weight batches of **82**, despite a drop in the measured surface area, indicating that as previously thought the measured surface area for the higher molecular weight batch does not represent the true microporosity of the material. The increased capacity between the two samples can be explained by the higher molecular weight batch possessing a greater concentration of smaller micropores, which are more suitable sites for CO₂ adsorption.

It is clear from the above results that polymer **83** had the highest measured adsorption capacity for CO₂ out of those tested, but this could have been due to two reasons. The first explanation is that the presence of bromine atoms in the structure of the polymer enhances affinity towards carbon dioxide, thus resulting in an increased capacity compared to the analogous polymer **82**, which lacks bromine substituents. An alternative explanation is that the presence of bromine atoms in the polymer structure results in a packing conformation that results in a greater concentration of smaller micropores, which are more suitable for CO₂ adsorption than N₂ adsorption.

Polymer **85** was also one of the best performing polymers, which can be explained by the high microporosity of the network framework, as well as its high nitrogen content (3 atoms per unit cell). It is strange that polymer **85** did not perform as well as the higher molecular weight batch of polymer **82**, considering that it has both an increased nitrogen content and substantially higher microporosity. One possible explanation is that polymer **85** exhibits slower gas adsorption than polymer **82**, so showed a lower capacity from the rapid zlc analysis due to adsorption kinetics.

Polymer **87** displayed reasonable CO₂ capacity despite the low microporosity of the material. This shows that as predicted the presence of the large heterocyclic crown ether ring system enhances affinity for carbon dioxide, but this is limited due to flexibility that polymer **87** possesses as a consequence of this structural feature, allowing efficient packing of the polymer chains.

Polymer **88** displayed lower capacity for CO₂ from zlc analysis than had been expected from its high microporosity; this may be consequence of slow adsorption kinetics caused by π -stacking between polymer chains. Results from the two related polymers **89** and **90** show lower CO₂ capacity than for **88**, but higher than what would be expected from the low microporosity of these polymers, suggesting that the quaternary process may be worthwhile. Analysis found that polymer **90** had a higher capacity than for polymer **89**, which is a consequence of the sulphate anion being able to stabilise two positive nitrogens, whilst the iodine anion can only stabilise one, so less pore space is consumed in polymer **90**. As predicted the presence of quaternary nitrogen atoms in both polymers does appear to enhance affinity for CO₂, but this is countered by the drastic reduction in microporosity that occurs as a consequence of forming the quaternary polymer and substantially reduces CO₂ capacity. This means that converting the polymer to the quaternary amine form is of limited usefulness, at least for this example, but smaller counter anions (e.g. F⁻) may prove to be more useful.

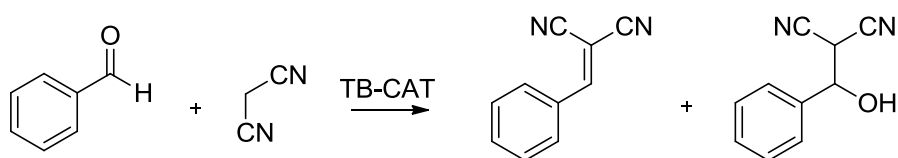
Polymer **91** showed impressive CO₂ capacity that exceeded that measured for polymers exhibiting higher microporosity. However, this can be explained by the high nitrogen content of polymer **91**, which is higher than that for any of the other polymers and results in strong affinity for CO₂. This suggests that if a membrane could be successfully prepared from **91** it would display impressive gas separation properties, particularly for CO₂/N₂.

Finally, the results from zlc analysis for polymers **93**, **95** and **97** show a trend for CO₂ capacity that is clearly influenced by the differing microporosity of the three polymers. Polymer **93** demonstrates the lowest CO₂ capacity since it possesses the lowest microporosity of the three polymers. Similarly, polymer **95** has the middle microporosity and middle CO₂ capacity of the three polymers, whilst polymer **97** possesses a significantly higher microporosity and consequently the highest CO₂ capacity of the three polymers. This clearly indicates that CO₂ capacity is directly influenced by the microporosity of the polymer.

Most of the other polymers that have previously been discussed in this chapter have been sent for zlc analysis, but unfortunately due to the large influx of samples being sent from the different universities that form the collaboration they have not yet been analysed.

4.6 TB network polymers as heterogeneous catalysts

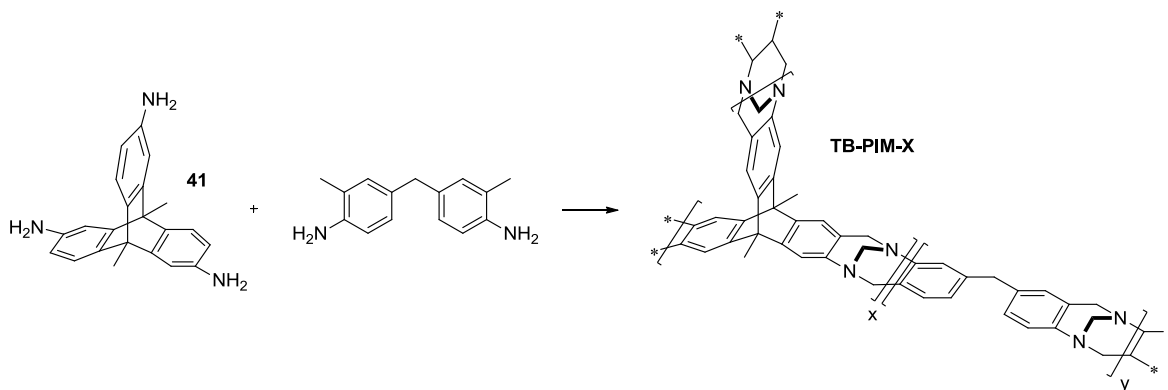
Dibenzodioxane-based PIMs have previously found use in catalytic applications⁸⁵ and TB has also been used successfully as a catalyst¹²⁰. Therefore logic suggested that a TB PIM would make a very useful heterogeneous catalyst, since it would benefit from possessing a large accessible surface area together with a high content of strongly basic nitrogen atoms. The Knoevenagel condensation reaction (Scheme 107) between benzaldehyde and malonitrile was chosen to assess this theory. This reaction has previously been used to test the catalytic performance of a number of materials, including TB, which was used as a homogeneous catalyst¹⁸². The catalytic study¹⁸³ was carried out by Dr. Mariolino Carta, so no further details are included elsewhere in this thesis.



Scheme 107: The Knoevenagel condensation reaction. TB-CAT = TB PIM catalyst. *Reagents and conditions:* Benzaldehyde (180 mmol), malonitrile (60 mmol), TB-CAT (0.5, 1.0 or 1.7 molar %), 18°C.

Polymers **85** and **86** were identified as potentially useful heterogeneous catalysts, due to their high microporosity (1035 and 750 m²/g, respectively), rigid structures, high content of strongly basic nitrogen and insoluble nature. A similar polymer, TB-PIM-X, was also

prepared using compound **41** and the commercially available bis(4-amino-3-methylphenyl)methane (Scheme 108). A 3:2 molar ratio of the two monomers was used in order to generate a similar TB-PIM with low microporosity ($1.5 \text{ m}^2/\text{g}$).



Scheme 108: The preparation of TB-PIM-X. *Reagents and conditions:* Dimethoxymethane, TFA, $0 \text{ }^\circ\text{C}$, 48 hours.

Together the three analogous TB polymers (Figure 55) enabled a more complete understanding of the importance of microporosity to catalytic efficiency to be made since they contained roughly the same level of strongly basic nitrogen, but showed great variation in their microporosity. The catalytic study was performed with increasing amounts of polymer as catalyst, always keeping the proportions between 0.5% M as a minimum and 1.7% M as maximum. Samples from the reaction mixture were taken out at regular intervals and analysed by GC-MS and NMR techniques. The total conversion was calculated by assessing how much malonitrile remained, as it could only be consumed in the Knoevenagel reaction. From this data the turnover rate (TON) and turnover frequency (TOF) were calculated to assess the catalytic efficiency of the catalyst.

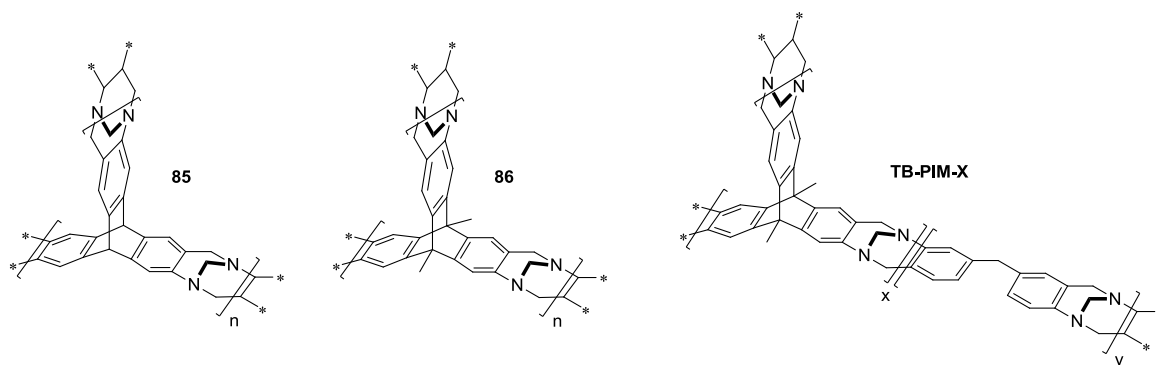


Figure 55: The three analogous TB polymers chosen for catalytic study.

The results of the catalytic study are summarised in Table 17. They show that polymer **85** demonstrated the highest catalytic activity, with polymer **86** showing only slightly reduced activity by comparison, caused by the slight difference in microporosity. TB-PIM-X exhibited similar catalytic activity to the homogeneous reaction using TB, which was significantly lower than for polymers **85** and **86**. For example, polymers **85** and **86** at 0.5% behaved similarly to TB-PIM-X at 1.0% and TB at 1.7%, which suggests that the high microporosity of polymers **85** and **86** has a considerable effect on the efficiency of the catalyst. Comparing the turnover number (TON) and turnover frequency (TOF) indicates that the TB units are more than twice as active when part of a microporous material than when used as a homogeneous catalyst dissolved in the reaction mixture. This increased activity may be a result of rapid adsorption of malonitrile into the pores of the polymer, where deprotonation can occur more rapidly due to nucleophilic attack by the embedded nitrogen atoms. Furthermore, polymer **85** was found to maintain activity after multiple cycles of reuse, with the same catalytic sample achieving a conversion of malonitrile of over 95% after eight consecutive reactions.

Polymer (molar %)	Conversion at x min (%) ^[A]				TON ^[B]	TOF ^[C]
	15	30	60	120		
85 (1.7%)	64	82	94	100	37	2.5
85 (1.0%)	38	55	74	93	35	2.3
85 (0.5%)	18	33	51	72	36	2.4
86 (1.7%)	61	78	90	96	36	2.4
86 (1.0%)	35	52	74	89	35	2.3
86 (0.5%)	16	28	47	65	34	2.3
TB-PIM-X (1.7%)	24	44	64	76	14	0.9
TB-PIM-X (1.0%)	14	25	41	61	14	0.9
TB-PIM-X (0.5%)	7	13	24	47	14	0.9
TB (1.7%) ^[D]	15	29	52	73	15	1.0

Table 17: The results of the TB catalytic study. [A] Conversion of malonitrile from GC-MS and NMR. [B] Turnover number after 15 minutes calculated from number of moles of malonitrile consumed versus number of mole equivalents of TB catalyst. [C] Turnover frequency calculated from turnover number per minute. [D] Homogeneous reaction.

Chapter 5: Future work

The research on TB polymerisation detailed in this thesis has contributed towards an International Patent¹²² and a paper in Science¹²³ so can be deemed to have been successful, but ultimately, the project ended before sufficient time was found to repeat and complete some of the work detailed in this thesis. One of the key areas where further work is required is the repeated polymerisation of several of the most promising monomers, compounds **64**, **71** and **74** (Figure 56), using the optimised polymerisation procedure, wherein the monomer is initially dissolved in a mixture of dichloromethane and dimethoxymethane prior to the slow addition of trifluoroacetic acid. This procedure was found to significantly increase the molecular weight of polymers **82** and **97**, thereby allowing the preparation of robust and self-standing membranes, which were used for measurement of gas separation properties. If membranes can be prepared for polymers **95**, **102** and **103** it will give further evidence that this altered procedure aids in the generation of high molecular weight material and the resulting membrane analysis will provide further useful information on the gas separation properties of TB PIMs. Furthermore, performing this work should prove straightforward since the synthesis of the four monomers has been optimised during this project and is reported in this thesis.

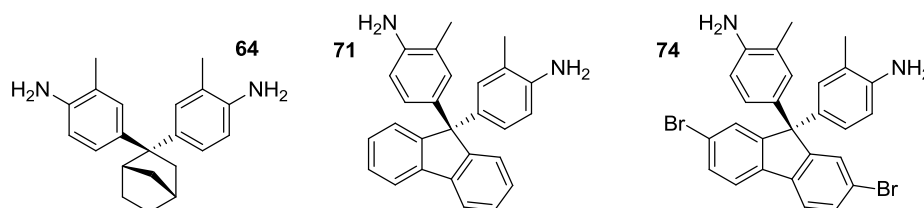


Figure 56: The monomers that need to be polymerised using the altered polymerisation procedure.

Another area where further work is needed is in forming membranes from polymers **93** and **101** (Figure 57), since gas permeability analysis was not performed for these two polymers after treatment with methanol, meaning the results obtained are not accurate. However, the data that exist for these polymers was very promising, but without methanol treatment the true performance of these materials cannot be known. This work would require both polymers to be synthesised again, but once again the preparation of the two monomers, compounds **62** and **70**, has been optimised during this project and is reported in this thesis so this work should prove relatively simple. It is also possible that the excellent molecular

weight of these two polymers could be improved by using the altered polymerisation procedure so that an even stronger polymer membrane could be generated.

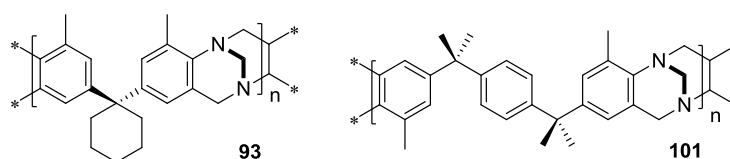
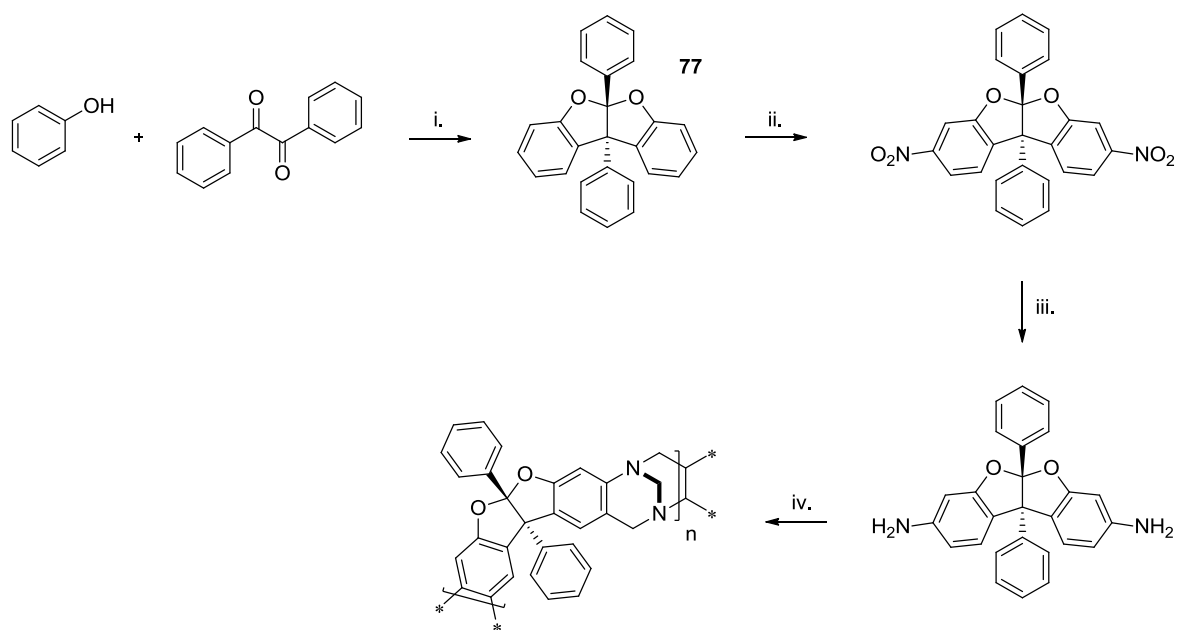


Figure 57: The two polymers that are capable of resistant membranes, but require further analysis.

Clearly since synthesis of a coumaron-based PIM was unsuccessful this is an area where further research is required. Unfortunately, work reported in this thesis has found that compound **80** is not a suitable monomer for PIM synthesis, due to its unstable nature. It is likely that the derivatives of this compound would exhibit similar stability problems, so traditional PIM synthesis must be disregarded since it would not likely be successful. However, TB polymerisation may provide the solution as a coumaron-based diamine may exhibit higher stability than observed for compound **80** and allow the preparation of a coumaron-based TB PIM.

The synthesis of a suitable monomer should prove relatively simple (Scheme 109), beginning with the preparation of compound **77**, which was successfully achieved during this project and is described in this thesis. The yield from this reaction is low (20%), but the reaction could be easily scaled up to generate a sufficient amount of the coumaron. This compound could then be nitrated using the potassium nitrate method of nitration reported in this thesis, since this allows the stoichiometry of the reaction to be better controlled, which is essential considering there are several phenyl rings that could become nitrated. It is likely that this reaction will result in a mixture of products, but the major product should be the compound possessing two nitro groups on the fused ring component, since the presence of the oxygen atoms will activate these rings. After purification of the desired compound the monomer could be synthesised from a reduction reaction using hydrazine, also reported in this thesis and should give the monomer in excellent yield. Finally, the monomer could be polymerised using dimethoxymethane, dichloromethane and trifluoroacetic acid to generate a coumaron-based TB PIM.



Scheme 109: The synthesis of a coumaron-based TB polymer. *Reagents and conditions:* I. Glacial acetic acid, HCl, chloroform, 62 °C, 48 hours. II. KNO₃, TFAA, MeCN, 60 °C, 16 hours. III. Hydrazine monohydrate, Raney nickel, THF, 60 °C, 16 hours. IV. Dimethoxymethane, TFA, 0 °C, 48 hours.

Chapter 6: Experimental

6.1 Experimental techniques

Where possible reagents were purchased from commercial sources and used without further purification, except where noted. Anhydrous dichloromethane was obtained by distillation over calcium hydride under a nitrogen atmosphere. For air/moisture sensitive reagents, reactions were performed in oven-dried or flame-dried apparatus, under a nitrogen atmosphere. Reactions were analysed by thin layer chromatography (TLC) using aluminium-backed plates coated with Merck Kieselgel 60 GF254, with product spots viewed either by the quenching of UV fluorescence under a UV lamp, or by staining with a solution of cerium sulphate in aqueous H₂SO₄. Silica chromatography was performed on 60Å (35-70 micron) chromatography grade silica gel purchased from Fisher Scientific.

Melting point analysis

Melting points were recorded using a Gallenkamp Melting Point Apparatus and are uncorrected. Infra-red spectra were recorded in the range 4000-700 cm⁻¹ using a Perkin-Elmer 1600 series FTIR instrument as a thin film between sodium chloride plates. Where possible melting points of known compounds have been reported, when this information is not present either the information could not be found or the compound is novel.

NMR analysis

¹H NMR spectra were recorded in the solvent stated using an Avance Bruker DPX 400 (400 MHz) instrument, with ¹³C NMR spectra recorded at 100 MHz. Chemical shifts (δ_{H} and δ_{C}) were recorded in parts per million (ppm) from tetramethylsilane (or chloroform) and are corrected to 0.00 (TMS) and 7.26 (CHCl₃) for ¹H NMR and 77.00 (CHCl₃), centre line, for ¹³C NMR. Solid state ¹³C NMR was measured externally at EPSRC UK National Solid-state NMR Service at Durham using a Varian VNMRS 400. The abbreviations s, d, t, q, m and br. denote singlet, doublet, triplet, quartet, multiplet and broadened resonances; all coupling constants were recorded in Hertz (Hz).

Mass spectrometry analysis

Low-resolution mass spectrometric data were determined using a Fisons VG Platform II quadrupole instrument using electron impact ionization (EI) unless otherwise stated. High-resolution mass spectrometric data was obtained by electron impact ionization (EI) unless otherwise reported, on a Waters Q-TOF micromass spectrometer.

BET surface area and isotherm analysis

Low-temperature (77 K) N₂ adsorption/desorption measurements of PIM powders were made using a Coulter SA3100 at a pressure range of 0.01 to 1000 mm Hg. Samples were degassed for 900 minutes at 135 °C under high vacuum prior to analysis.

Thermogravimetric analysis

Thermal gravimetric analysis (TGA) was performed using the device Thermal Analysis SDT Q600 at a heating rate of 10 °C/min from room temperature to 1000 °C. Where no analysis is present the polymer was synthesised after the facilities at Cardiff University were no longer available due to equipment failure.

Elemental analysis

Elemental analysis has been performed externally by MEDAC Ltd.

Single crystal X-ray diffraction analysis

Single crystal XRD analysis data was collected at Cardiff University using a Bruker-Nonius Kappa CCD area-detector diffractometer equipped with an Oxford Cryostream low temperature cooling device operating at 150(2) K, Mo K α radiation ($\lambda = 0.71073 \text{ \AA}$) or the Diamond Light Source (Station I19) using a Rigaku Saturn 724 CCD diffractometer (graphite monochromated radiation). The structures were solved by direct methods and all calculations were carried out by using the SHELX-97 package. Non-H atoms were refined anisotropically, except some of the disordered atoms. H atoms were included in calculated positions, except those bonded to solvent molecules.

Gel Permeation Chromatography

Gel Permeation Chromatography was carried out using a Viscotek GPC Max1000 system, which includes a refractive index detector and two 2 columns (KF-805L Shodex). A dilute solution of polymer in chloroform (1 mg in 1 ml) was used for the analysis and the retention time compared to polystyrene standards (up to $1 \times 10^6 \text{ g mol}^{-1}$). Due to this comparison it is possible that the measured molecular weights of the PIMs detailed in this thesis are an over-estimation of the actual molecular weights of the polymers. This is because PIMs are a lot less flexible than the polystyrene standards so consequently a PIM of a particular molecular weight may spend less time in the porous beads of the column and elute faster than polystyrene with the same or similar molecular weight.

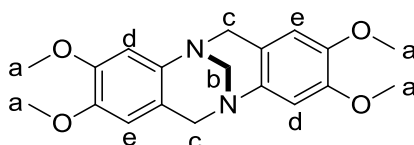
Film formation and pure gas permeation analysis

Film formation was achieved by preparing a solution of polymer (600 – 700 mg) in chloroform (20 ml), filtering it through glass wool, pouring it into a 9 cm circular Teflon mould and allowing the chloroform to evaporate slowly over at least 96 hours. Unless otherwise stated, membranes were not further treated after formation, meaning that traces of residual chloroform and water were present during analysis.

Membranes were analysed externally at the Institute for Membrane Technology (ITM-CNR) in Italy or at Helmholtz-Zentrum Geesthacht Centre for Materials and Coastal Research (GKSS) in Germany.

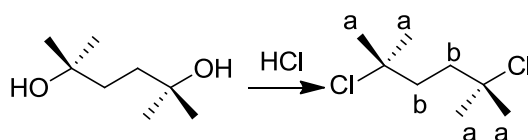
6.2 Monomer and model compound synthesis

Preparation of Tröger's base from 3,4-dimethoxyaniline(1):



3,4-Dimethoxyaniline (1.00 g, 6.53 mmol) was dissolved in trifluoroacetic acid (10 ml) at 0 °C with stirring. Once dissolved, hexamine (1.83 g, 13.07 mmol) was added and the reaction mixture stirred for 16 hours. The reaction was then quenched with saturated sodium hydroxide (100 ml) and the product extracted with chloroform (3 x 100 ml). The organic solution was concentrated under reduced pressure to give the crude product as a brown solid. This was washed with hot methanol to give the product as an off-white flaky solid (0.48 g, 1.39 mmol, 42.5%). Mp 198 – 200 °C; ^1H NMR (400 MHz, CDCl_3) δ ppm 3.77 (6H, s, H_a), 3.85 (6H, s, H_a), 4.05 (1H, s, H_b), 4.09 (1H, s, H_b), 4.28 (2H, s, H_c), 4.59 (1H, s, H_c), 4.63 (1H, s, H_c), 6.38 (2H, s, H_d), 6.65 (2H, s, H_e); ^{13}C NMR (100 MHz, CDCl_3) δ ppm 56.0, 58.0, 67.2, 108.2, 109.1, 118.9, 140.6, 146.3, 148.5; LRMS m/z (ES, MH^+) = 343.17; IR (NaCl): 2926, 2831, 1692, 1610, 1505, 1465, 1437, 1404, 1378, 1360, 1334, 1310, 1229, 1189, 1172, 1119, 1093, 1067, 1030, 1002 cm^{-1} .

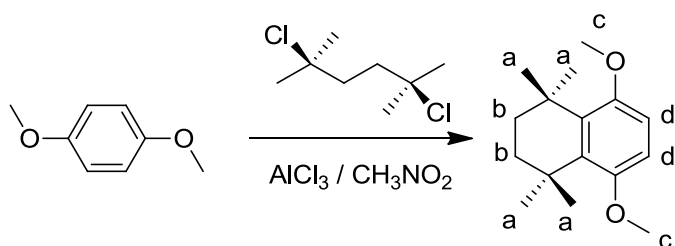
Synthesis of 2,5-dichloro-2,5-dimethylhexane (2):



Based upon the procedure detailed by S. A. Miller *et al.*¹⁸⁴, 2,5-dimethyl-2,5-hexanediol (10.75g, 73.5 mmol) and concentrated hydrochloric acid (37%, 55 ml, 671.0 mmol) were stirred at room temperature for 16 hours. The mixture was then filtered and the precipitate washed with water (50 ml). The white solid was added to water (30 ml) and extracted with diethyl ether (3 x 50 ml) before the solution was concentrated under reduced pressure giving the product as a white powder (9.75 g, 53.6 mmol, 78.4%). Mp 64 – 66 °C; lit. mp = 63 – 64 °C¹⁸⁴; ^1H NMR (400 MHz, CDCl_3) δ ppm 1.53 (12H, s, H_a), 1.88 (4H, s, H_b); ^{13}C

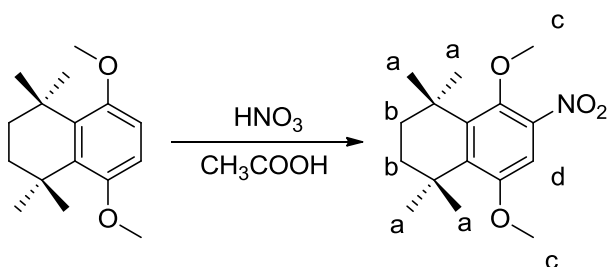
NMR (100 MHz, CDCl₃) δ ppm 32.6, 41.2, 70.4; LRMS m/z (EI, MH - 2Cl⁺) = 111.11; IR (NaCl): 2966, 2922, 1450, 1372, 1306, 1266, 1250, 1209, 1145, 1084, 955, 821, 740 cm⁻¹.

Synthesis of 5,8-dimethoxy-1,1,4,4-tetramethyl-1,2,3,4-tetrahydronaphthalene (3):



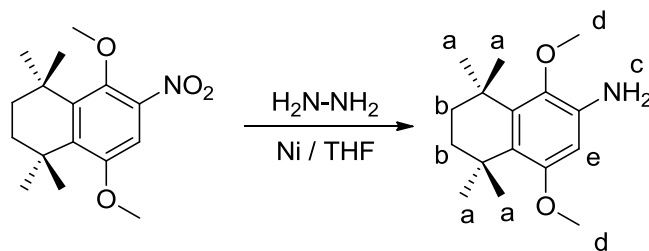
1,4-Dimethoxybenzene (6.40 g, 46.3 mmol) and 2,5-dichloro-2,5-dimethylhexane (10.10 g, 55.5 mmol) were dissolved in dichloromethane (90 ml) in a nitrogen purged flask. Aluminium trichloride (8.40 g, 62.9 mmol) in dichloromethane (40 ml) was added dropwise and the black solution stirred for 16 hours under nitrogen. The reaction was then quenched in ice water (100 ml), stirred for 30 minutes and the crude product extracted with dichloromethane (2 x 100 ml). The solution was concentrated under reduced pressure to give a brown oil, which was passed through a short column of silica (1:4 dichloromethane:hexane). Recrystallisation from ethanol gave the product as a yellow crystalline solid (7.58 g, 30.6 mmol, 66.1%). Mp 68 – 70 °C; ¹H NMR (400 MHz, CDCl₃) δ ppm 1.38 (12 H, s, H_a), 1.60 (4H, s, H_b), 3.77 (6H, s, H_c), 6.69 (2H, s, H_d); ¹³C NMR (100 MHz, CDCl₃) δ ppm 34.9, 38.1, 55.4, 109.3, 135.7, 153.2; HRMS Calc. for C₁₆H₂₄O₂ m/z = 248, found 248.1776 gmol⁻¹; IR (NaCl): 2945, 1457, 1359, 1241, 1053 cm⁻¹.

Synthesis of 5,8-dimethoxy-1,1,4,4-tetramethyl-6-nitro-1,2,3,4-tetrahydronaphthalene (4):



Concentrated nitric acid (70%, 2 ml) was added dropwise to a solution of 5,8-dimethoxy-1,1,4,4-tetramethyl-1,2,3,4-tetrahydronaphthalene (6.30 g, 25.4 mmol) in glacial acetic acid (100 ml) at 0 °C. The reaction was stirred for 16 hours whilst gradually allowed to warm to room temperature. Water (350 ml) was added and after brief stirring the mixture was extracted with dichloromethane (3 x 50 ml), before the solution was concentrated under reduced pressure. Recrystallisation from ethanol gave the product as yellow crystals (7.14 g, 24.4 mmol, 96.1 %). Mp 74 – 76 °C; ¹H NMR (400 MHz, CDCl₃) δ ppm 1.36 (6H, s, H_a), 1.40 (6H, s, H_a), 1.61 (4H, s, H_b), 3.74 (3H, s, H_c), 3.82 (3H, s, H_c), 7.15 (1H, s, H_d); ¹³C NMR (100 MHz, CDCl₃) δ ppm 28.0, 29.3, 30.9, 32.5, 35.7, 35.9, 37.7, 38.1, 47.9, 55.5, 61.5, 104.4, 105.5, 141.0, 142.1, 142.6, 148.2, 154.0; HRMS Calc. for C₁₆H₂₃NO₄m/z = 293 gmol⁻¹, found 293.1630 gmol⁻¹; IR (NaCl): 2931, 1578, 1521, 1451, 1418, 1391, 1377, 1361, 1270, 1243, 1225, 1058, 1034, 978, 962, 901, 841, 814, 785, 741 cm⁻¹.

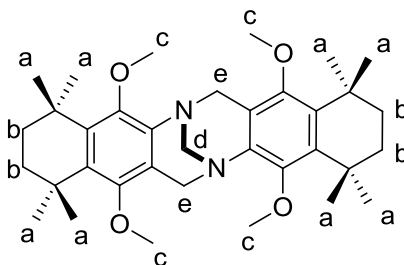
Synthesis of 5,8-dimethoxy-1,1,4,4-tetramethyl-6-amino-1,2,3,4-tetrahydronaphthalene (5):



5,8-Dimethoxy-1,1,4,4-tetramethyl-6-nitro-1,2,3,4-tetrahydronaphthalene (1.00 g, 3.41 mmol) was dissolved in THF (30 ml) with stirring under nitrogen. Raney nickel (catalytic amount) and hydrazine monohydrate (0.5 ml, 10.24 mmol) were added slowly, before the mixture was heated to 60 °C and stirred under nitrogen for 16 hours. The mixture was then filtered and the solution concentrated under reduced pressure. The resulting material was added to water (100 ml) and the product extracted with chloroform (3 x 50 ml). This solution was concentrated under reduced pressure, giving the product as white crystals (0.82 g, 3.12 mmol, 91.4%). Mp 126 – 128 °C; ¹H NMR (400 MHz, CDCl₃) δ ppm 1.33 (6H, s, H_a), 1.39 (6H, s, H_a), 1.56 (4H, s, H_b), 3.55 (2H, s, H_c), 3.73 (3H, s, H_d), 3.74 (3H, s, H_d), 6.23 (1H, s, H_e); ¹³C NMR (100 MHz, CDCl₃) δ ppm 28.9, 30.0, 34.2, 34.7, 38.5, 55.2, 59.4, 99.4, 125.0, 137.9, 140.0, 141.3, 155.3; HRMS Calc. for C₁₆H₂₅NO₂m/z = 263,

found 263.1885 g mol^{-1} ; IR (NaCl): 3452, 3353, 2987, 2957, 2927, 2861, 1618, 1574, 1445, 1409, 1384, 1358, 1330, 1279, 1229, 1200, 1092, 1030, 832, 797, 768 cm^{-1} .

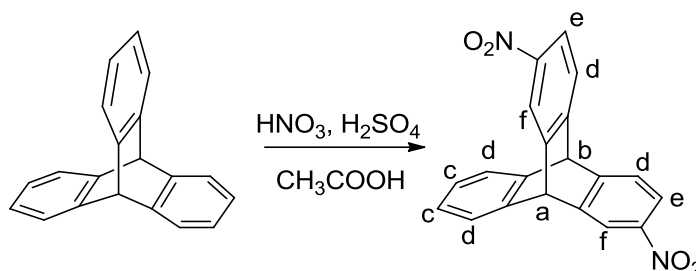
Synthesis of Tröger's base from 5,8-dimethoxy-1,1,4,4-tetramethyl-6-amino-1,2,3,4-tetrahydronaphthalene (6):



5,8-Dimethoxy-1,1,4,4-tetramethyl-6-amino-1,2,3,4-tetrahydronaphthalene (1.00 g, 3.80 mmol) was dissolved in trifluoroacetic acid (10 ml) at 0 °C. Dimethoxymethane (0.7 ml, 7.60 mmol) was then added dropwise and the mixture left stirring for 16 hours. The reaction was quenched in water (100 ml) and saturated sodium hydroxide solution added until a pH of 12 was achieved. After stirring vigorously for 2 hours the precipitate was collected by filtration. It was refluxed in methanol for 16 hours before being filtered and dried under vacuum, giving the product as a white powder (0.83 g, 1.48 mmol, 77.8%). Mp 216 – 218 °C; ^1H NMR (400 MHz, CDCl_3) δ ppm 1.31 (18H, br. m, H_a), 1.40 (6H, s, H_a), 1.54 (8H, br. m, H_b), 3.69 (6H, s, H_c), 4.02 (6H, s, H_c), 4.19 (2H, s, H_d), 4.41 (4H, m, H_e); ^{13}C NMR (100 MHz, CDCl_3) δ ppm 29.2, 29.7, 29.9, 31.0, 34.7, 35.0, 38.4, 38.6, 50.7, 59.7, 61.0, 66.8, 121.0, 134.0, 137.9, 149.4, 153.1; HRMS Calc. for $\text{C}_{35}\text{H}_{50}\text{N}_2\text{O}_4\text{m/z} = 562$, found 563.3831 g mol^{-1} ; IR (NaCl): 2926, 1574, 1442, 1389, 1357, 1320, 1269, 1242, 1201, 1155, 1099, 1045, 1026, 1000, 959, 920, 857, 739, 705, 633 cm^{-1} . Crystals were prepared by a slow diffusion of hexane into a solution of the compound in chloroform. Crystal properties: system = Orthorhombic, space group = $P -1$, $a = 9.6255(3)$, $b = 13.8598(6)$, $c = 14.8971(6)$, $\alpha = 111.57(2)$, $\beta = 101.44(2)$, $\gamma = 100.77(2)$, $V = 1736.37\text{\AA}^3$; $Z = 2$.

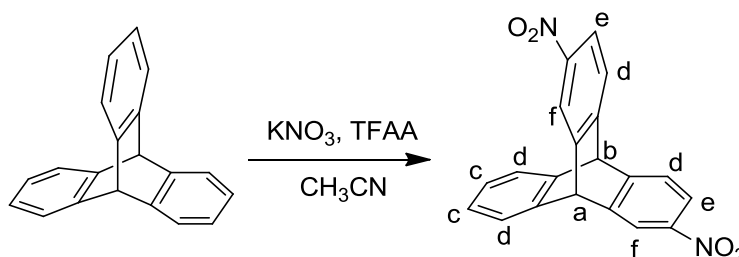
Synthesis of 2,6(7)-dinitrotritycene (7):

Nitric acid method:



Using a modified version of the procedure reported by B. H. Klanderman and W. C. Perkins¹³², triptycene (1.00 g, 3.93 mmol), concentrated nitric acid (70%, 0.6 ml, 9.43 mmol) and concentrated sulphuric acid (95%, 2 ml) were added to glacial acetic acid (20 ml) at room temperature. The resulting mixture was heated to 70 °C and stirred for 48 hours under nitrogen, when the reaction was quenched in water (50 ml). The crude product was extracted with dichloromethane (3 x 10 ml) and the dichloromethane removed under reduced pressure. This material was purified by silica column chromatography (7:3 dichloromethane:hexane) giving the product as a yellow powder (0.56 g, 1.63 mmol, 41.4%).

Potassium nitrate method:

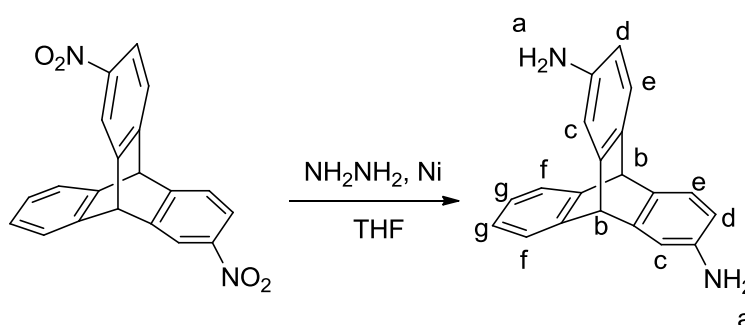


Based upon the nitration procedure reported by J. V. Crivello¹³³, triptycene (2.00 g, 7.87 mmol) was dissolved in acetonitrile (60 ml); to this solution was added trifluoroacetic anhydride (7.66 ml, 55.11 mmol) and potassium nitrate (1.59 g, 15.74 mmol). The mixture was left stirring for 16 hours, quenched in water (150 ml) and extracted with dichloromethane (3 x 30 ml). The dichloromethane was removed under reduced pressure giving the crude product as a yellow powder. This material was passed through a silica

column (2:1 dichloromethane:hexane) giving the product as a yellow powder (2.17 g, 6.32 mmol, 80.3%, Rf = 0.80). Other products that eluted were 2,6(7),14-trinitrotritycene (0.18 g, 0.46 mmol, 5.9%, Rf = 0.75) and 2-nitrotritycene (0.20 g, 0.69 mmol, 8.8%, Rf = 0.85).

Characterisation: Mp 240-242 °C; Lit. Mp > 350 °C (isomerically pure)¹³²; ¹H NMR (400 MHz, CDCl₃) δ ppm 5.69 (1H, s, H_a), 5.72 (1H, s, H_b), 7.12 (2H, m, H_c), 7.53 (4H, m, H_d), 7.96 (2H, d, J = 8.1 Hz, H_e), 8.25 (2H, s, H_f); ¹³C NMR (100 MHz, CDCl₃) δ ppm 53.5, 53.6, 53.8, 119.1, 119.2, 122.0, 124.4, 124.5, 126.5, 126.6, 141.9, 142.3, 142.8, 145.4, 145.9, 150.6, 151.0; LRMS m/z (EI, M⁺) = 344.06, IR (NaCl): 3071, 1591, 1516, 1458, 1343, 801, 738 cm⁻¹.

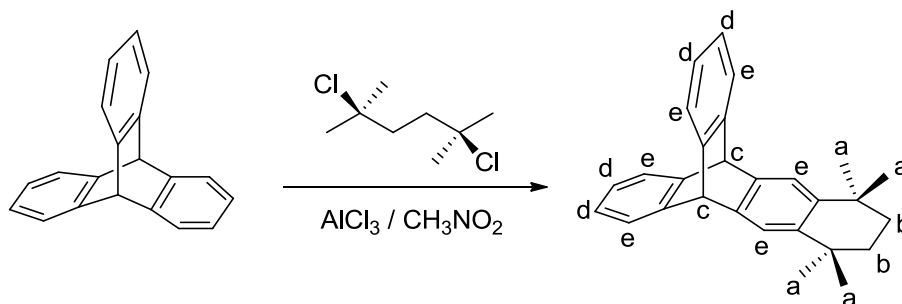
Synthesis of 2,6(7)-diaminotritycene (8):



Following the procedure described by T. M. Swager and Z. Chen¹³⁴, 2, 6(7)-dinitrotritycene (1.00 g, 2.90 mmol) was dissolved in THF (40 ml) with stirring under nitrogen. Raney nickel (catalytic amount) and hydrazine monohydrate (0.9 ml, 17.4 mmol) were slowly added to the solution before the temperature was increased to 60 °C. This mixture was stirred under nitrogen for 16 hours, then filtered and the solvent removed under reduced pressure. The resulting oil was added to water (50 ml), the product extracted with chloroform (3 x 10 ml) and the solvent removed under reduced pressure giving the product as a cream-white powder (0.82 g, 2.89 mmol, 99.6%). Mp 230 – 232 °C; Lit. Mp = 219 – 221 °C (CH₂Cl₂)¹³⁴; ¹H NMR (400 MHz, CDCl₃) δ ppm 3.36 (4H, s, H_a), 5.19 (2H, m, H_b), 6.26 (2H, m, H_c), 6.77 (2H, m, H_d), 6.99 (2H, m, H_e), 7.11 (2H, m, H_f), 7.34 (2H, m, H_g); ¹³C NMR (100 MHz, CDCl₃) δ ppm 52.4, 53.4, 54.4, 110.6, 110.9, 111.5, 111.7, 122.9, 123.1, 123.4, 123.7, 124.0, 124.7, 124.9, 125.1, 135.7, 136.6, 143.6, 143.8, 145.1,

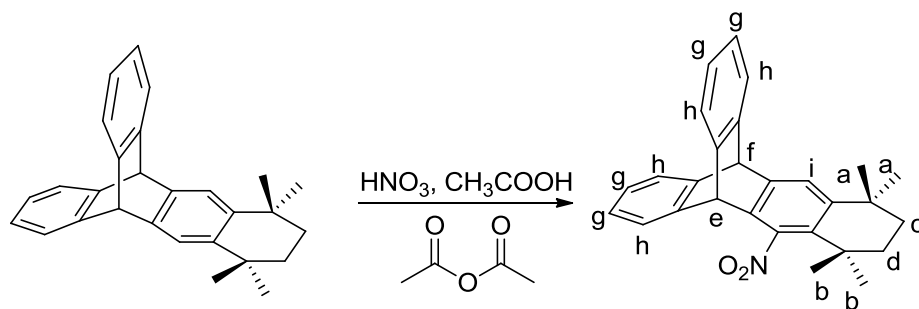
145.9, 146.5, 146.6, 147.2; LRMS m/z (EI, M^+) = 284.13; IR (NaCl): 3347, 3011, 2954, 1623, 1494, 1479, 1330, 1294, 1263 cm^{-1} .

Synthesis of 2,2,5,5-tetramethyl-2,3,4,5-tetrahydrobenzotriptycene (9):



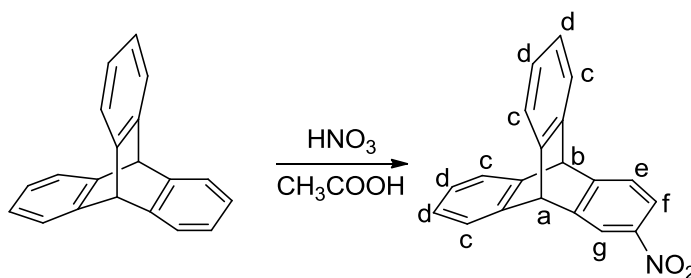
Triptycene (2.00 g, 7.87 mmol) and 2,5-dichloro-2,5-dimethylhexane (1.50 g, 8.27 mmol) were dissolved in nitromethane (80 ml) with stirring under nitrogen. A solution of aluminium trichloride (2.73 g, 20.46 mmol) in nitromethane (40 ml) was added dropwise to the reaction before the reaction was left stirring under nitrogen for 16 hours. The reaction was then quenched with water (400 ml) and the mixture stirred at 60 °C for 4 hours before the precipitate was collected by filtration. The solid was added to a mixture of dichloromethane (30 ml) and saturated sodium hydroxide solution (30 ml) and the product extracted with dichloromethane (3 x 30 ml). The solution was concentrated under reduced pressure, giving the crude product as orange-brown powder. This was triturated in methanol (100 ml), collected by filtration and dried under vacuum, giving the product as a cream coloured powder (2.53 g, 6.95 mmol, 88.4%). Mp 248 – 250 °C; ^1H NMR (400 MHz, CDCl_3) δ ppm 1.23 (12H, s, H_a), 1.52 (4H, m, H_b), 5.51 (2H, m, H_c), 7.17 (4H, m, H_d), 7.58 (6H, m, H_e); ^{13}C NMR (100 MHz, CDCl_3) δ ppm 31.9, 32.0, 34.2, 35.3, 53.5, 53.8, 54.0, 54.2, 121.4, 121.5, 121.6, 123.4, 123.5, 123.6, 124.1, 124.8, 125.0, 125.2, 125.9, 141.0, 141.1, 141.3, 141.9, 142.3, 142.9, 145.3, 145.8, 146.3; LRMS m/z (EI, M^+) = 364.23 g mol^{-1} ; HRMS Calc. for $\text{C}_{28}\text{H}_{28}$ m/z = 364, found 364.2182 g mol^{-1} ; IR (NaCl): 2958, 1458, 1362, 1265, 1192, 796, 741, 625 cm^{-1} .

Preparation of 2,2,5,5-tetramethyl-1-nitro-2,3,4,5-tetrahydrobenzotriptycene (10):



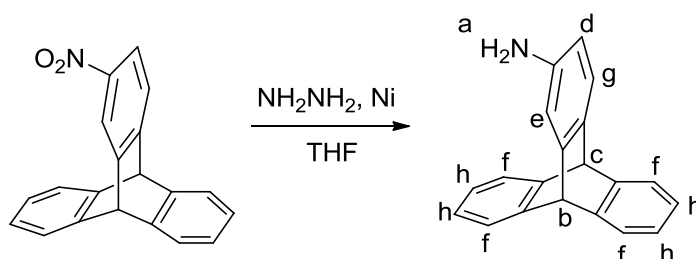
7,7,10,10-Tetramethyl-5,7,8,9,10,12-hexahydrotriptycene (3.00 g, 8.24 mmol) was dissolved in boiling acetic anhydride (45 ml). The solution was cooled slowly to 0 °C before acetic acid (0.94 ml, 16.48 mmol) was added, concentrated nitric acid (70%, 1.20 ml, 27.19 mmol) was then added dropwise. After stirring for 24 hours the reaction was quenched in water (100 ml) and stirred for 1 hour. The crude product was extracted with dichloromethane (3 x 50 ml) and the solution dried under reduced pressure, giving the crude product as a pale yellow powder. This material was passed through a silica column (4:1 hexane:dichloromethane). This gave the product as a white powder (0.46 g, 1.12 mmol, 13.6%). Mp 308 – 310 °C; ¹H NMR (400 MHz, CDCl₃) δ ppm 1.25 (6H, s, H_a), 1.29 (6H, s, H_b), 1.58 (2H, m, H_c), 1.68 (2H, m, H_d), 5.23 (1H, s, H_e), 5.44 (1H, s, H_f), 7.05 (4H, m, H_g), 7.40 (4H, m, H_h), 7.45 (1H, s, H_i); ¹³C NMR (100 MHz, CDCl₃) δ ppm 29.0, 32.6, 34.4, 34.8, 35.1, 38.2, 49.9, 53.5, 123.7, 124.2, 125.7, 131.1, 135.25, 143.7, 144.5, 144.8, 147.8; HRMS Calc. for C₂₈H₂₇NO₂ *m/z* = 409, found 409.2038 gmol⁻¹; IR (NaCl): 2962, 2932, 1520, 1459, 1384, 1366, 1277, 1261, 1216, 1194, 1163, 1120, 1085, 1058, 1020 cm⁻¹.

Synthesis of 2-nitrotriptycene (11):



Following the procedure reported by J. H. Chong and M. J. MacLachlan¹³⁵, triptycene (4.00 g, 15.75 mmol) was added to a mixture of concentrated nitric acid (70%, 50 ml) and glacial acetic acid (120 ml). The mixture was heated to 75 °C and stirred for 16 hours before the cloudy yellow solution was cooled to room temperature and quenched in water (150 ml). The crude product was extracted with dichloromethane (3 x 80 ml) before the solvent was removed under reduced pressure. This material was purified by silica column chromatography (1:4 dichloromethane:hexane) and concentrated to yield the product as a yellow powder (3.48 g, 11.63 mmol, 73.8%). Mp 254-258 °C; Lit. Mp = 268 – 271 °C¹³⁵; ¹H NMR (400 MHz, CDCl₃) δ ppm 5.54 (1H, s, H_a), 5.55 (1H, s, H_b), 7.05 (4H, m, H_c), 7.43 (4H, m, H_d), 7.50 (1H, d, *J* = 8.2 Hz, H_e), 7.95 (1H, dd, *J* = 8.2 Hz, H_f), 8.22 (1H, s, H_g); ¹³C NMR (100 MHz, CDCl₃) δ ppm 53.9, 54.0, 118.7, 121.4, 123.9, 124.0, 124.1, 125.8, 125.9, 143.6, 144.0, 145.5, 147.1, 152.4; LRMS *m/z* (EI, M⁺) = 299.10; IR (NaCl): 3069, 1592, 1518, 1460, 1342, 1194, 801, 751 cm⁻¹.

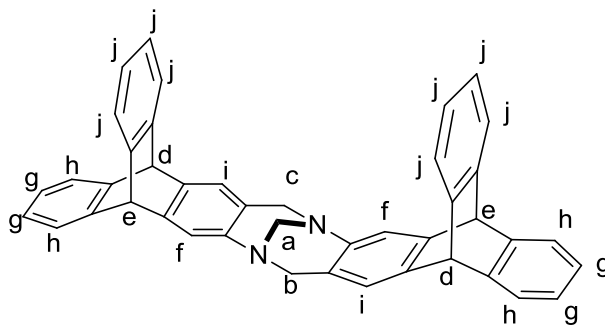
Synthesis of 2-aminotriptycene (12):



Following the procedure reported by J. H. Chong and M. J. MacLachlan¹³⁵, 2-nitrotriptycene (1.00 g, 3.30 mmol) was dissolved in THF (40 ml) with stirring under nitrogen. Raney nickel (catalytic amount) and hydrazine monohydrate (0.5 ml, 10.00 mmol) were added slowly before the temperature was increased to 60 °C. The mixture was stirred under nitrogen for 16 hours, then filtered and the solvent removed under reduced pressure. The resulting oil was added to water (50 ml), the product extracted with chloroform (3 x 10 ml) before the solvent was removed under reduced pressure, giving the product as a white powder (0.85 g, 3.10 mmol, 94.6%). Mp 233 – 235 °C, Lit. Mp = 246 °C (decomposes)¹³⁵; ¹H NMR (400 MHz, CDCl₃) δ ppm 3.34 (2H, broad s, H_a), 5.31 (1H, s, H_b), 5.33 (1H, s, H_c), 6.29 (1H, d, *J* = 7.8 Hz, H_d), 6.81 (1H, s, H_e), 6.99 (4H, m, H_f), 7.16 (1H, d, *J* = 7.8 Hz, H_g), 7.37 (4H, m, H_h); ¹³C NMR (100 MHz, CDCl₃) δ ppm 53.3,

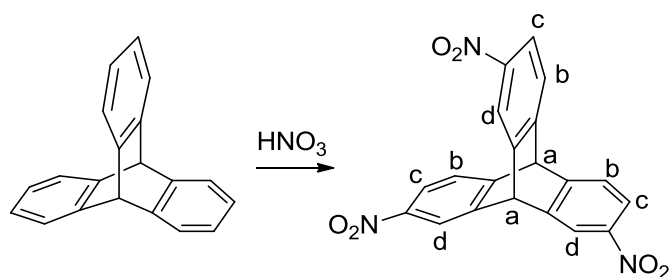
54.3, 110.9, 111.8, 123.3, 123.5, 123.7, 124.1, 125.0, 125.2, 135.8, 143.8, 145.3, 146.0, 146.6; LRMS m/z (ES, $M + \text{MeCNH}^+$) = 311.15; IR (NaCl): 3468, 3378, 3015, 2960, 1618, 1472, 1457, 1336, 794, 741 cm^{-1} .

Synthesis of Tröger's base from 2-aminotriptycene (13):



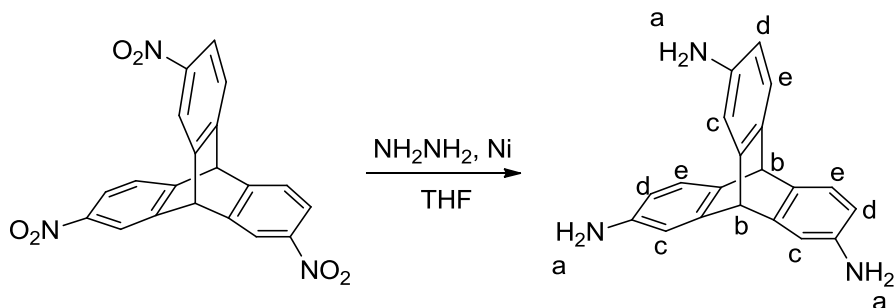
Dimethoxymethane (1.48 ml, 16.74 mmol) was added to trifluoroacetic acid (20 ml) at 0 °C. To this 2-aminotriptycene (1.50 g, 5.58 mmol) was added in small portions before the mixture was left stirring for 16 hours. The reaction was then quenched with water (150 ml) and saturated sodium hydroxide solution added until a pH of 12 was achieved. This was stirred vigorously for 2 hours before the precipitate was collected by filtration. The solid was added to saturated sodium hydroxide solution (30 ml) and extracted with dichloromethane (3 x 30 ml). The solution was concentrated under reduced pressure giving the product as a white powder (1.10 g, 1.92 mmol, 68.9%). TGA (nitrogen): 10.5% loss of weight occurred at ~205 °C. Initial weight loss due to thermal degradation started at 387 °C and totalled 31%. ^1H NMR (400 MHz, CDCl_3) δ ppm 4.13 (2H, m, H_a), 4.17 (2H, s, H_b), 4.70 (2H, s, H_c), 5.40 (2H, s, H_d), 5.48 (2H, s, H_e), 7.01 (2H, s, H_f), 7.05 (4H, m, H_g), 7.11 (4H, m, H_h), 7.14 (2H, s, H_i), 7.40 (2H, m, H_j), 7.51 (6H, m, H_j); ^{13}C NMR (100 MHz, CDCl_3) δ ppm 53.5, 53.8, 58.2, 66.8, 120.4, 121.8, 123.4, 123.5, 123.6, 124.0, 125.1, 125.2, 125.3, 140.9, 144.3, 144.9, 145.0, 145.2; HRMS Calc. for $\text{C}_{43}\text{H}_{30}\text{N}_2$ m/z = 574, found 575.2501 g mol^{-1} ; IR (NaCl): 3067, 3018, 2956, 2898, 2845, 1783, 1622, 1572, 1459, 1420, 1341, 1293, 1265 cm^{-1} . Crystals were prepared by a slow diffusion of hexane into a solution of the compound in ethyl acetate. Crystal properties: system = Orthorhombic, space group = $P bca$, a = 19.6400(2), b = 17.8250(19), c = 41.9200(5), α = 90.00, β = 90.00, γ = 90.00, V = 14675.50 \AA^3 ; Z = 16.

Synthesis of 2,6(7),14-trinitrotritycene (14):



Based upon the procedure detailed by C. Zhang and C. Chen¹³⁶, triptycene (5.00 g, 19.69 mmol) was added to a mixture of concentrated nitric acid (70%, 200 ml) and concentrated sulphuric acid (95%, 15 ml). The mixture was heated to 80 °C and stirred for 16 hours, before the temperature was increased to 100 °C for 2 hours, until all remaining solid had dissolved. The reaction was then quenched in water (1000 ml) and stirred for an hour. The crude product was extracted with chloroform (3 x 150 ml) and the chloroform removed under reduced pressure. The crude material was purified by column chromatography (4:1 dichloromethane:hexane), giving the product as a light yellow powder (4.97 g, 12.78 mmol, 64.9%). Mp 172-174 °C; Lit. Mp = 173 – 176 °C¹³⁶; ¹H NMR (400 MHz, CDCl₃) δ ppm 5.83 (2H, m, H_a), 7.64 (3H, m, H_b), 8.05 (3H, m, H_c), 8.34 (3H, m, H_d). ¹³C NMR (100 MHz, CDCl₃) δ ppm 53.1, 53.2, 53.4, 53.5, 119.6, 121.0, 122.5, 122.6, 125.0, 143.9, 144.3, 144.7, 146.3, 148.9, 149.2, 149.6; LRMS *m/z* (EI, M⁺) = 389.07; IR (NaCl): 3092, 1591, 1521, 1459.9, 1346.1, 1197.6, 794.5, 735.7 cm⁻¹.

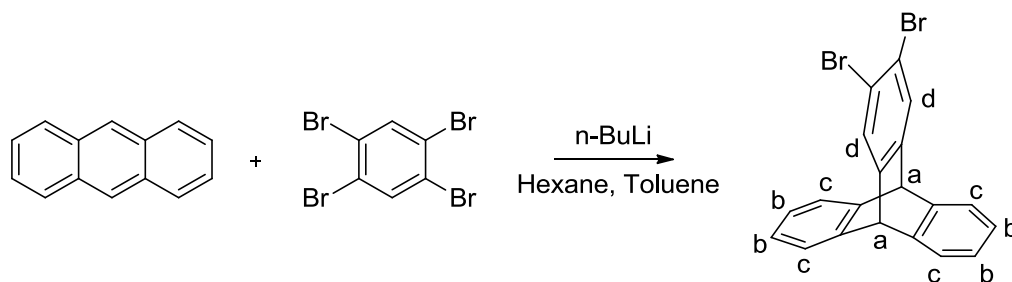
Synthesis of 2,6(7),14-triaminotriptycene (15):



Following the procedure described by C. Zhang and C. Chen¹³⁶, 2,6(7),14-Trinitrotritycene (1.00 g, 2.64 mmol) was dissolved in THF (40 ml) with stirring under

nitrogen. Raney nickel (catalytic amount) and hydrazine monohydrate (1.2 ml, 23.8 mmol) were added slowly to the solution before the temperature was increased to 60 °C. This was stirred under nitrogen for 16 hours, then filtered and the solvent removed under reduced pressure. The resulting oil was added to water (50 ml), the product extracted with chloroform (3 x 10 ml) and the solvent removed under reduced pressure, giving the product as a cream-white powder (0.80 g, 2.61 mmol, 98.8%). Mp 160-162 °C; Lit. Mp = 279 – 283 °C (isomerically pure)¹³⁶; ¹H NMR (400 MHz, CDCl₃) δ ppm 3.48 (6H, br. s, H_a), 5.03 (2H, m, H_b), 6.25 (3H, m, H_c), 6.72 (3H, m, H_d), 7.06 (3H, m, H_e); ¹³C NMR (100 MHz, *d6*-acetone) δ ppm 52.2, 53.3, 54.4, 55.5, 110.3, 110.5, 110.9, 111.3, 111.5, 111.9, 123.6, 124.0, 124.2, 135.5, 136.4, 137.3, 145.9, 146.3, 146.5, 147.6, 148.4, 149.2; LRMS *m/z* (ES, M⁺) = 299.14; IR (NaCl): 3341, 3209, 3007, 2957, 1620, 1479, 1329, 1188, 819, 730 cm⁻¹.

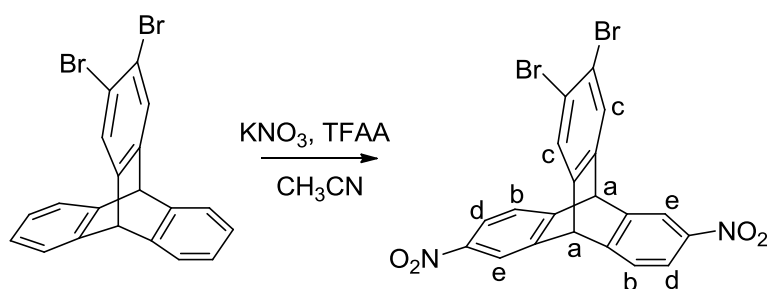
Preparation of 2,3-dibromotriptycene (16):



Following the procedure reported by H. Hart *et al.*¹³⁷, anthracene (8.00 g, 44.89 mmol) and 1,2,4,5-tetrabromobenzene (23.00 g, 58.35 mmol) were dissolved in toluene (640 ml) at room temperature. The solution was cooled to 0 °C before *n*-butyl lithium (2.5 M in hexane, 27 ml, 67.33 mmol) in hexane (140 ml) was added dropwise over 30 minutes. The solution was allowed to warm to room temperature and stirred for 16 hours under nitrogen before it was concentrated under reduced pressure. The resulting residue was added to water (300 ml), extracted with chloroform (4 x 100 ml), washed with sodium hydroxide (100 ml) and the solvent then removed under reduced pressure, giving the crude product as a brown powder. This was triturated in acetone at 0 °C for 1 hour before the solid was removed by filtration and the solution dried under reduced pressure. This gave a brown powder, which was passed through a silica column (using 9:1 hexane:dichloromethane) to purify the material. This gave the product as an off-white powder (10.65 g, 25.84 mmol,

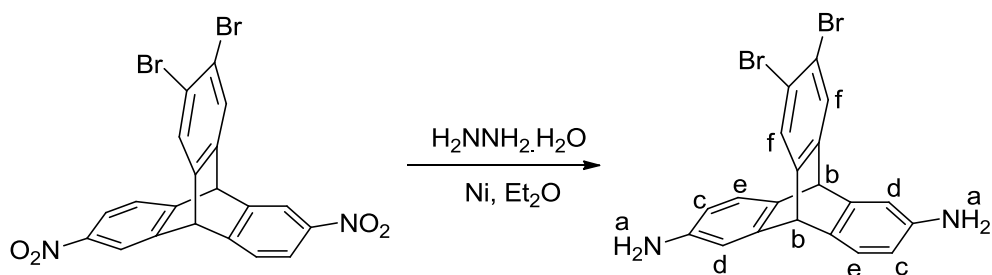
57.6%). Mp 177 – 179 °C; Lit. Mp = 191 – 192 °C¹³⁷; ¹H NMR (400 MHz, CDCl₃) δ ppm 5.37 (2H, s, H_a), 7.03 (4H, m, H_b), 7.38 (4H, m, H_c), 7.63 (2H, s, H_d); ¹³C NMR (100 MHz, CDCl₃) δ ppm 53.3, 120.7, 124.2, 125.8, 128.0, 144.3, 146.5; LRMS *m/z* (EI, M⁺) = 411.92 gmol⁻¹; IR (NaCl): 3067, 3040, 3020, 2963, 1908, 1590, 1557, 1458, 1442, 1365, 1296, 1216, 1189, 1156, 1128, 1097, 1024 cm⁻¹.

Preparation of 2,3-dibromo-6(7),14-dinitrotriptycene (17):



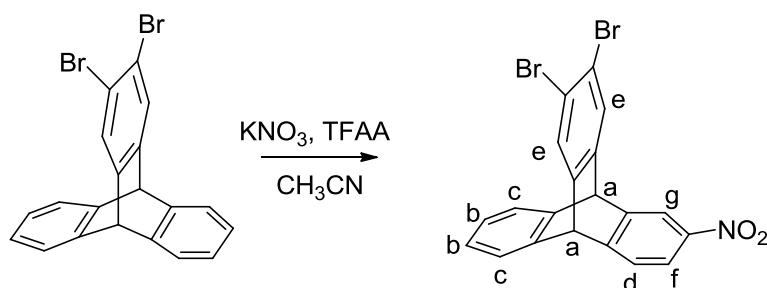
2,3-Dibromotriptycene (2.00 g, 4.85 mmol) was dissolved in acetonitrile (100 ml) before potassium nitrate (1.47 g, 14.56 mmol) and trifluoroacetic anhydride (4.73 ml, 33.95 mmol) were added. The reaction was left stirring for 16 hours at room temperature and then concentrated under reduced pressure. The resulting residue was added to water (300 ml) and the product extracted with chloroform (5 x 60 ml). The chloroform solution was filtered and concentrated under reduced pressure to give the product as an orange powder (2.43 g, 4.84 mmol, 99.0%). Mp 222 – 224 °C; ¹H NMR (400 MHz, CDCl₃) δ ppm 5.63 (2H, m, H_a), 7.58 (2H, m, H_b), 7.73 (2H, m, H_c), 8.03 (2H, m, H_d), 8.27 (2H, m, H_e); ¹³C NMR (100 MHz, CDCl₃) δ ppm 52.6, 119.4, 122.3, 124.8, 129.5, 142.9, 143.3, 143.7, 144.9, 146.1, 149.4, 149.9; HRMS Calc. for C₂₀H₁₀N₂O₄Br₂*m/z* = 502, found 501.8844 gmol⁻¹; IR (NaCl): 3435, 2987, 1785, 1590, 1522, 1458, 1443, 1344, 1290, 1265, 1163 cm⁻¹.

Preparation of 2,3-dibromo-6(7),14-diaminotriptycene (18):



2,3-Dibromo-6(7),14-dinitrotriptycene (2.44 g, 4.86 mmol), diethyl ether (100 ml), hydrazine monohydrate (3.80 ml, 48.60 mmol) and Raney nickel (catalytic amount) were mixed together. The reaction mixture was heated to 30 °C and left stirring for 16 hours under nitrogen. It was then filtered and dried under reduced pressure, leaving a residue which was added to water (150 ml) and extracted with chloroform (3 x 100 ml). The solution was dried under reduced pressure, giving the product as an orange/brown powder (2.12 g, 4.81 mmol, 99.0%). Mp 168-170 °C; ¹H NMR (400 MHz, CDCl₃) δ ppm 3.51 (4H, br. s, H_a), 5.12 (2H, m, H_b), 6.27 (2H, m, H_c), 6.74 (2H, m, H_d), 7.10 (2H, m, H_e), 7.55 (2H, m, H_f); ¹³C NMR (100 MHz, CDCl₃) δ ppm 53.0, 111.1, 111.7, 118.3, 124.1, 126.6, 127.8, 135.7, 144.0, 145.7, 146.5; HRMS Calc. for C₂₀H₁₄N₂Br₂m/z = 442, found 441.9540 gmol⁻¹; IR (NaCl): 3433, 2960, 2089, 1624, 1441, 1363, 1215, 1096 cm⁻¹.

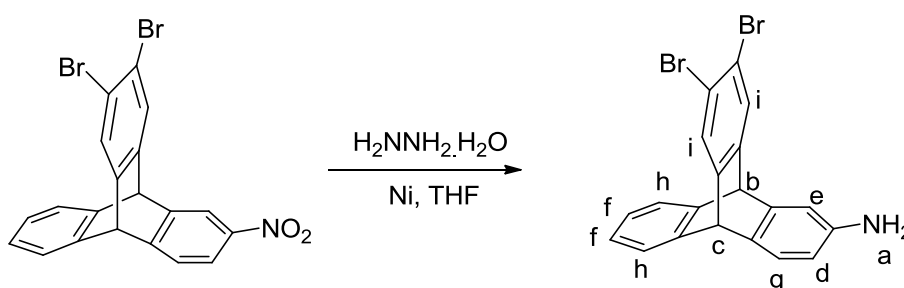
Preparation of 2,3-dibromo-6(7)-nitrotriptycene (19):



2,3-Dibromotriptycene (1.00 g, 2.43 mmol) was dissolved in acetonitrile (60 ml). Once dissolved, potassium nitrate (0.28 g, 2.67 mmol) and trifluoroacetic acid (2.36 ml, 16.98 mmol) were added before the reaction was heated to 50 °C and left stirring for 16 hours. The mixture was then concentrated under reduced pressure and the resulting oil added to water (100 ml). The mixture was extracted with chloroform (3 x 20 ml), and the

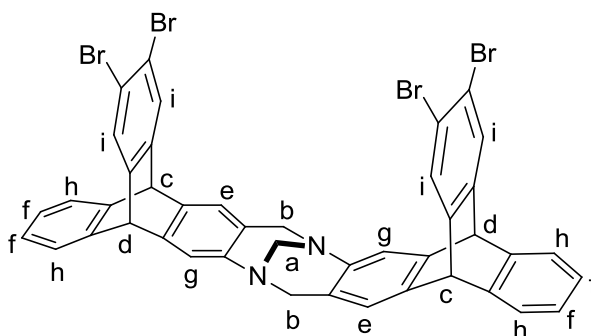
chloroform removed under reduced pressure to give the crude product as a cream powder. This was passed through a silica column (using 9:1 hexane:dichloromethane), giving the product as an off-white powder (0.91 g, 2.00 mmol, 82.2%). Mp 170 – 172 °C; ^1H NMR (400 MHz, CDCl_3) δ ppm 5.49 (2H, s, H_a), 7.08 (2H, m, H_b), 7.42 (2H, m, H_c), 7.51 (1H, d, $J = 8.0$ Hz, H_d), 7.67 (1H, s, H_e), 7.68 (1H, s, H_e), 7.96 (1H, d, $J = 8.0$ Hz, H_f), 8.21 (1H, s, H_g); ^{13}C NMR (100 MHz, CDCl_3) δ ppm 52.8, 118.9, 121.4, 121.5, 124.3, 129.0, 129.5, 142.5, 142.9, 144.5, 145.0, 145.8, 146.0, 151.2; HRMS Calc. for $\text{C}_{20}\text{H}_{11}\text{NO}_2\text{Br}_2$ $m/z = 457$, found 456.9178 g mol^{-1} ; IR (NaCl): 3019, 2400, 2360, 2253, 1526, 1459, 1345, 1216, 1098 cm^{-1} .

Preparation of 2,3-dibromo-6(7)-aminotriptycene (20):



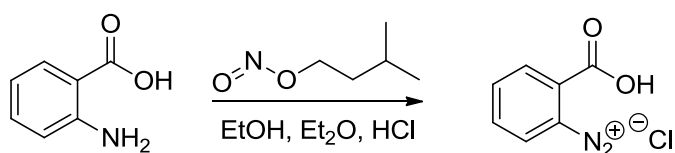
2,3-Dibromo-6(7)-dinitrotriptycene (0.74 g, 1.62 mmol) was dissolved in THF (30 ml) at room temperature. Once dissolved, hydrazine monohydrate (0.41 ml, 8.09 mmol) and Raney nickel (catalytic amount) were added before the mixture was heated to 50 °C and left stirring under nitrogen for 16 hours. Following this, the mixture was filtered and concentrated under reduced pressure to give the crude product as a brown oil. This was added to water (100 ml) and extracted with chloroform (3 x 30 ml). The chloroform was removed under reduced pressure to give the product as a fluffy cream powder (0.69 g, 1.62 mmol, 99%). Mp 180 – 182 °C; ^1H NMR (400 MHz, CDCl_3) δ ppm 2.90 (2H, br. s, H_a), 5.22 (1H, s, H_b), 5.24 (1H, s, H_c), 6.31 (1H, d, $J = 7.4$ Hz, H_d), 6.78 (1H, s, H_e), 7.01 (2H, m, H_f), 7.13 (1H, d, $J = 7.4$ Hz, H_g), 7.34 (2H, m, H_h), 7.58 (2H, s, H_i), ^{13}C NMR (100 MHz, CDCl_3) δ ppm 52.3, 53.3, 111.3, 111.8, 120.3, 120.6, 123.5, 123.7, 124.4, 125.6, 128.5, 134.5, 144.0, 144.8, 145.4, 146.3, 147.1; HRMS Calc. for $\text{C}_{20}\text{H}_{13}\text{NBr}_2$ $m/z = 427$, found 426.9423 g mol^{-1} ; IR (NaCl): 3418, 2925, 2854, 2360, 1625, 1457, 1201 cm^{-1} .

Preparation of Tröger's base from 2,3-dibromotriptycene (21):



2,3-Dibromo-6(7)-diaminotriptycene (0.55 g, 1.29 mmol) was dissolved in trifluoroacetic acid (8 ml) with stirring at 0 °C. Once dissolved, dimethoxymethane (0.23 ml, 2.58 mmol) was added and the reaction mixture left stirring for 16 hours. The reaction was then quenched in a mixture of aqueous ammonia (35%, 100 ml) and ice (50 g). It was stirred for 2 hours before the product was extracted with chloroform (3 x 50 ml). The chloroform solution was concentrated under reduced pressure to give the product as a light brown powder (0.59 g, 0.65 mmol, 99%). Mp > 350 °C; ¹H NMR (400 MHz, CDCl₃) δ ppm 3.98 (2H, m, H_a), 4.12 (2H, m, H_b), 4.51 (2H, m, H_b), 5.17 (1H, s, H_c), 5.18 (1H, s, H_c), 5.24 (1H, s, H_d), 5.25 (1H, s, H_d), 6.83 (1H, s, H_e), 6.86 (1H, m, H_e), 7.00 (4H, m, H_f), 7.08 (2H, m, H_g), 7.32 (4H, m, H_h), 7.48 (1H, m, H_i), 7.56 (2H, m, H_i), 7.60 (1H, m, H_i); ¹³C NMR (100 MHz, CDCl₃) δ ppm 52.6, 53.4, 58.4, 66.8, 124.4, 125.5, 125.6, 125.7, 125.8, 128.5, 139.5, 143.2, 143.9, 144.4, 145.2, 146.3. HRMS Calc. for C₄₃H₂₆N₂Br₄m/z = 890, found 889.8767 g mol⁻¹; IR (NaCl): 3419, 3010, 2960, 1734, 1625, 1462, 1443, 1422, 1364, 1341, 1296, 1214, 1154, 1098, 1078, 1030 cm⁻¹.

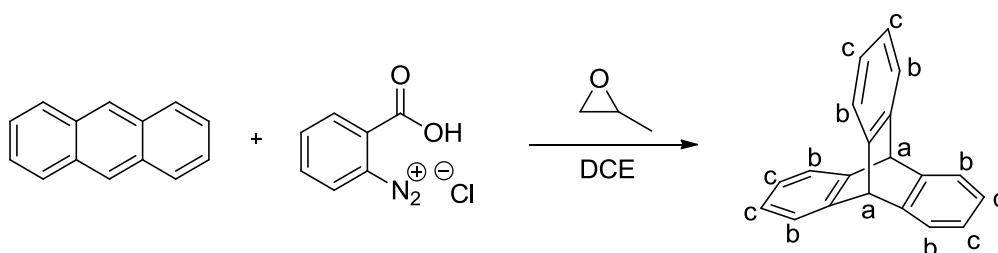
Preparation of benzenediazonium-2-carboxylatechloride (22):



Based upon the procedure detailed by B. H. Klanderman and T. H. Criswell¹⁸⁵, 2-aminobenzoic acid (31.00 g, 226.3 mmol) was added to ethanol (700 ml) at 0 °C. After stirring for 15 minutes concentrated hydrochloric acid (37%, 25 ml) was added, causing

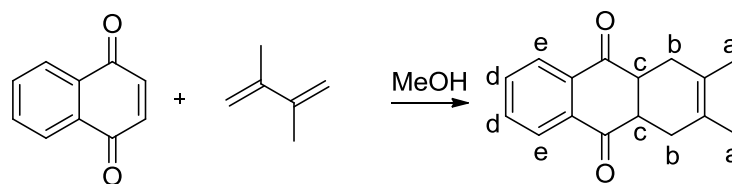
the solid to dissolve. After a further 15 minutes isoamyl nitrite (54.70 ml, 407.30 mmol) was added, after which the solution was stirred for another 15 minutes. Diethyl ether (700 ml) was then added, causing the product to crash out, and after stirring for 15 minutes the solid was collected by filtration. The solid was washed with diethyl ether (700 ml) and dried under vacuum. This gave the product as a cream coloured powder (39.87 g, 216.00 mmol, 95.5%). No characterisation was performed due to the instability of the product.

Preparation of triptycene (23):



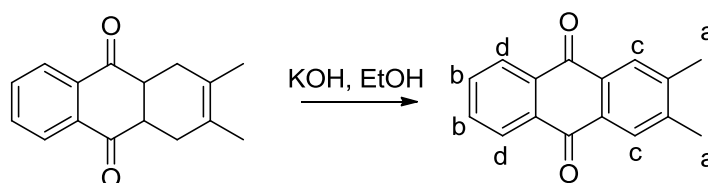
Based upon the procedures described by L. Friedman et al.¹³⁸ and J. M. Chance et al.¹⁴³, anthracene (4.50 g, 25.28 mmol) was added to dichloroethane (250 ml) and the mixture heated to 60 °C. Once at temperature, benzenediazonium-2-carboxylate (23.09 g, 126.40 mmol) and 1,2-epoxypropane (75 ml) were added before the mixture was refluxed at 85 °C for 48 hours under a nitrogen atmosphere. It was then cooled to room temperature and the concentrated under reduced pressure, giving a brown oil. The oil was added to a mixture of maleic anhydride (2.48 g, 25.28 mmol) and o-xylene (200 ml). This was heated to 110 °C for an hour before being allowed to cool to room temperature and added to water (300 ml). The crude material was extracted with dichloromethane (3 x 100 ml) and the organic solution washed with aqueous potassium hydroxide (15%, 2 x 150 ml). The organic solution was then dried under reduced pressure, giving a red residue, which was triturated in methanol (200 ml) for 16 hours. The resulting solid was collected by filtration and dried under vacuum giving the product as a light brown powder (4.02 g, 15.83 mmol, 62.6%). Mp 242 – 244 °C; Lit. Mp = 253 – 254 °C¹³⁸; ¹H NMR (400 MHz, CDCl₃) δ ppm 5.47 (2H, s, H_a), 7.03 (6H, m, H_b), 7.43 (6H, m, H_c); ¹³C NMR (100 MHz, CDCl₃) δ ppm 54.2, 123.8, 125.2, 145.4; LRMS m/z (EI, M⁺) = 254.10 g mol⁻¹; IR (NaCl): 3069, 3020, 2968, 1906, 1454, 1310, 1215, 1196, 1163, 1027, 1016 cm⁻¹.

Preparation of 2,3-dimethylbutadiene- α -naphthoquinone (24):



Following the procedure reported by C. F. H. Allen and A. Bell¹⁴⁰, 2,3-dimethyl-1,3-butadiene (60.1 ml, 531.11 mmol), α -naphthoquinone (30.00 g, 189.68 mmol) and methanol (160 ml) were mixed together and then heated to 70 °C. The mixture was left stirring for 16 hours under a nitrogen atmosphere. It was then cooled to room temperature and the resulting precipitate filtered off. The solid was washed with methanol (400 ml) before being ground up. This gave the product as an off-white powder (44.70 g, 186.25 mmol, 98.2%). Mp 142 – 144 °C; lit. mp = 147 -149 °C¹⁴⁰; ¹H NMR (400 MHz, CDCl₃) δ ppm 1.63 (6H, s, H_a), 2.14 (2H, m, H_b), 2.45 (2H, d, m, H_b), 3.36 (2H, m, H_c), 7.73 (2H, m, H_d), 8.04 (2H, m, H_e); ¹³C NMR (100 MHz, CDCl₃) δ ppm 18.9, 30.7, 47.4, 123.5, 126.8, 134.2, 198.3; LRMS *m/z* (EI, M⁺) = 240.12 gmol⁻¹; IR (NaCl): 2913, 2888, 1685, 1592, 1446, 1421, 1370, 1345, 1284, 1251, 1205, 1160, 1143, 1074, 1028 cm⁻¹.

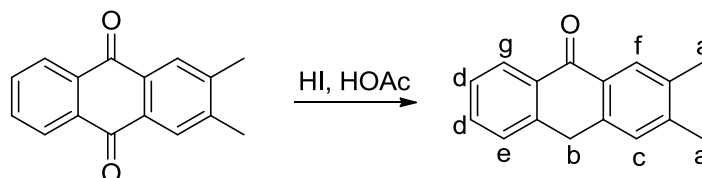
Preparation of 2,3-dimethylantraquinone (25):



Following the procedure reported by C. F. H. Allen and A. Bell¹⁴⁰, 2,3-dimethylbutadiene- α -naphthoquinone (20.00 g, 83.33 mmol) was stirred in ethanolic potassium hydroxide solution (5%, 300 ml) for 72 hours. This caused the colour to change from white to green. The precipitate was collected by filtration, washed with water (3 x 200 ml), ethanol (200 ml) and diethyl ether (100 ml). This gave the product as a light green powder (18.15 g, 76.9 mmol, 92.3%). Mp 200 – 202 °C; lit. mp = 209- 210 °C¹⁴⁰; ¹H NMR (400 MHz, CDCl₃) δ ppm 2.39 (6H, s, H_a), 7.74 (2H, m, H_b), 7.97 (2H, s, H_c), 8.24 (2H, m, H_d); ¹³C NMR (100 MHz, CDCl₃) δ ppm 20.2, 127.0, 128.1, 131.5, 133.8, 144.0, 183.2; LRMS

$m/z(\text{EI}, \text{M}^+) = 236.09 \text{ g mol}^{-1}$; IR (NaCl): 2948, 1671, 1589, 1443, 1383, 1331, 1294, 1221, 1168, 1068, 1022 cm^{-1} .

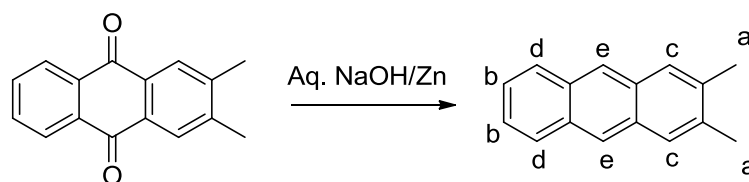
Preparation of 2,3-dimethylanthrone (26):



Following the procedure (for the synthesis of anthracene from anthraquinone) described by R. Sangaiah and A. Gold¹⁴², 2,3-dimethylantraquinone (5.00 g, 24.27 mmol) was added to a mixture of glacial acetic acid (180 ml) and hydroiodic acid (20 ml). The mixture was refluxed for 6 hours and then cooled to room temperature. The reaction was quenched in saturated sodium thiosulphate solution (500 ml), and immediately a precipitate began to crash out. The mixture was left stirring for 16 hours before the pale yellow solid was collected by filtration. The solid was washed with ethanol (100 ml) and diethyl ether (50 ml) before being dissolved in chloroform (300 ml). The solution was the solvent removed under reduced pressure and the resulting solid triturated in ethanol for 30 minutes. Filtration gave the product as a pale yellow powder (4.84 g, 21.82 mmol, 90%). Mp 128 – 130 °C; Lit. Mp = 153 – 157 °C¹⁸⁶; ¹HNMR (400 MHz, CDCl₃) δ ppm 2.35 (6H, s, H_a), 4.26 (2H, s, H_b), 7.22 (1H, s, H_c), 7.44 (2H, m, H_d), 7.57 (1H, m, H_e), 8.11 (1H, s, H_f), 8.35 (1H, m, H_g); ¹³C NMR (100 MHz, CDCl₃) δ ppm 19.5, 20.1, 31.9, 124.8, 126.8, 127.5, 128.1, 129.4, 130.0, 132.3, 135.7, 138.2, 140.6, 142.6, 184.2; LRMS m/z (ES +, M + H⁺) = 223.11 g mol^{-1} ; IR (NaCl): 3066, 2970, 2917, 2249, 1659, 1613, 1485, 1462, 1450, 1409, 1395, 1384, 1371, 1342, 1329, 1297, 1267, 1232, 1186, 1166, 1105, 1077, 1025 cm^{-1} .

Preparation of 2,3-dimethylantracene (27):

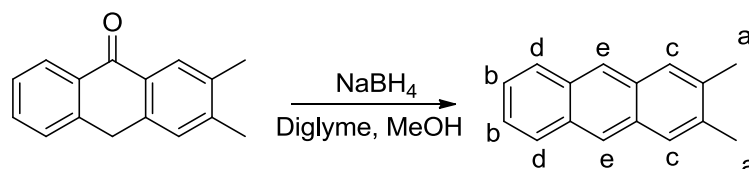
Zinc method (27a):



Activation of zinc: Based upon the procedure detailed by L. Guo-Yuan¹⁴¹, zinc (200.00 g, 3.06 mmol) was stirred in dilute hydrochloric acid (5%, 280 ml) for an hour. The zinc was then filtered off and washed with water (2 x 200 ml), methanol (200 ml) and diethyl ether (200 ml). This gave the activated zinc as a grey powder.

Reaction: Active zinc powder (34.89 g, 533.61 mmol) and 2,3-dimethylanthraquinone (2.00 g, 8.47 mmol), were added to a solution of sodium hydroxide (10.53 g, 262.57 mmol) in water (130 ml). The mixture was refluxed for 48 hours under a nitrogen atmosphere. After cooling to room temperature the mixture was poured into concentrated hydrochloric acid (37%, 200 ml) and stirred for 30 minutes. The solid was collected by filtration and washed with ethanol (300 ml), giving the product as an off-white powder (1.63 g, 7.91 mmol, 93.4%).

Sodium borohydride method (27b):

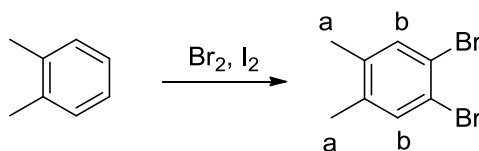


Following the procedure reported by D. J. Marquardt¹⁴³, 2,3-dimethylantrone (2.00 g, 9.01 mmol) was suspended in diglyme (40 ml) for 20 minutes under a nitrogen atmosphere. Sodium borohydride (1.00 g, 26.43 mmol) was added and immediate hydrogen evolution was observed with a colour change from pale yellow to orange. After 30 minutes, when the anthrone had dissolved, the reaction was transferred to a cold water

bath. Methanol (20 ml) and sodium borohydride (0.50 g, 13.22 mmol) were then slowly added. An immediate strong evolution of gas was observed. The mixture was stirred overnight before the reaction was quenched by addition of glacial acetic acid until a pH of 3 was reached. The mixture was stirred for two hours before water (400 ml) was slowly added. Immediately a precipitate was observed and the solid collected by filtration. The solid was washed with water (200 ml) and ethanol (100 ml) before being dried under vacuum. This gave the product as an off-white powder (1.69 g, 8.26 mmol, 91.5%).

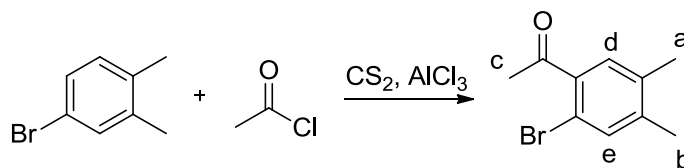
Characterisation (both): Mp 242 – 244 °C; Lit. Mp = 248 °C¹⁸⁷; ¹HNMR (400 MHz, CDCl₃) δ ppm 2.48 (6H, s, H_a), 7.42 (2H, m, H_b), 7.75 (2H, s, H_c), 7.97 (2H, m, H_d), 8.29 (2H, s, H_e); ¹³C NMR (100 MHz, CDCl₃) δ ppm 20.4, 123.3, 124.8, 127.0, 128.1, 131.4, 135.5; HRMS Calc. for C₁₆H₁₄m/z = 206, found 206.1101 gmol⁻¹; IR (NaCl): 2933, 1636, 1450, 1348, 1120, 1024 cm⁻¹.

Preparation of 1,2-dibromo-4,5-dimethylbenzene (28):



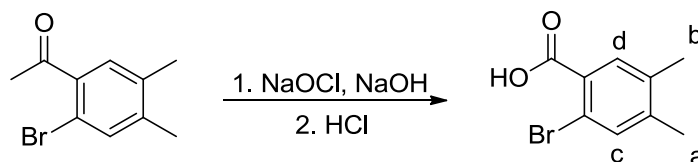
Following the procedure described by Y. Chen et al.¹⁴⁴, bromine (80 ml, 1574.98 mmol) was added dropwise to a mixture of iodine (0.40 g, 1.58 mmol) in o-xylene (95 ml, 787.49 mmol) that had been cooled to 0 °C. The mixture was left stirring for 72 hours, after which time diethyl ether (500 ml) was added to dissolve the solid reaction mixture. The resulting solution was then washed with sodium hydroxide solution (2M, 600 ml) and water (600 ml). The ether was removed under reduced pressure to give a colourless oil that crystallised at room temperature. Recrystallisation from methanol (500 ml) gave the product as a white powder (78.95 g, 299.28 mmol, 38.0%). Mp 82 – 84 °C; Lit. Mp = 86 – 87 °C¹⁸⁸; ¹HNMR (400 MHz, CDCl₃) δ ppm 2.17 (6H, s, H_a), 7.36 (2H, s, H_b); ¹³C NMR (100 MHz, CDCl₃) δ ppm 19.2, 121.1, 134.0, 137.6; LRMS m/z (EI, M⁺) = 263.89 gmol⁻¹; IR (NaCl): 2947, 1473, 1442, 1374, 1342, 1157, 1118, 1019 cm⁻¹.

Preparation of 2-bromo-4,5-dimethylacetophenone (29):



Following the procedure reported by A. Brändström and S. A. I. Carlsson¹⁴⁵, acetyl chloride (43.9 ml, 615.98 mmol), 1-bromo-3,4-dimethylbenzene (95.00 g, 513.32 mmol) and carbon disulphide (60 ml) were mixed together under a nitrogen atmosphere. To the mixture aluminium trichloride (75.29 g, 564.65 mmol) was added in one portion and the temperature slowly increased to 60 °C, when the mixture began to reflux. The mixture was stirred for two hours before the temperature was increased to 70 °C for a further final hour. The carbon disulphide was evaporated off and the mixture then cooled to room temperature. The reaction was quenched by addition to ice (1 L) and stirred for an hour before the product was extracted with dichloromethane (4 x 200 ml). The solvent was removed under reduced pressure, giving a dark oil. Recrystallisation from petroleum ether (40 – 60 °C) gave the product as dark needles (90.26 g, 396.05 mmol, 77.2%). Mp 24 – 26 °C; Lit. Mp = 31 – 32 °C¹⁴⁵; ¹HNMR (400 MHz, CDCl₃) δ ppm 2.22 (3H, s, H_a), 2.24 (3H, s, H_b), 2.60 (2H, s, H_c), 7.28 (1H, s, H_d), 7.36 (1H, s, H_e); ¹³C NMR (100 MHz, CDCl₃) δ ppm 19.1, 19.4, 30.2, 116.1, 130.5, 134.7, 136.1, 138.4, 141.6, 200.8; LRMS m/z (EI, M⁺) = 227.01 gmol⁻¹; IR (NaCl): 2974, 2921, 1695, 1598, 1551, 1480, 1447, 1380, 1363, 1286, 1256, 1216, 1157, 1105, 1021 cm⁻¹.

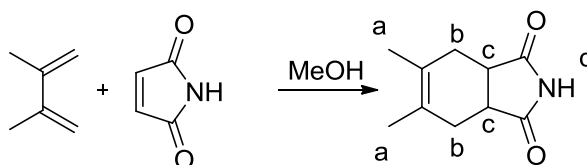
Preparation of 2-bromo-3,4-dimethylbenzoic acid (30):



Following the procedure reported by A. Brändström and S. A. I. Carlsson¹⁴⁵, 2-bromo-4,5-dimethylacetophenone (5.00 g, 22.04 mmol), sodium hypochlorite (10%, 100 ml, 161.97 mmol), sodium hydroxide solution (10%, 15 ml) and sodium 1-dodecanesulphonate (catalytic amount) were mixed together at room temperature. The mixture was heated to 75

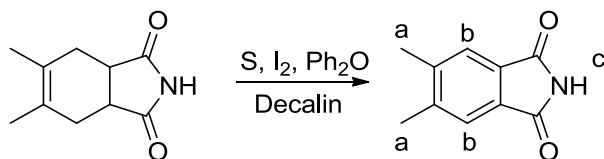
°C and stirred for 16 hours. The reaction was then quenched by addition of sodium metabisulphite (spatula tip) and stirred for 30 minutes. The mixture was cooled to room temperature and made acidic by addition of concentrated hydrochloric acid (37%) until a pH of 1 was reached. After stirring for 1 hour water (100 ml) was added and the mixture stirred for a further 10 minutes. The solid was then collected by filtration, washed with water (100 ml), dissolved in acetone (300 ml) and the solvent removed under reduced pressure, giving the crude product as a yellow solid. Recrystallisation from toluene gave the product as a cream powder (4.87 g, 21.28 mmol, 96.5%). Mp 172 – 174 °C; Lit. Mp = 195 - 196 °C¹⁴⁵; ¹HNMR (400 MHz, CDCl₃) δ ppm 2.26 (3H, s, H_a), 2.29 (3H, s, H_b), 7.48 (1H, s, H_c), 7.81 (1H, s, H_d); ¹³C NMR (100 MHz, CDCl₃) δ ppm 19.1, 19.5, 119.6, 127.2, 133.6, 135.7, 136.0, 143.6, 170.5; LRMS m/z (EI, M⁺) = 227.98 gmol⁻¹; IR (NaCl): 3433, 1664, 1600, 1488, 1401, 1304, 1260, 1162 cm⁻¹.

Preparation of 3,4-dimethyltetrahydrophthalimide (31):



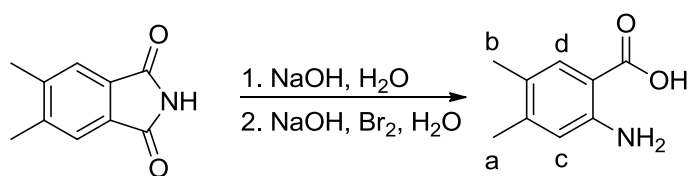
Following the procedure described by H.-J. Hess et al.¹⁵⁰, 2,3-dimethyl-1,3-butadiene (56.00 ml, 494.40 mmol) was added to a solution of maleimide (25.00 g, 257.73 mmol) in methanol (300 ml). The mixture was heated to 70 °C and stirred for 16 hours, before it was cooled to room temperature and the solvent removed under reduced pressure, giving a white residue. This was dissolved in chloroform (200 ml) and dried on the rotavap, giving the product as an off-white powder (45.32 g, 252.90 mmol, 98.1%). Mp 124 – 126 °C; Lit. Mp = 121 – 124 °C¹⁵⁰; ¹HNMR (400 MHz, CDCl₃) δ ppm 1.65 (6H, s, H_a), 2.16 (1H, m, H_b), 2.20 (1H, m, H_b), 2.36 (1H, s, H_b), 2.39 (1H, s, H_b), 3.04 (2H, m, H_c), 9.16 (1H, s, H_d); ¹³C NMR (100 MHz, CDCl₃) δ ppm 19.2, 30.4, 41.1, 126.8, 181.1; LRMS m/z (EI, M⁺) = 179.08 gmol⁻¹; IR (NaCl): 3223, 3073, 2989, 2940, 2930, 2892, 2846, 2757, 1821, 1749, 1696, 1433, 1360, 1333, 1316, 1278, 1260, 1211, 1187, 1118, 1084, 1033 cm⁻¹.

Preparation of 3,4-dimethylphthalimide (32):



Following the procedure described by H.-J. Hess et al.¹⁵⁰, a mixture of 3,4-dimethyltetrahydrophthalimide (30.00 g, 167.60 mmol), sulphur (13.43 g, 418.99 mmol), iodine (0.18 g, 0.70 mmol), diphenyl ether (5.58 ml, 35.20 mmol) and decalin (200 ml) was heated to 190 °C and stirred for 24 hours. The mixture was then cooled to room temperature, which caused a large amount of brown solid to crash out. The solid was broken up, collected by filtration, washed with diethyl ether (50 ml) and dried under vacuum. It was then triturated in diethyl ether (100 ml) for 16 hours before being collected by filtration and dried under vacuum. This gave the product as a light brown powder (26.23 g, 149.89 mmol, 89.4%). Mp 234 – 236 °C; Lit. Mp = 228 – 232 °C¹⁵⁰; ¹H NMR (400 MHz, CDCl₃) δ ppm 2.41 (6H, s, H_a), 7.61 (2H, s, H_b), 7.75 (1H, s, H_c); ¹³C NMR (100 MHz, CDCl₃) δ ppm 20.6, 124.5, 130.7, 144.1, 168.3; LRMS m/z (EI, M⁺) = 175.05 g mol⁻¹; IR (NaCl): 3424, 2951, 1644, 1390, 1348, 1299, 1105 cm⁻¹.

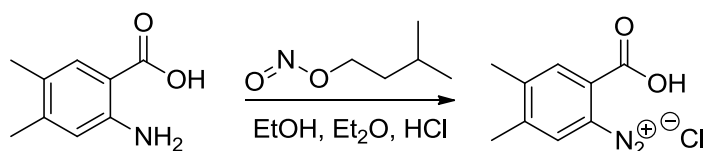
Preparation of 4,5-dimethylantranilic acid (33):



Based upon the procedure detailed by M. Teng et al.¹⁵¹, bromine (11.46 ml, 222.54 mmol) was added to aqueous sodium hydroxide (25%, 150 ml) with stirring at 0 °C, forming a yellow solution. 3,4-dimethylphthalimide (35.00 g, 202.31 mmol) was added to aqueous sodium hydroxide (10%, 340 ml) at 60 °C. Once dissolved, this second solution was cooled to 0 °C, forming a thick brown paste, which was added to the first solution. The mixture was stirred vigorously for 5 minutes before being heated to 80 °C for an hour. It was then cooled to room temperature and concentrated hydrochloric acid (37%) added until a pH of 5 was reached. This caused the product to crash out; it was collected by

filtration, washed with water (200 ml) and dried under vacuum. Recrystallisation with 1:1 chloroform:ethanol gave the product as a brown powder (20.68 g, 125.33 mmol, 62.0%). Mp 200 – 202 °C; Lit. Mp = 193 – 195 °C (decomposes)¹⁵⁰; ¹HNMR (400 MHz, CDCl₃) δ ppm 2.16 (3H, s, H_a), 2.21 (3H, s, H_b), 6.50 (1H, s, H_c), 7.66 (1H, s, H_d); ¹³C NMR (100 MHz, CDCl₃) δ ppm 18.6, 20.2, 107.4, 117.8, 125.0, 132.0, 145.1, 149.4, 172.8; HRMS Calc. for [C₉H₁₁NO₂]⁺ m/z = 165, found 165.0792 g mol⁻¹; IR (NaCl): 3381, 2939, 1657, 1630, 1589, 1539, 1494, 1471, 1442, 1415, 1354, 1302, 1283, 1243, 1209, 1160, 1065, 1024 cm⁻¹.

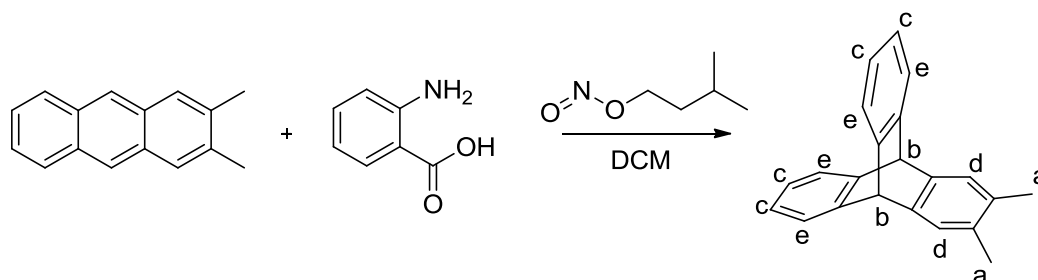
Preparation of 4,5-dimethylbenzenediazonium-2-carboxylatechloride (34):



4,5-Dimethyl-2-aminobenzoic acid (23.00 g, 139.39 mmol) was added to ethanol (500 ml) at 0 °C. After stirring for 15 minutes concentrated hydrochloric acid (37%, 23 ml) was added, causing the solid to dissolve. After a further 15 minutes isoamyl nitrite (33.71 ml, 250.91 mmol) was added, after which the solution was stirred for another 15 minutes. Diethyl ether (500 ml) was then added, which caused the product to crash out, and after stirring for 15 minutes the solid was collected by filtration. The solid was washed with diethyl ether (500 ml) and dried under vacuum. This gave the product as a cream coloured powder (24.49 g, 115.17 mmol, 82.6%). No characterisation was performed due to the instability of the product.

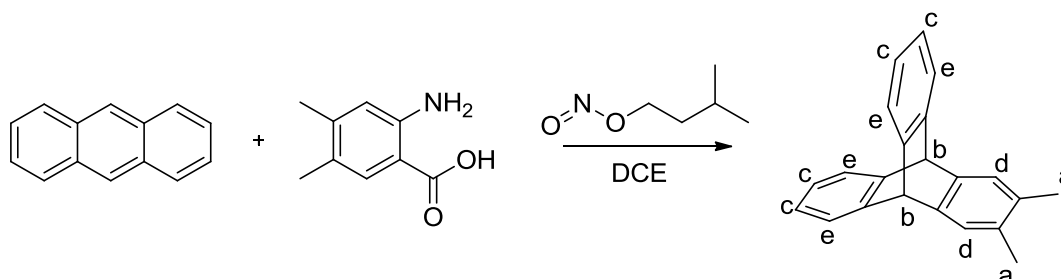
Preparation of 2,3-dimethyltriptycene (35):

2,3-Dimethylantracene route (35a):



A solution of anthranilic acid (18.00 g, 131.40 mmol) in acetone (60 ml) was added dropwise over a few hours to a refluxing mixture of 2,3-dimethylantracene (6.00 g, 43.80 mmol) and amyl nitrite (17.65 ml, 131.40 mmol) in dichloromethane (90 ml). The mixture was refluxed for 16 hours under a nitrogen atmosphere. It was then cooled to room temperature and concentrated under reduced pressure, giving a dark oil. The oil was added to a mixture of maleic anhydride (4.32 g, 43.80 mmol) and *o*-xylene (50 ml). This was heated to 110 °C for two hours before being cooled to room temperature. Water (150 ml) was added and the product extracted with dichloromethane (3 x 50 ml). The organic solution was washed with aqueous potassium hydroxide (15%, 2 x 100 ml) before being dried under reduced pressure. This gave a red residue, which was triturated in methanol (50 ml) for 16 hours. The resulting solid was collected by filtration and dried under vacuum. This gave the product as a light brown powder (0.58 g, 2.06 mmol, 4.7%).

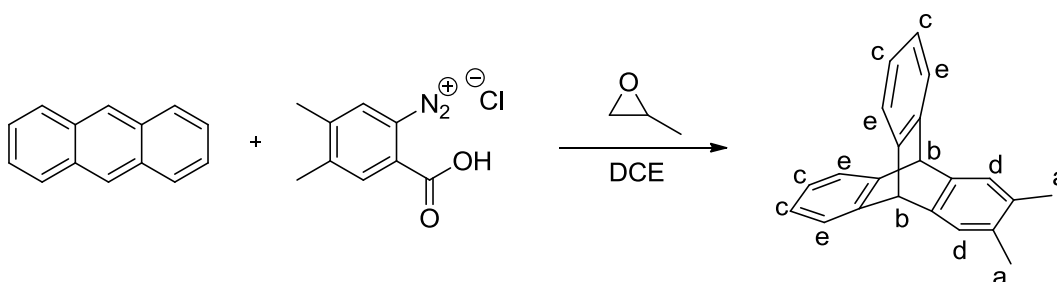
4,5-Dimethylanthranilic acid route (35b):



Based upon the procedure reported by K. Mislow et al.¹⁵², a solution of 3,4-dimethylanthranilic acid (5.00 g, 30.30 mmol) in acetone (50 ml) was added dropwise to a

refluxing mixture of anthracene (1.08 g, 6.06 mmol) and amyl nitrite (4.88 ml, 36.36 mmol) in dichloroethane (100 ml). The mixture was refluxed for 16 hours under a nitrogen atmosphere. It was then cooled to room temperature and the solvent removed under reduced pressure, giving a dark oil. This was added to a mixture of maleic anhydride (0.59 g, 6.06 mmol) and *o*-xylene (60 ml). This was heated to 110 °C for 2 hours before being cooled to room temperature. Water (150 ml) was added and the product extracted with dichloromethane (3 x 50 ml). The organic solution was washed with aqueous potassium hydroxide (15%, 3 x 50 ml) before being dried under reduced pressure. This gave a red residue, which was triturated in methanol (50 ml) for 16 hours. The resulting solid was collected by filtration and dried under vacuum. This gave the product as a light brown powder (0.44 g, 1.58 mmol, 26.1%).

Diazonium route (35c):

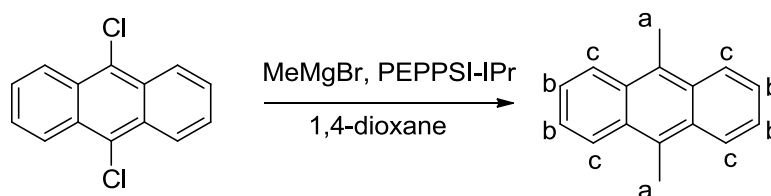


Anthracene (3.20 g, 17.98 mmol) was added to dichloroethane (170 ml) and heated to 60 °C. Once at temperature, 4,5-dimethylbenzenediazonium-2-carboxylatechloride (18.94 g, 89.89 mmol) and 1,2-epoxypropane (48 ml) were added. The mixture was refluxed at 85 °C for 72 hours under a nitrogen atmosphere. It was then cooled to room temperature and concentrated to a dark oil under reduced pressure. The oil was added to a mixture of maleic anhydride (1.96 g, 17.98 mmol) and *o*-xylene (150 ml). This was heated to 110 °C for two hours before being allowed to cool to room temperature. The mixture was then added to water (200 ml) and the product extracted with dichloromethane (3 x 100 ml). The organic solution was washed with aqueous potassium hydroxide (15%, 2 x 100 ml) before being concentrated to a red oil. This was loaded onto silica and passed through a silica column (9:1 hexane:dichloromethane), which gave the crude product as a yellow powder. Finally,

trituration in methanol (50 ml) for 16 hours gave the product as an off-white powder (3.06 g, 10.85 mmol, 60.4%)

Characterisation: Mp 226 – 228 °C; Lit. Mp = 240 – 242 °C¹⁵²; ¹H NMR (400 MHz, CDCl₃) δ ppm 2.19 (6H, s, H_a), 5.39 (2H, s, H_b), 7.00 (2H, m, H_c), 7.22 (2H, s, H_d), 7.39 (2H, m, H_e); ¹³C NMR (100 MHz, CDCl₃) δ ppm 19.5, 53.8, 123.5, 125.1, 132.9, 143.0, 145.6; LRMS m/z (EI, M⁺) = 282.14 gmol⁻¹; IR (NaCl): 3067, 3006, 2960, 1639, 1468, 1457, 1217, 1190, 1153, 1022 cm⁻¹.

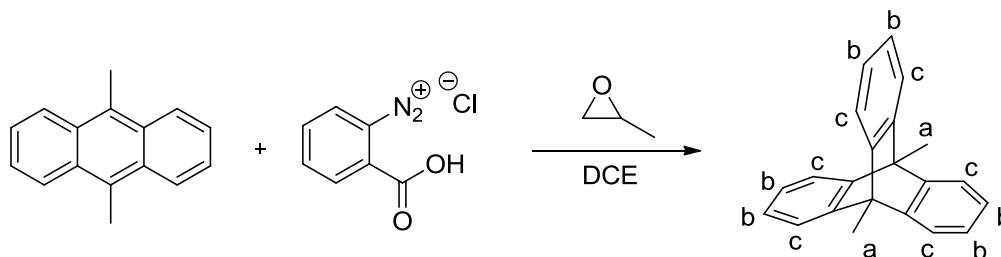
Preparation of 9,10-dimethylantracene (36):



Following the procedure described by C. J. Douglas and E. Yagodkin¹⁵³, in an oven-dried nitrogen purged flask was added 9,10-dichloroanthracene (15.00 g, 60.70 mmol), PEPPSI-IPr catalyst (2.68 g, 3.95 mmol) and 1,4-dioxane (1.2 L). This was stirred under a nitrogen atmosphere for thirty minutes before methyl magnesium bromide (3 M in ether, 121.40 ml, 364.20 mmol) was slowly added. The mixture was then left stirring for 24 hours under a nitrogen atmosphere. The reaction was quenched by addition to water (2 L) and stirred for an hour before the product was extracted with ethyl acetate (3 x 250 ml). The ethyl acetate solution was filtered through cotton wool and washed with saturated sodium chloride solution (500 ml). The solution was then filtered through filter paper and the solvent removed under reduced pressure, giving the crude product as a yellow solid. This was triturated with acetone (100 ml) and the solid collected by filtration. The acetone solution was dried under reduced pressure and the resulting solid triturated in acetone two further times, each time using less acetone. The solid fractions were combined and dried under vacuum. This gave the product as a yellow powder (12.26 g, 59.43 mmol, 97.9%). Mp 174 – 176 °C; Lit. Mp = 181 – 183 °C¹⁵³; ¹H NMR (400 MHz, CDCl₃) δ ppm 3.11 (6H, s, H_a), 7.53 (4H, m, H_b), 8.35 (4H, m, H_c); ¹³C NMR (100 MHz, CDCl₃) δ ppm 14.1, 124.7,

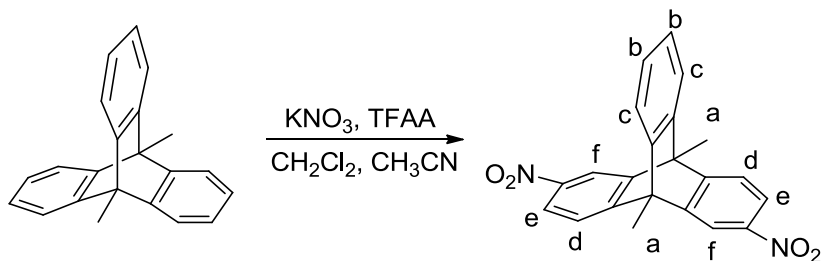
125.3, 128.3, 129.9; LRMS m/z (EI, M^+) = 206.10 g mol^{-1} ; IR (NaCl): 2982, 1618, 1463, 1377, 1305, 1284, 1233, 1150, 1100, 1071, 1050, 1022 cm^{-1} .

Preparation of 9,10-dimethyltriptycene (37):



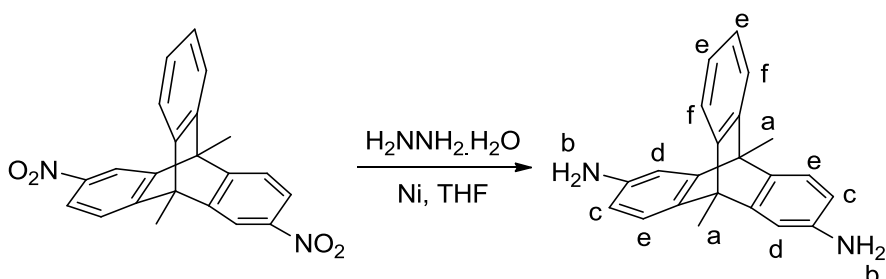
9,10-Dimethylanthracene (7.00 g, 33.98 mmol) was dissolved in dichloroethane (350 ml) at 60 °C with stirring. Benzenediazonium-2-carboxylatechloride (31.04 g, 169.90 mmol) and 1,2-epoxypropane (100 ml) were added to the solution before the mixture was refluxed at 85 °C for 40 hours under a nitrogen atmosphere. It was then allowed to cool to room temperature and concentrated under reduced pressure, giving a dark oil. The oil was added to a mixture of maleic anhydride (1.67 g, 16.99 mmol) and *o*-xylene (200 ml). This was heated to 110 °C for an hour before being allowed to cool to room temperature and added to water (350 ml). The crude material was extracted with dichloromethane (3 x 150 ml) and the organic solution washed with aqueous potassium hydroxide (15%, 2 x 150 ml). The solution was then dried under reduced pressure, giving a red residue, which was triturated in methanol (150 ml) for 16 hours. The resulting solid was collected by filtration and dried under vacuum, giving the product as a light brown powder (7.76 g, 27.52 mmol, 81.0%). Mp 324 – 326 °C; Lit. Mp = > 300 °C¹⁸⁹; ¹H NMR (400 MHz, CDCl₃) δ ppm 2.44 (6H, s, H_a), 7.04 (6H, m, H_b), 7.38 (6H, m, H_c); ¹³C NMR (100 MHz, CDCl₃) δ ppm 13.8, 48.8, 120.7, 125.0, 148.5; HRMS Calc. for [C₂₂H₁₈]⁺ m/z = 282, found 282.1407 g mol^{-1} ; IR (NaCl): 3067, 2976, 1469, 1448, 1375, 1141, 1089, 1024 cm^{-1} .

Preparation of 2,6(7)-dinitro-9,10-dimethyltritycene (38):



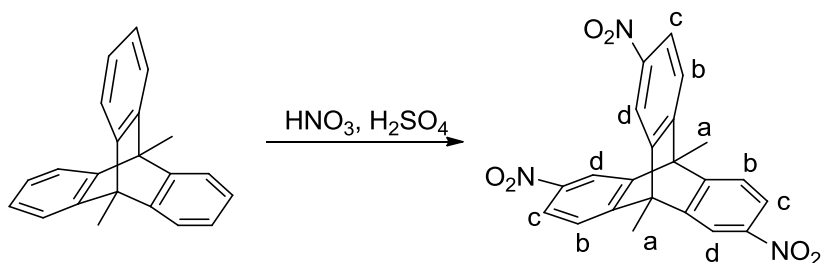
9,10-Dimethyltritycene (2.00 g, 7.09 mmol) was dissolved in a mixture of dichloromethane (40 ml) and acetonitrile (160 ml) at room temperature. To the resulting solution was added potassium nitrate (1.43 g, 14.18 mmol) and trifluoroacetic anhydride (3.45 ml, 24.82 mmol). The reaction mixture was heated to 50 °C and stirred for 72 hours. It was then cooled to room temperature and concentrated to an orange residue under reduced pressure. The residue was added to water (300 ml) and the product extracted with chloroform (3 x 70 ml). The chloroform was removed under reduced pressure, giving the product as an off-white powder. This was passed through a silica column (4:1 dichloromethane:hexane) to give the product as a pale yellow powder (2.43 g, 6.53 mmol, 92.1%). Mp 222 – 224 °C; ¹H NMR (400 MHz, CDCl₃) δ ppm 2.54 (6H, m, H_a), 7.15 (2H, m, H_b), 7.44 (2H, m, H_c), 7.51 (2H, m, H_d), 7.99 (2H, m, H_e), 8.20 (2H, m, H_f); ¹³C NMR (100 MHz, CDCl₃) δ ppm 13.5, 49.3, 116.1, 121.3, 121.4, 121.5, 126.1, 145.1, 145.5, 145.9, 148.9, 149.3, 153.7, 154.1; HRMS Calc. for [C₂₂H₁₆N₂O₄]⁺ m/z = 372, found 372.1115 gmol⁻¹; IR (NaCl): 3075, 3025, 2977, 2947, 2886, 1587, 1522, 1449, 1383, 1341, 1275, 1216, 1180, 1162, 1143, 1111, 1095, 1044, 1037 cm⁻¹.

Preparation of 2,6(7)-diamino-9,10-dimethyltritycene (39):



2,6(7)-Dinitro-9,10-dimethyltritycene (3.10 g, 8.33 mmol) was dissolved in THF (100 ml) at room temperature. To this solution was added hydrazine monohydrate (6.52 ml, 83.33 mmol) and Raney nickel (catalytic amount) and the reaction mixture was heated to 60 °C and stirred for 16 hours under a nitrogen atmosphere. The mixture was then cooled to room temperature, filtered to remove the nickel and concentrated under reduced pressure to give the crude product as a yellow oil. The oil was added to water (200 ml) and the product extracted with chloroform (3 x 70 ml). The chloroform was then removed under reduced pressure, giving the product as a yellow powder (2.52 g, 8.08 mmol, 97.0%). Mp 292 – 294 °C; ¹H NMR (400 MHz, CDCl₃) δ ppm 2.33 (6H, m, H_a), 3.34 (4H, br. s, H_b), 6.33 (2H, s, H_c), 6.74 (2H, s, H_d), 7.09 (4H, m, H_e), 7.35 (2H, s, H_f); ¹³C NMR (100 MHz, CDCl₃) δ ppm 13.6, 47.1, 47.7, 48.4, 108.9, 110.3, 120.1, 120.4, 120.8, 121.0, 124.5, 124.8, 125.6, 136.0, 138.9, 139.6, 143.5, 148.2, 148.8, 149.4, 149.6, 150.0; HRMS Calc. for [C₂₂H₂₀N₂]⁺ m/z = 312, found 312.1617 gmol⁻¹; IR (NaCl): 3348, 3214, 3007, 2969, 2878, 1618, 1500, 1475, 1456, 1379, 1321, 1250, 1217, 1188, 1147, 1123, 1086, 1026 cm⁻¹.

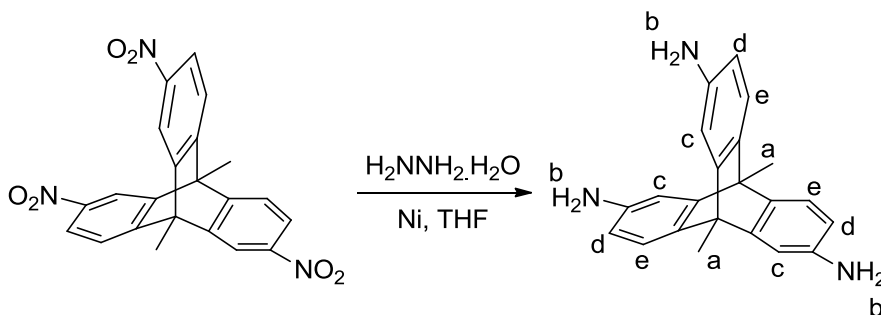
Preparation of 2,6(7),14-trinitro-9,10-dimethyltritycene (40):



9,10-Dimethyltritycene (1.50 g, 5.32 mmol) was added to a mixture of concentrated nitric acid (70 %, 50 ml) and concentrated sulphuric acid (95 %, 2.5 ml). The reaction mixture was heated to 80 °C for 40 hours, leaving a yellow solution. The reaction was then quenched in water (250 ml) and stirred for an hour. The product was extracted with chloroform (3 x 50 ml) and the chloroform removed under reduced pressure. This gave the crude product as a yellow powder, which was loaded onto silica and passed through a silica column (4:1 dichloromethane:hexane). This gave the product as a pale yellow powder (2.14 g, 5.13 mmol, 96.5%). Mp > 350 °C; ¹H NMR (400 MHz, CDCl₃) δ ppm 2.62 (6H, m, H_a), 7.58 (3H, m, H_b), 8.06 (3H, m, H_c), 8.26 (3H, m, H_d); ¹³C NMR (100 MHz, CDCl₃)

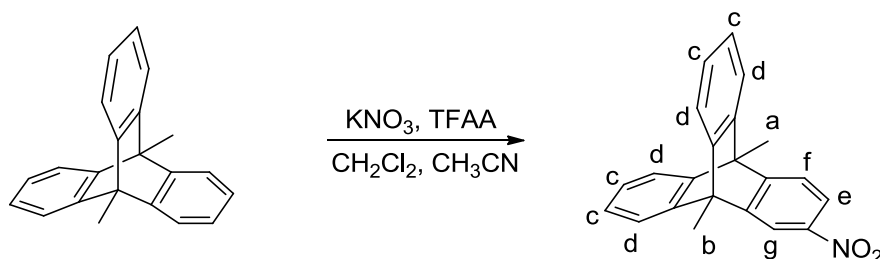
δ ppm 13.4, 49.5, 116.6, 122.1, 122.2, 146.2, 147.5, 147.8, 148.1, 152.1, 152.4, 152.8; HRMS Calc. for $[\text{C}_{22}\text{H}_{15}\text{N}_3\text{O}_6]^+$ $m/z = 417$, found 417.0966 g mol^{-1} ; IR (NaCl): 3092, 2925, 2854, 1595, 1525, 1450, 1383, 1344, 1288, 1268, 1216, 1145, 1097, 1044 cm^{-1} .

Preparation of 2,6(7),14-triamino-9,10-dimethyltriptycene (41):



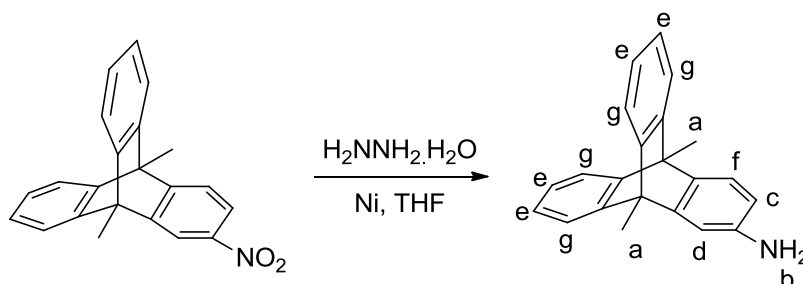
2,6(7),14-Trinitro-9,10-dimethyltriptycene (3.00 g, 7.19 mmol) was dissolved in THF (100 ml) at room temperature. To this solution was added hydrazine monohydrate (8.44 ml, 107.91 mmol) and Raney nickel (catalytic amount) before the reaction mixture was heated to 60 °C and stirred for 16 hours under a nitrogen atmosphere. It was then cooled to room temperature and filtered to remove the nickel, before the solution was concentrated to an oil under reduced pressure. The oil was added to water (200 ml) and the product extracted with chloroform (3 x 80 ml). The chloroform was removed under reduced pressure, giving the product as a peach coloured powder (2.27 g, 6.94 mmol, 96.5%). Mp 298 – 300 °C; ^1H NMR (400 MHz, CDCl_3) δ ppm 2.23 (6H, m, H_a), 3.50 (6H, br. s, H_b), 6.28 (3H, m, H_c), 6.67 (3H, m, H_d), 7.03 (3H, d, $J = 8.0$ Hz, H_e); ^{13}C NMR (100 MHz, CDCl_3) δ ppm 13.6, 47.0, 108.5, 108.8, 109.1, 110.0, 110.3, 110.5, 120.3, 120.6, 120.9, 125.5, 138.7, 139.4, 140.2, 143.1, 143.3, 143.5, 149.4, 150.0, 150.6; HRMS Calc. for $[\text{C}_{22}\text{H}_{21}\text{N}_3]^+$ $m/z = 327$, found 327.1734 g mol^{-1} ; IR (NaCl): 3338, 3213, 3006, 2968, 2877, 1619, 1502, 1476, 1454, 1378, 1321, 1287, 1249, 1215, 1147, 1083 cm^{-1} .

Preparation of 2-nitro-9,10-dimethyltritycene (42):



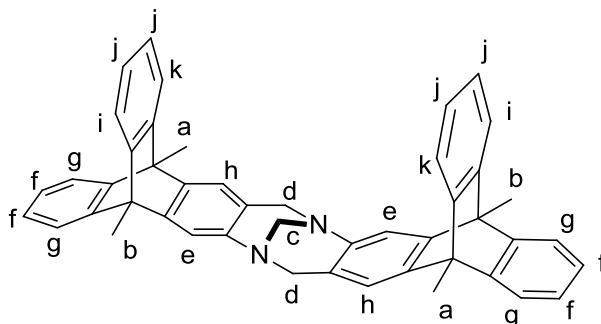
9,10-Dimethyltritycene (1.00 g, 3.55 mmol) was dissolved in a mixture of dichloromethane (20 ml) and acetonitrile (80 ml). To the solution was added potassium nitrate (0.38 g, 3.72 mmol) and trifluoroacetic anhydride (1.73 ml, 12.43 mmol) before the mixture was heated to 50 °C and stirred for 16 hours. It was then concentrated to an orange residue under reduced pressure, before being added to water (200 ml) and the product extracted with chloroform (3 x 50 ml). The chloroform was removed under reduced pressure, giving the crude product as a yellow powder. This was loaded onto silica and passed through a silica column (2:1 hexane:dichloromethane). This gave the product as a white powder (1.10 g, 3.36 mmol, 94.8%). Mp 226 – 228 °C; Lit. MP = 241 – 242 °C¹⁹⁰; ¹H NMR (400 MHz, CDCl₃) δ ppm 2.47 (3H, s, H_a), 2.49 (3H, s, H_b), 7.09 (4H, m, H_c), 7.40 (4H, m, H_d), 7.45 (1H, d, J = 8.2 Hz, H_e), 7.94 (1H, dd, J = 8.4 Hz, H_f), 8.17 (1H, s, H_g); ¹³C NMR (100 MHz, CDCl₃) δ ppm 13.4, 13.6, 48.8, 49.1, 115.7, 121.0, 121.2, 125.2, 125.4, 145.5, 146.7, 147.1, 150.4, 155.5; HRMS Calc. for [C₂₂H₁₇NO₂ + H]⁺ m/z = 328, found 328.1330 gmol⁻¹; IR (NaCl): 3072, 3020, 2973, 2944, 2884, 1604, 1585, 1519, 1448, 1418, 1381, 1340, 1273, 1216, 1181, 1160, 1143, 1118, 1094, 1047, 1038, 1027 cm⁻¹.

Preparation of 2-amino-9,10-dimethyltritycene (43):



2-Nitro-9,10-dimethyltryptycene (1.50 g, 4.59 mmol) was dissolved in THF (100 ml) at room temperature. To this solution was added hydrazine monohydrate (1.79 ml, 22.94 mmol) and Raney nickel (catalytic amount). The mixture was heated to 60 °C and left stirring for 48 hours under a nitrogen atmosphere. It was then cooled to room temperature and filtered to remove the nickel. The solution was concentrated to an oil under reduced pressure, and the oil added to water (200 ml). The product was extracted with chloroform (3 x 40 ml) and the chloroform removed under reduced pressure. This gave the product as a pale yellow powder (1.31 g, 4.41 mmol, 96.1%). Mp 294 – 296 °C; Lit. Mp = 297 – 300 °C¹⁹⁰; ¹H NMR (400 MHz, CDCl₃) δ ppm 2.40 (6H, s, H_a), 3.50 (2H, br. s, H_b), 6.34 (1H, d, J = 7.3 Hz, H_c), 6.78 (1H, s, H_d), 7.06 (4H, s, H_e), 7.15 (1H, d, J = 7.3 Hz, H_f), 7.37 (4H, s, H_g); ¹³C NMR (100 MHz, CDCl₃) δ ppm 13.6, 47.8, 48.5, 109.2, 110.6, 120.1, 120.4, 121.2, 124.5, 124.8, 125.6, 139.1, 143.2, 148.2, 148.8, 149.7; HRMS Calc. for [C₂₂H₁₇ + H]⁺ m/z = 282, found 282.1268 gmol⁻¹; IR (NaCl): 3364, 3063, 3015, 2971, 2880, 1616, 1496, 1472, 1448, 1376, 1332, 1312, 1299, 1269, 1222, 1187, 1144, 1119, 1089, 1024 cm⁻¹.

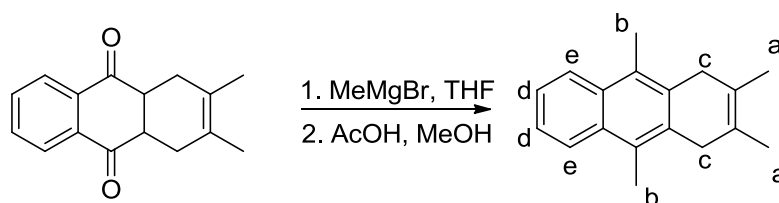
Preparation of Tröger's base from 9,10-dimethyltryptycene (44):



2-Amino-9,10-dimethyltryptycene (1.10 g, 3.70 mmol) was dissolved in trifluoroacetic acid (11 ml) at 0 °C with stirring. Dimethoxymethane (0.66 ml, 7.41 mmol) was slowly added over a few minutes and the mixture left stirring for 48 hours under a nitrogen atmosphere. The reaction was then quenched by addition of water (50 ml) and aqueous ammonia (35%, 100 ml). After stirring for 30 minutes the product was extracted with chloroform (3 x 50 ml). The chloroform solution was washed with water (100 ml) before the solvent was removed under reduced pressure, giving a red solid. This was loaded onto silica and passed through a silica column (starting with pure dichloromethane and slowly increasing the

polarity with ethyl acetate until using pure ethyl acetate). This gave a red oil, which was recrystallised from methanol, giving the product as an off-white powder (0.72 g, 1.14 mmol, 61.8%). Mp > 350 °C; ^1H NMR (400 MHz, CDCl_3) δ ppm 2.28 (6H, s, H_a), 2.36 (6H, s, H_b), 3.99 (1H, s, H_c), 4.02 (1H, s, H_c), 4.14 (2H, s, H_d), 4.52 (1H, s, H_d), 4.56 (1H, s, H_d), 6.79 (2H, s, H_e), 6.93 (4H, m, H_f), 7.00 (4H, m, H_g), 7.06 (2H, s, H_h), 7.20 (2H, m, H_i), 7.28 (4H, m, H_j), 7.32 (2H, m, H_k); ^{13}C NMR (100 MHz, CDCl_3) δ ppm 13.5, 47.8, 48.2, 58.3, 66.9, 117.5, 118.9, 120.3, 120.4, 120.5, 123.3, 124.6, 124.8, 124.9, 144.0, 144.2, 147.5, 147.9, 148.1; HRMS Calc. for $[\text{C}_{47}\text{H}_{38}\text{N}_2]^+$ $m/z = 630$, found 630.3040 g mol^{-1} ; IR (NaCl): 3062, 3016, 2970, 2943, 2882, 2845, 1618, 1593, 1569, 1449, 1410, 1378, 1338, 1314, 1301, 1241, 1217, 1198, 1161, 1301, 1241, 1217, 1198, 1161, 1144, 1123, 1102, 1088, 1068, 1023 cm^{-1} .

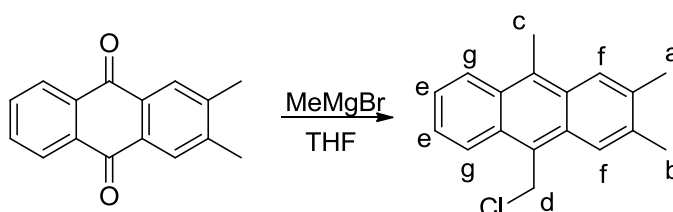
Preparation of 2,3,9,10-tetramethyl-1,4-dihydroanthracene (45):



Following the procedure reported by L. F. Fieser and T. G. Webber¹⁵⁴, 2,3-dimethylbutadiene- α -naphthoquinone (10.00 g, 41.67 mmol) was dissolved in dry THF (120 ml) and cooled to 0 °C. Methylmagnesium bromide (3 M in ether, 83.33 ml, 250.00 mmol) was then added dropwise to the mixture. Upon completion of addition the mixture was heated to 50 °C and stirred overnight under a nitrogen atmosphere. The reaction was quenched in a mixture of water (200 ml) and dilute hydrochloric acid (2M, 200 ml). The intermediate was extracted with diethyl ether (3 x 150 ml), and the solvent removed under reduced pressure. The resulting residue was dissolved in chloroform (150 ml) and filtered, removing the black precipitate. The chloroform was removed under reduced pressure and the resulting oil dissolved in a mixture of methanol (70 ml) and glacial acetic acid (70 ml). This mixture was refluxed for 16 hours and cooled to room temperature before the solid was collected. It was washed with water (200 ml) and ethanol (100 ml), giving the product as an off-white powder (1.98 g, 8.39 mmol, 20.1%). Mp 174 – 176 °C; Lit. Mp = 175 – 176 °C¹⁵⁴; ^1H NMR (400 MHz, CDCl_3) δ ppm 1.86 (6H, s, H_a), 2.60 (6H, s, H_b), 3.44 (4H,

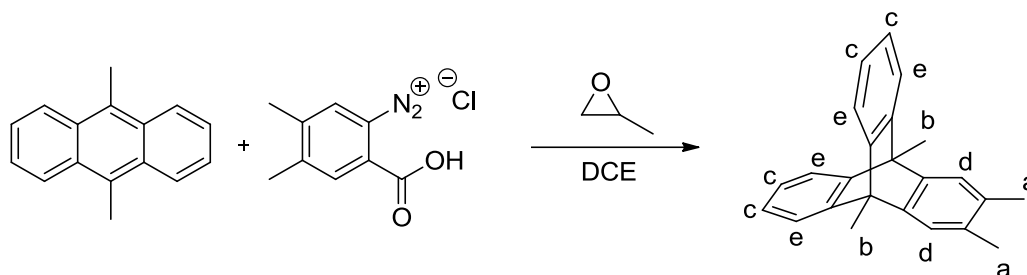
s, H_c), 7.47 (2H, m, H_d), 8.09 (2H, m, H_e); ¹³C NMR (100 MHz, CDCl₃) δ ppm 14.1, 18.7, 36.1, 122.9, 124.2, 124.5, 127.8, 131.2; HRMS Calc. for C₁₈H₂₀ m/z = 236, found 236.1571 g mol⁻¹; IR (NaCl): 3079, 2913, 2860, 1583, 1446, 1383, 1312, 1193, 1124, 1015 cm⁻¹.

Preparation of 2,3,9-trimethyl-10-chloromethylantracene (46):



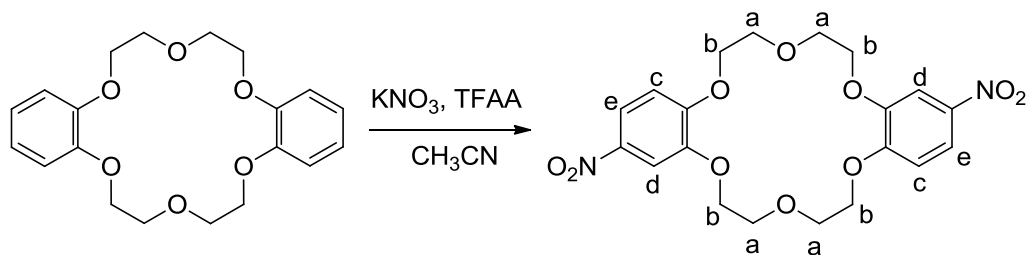
Based upon the procedure (for the synthesis of anthracene from anthraquinone) reported by M. Konieczny and R. G. Harvey¹⁹¹, 2,3-dimethylanthraquinone (2.00 g, 8.47 mmol) was dissolved in THF (30 ml) with stirring at 0 °C under a nitrogen atmosphere. Methylmagnesium bromide (3 M in ether, 11.30 ml, 33.90 mmol) was added dropwise to the solution before it was stirred at room temperature for 16 hours. The reaction was then quenched in water (150 ml) and the intermediate extracted with diethyl ether (3 x 100 ml). The ether solution was washed with concentrated hydrochloric acid (37%, 100 ml), and an immediate colour change from green to yellow was observed. The ether solution was dried under reduced pressure and the resulting residue triturated in hexane (100 ml) for two hours. The solid was then collected by filtration and dried under vacuum. This gave the product as a yellow solid (1.00 g, 4.27 mmol, 50.4%). Mp 132 – 134 °C; ¹H NMR (400 MHz, CDCl₃) δ ppm 2.50 (3H, s, H_a), 2.53 (3H, s, H_b), 3.03 (3H, s, H_c), 5.55 (2H, s, H_d), 7.55 (2H, m, H_e), 8.02 (2H, m, H_f), 8.29 (2H, m, H_g); ¹³C NMR (100 MHz, CDCl₃) δ ppm 14.4, 19.7, 39.8, 123.0, 124.4, 124.6, 124.9, 125.0, 125.2, 129.4, 131.7, 133.0, 135.1, 136.6; HRMS Calc. for [C₁₈H₁₇]⁺ m/z = 233, found 233.1331 g mol⁻¹; LRMS (C₁₈H₁₇Cl) m/z (ES +, M + H⁺) = 269.09 g mol⁻¹; IR (NaCl): 3023, 2967, 2917, 1495, 1464, 1376, 1281, 1249, 1216, 1023 cm⁻¹.

Preparation of 2,3,9,10-tetramethylantracene (47):



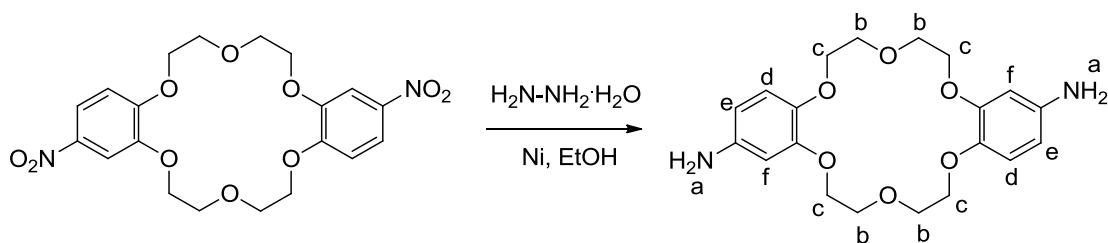
9,10-Dimethylantracene (5.48 g, 26.58 mmol) was dissolved in dichloroethane (250 ml) at 60 °C with stirring. 4,5-dimethylbenzenediazonium-2-carboxylatechloride (28.00 g, 132.90 mmol) and 1,2-epoxypropane (80 ml) were added to the solution before the mixture was refluxed at 85 °C for 40 hours under a nitrogen atmosphere. After cooling to room temperature the mixture was concentrated under reduced pressure, giving a dark oil. This oil was added to a mixture of maleic anhydride (1.30 g, 13.29 mmol) and o-xylene (200 ml). This was heated to 110 °C for an hour before being allowed to cool to room temperature and added to water (300 ml). The crude material was extracted with dichloromethane (3 x 150 ml) and the organic solution washed with aqueous potassium hydroxide (15%, 2 x 150 ml). The solution was then dried under reduced pressure, giving a red residue, which was loaded onto silica and passed through a silica column (9:1 hexane:dichloromethane). This gave the crude product as a yellow powder, which was triturated in methanol (150 ml) for 16 hours. The resulting solid was collected by filtration and dried under vacuum, giving the product as an off-white powder (6.99 g, 22.55 mmol, 84.8%). Mp 230 – 232 °C; ^1H NMR (400 MHz, CDCl_3) δ ppm 2.23 (6H, s, H_a), 2.45 (6H, s, H_b), 7.05 (4H, m, H_c), 7.19 (2H, s, H_d), 7.38 (4H, m, H_e); ^{13}C NMR (100 MHz, CDCl_3) δ ppm 13.6, 19.6, 48.2, 120.3, 122.2, 124.7, 132.5, 146.0, 148.6; HRMS Calc. for $[\text{C}_{24}\text{H}_{22}]^+$ $m/z = 310$, found 310.1720 g mol^{-1} ; IR (NaCl): 3064, 3017, 2970, 2941, 2919, 2881, 1497, 1471, 1451, 1398, 1377, 1301, 1243, 1217, 1178, 1160, 1108, 1087, 1028 cm^{-1} .

Synthesis of 2,13(14)-dinitrodibenzo-18-crown-6 (48):



Dibenzo-18-crown-6 (3.00 g, 8.32 mmol) was dissolved in acetonitrile (100 ml); once dissolved, potassium nitrate (1.68 g, 16.65 mmol) and trifluoroacetic acid (8.11 ml, 58.27 mmol) were added. The mixture was heated to 50 °C and left stirring for 16 hours. After cooling to room temperature the solution was concentrated under reduced pressure. The residue was added to water (100 ml), extracted with dichloromethane (3 x 80 ml), filtered and dried under reduced pressure giving a brown powder (3.52 g). This was washed with hot methanol, filtered off and dried in a vacuum oven to give the product as a cream powder (3.25 g, 7.22 mmol, 86.7%). Mp 208 – 210 °C; Lit. Mp = 203 - 205 °C (*cis* isomer), 237 – 242 °C (mixture of isomers)¹⁵⁵; ¹H NMR (400 MHz, CDCl₃) δ ppm 4.03 (8H, m, H_a), 4.24 (8H, m, H_b), 6.86 (2H, d, J = 8.9 Hz, H_c), 7.70 (2H, s, H_d), 7.88 (2H, d, J = 8.9 Hz, H_e); ¹³C NMR (100 MHz, CDCl₃) δ ppm 68.5, 68.6, 69.2, 107.2, 110.6, 117.9, 118.0, 141.5, 148.1, 153.8; HRMS Calc. for C₂₀H₂₂N₂O₁₀ *m/z* = 450, found 450.1259 gmol⁻¹; IR (NaCl): 3434, 3092, 2948, 2886, 2309, 1634, 1591, 1511, 1473, 1454, 1347, 1275, 1236, 1137 cm⁻¹.

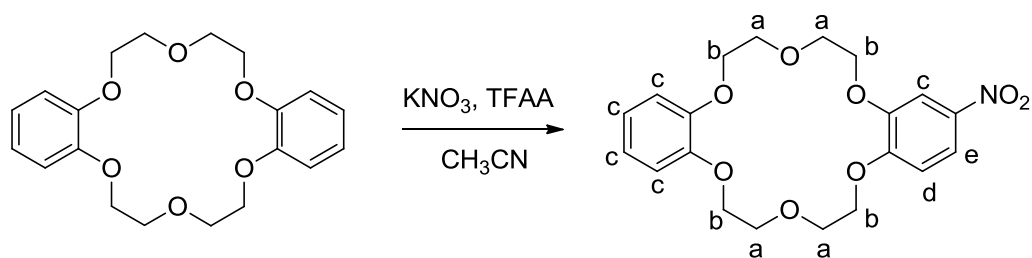
Synthesis of 2,13(14)-diaminodibenzo-18-crown-6 (49):



2,13-Dinitrobenzo-18-crown-6 (2.00 g, 4.44 mmol) was added to ethanol (60 ml). To this was added Raney nickel (catalytic amount) and hydrazine monohydrate (3.47 ml, 44.40 mmol). The reaction was heated to 60 °C and left to react for 16 hours under nitrogen. The

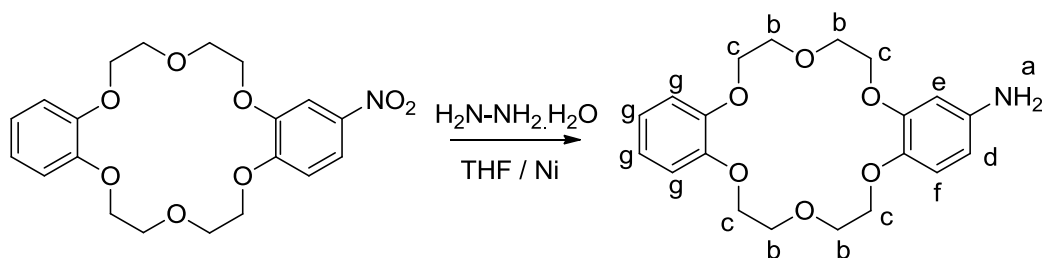
mixture was then filtered and the solution dried under reduced pressure. The resulting oil was added to water (100 ml), extracted with chloroform (3 x 80 ml) and dried under reduced pressure. The residue was treated with diethyl ether (200 ml) and hexane (100 ml) giving the product as a brown powder (1.42 g, 3.64 mmol, 82.1 %). Mp 158 – 162 °C; Lit. Mp = 178 – 182 °C (*cis* isomer)¹⁵⁵; ¹H NMR (400 MHz, CDCl₃) δ ppm 3.26 (4H, s, H_a), 3.90 (8H, m, H_b), 4.07 (8H, m, H_c), 6.26 (2H, d, J = 8.6 Hz, H_d), 6.43 (2H, s, H_e), 6.71 (2H, s, J = 8.6 Hz, H_f); ¹³C NMR (100 MHz, MeOD) δ ppm 68.5, 68.6, 68.9, 69.0, 70.6, 70.7, 70.8, 70.9, 102.6, 108.7, 114.1, 122.6, 141.7, 142.8, 149.3; HRMS Calc. for C₂₀H₂₆N₂O₆ *m/z* = 390, found 390.1808 g mol⁻¹; IR (NaCl): 3353, 2931, 1695, 1517, 1457, 1360, 1284, 1231, 1201, 1186, 1124, 1063 cm⁻¹.

Preparation of 2-nitrodibenzo-18-crown-6 (50):



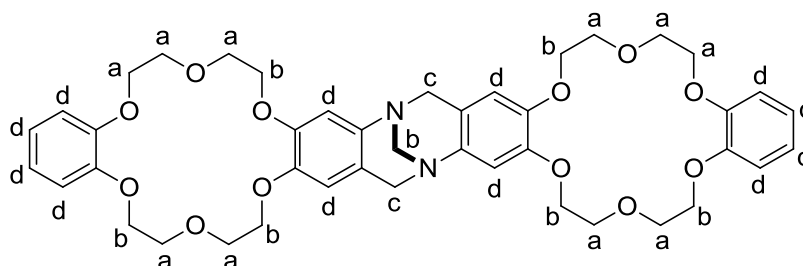
Dibenzo-18-crown-6 (3.00 g, 8.32 mmol) was dissolved in a mixture of acetonitrile (50 ml) and dichloromethane (15 ml). To this was added potassium nitrate (0.84 g, 8.32 mmol) and trifluoroacetic anhydride (4.05 ml, 29.13 mmol). The mixture was heated to 50 °C and left stirring for 16 hours. It was then concentrated under reduced pressure to give an oil, which was added to water (100 ml), extracted with dichloromethane (3 x 100 ml) and dried under reduced pressure, giving the product as a light brown powder (3.37 g, 8.31 mmol, 99.8%). Mp 178 – 180 °C; Lit. Mp = 171 – 174 °C¹⁹²; ¹H NMR (400 MHz, CDCl₃) δ ppm 4.04 (8H, m, H_a), 4.17 (4H, m, H_b), 4.24 (4H, m, H_b), 6.88 (5H, m, H_c), 7.71 (1H, m, H_d), 7.88 (1H, d, J = 8.8 Hz, H_e); ¹³C NMR (100 MHz, MeOD) δ ppm 68.5, 68.7, 68.9, 69.2, 69.4, 70.0, 70.1, 70.2, 107.6, 110.9, 113.8, 117.9, 118.0, 121.4, 141.5, 148.3, 148.8; HRMS Calc. for C₂₀H₂₃NO₈ *m/z* = 405, found 405.1432 g mol⁻¹; IR (NaCl): 3434, 2931, 2349, 2070, 1637, 1592, 1507, 1453, 1336, 1276, 1254, 1230, 1134, 1097, 1060 cm⁻¹.

Preparation of 2-aminodibenzo-18-crown-6 (51):



2-Nitrodibenzo-18-crown-6 (2.00 g, 4.93 mmol) was dissolved in THF (80 ml). Raney nickel (catalytic amount) and hydrazine monohydrate (1.93 ml, 24.67 mmol) were then added to the solution. The mixture was heated to 50 °C and left stirring for 24 hours under nitrogen before it was filtered and the solvent removed under reduced pressure. The residue was added to water (100 ml), extracted with chloroform (3 x 80 ml) and dried under reduced pressure, giving the product as a grey/brown powder (1.83 g, 4.88 mmol, 98.9%). Mp 134 – 138 °C; Lit. Mp = 158 °C¹⁹²; ¹H NMR (400 MHz, MeOD) δ ppm 3.25 (4H, br. s, H_a), 3.89 (8H, m, H_b), 4.01 (4H, m, H_c), 4.09 (4H, m, H_c), 6.23 (1H, d, J = 8.1 Hz, H_d), 6.37 (1H, s, H_e), 6.68 (1H, d, J = 8.1 Hz, H_f), 6.86 (4H, s, H_g); ¹³C NMR (100 MHz, MeOD) δ ppm 52.0, 52.4, 52.9, 72.3, 73.4, 73.7, 117.4, 125.0, 152.2; HRMS Calc. for C₂₀H₂₅NO₆m/z = 375, found 375.1689 gmol⁻¹; IR (NaCl): 3618, 3363, 2923, 2357, 1593, 1507, 1452, 1361, 1332, 1276, 1254, 1230, 1189, 1129, 1061 cm⁻¹.

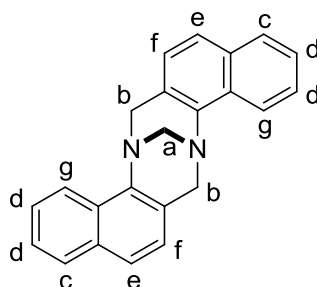
Preparation of Tröger's base from 2-aminodibenzo-18-crown-6 (52):



2-Aminodibenzo-18-crown-6 (1.00 g, 2.66 mmol) was dissolved in trifluoroacetic acid (10 ml) at -15 °C. Paraformaldehyde (0.16 g, 5.33 mmol) was added and the reaction left stirring for 16 hours. The reaction was then quenched in a mixture of ice (100 ml) and aqueous ammonia (35%, 50 ml). This was stirred for 2 hours before the product was

extracted with a mixture of methanol and dichloromethane (10 ml + 50 ml x 3). The brown solution was dried under reduced pressure, giving the product as a grey/brown powder (1.03 g, 1.31 mmol, 98.5%). Mp 162 – 164 °C; ¹H NMR (400 MHz, CDCl₃) δ ppm 4.03 (20H, m, H_a), 4.17 (14H, m, H_b), 4.24 (4H, m, H_c), 6.88 (12H, m, H_d); ¹³C NMR (100 MHz, *solid state*) δ ppm 58.5, 69.7, 111.7, 121.1, 133.3, 141.4, 148.2; HRMS Calc. for C₄₃H₅₀N₂O₁₂ *m/z* = 786, found 785.32 *gmol*⁻¹; IR (NaCl): 3395, 2840, 2515, 2129, 1655, 1510, 1451, 1415, 1256, 1205, 1118, 1016 *cm*⁻¹.

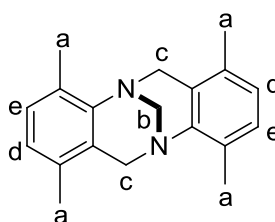
Synthesis of Tröger's base from 1-naphthylamine (53):



Based upon the procedure detailed by S. Sergeyev *et al.*¹⁵⁶, 1-naphthylamine (4.00 g, 27.93 mmol) was dissolved in trifluoroacetic acid (40 ml) at -15 °C. Once dissolved, paraformaldehyde (1.68 g, 55.87 mmol) was added and the reaction left stirring for 16 hours. The reaction was quenched in a mixture of ice (100 ml) and aqueous ammonia (35%, 50 ml). This mixture was stirred for an hour before the crude product was extracted with dichloromethane (3 x 150 ml). The solution was dried under reduced pressure giving the crude product as a pale brown powder, which was passed through a silica column (neat dichloromethane) to give the product as a pale yellow powder (0.88 g, 2.72 mmol, 19.5%). Mp 196 – 198 °C; Lit. Mp = 209 – 211 °C¹⁵⁶; ¹H NMR (400 MHz, CDCl₃) δ ppm 4.41 (1H, s, H_a), 4.46 (1H, s, H_a), 4.63 (2H, s, H_b), 4.93 (1H, s, H_b), 4.97 (1H, s, H_b), 6.95 (2H, d, J = 8.4 Hz, H_c), 7.48 (4H, m, H_d), 7.60 (2H, m, H_e), 7.77 (2H, d, J = 8.0 Hz, H_f), 8.39 (2H, d, J = 8.4 Hz, H_g); ¹³C NMR (100 MHz, CDCl₃) δ ppm 56.2, 67.7, 122.5, 124.4, 124.7, 125.6, 126.0, 128.4, 129.2, 133.4, 142.6; LRMS *m/z* (EI, M⁺) = 322.14; IR (NaCl): 3049, 2945, 2886, 2843, 1597, 1569, 1506, 1462, 1430, 1390, 1363, 1304, 1263, 1219, 1199, 1174, 1151, 1107, 1090, 1064, 1038, 1025, 1002, 973 *cm*⁻¹. Elemental analysis calc. (%) for repeating unit [C₁₃H₁₀N₂]: C 80.39, H 5.19, N 14.42 (calculated), C 71.50, H 4.43,

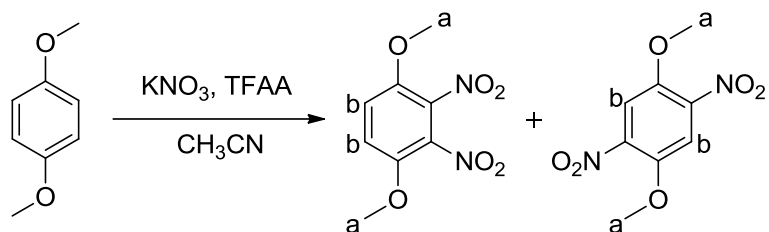
N 12.54 (found). Crystals were prepared by a slow diffusion of hexane into a solution of the compound in THF. Crystal properties: system = Monoclinic, space group = $P21/c$, $a = 10.9661(5)$, $b = 13.1191(8)$, $c = 11.3187(5)$, $\alpha = 90.00$, $\beta = 93.95(3)$, $\gamma = 90.00$, $V = 1624.50 \text{ \AA}^3$; $Z = 0$.

Synthesis of Tröger's base from 2,5-dimethylaniline (54):



Based upon the procedure reported by S. Sergeyev et al.¹¹⁵, 2,5-dimethylaniline (4.11 ml, 33.0 mmol) was dissolved in trifluoroacetic acid (40 ml) at $-15 \text{ }^\circ\text{C}$. Once dissolved, paraformaldehyde (1.98 g, 66.0 mmol) was added and the mixture left stirring for 16 hours. The reaction mixture was then quenched in a mixture of ice (100 ml) and aqueous ammonia (35%, 50 ml). This was stirred for two hours before the crude product was extracted with dichloromethane (3 x 50 ml). The organic solution was concentrated under reduced pressure to give the crude product as a pale yellow powder. This material was passed through a silica column (using a solvent system of 1:49 ethyl acetate:dichloromethane), giving the purified product as a cream powder (1.097 g, 3.94 mmol, 23.9%). Mp $180 - 182 \text{ }^\circ\text{C}$; Lit. Mp = $195 - 197 \text{ }^\circ\text{C}$ ¹¹⁵; $^1\text{H NMR}$ (400 MHz, CDCl_3) δ ppm 2.07 (6H, s, H_a), 2.42 (6H, s, H_a), 3.91 (1H, s, H_c), 3.96 (1H, s, H_c), 4.29 (2H, s, H_c), 4.41 (1H, s, H_c), 4.45 (1H, s, H_c), 6.78 (2H, d, $J = 7.6 \text{ Hz}$, H_d), 6.99 (2H, d, $J = 7.6 \text{ Hz}$, H_e); $^{13}\text{C NMR}$ (100 MHz, CDCl_3) δ ppm 17.1, 17.8, 53.7, 66.4, 125.1, 126.5, 128.5, 130.4, 132.8, 146.5); LRMS m/z (EI, M^+) = 278.17; IR (NaCl): 3066, 3012, 2943, 2920, 2891, 2853, 1852, 1598, 1580, 1485, 1478, 1463, 1436, 1410, 1402, 1373, 1359, 1347, 1334, 1304, 1265, 1245, 1216, 1201, 1160, 1154, 1096, 1062, 1032 cm^{-1} . Crystals were prepared by a slow diffusion of hexane into a solution of the compound in chloroform. Crystal properties: system = Monoclinic, space group = $P 21/c$, $a = 13.0370(3)$, $b = 13.8370(3)$, $c = 8.2433(16)$, $\alpha = 90.00$, $\beta = 103.32(3)$, $\gamma = 90.00$, $V = 1447.03 \text{ \AA}^3$; $Z = 4$.

Preparation of 1,4-dimethoxy-2,3(5)-dinitrobenzene (55):

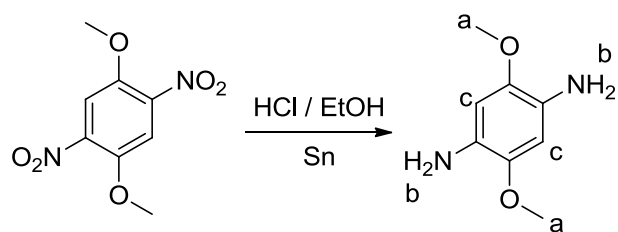


1,4-Dimethoxybenzene (2.00 g, 14.48 mmol) was dissolved in acetonitrile (70 ml) with stirring. After complete dissolution potassium nitrate (2.93 g, 28.95 mmol) and trifluoroacetic anhydride (14.1 ml, 101.33 mmol) were added and the mixture heated to 50 °C. The mixture was left stirring for 16 hours under nitrogen, before it was concentrated under reduced pressure. The residue was added to water (200 ml) and extracted with chloroform (3 x 100 ml) before the solution was concentrated under reduced pressure. The resulting yellow powder was purified by silica column chromatography (1:1 ethyl acetate: hexane) to yield the two products as yellow powders: 1,4-dimethoxy-2,3-dinitrobenzene (1.82 g, 7.95 mmol, 54.9%), and 1,4-dimethoxy-2,5-dinitrobenzene (0.64 g, 2.81 mmol, 19.4%). 1,4-dimethoxy-2,5-dinitrobenzene was further purified by recrystallisation from methanol, which gave the product as a yellow crystalline powder (0.62 g, 2.72 mmol, 18.8%).

1,4-Dimethoxy-2,3-dinitrobenzene (55a): Mp 172 – 174 °C; Lit. Mp = 182 - 183 °C¹⁹³; ¹H NMR (400 MHz, CDCl₃) δ ppm 3.93 (6H, s, H_a), 7.20 (2H, s, H_b); ¹³C NMR (100 MHz, CDCl₃) δ ppm 57.6, 116.7, 134.4, 145.4; LRMS *m/z* (EI, M⁺) = 228.04; IR (NaCl): 3408, 2980, 2946, 2846, 2349, 2283, 1631, 1574, 1536, 1492, 1447, 1431, 1368, 1276, 1193, 1056, 934, 816, 809, 794 cm⁻¹.

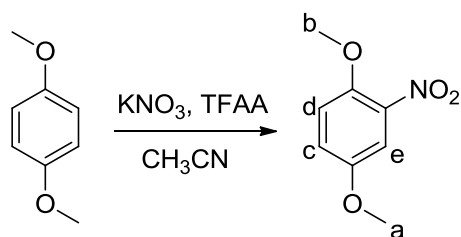
1,4-Dimethoxy-2,5-dinitrobenzene (55b): Mp 188 – 190 °C; Lit. Mp = 201 – 202 °C¹⁹³; ¹H NMR (400 MHz, CDCl₃) δ ppm 3.98 (6H, s, H_a), 7.57 (2H, s, H_b); ¹³C NMR (100 MHz, CDCl₃) δ ppm 57.5, 111.2, 141.8, 146.2; LRMS *m/z* (EI, M⁺) = 228.04; IR (NaCl): 3434, 2102, 1640, 1538, 1396, 1359, 1281, 1233, 1186, 1019 cm⁻¹.

Preparation of 1,4-dimethoxy-2,5-phenylenediamine (**56**):



Based upon the procedure described by N. R. Branda *et al.*¹⁵⁸, 1,4-dimethoxy-2,5-phenylenediamine (1.00 g, 4.39 mmol) was dissolved in a mixture of concentrated hydrochloric acid (30 ml) and ethanol (30 ml). The mixture was heated to 80 °C with stirring under a nitrogen atmosphere. Once at temperature, tin powder (5.21 g, 43.86 mmol) was slowly added before the temperature was increased to 120 °C. The mixture was stirred for 16 hours before the condenser was removed to evaporate off the remaining ethanol. The remaining solution had sodium hydroxide added until a pH of 12 was achieved. This was added to water (100 ml) and the crude product extracted with chloroform (5 x 50 ml). The organic solution was concentrated under reduced pressure giving a purple crystalline solid, which was washed with diethyl ether to give the pure product as an off-white crystalline solid (0.45 g, 2.70 mmol, 61.6%). Mp 202 – 204 °C; Lit. Mp = 212 – 214 °C¹⁹⁴; ¹H NMR (400 MHz, CDCl₃) δ ppm 1.58 (6H, s, H_a), 3.77 (4H, s, H_b), 6.35 (2H, s, H_c); ¹³C NMR (100 MHz, CDCl₃) δ ppm 21.2, 30.3, 34.2, 102.0, 125.5, 128.3, 135.8, 151.5; LRMS *m/z* (AP, M+H⁺) = 169.1; IR (NaCl): 3377, 3173, 2976, 2842, 2343, 1532, 1462, 1432, 1265, 1240, 1207, 1186, 1038 cm⁻¹.

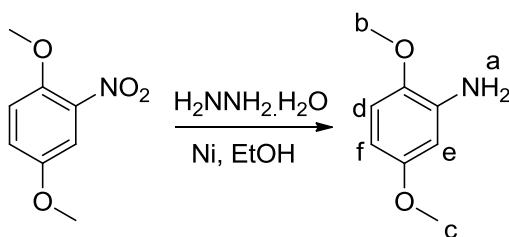
Preparation of 1,4-dimethoxy-2-nitrobenzene (**57**):



1,4-Dimethoxybenzene (10.00 g, 72.38 mmol) was dissolved in acetonitrile (200 ml) with stirring. Once dissolved, potassium nitrate (7.32 g, 72.38 mmol) and trifluoroacetic

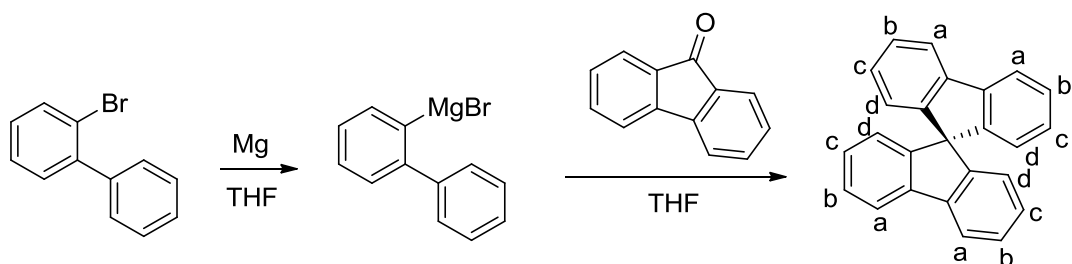
anhydride (35.26 ml, 253.33 mmol) were added. The mixture was heated to 50 °C and stirred for 16 hours before being concentrated under reduced pressure. The residue was added to water (200 ml), extracted with chloroform (3 x 150 ml) and the solution concentrated under reduced pressure, giving the product as a yellow powder (13.14 g, 71.75 mmol, 99.1%). Mp 64 – 66 °C; Lit. Mp = 68 – 70 °C¹⁹⁵; ¹H NMR (400 MHz, CDCl₃) δ ppm 3.81 (3H, s, H_a), 3.91 (3H, s, H_b), 7.03 (1H, m, H_c), 7.10 (1H, m, H_d), 7.39 (1H, m, H_e); ¹³C NMR (100 MHz, CDCl₃) δ ppm 56.1, 57.1, 110.0, 115.2, 120.9, 139.6, 147.4, 152.9; LRMS *m/z* (EI, M⁺) = 183.04; IR (NaCl): 2982, 2848, 1576, 1527, 1498, 1466, 1445, 1355, 1284, 1273, 1220, 1190, 1162, 1039, 1016 cm⁻¹.

Preparation of 1,4-dimethoxy-2-aminobenzene (58):



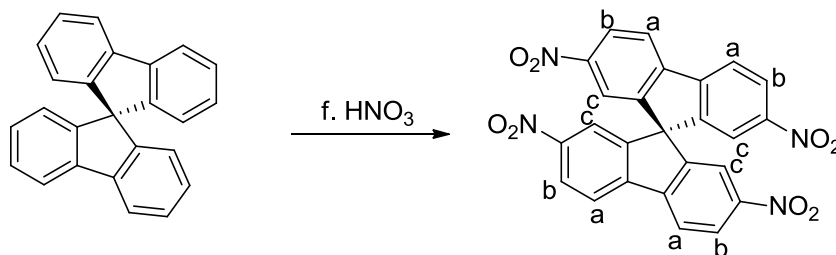
1,4-Dimethoxy-2-nitrobenzene (1.00 g, 5.46 mmol), ethanol (60 ml), Raney nickel (catalytic amount) and hydrazine monohydrate (2.14 ml, 27.32 mmol) were briefly mixed together at room temperature. The reaction mixture was then heated to 60 °C and left stirring for 16 hours under nitrogen. Following this the mixture was filtered and concentrated under reduced pressure. The resulting material was added to water (100 ml) and the product extracted with chloroform (3 x 50 ml). This solution was concentrated under reduced pressure, giving the product as a light grey powder (0.80 g, 5.24 mmol, 95.9%). Mp 68 – 70 °C; Lit. Mp = 74 - 76 °C¹⁹⁶; ¹H NMR (400 MHz, CDCl₃) δ ppm 2.82 (2H, br. s, H_a), 3.73 (3H, s, H_b), 3.81 (3H, s, H_c), 6.24 (1H, d, J = 8.6 Hz, H_d), 6.34 (1H, s, H_e), 6.71 (1H, d, J = 8.6 Hz, H_f); ¹³C NMR (100 MHz, CDCl₃) δ ppm 30.9, 55.7, 56.2, 102.1, 102.2, 111.4, 137.1, 141.9, 154.4; LRMS *m/z* (EI, M⁺) = 153.07; IR (NaCl): 3801, 3460, 3369, 2838, 1621, 1520, 1466, 1310, 1227, 1182, 1037 cm⁻¹.

Preparation of 9,9'-spirobisfluorene (**59**):



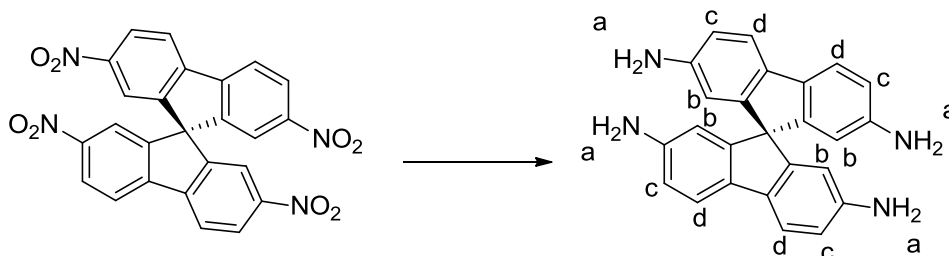
Based upon the procedure described by J. Pei *et al.*¹⁶⁰, a solution of 2-bromobiphenyl (10.00 ml, 58.00 mmol) in dry THF (150 ml) was added to dry powdered magnesium (1.48 g, 60.90 mmol). This was heated to reflux (85 °C) and stirred for 1.5 hours under a nitrogen atmosphere. At regular intervals during this period an iodine crystal was added to the mixture. After this time all the magnesium had been consumed and the solution appeared as a clear grey solution. This was added to a solution of 9-fluorenone (11.50 g, 63.80 mmol) in dry THF (250 ml). The resulting mixture was stirred at 70 °C for 16 hours under a nitrogen atmosphere. The intermediate was then collected by filtration and washed with THF (100 ml). The solid was stirred in ice-cold saturated ammonium chloride solution (250 ml) for 16 hours before being added to a mixture of acetic acid (100 ml) and concentrated hydrochloric acid (37%, 5 ml). This was stirred at reflux for 2 hours before the product was collected by filtration. It was washed with water (200 ml) and ethanol (100 ml). Finally, the solid was boiled in ethanol (100 ml) for a few minutes, cooled to room temperature and the product collected by filtration. After drying under vacuum, the product appeared as a white crystalline solid (10.85 g, 34.33 mmol, 59.2%). Mp 180 – 182 °C; Lit. Mp = 202 °C¹⁹⁷; ¹H NMR (400 MHz, CDCl₃) δ ppm 6.77 (4H, d, J = 7.6 Hz, H_a), 7.13 (4H, dt, J = 7.6, 1.0 Hz, H_b), 7.39 (4H, dt, J = 7.6, 1.0 Hz, H_c), 7.88 (4H, d, J = 7.6 Hz, H_d); ¹³C NMR (100 MHz, CDCl₃) δ ppm 66.0, 119.7, 120.0, 123.8, 124.08, 127.7, 127.8, 141.8, 148.8; LRMS *m/z* (EI, M⁺) = 316.12; IR (NaCl): 3061, 3036, 3016, 1950, 1919, 1603, 1581, 1473, 1446, 1282, 1213, 1153, 1102, 1030, 1020, 1005 cm⁻¹.

Preparation of 2,2',7,7'-tetranitro-9,9'-spirobisfluorene (**60**):



Based upon the procedure detailed by J. D. Wuest *et al.*¹⁶¹, fuming nitric acid (40 ml) was cooled to -45 °C and stirred for 30 minutes. 9,9'-Spirobisfluorene (4.00 g, 12.66 mmol) was then slowly added to the acid in portions over 20 minutes. The mixture was given a further 20 minutes of stirring before the reaction was quenched by addition of water (250 ml). This was stirred briefly before the product was extracted with dichloromethane (3 x 80 ml). The dichloromethane was removed under reduced pressure and the resulting solid boiled in THF:hexane (1:1, 100 ml) for a few minutes. Finally, the mixture was cooled to room temperature, the product collected by filtration and dried under vacuum. This gave the product as a pale yellow powder (4.95 g, 9.98 mmol, 78.8%). Mp > 350 °C; Lit. Mp > 300 °C¹⁶¹; ¹H NMR (400 MHz, (CD₃)₂SO) δ ppm 7.63 (4H, d, J = 2.1 Hz, H_a), 8.45 (2H, d, J = 2.1 Hz, H_b), 8.47 (2H, d, J = 2.1 Hz, H_b), 8.57 (2H, s, H_c), 8.59 (2H, m, H_c); ¹³C NMR (100 MHz, (CD₃)₂SO) δ ppm 65.0, 119.1, 124.0, 125.3, 145.7, 147.6, 148.5; LRMS *m/z* (EI, M⁺) = 496.06; IR (NaCl): 2978, 1635, 1520, 1485, 1411, 1340, 1257, 1126, 1079 cm⁻¹.

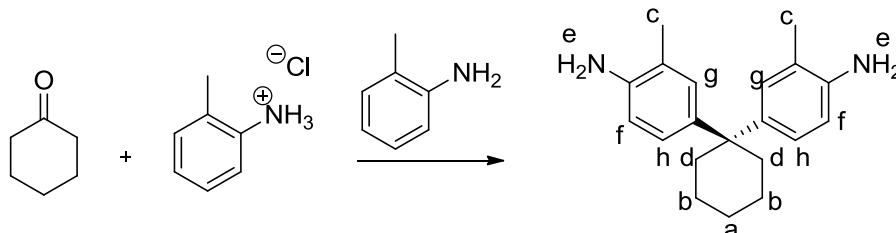
Preparation of 2,2',7,7'-tetraamino-9,9'-spirobisfluorene (**61**):



Under a nitrogen atmosphere, tin metal (3.60 g, 30.30 mmol) was added in small portions to a suspension of tetranitrospirobisfluorene (1.00 g, 2.02 mmol) in concentrated hydrochloric acid (37%, 15 ml). This mixture was heated to 140 °C for 16 hours to

dissolve any residual tin metal. This was accompanied by a colour change from yellow to off-white. The mixture was then cooled to room temperature and the white crystalline powder collected by filtration. This was washed with concentrated hydrochloric acid (37%, 50 ml), chloroform (50 ml) and diethyl ether (50 ml). The powder was then dissolved in water (100 ml) and the pH of the solution increased to 10 by addition of aqueous ammonia (35%, 20 ml). This caused a cream coloured powder to precipitate, which was extracted with dichloromethane (3 x 50 ml). The resulting solution was dried under reduced pressure. This gave the product as a cream coloured powder (0.51 g, 1.36 mmol, 67.1%). Mp > 360 °C; Lit. Mp > 210 °C (decomposes)¹⁶¹; ¹H NMR (400 MHz, *DMSO*) δ ppm 4.81 (8H, s, H_a), 5.85 (4H, s, H_b), 6.46 (4H, d, J = 7.8 Hz, H_c), 7.32 (4H, d, J = 7.8 Hz, H_d); ¹³C NMR (100 MHz, *MeOD*) δ ppm 66.8, 112.6, 116.0, 120.2, 134.6, 147.1, 152.0; HRMS Calc. for C₂₅H₂₀N₄m/z = 376, found 376.1683 gmol⁻¹; IR (NaCl): 3409, 2518, 1469, 1304, 1244, 1121 cm⁻¹.

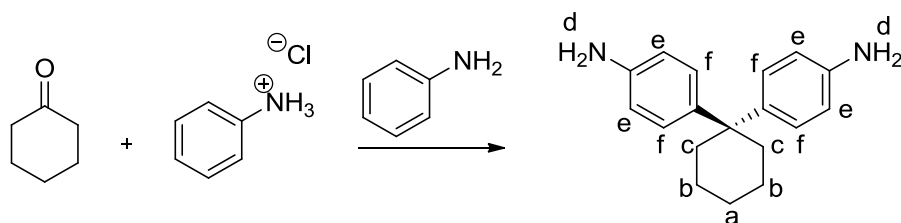
Preparation of 2,2-bis(3-methyl-4-aminophenyl)cyclohexane (62):



Based upon the procedure described by K.-Y. Choi *et al.*¹⁶⁴, cyclohexanone (7.39 ml, 71.33 mmol), 2-methylaniline (22.84 ml, 213.98 mmol) and 2-methylaniline hydrochloride (20.49 g, 142.65 mmol) were mixed together. The mixture was heated to 150 °C and stirred for 20 hours under nitrogen. The reaction was then quenched by addition of water (100 ml), and stirred for an hour before aqueous ammonia (35%, 100 ml) was added. After brief stirring the crude product was extracted with chloroform (3 x 100 ml) and the solution concentrated under reduced pressure, giving a brown oil, which was passed through a silica column (6:4 hexane:ethyl acetate). This gave the product as a cream powder (14.69 g, 49.97 mmol, 70.1%). Mp 167 – 169 °C; Lit. Mp = 162 – 163 °C¹⁶³; ¹H NMR (400 MHz, CDCl₃) δ ppm 1.48 (2H, m, H_a), 1.54 (4H, m, H_b), 2.13 (6H, s, H_c), 2.19 (4H, m, H_d), 3.45 (4H, br. s, H_e), 6.60 (2H, d, J = 8.0 Hz, H_f), 6.93 (2H, m, H_g), 6.96 (2H,

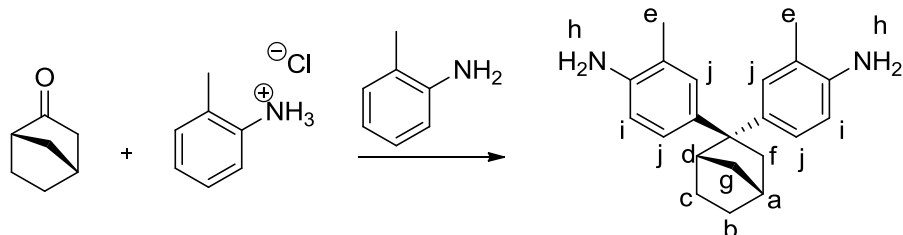
m, H_h); ¹³C NMR (100 MHz, CDCl₃) δ ppm 17.8, 23.1, 26.6, 37.5, 44.8, 115.0, 122.1, 125.7, 129.2, 139.7, 141.6; HRMS Calc. for C₂₀H₂₆N₂m/z = 294, found 294.2106 gmol⁻¹; IR (NaCl): 3464, 3430, 3380, 3355, 3016, 2932, 2854, 1621, 1505, 1470, 1454, 1409, 1286, 1270, 1182, 1158, 1109, 1035 cm⁻¹. Crystals were prepared by a slow diffusion of hexane into a solution of the compound in chloroform. Crystal properties: system = Tetragonal, space group = *I41/a*, *a* = 31.3432(18), *b* = 31.4883(18), *c* = 6.5834(5), α = 89.88, β = 89.82, γ = 89.83, *V* = 6497.37 Å³; *Z* = 18.

Preparation of 2,2-bis(4-aminophenyl)cyclohexane (63):



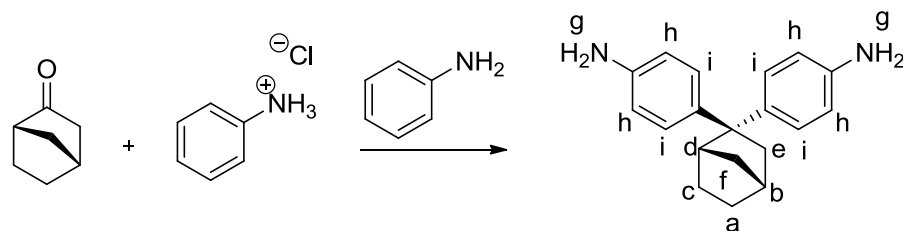
Cyclohexanone (21.10 ml, 203.77 mmol), aniline (55.68 ml, 611.31 mmol) and 2-methylaniline hydrochloride (58.09 g, 448.29 mmol) were mixed together at room temperature. The mixture was heated to 150 °C and stirred for 20 hours under nitrogen. The temperature was then decreased to 140 °C and the reaction quenched by addition of water (100 ml) and aqueous ammonia (35%, 200 ml). After brief stirring the crude product was extracted with chloroform (3 x 150 ml). The solution was washed with water (300 ml) before being concentrated under reduced pressure, giving a brown oil. Most of the unreacted aniline was distilled off at 1.7 torr and 70 – 100 °C, with the conditions maintained for an hour. The resulting residue was passed through a silica column (6:4 hexane:ethyl acetate), which gave a red oil. This was then passed through another silica column (6:4 hexane:ethyl acetate), giving the product as a brown powder (22.61 g, 99.98 mmol, 49.1%). Mp 100 – 102 °C; Lit. Mp = 112 °C¹⁶²; ¹H NMR (400 MHz, CDCl₃) δ ppm 1.50 (2H, m, H_a), 1.55 (4H, m, H_b), 2.19 (4H, m, H_c), 3.52 (4H, br. s, H_d), 6.60 (4H, m, H_e), 7.06 (4H, m, H_f); ¹³C NMR (100 MHz, CDCl₃) δ ppm 22.9, 26.6, 37.4, 44.9, 115.1, 128.0, 139.5, 143.6; HRMS Calc. for C₁₈H₂₂N₂m/z = 266, found 266.1785 gmol⁻¹; IR (NaCl): 3349, 3216, 3027, 2934, 2857, 1622, 1512, 1467, 1452, 1353, 1278, 1216, 1187, 1138, 1010 cm⁻¹.

Preparation of 2,2-bis(3-methyl-4-aminophenyl)bicyclo[2.2.1]heptane (**64**):



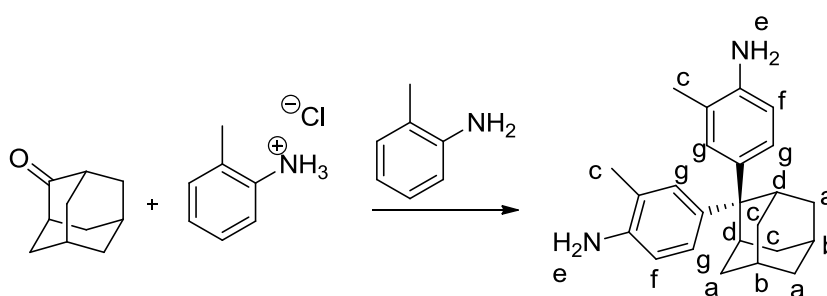
Norcamphor (7.00 g, 63.64 mmol), 2-methylaniline (20.38 ml, 190.91 mmol) and 2-methylaniline hydrochloride (18.28 g, 127.27 mmol) were mixed together at room temperature. The mixture was heated to 150 °C and stirred for 20 hours under nitrogen before the reaction was quenched by addition of water (100 ml). After stirring for an hour, aqueous ammonia (35%, 100 ml) was added and after brief stirring the crude product was extracted with chloroform (3 x 100 ml). The solvent was removed under reduced pressure, giving a brown oil, which was then passed through a silica column (6:4 hexane:ethyl acetate). This gave the product as a cream powder (4.95 g, 16.16 mmol, 25.4%). Mp 98 – 100 °C; ¹H NMR (400 MHz, CDCl₃) δ ppm 1.16 (1H, m, H_a), 1.30 (2H, m, H_b), 1.44 (2H, m, H_c), 1.70 (1H, m, H_d), 2.10 (6H, s, H_e), 2.23 (2H, m, H_f), 2.33 (1H, s, H_g), 3.07 (1H, s, H_g), 3.38 (4H, s, H_h), 6.54 (2H, d, J = 8.2 Hz, H_i), 6.97 (4H, m, H_j); ¹³C NMR (100 MHz, CDCl₃) δ ppm 17.7, 24.8, 29.8, 38.3, 43.5, 44.8, 54.8, 114.8, 121.8, 122.0, 125.1, 126.2, 129.1, 130.0, 139.6, 141.1, 141.4, 143.7; HRMS Calc. for C₂₁H₂₆N₂m/z = 306, found 306.2097 gmol⁻¹; IR (NaCl): 3449, 3368, 3219, 2958, 2870, 2734, 2240, 1869, 1738, 1623, 1582, 1505, 1454, 1407, 1379, 1288, 1217, 1156, 1068, 1033 cm⁻¹. Crystals were prepared by a slow diffusion of hexane into a solution of the compound in THF. Crystal properties: system = Monoclinic, space group = *P bca*, *a* = 29.7279(8), *b* = 6.9561(3), *c* = 18.1863(8), α = 90.00, β = 114.29, γ = 90.00, *V* = 3427.94 Å³; *Z* = 8.

Preparation of 2,2-bis(4-aminophenyl)bicyclo[2.2.1]heptane (**65**):



Norcamphor (8.69 g, 79.02 mmol) and aniline hydrochloride (22.53 g, 173.84 mmol) were mixed together. The mixture was heated to 170 °C and stirred for 18 hours under nitrogen. The temperature was then decreased to 140 °C and the reaction quenched by addition of water (100 ml) and aqueous ammonia (35%, 100 ml). After brief stirring the crude product was extracted with chloroform (4 x 80 ml). The solution was washed with water (100 ml) before the solvent was removed under reduced pressure, giving a brown oil, which was then passed through a silica column (6:4 hexane:ethyl acetate). This gave the product as a cream powder (3.86 g, 13.88 mmol, 17.6%). Mp 190 – 192 °C; Lit. Mp = 202 °C¹⁶⁴; ¹H NMR (400 MHz, CDCl₃) δ ppm 1.30 (5H, m, H_a, H_b, H_c), 1.70 (1H, d, J = 9.4 Hz, H_d), 2.21 (2H, br. s, H_e), 2.33 (1H, s, H_f), 3.03 (1H, s, H_f), 3.47 (4H, br. s, H_g), 6.55 (4H, d, J = 7.9 Hz, H_h), 7.03 (2H, d, J = 7.9 Hz, H_i), 7.08 (2H, d, J = 7.9 Hz, H_j); ¹³C NMR (100 MHz, CDCl₃) δ ppm 24.8, 29.7, 38.3, 43.4, 44.9, 54.8, 114.9, 115.0, 127.7, 128.6, 139.5, 143.3; HRMS Calc. for C₁₉H₂₂N₂m/z = 278, found 278.1777 gmol⁻¹; IR (NaCl): 3434, 3349, 3216, 3026, 2955, 2869, 1622, 1579, 1512, 1476, 1453, 1429, 1311, 1278, 1215, 1185, 1157, 1126, 1057, 1013 cm⁻¹. Crystals were prepared by a slow diffusion of hexane into a solution of the compound in THF. Crystal properties: system = Orthorhombic, space group = *P* 2₁2₁2₁, *a* = 6.4087(4), *b* = 10.7718(7), *c* = 10.7814(6), α = 90.00, β = 90.00, γ = 90.00, *V* = 744.28 Å³; *Z* = 4.

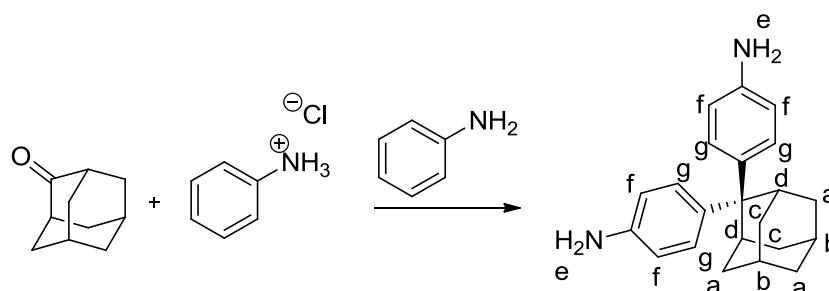
Preparation of 2,2-bis(3-methyl-4-aminophenyl)adamantane (66):



2-Adamantanone (20.00 g, 133.14 mmol), 2-methylaniline (42.80 ml, 399.41 mmol) and 2-methylaniline hydrochloride (42.06 g, 292.91 mmol) were mixed together at room temperature. The mixture was heated to 180 °C and stirred for 20 hours under nitrogen. The reaction was then quenched by addition of water (200 ml), and stirred for an hour before aqueous ammonia (35%, 200 ml) was added. After brief stirring the crude product

was extracted with chloroform (3 x 300 ml). The solvent was removed under reduced pressure, giving a brown oil, which was then passed through a silica column (6:4 hexane:ethyl acetate). Finally, washing the material with methanol (100 ml) gave the pure product as a cream powder (16.08 g, 46.47 mmol, 34.9%). Mp 261-263 °C; ¹H NMR (400 MHz, CDCl₃) δ ppm 1.71 (6H, br. s, H_a), 1.79 (2H, s, H_b), 2.10 (10H, m, H_c), 3.12 (6H, m, H_d + H_e), 6.55 (2H, d, J = 8.0 Hz, H_f), 7.05 (4H, m, H_g); ¹³C NMR (100 MHz, CDCl₃) δ ppm 17.9, 27.8, 32.0, 33.5, 38.3, 49.0, 115.3, 122.3, 124.1, 127.7, 139.7, 141.0; HRMS Calc. for C₂₄H₃₀N₂m/z = 346, found 346.2408 gmol⁻¹; IR (NaCl): 3448, 3376, 3019, 2910, 2853, 2734, 2676, 2239, 1866, 1624, 1508, 1469, 1450, 1411, 1378, 1359, 1308, 1288, 1216, 1149, 1119, 1101, 1076, 1033 cm⁻¹. Crystals were prepared by a slow diffusion of hexane into a solution of the compound in chloroform. Crystal properties: system = Tetragonal, space group = *I*-42*d*, *a* = 14.8398(14), *b* = 14.8373(18), *c* = 36.1380(5), α = 90.00, β = 90.00, γ = 90.00, *V* = 7956.96 Å³; *Z* = 18.

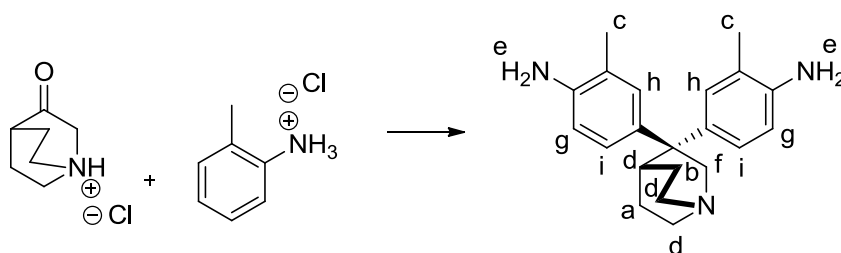
Preparation of 2,2-bis(4-aminophenyl)adamantane (67):



2-Adamantanone (20.00 g, 133.14 mmol), aniline (36.38 ml, 399.41 mmol) and aniline hydrochloride (37.96 g, 292.91 mmol) were mixed together at room temperature. The mixture was heated to 180 °C and stirred for 40 hours under nitrogen. The temperature was decreased to 140 °C before the reaction was quenched by addition of water (200 ml). This was stirred for an hour before aqueous ammonia (35%, 200 ml) was added. After brief stirring the crude product was extracted with chloroform (3 x 150 ml). The solution was washed with water (100 ml) before the solvent was removed under reduced pressure, giving a brown oil. Most of the unreacted aniline was removed by distillation, at 70 – 100 °C and a pressure of 0.66 Torr, the conditions were maintained for an hour. The resulting residue was then passed through a silica column (6:4 hexane:ethyl acetate). This gave the

product as a grey powder (13.16 g, 41.4 mmol, 31.1%). Mp 242 – 244 °C; Lit. Mp = 242 °C¹⁶⁴; ¹H NMR (400 MHz, CDCl₃) δ ppm 1.69 (6H, m, H_a), 1.79 (2H, br. s, H_b), 2.05 (4H, m, H_c), 3.11 (2H, s, H_d), 3.21 (4H, s, H_e), 6.56 (4H, d, J = 8.6 Hz, H_f), 7.14 (4H, d, J = 8.6 Hz, H_g); ¹³C NMR (100 MHz, CDCl₃) δ ppm 27.7, 32.0, 33.4, 38.2, 39.3, 49.1, 115.4, 126.4, 139.6, 142.9; HRMS Calc. for C₂₂H₂₆N₂m/z = 318, found 319.2166 gmol⁻¹ (M + H⁺); IR (NaCl): 3433, 3350, 3215, 3026, 3003, 2909, 2852, 2673, 1622, 1509, 1468, 1449, 1358, 1282, 1215, 1204, 1189, 1129, 1100, 1076, 1013 cm⁻¹. Crystals were prepared by a slow diffusion of hexane into a solution of the compound in THF. Crystal properties: system = Orthorhombic, space group = *P nma*, *a* = 12.2760(4), *b* = 12.6251(3), *c* = 36.1380(5), α = 90.00, β = 90.00, γ = 90.00, *V* = 3331.25 Å³; *Z* = 8.

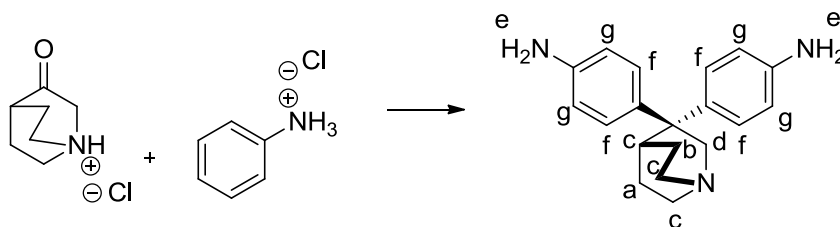
Preparation of 3,3-bis(3-methyl-4-aminophenyl)-1-azabicyclo[2,2,2]octane (68):



Based upon the procedure described by Y. S. Vygodskii et al.¹⁶⁵, a solution of 3-quinuclidone hydrochloride (8.45 g, 52.28 mmol) in water (200 ml) was added aqueous ammonia (35%, 100 ml). The mixture was thoroughly shaken and the ketone extracted with chloroform (3 x 60 ml). The chloroform solution was washed with water (200 ml) and the chloroform removed under reduced pressure, giving 3-quinuclidone as a colourless oil (6.42 g, 51.36 mmol). This was mixed with *o*-toluidine hydrochloride (16.52 g, 115.02 mmol) and heated to 170 °C before the mixture was stirred for 72 hours under a nitrogen atmosphere. The temperature was then decreased to 140 °C and water (50 ml) added to quench the reaction. The dark solution was allowed to cool to room temperature and treated with aqueous ammonia (35%, 100 ml). This was stirred for 30 minutes before the product was extracted with chloroform (3 x 80 ml). The chloroform solution was washed with water (200 ml) and dried under reduced pressure, giving the crude product as a dark oil. The unreacted *o*-toluidine was removed by distillation at a temperature of 180 – 220 °C and a pressure of 0.7 torr, these conditions were maintained for an hour. The mixture was

dried under reduced pressure, giving the product as a brown powder (11.30 g, 35.15 mmol, 67.2%). Mp 86 – 88 °C; ^1H NMR (400 MHz, CDCl_3) δ ppm 1.50 (2H, m, H_a), 1.68 (2H, m, H_b), 2.07 (6H, s, H_c), 2.73 (5H, m, H_d), 3.44 (4H, s, H_e), 3.72 (2H, s, H_f), 6.53 (2H, d, $J = 8.2$ Hz, H_g), 6.92 (2H, s, H_h), 6.95 (2H, d, $J = 8.2$ Hz, H_i); ^{13}C NMR (100 MHz, CDCl_3) δ ppm 17.8, 23.5, 28.9, 29.2, 30.9, 44.2, 47.1, 59.1, 114.7, 118.5, 122.1, 124.9, 129.0, 147.0; HRMS Calc. for $[\text{C}_{21}\text{H}_{27}\text{N}_3]^+$ $m/z = 321$, found 321.2206 g mol^{-1} ; IR (NaCl): 3357, 2944, 1625, 1507, 1456, 1282, 1153 cm^{-1} .

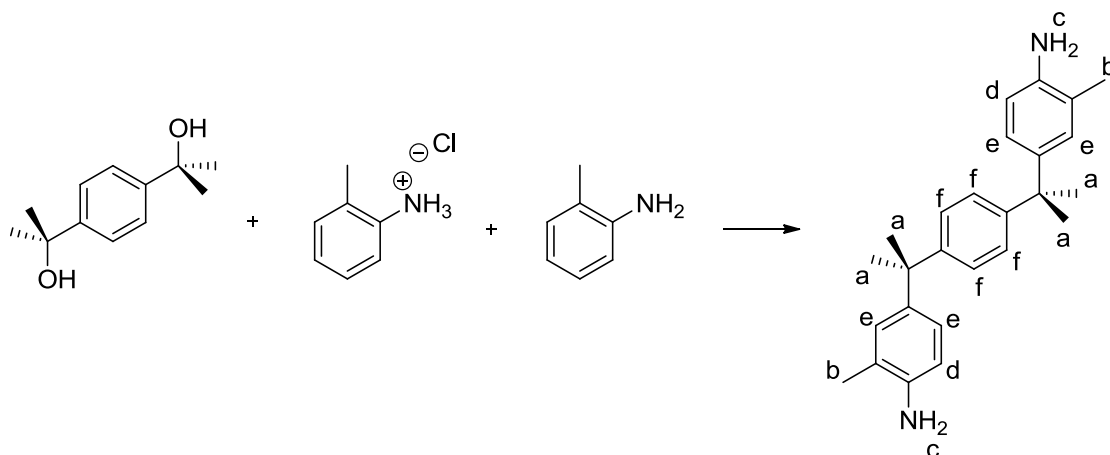
Preparation of 3,3-bis(4-aminophenyl)-1-azabicyclo[2,2,2]octane (69):



To a solution of 3-quinuclidone hydrochloride (10.00 g, 61.87 mmol) in water (200 ml) was added aqueous ammonia (35%, 100 ml). The mixture was thoroughly shaken and the ketone extracted with chloroform (3 x 80 ml). The chloroform solution was washed with water (200 ml) and dried under reduced pressure, giving 3-quinuclidone as a colourless oil (7.48 g, 59.86 mmol). This was mixed with aniline hydrochloride (17.64 g, 136.11 mmol) and heated to 170 °C before the mixture was stirred for 24 hours under a nitrogen atmosphere. The temperature was then decreased to 140 °C and water (50 ml) added to quench the reaction. The resulting dark solution was allowed to cool to room temperature and treated with aqueous ammonia (35%, 100 ml). This was stirred for 30 minutes before the product was extracted with chloroform (3 x 100 ml). The solution was washed with water (200 ml) before being dried under reduced pressure, this gave the crude product as a dark oil. The unreacted aniline was removed by distillation at a temperature of 160-200 °C and a pressure of 0.7 torr, these conditions were maintained for an hour. The resulting dark residue was dried under reduced pressure, giving the product as a light brown powder (12.78 g, 43.61 mmol, 70.5%). Mp 124 – 126 °C; ^1H NMR (400 MHz, CDCl_3) δ ppm 1.50 (2H, m, H_a), 1.67 (2H, m, H_b), 2.73 (5H, m, H_c), 3.41 (2H, s, H_d), 3.49 (4H, s, H_e), 6.54 (4H, d, $J = 8.4$ Hz, H_f), 7.04 (4H, d, $J = 8.4$ Hz, H_g); ^{13}C NMR (100 MHz, CDCl_3) δ ppm

23.4, 28.9, 44.3, 47.0, 50.3, 59.0, 115.1, 127.4, 139.4, 143.5; HRMS Calc. for $[C_{19}H_{23}N_3]^+$ $m/z = 293$, found 293.1894 $gmol^{-1}$; IR (NaCl): 3349, 2948, 2872, 1622, 1512, 1456, 1318, 1283, 1217, 1188, 1152, 1073, 1050 cm^{-1} .

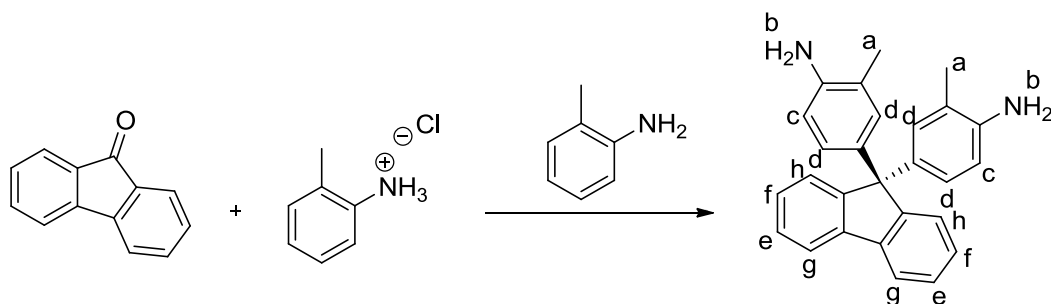
Preparation of 1,1',4,4'-tetramethyl-1,4-(3-methyl-4-aminophenyl)benzene (70):



1,4-Bis(2-hydroxyisopropyl)benzene (10.00 g, 51.55 mmol), 2-methyl aniline (16.57 ml, 154.64 mmol) and 2-methyl aniline hydrochloride (16.28 g, 113.41 mmol) were mixed together at room temperature. The mixture was heated to 170 °C and stirred for 72 hours under a nitrogen atmosphere. The temperature was then reduced to 140 °C and the reaction quenched by addition of water (100 ml). This was stirred for an hour whilst the mixture cooled down to room temperature. Aqueous ammonia (35%, 100 ml) was then added and after brief stirring the product was extracted with chloroform (3 x 150 ml). The chloroform solution was washed with water (200 ml) before being concentrated to a dark oil under reduced pressure. The oil was passed through a silica column (7:3 hexane:ethyl acetate), which gave the crude product as a yellow solid. This was triturated in methanol (100 ml) at 0 °C for an hour before the product was collected by filtration and dried under vacuum. This gave the product as an off-white solid (14.61 g, 39.27 mmol, 76.2%). Mp 124 – 126 °C; Lit. Mp = 131 °C¹⁹⁸; 1H NMR (400 MHz, $CDCl_3$) δ ppm 1.66 (12 H, s, H_a), 2.16 (6H, s, H_b), 3.51 (4H, br. s, H_c), 6.61 (2H, d, $J = 8.0$ Hz, H_d), 6.95 (4H, m, H_e), 7.15 (4H, s, H_f); ^{13}C NMR (100 MHz, $CDCl_3$) δ ppm 17.7, 31.2, 41.7, 114.7, 121.8, 125.3, 126.2, 128.9, 141.2, 142.1, 148.1; HRMS Calc. for $C_{26}H_{32}N_2$ $m/z = 372$, found 372.2558 $gmol^{-1}$; IR (NaCl): 3451, 3373, 2966, 2930, 2870, 1623, 1507, 1463, 1401, 1382, 1360, 1317, 1289,

1218, 1187, 1159, 1120, 1095, 1017 cm^{-1} . Crystals were prepared by a slow diffusion of hexane into a solution of the compound in THF. Crystal properties: system = Monoclinic, space group = $P 21/n$, $a = 10.0150(5)$, $b = 10.3320(5)$, $c = 21.4990(8)$, $\alpha = 90.00(5)$, $\beta = 111.37(5)$, $\gamma = 90.00(5)$, $V = 1037.87\text{\AA}^3$; $Z = 2$.

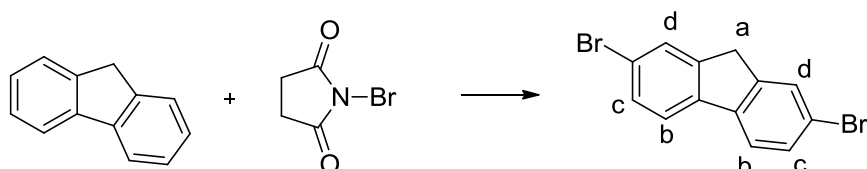
Preparation of 9,9'-(3-methyl-4-aminophenyl)-fluorene (71):



9-Fluorenone (15.00 g, 44.40 mmol), 2-methylaniline (45.00 ml, 419.93 mmol) and 2-methylaniline hydrochloride (14.03 g, 97.68 mmol) were mixed together at room temperature. The mixture was heated to 170 °C and stirred for 48 hours under a nitrogen atmosphere. The temperature was then reduced to 140 °C and the reaction quenched by addition of water (200 ml). After stirring for 30 minutes the mixture was cooled to room temperature and aqueous ammonia (35%, 200 ml) added. This was stirred briefly before the product was extracted with chloroform (3 x 200 ml). The chloroform solution was washed with water (200 ml) and concentrated to a dark oil under reduced pressure. The oil was passed through a silica column (6:4 hexane:ethyl acetate), which removed most of the impurities and gave the crude product as a brown solid. This was passed through a second silica column (6:4 hexane:ethyl acetate) before drying under vacuum. This gave the product as a white powder (11.28 g, 30.00 mmol, 67.6%). Mp 222 – 224 °C; ^1H NMR (400 MHz, CDCl_3) δ ppm 2.05 (6H, s, H_a), 3.67 (4H, br. s, H_b), 6.53 (2H, d, $J = 9.0$ Hz, H_c), 6.89 (4H, m, H_d), 7.24 (2H, dt, $J = 7.4, 1.2$ Hz, H_e), 7.33 (2H, dt, $J = 7.4, 1.2$ Hz, H_f), 7.39 (2H, d, $J = 7.4$ Hz, H_g), 7.73 (2H, d, $J = 7.4$ Hz, H_h); ^{13}C NMR (100 MHz, CDCl_3) δ ppm 17.5, 64.3, 114.8, 119.9, 122.0, 126.1, 126.9, 127.0, 127.5, 130.1, 136.4, 140.0, 142.9, 152.4; HRMS Calc. for $\text{C}_{27}\text{H}_{24}\text{N}_2$ $m/z = 376$, found 376.1933 g mol^{-1} ; IR (NaCl): 3458, 3375, 3017, 2926, 1722, 1622, 1503, 1475, 1446, 1409, 1289, 1217, 1154, 1096, 1032, 1006 cm^{-1} . Crystals were prepared by a slow diffusion of hexane into a solution of the

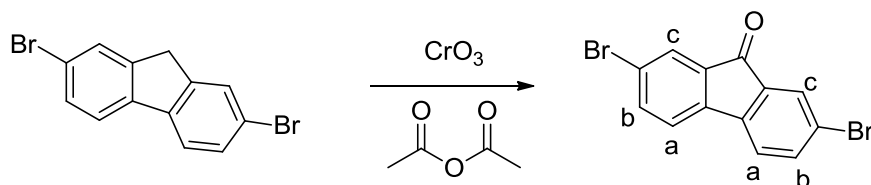
compound in THF. Crystal properties: system = Monoclinic, space group = $P 21/n$, $a = 13.4303(7)$, $b = 11.9346(6)$, $c = 13.4861(5)$, $\alpha = 90.00$, $\beta = 114.21(3)$, $\gamma = 90.00$, $V = 1971.49 \text{ \AA}^3$; $Z = 4$.

Preparation of 2,7-dibromo-9-fluorene (72):



Following the procedure reported by W. Y. Huang *et al.*¹⁶⁷, a mixture of fluorene (30.00 g, 180.72 mmol), *N*-bromosuccinimide (65.62 g, 368.67 mmol) and propylene carbonate (250 ml) was refluxed for 4 hours before the dark solution was cooled to room temperature. It was then poured into methanol (1 L) and stirred vigorously for 16 hours. The precipitated solid was collected by filtration and dried under vacuum. This gave the product as a peach coloured powder (36.25 g, 111.95 mmol, 61.9%). Mp 136 – 138 °C; Lit. Mp = 156 – 160 °C (dichloromethane)¹⁹⁹; ¹H NMR (400 MHz, CDCl₃) δ ppm 3.81 (2H, s, H_a), 7.48 (2H, d, $J = 8.1$ Hz, H_b), 7.56 (2H, d, $J = 8.1$ Hz, H_c), 7.63 (2H, s, H_d); ¹³C NMR (100 MHz, CDCl₃) δ ppm 36.6, 121.1, 128.3, 130.2, 139.7, 144.8; LRMS m/z (EI, M⁺) = 323.88; IR (NaCl): 3058, 2921, 2897, 1883, 1795, 1598, 1569, 1456, 1417, 1399, 1391, 1332, 1291, 1274, 1215, 1160, 1127, 1118, 1055, 1005 cm⁻¹.

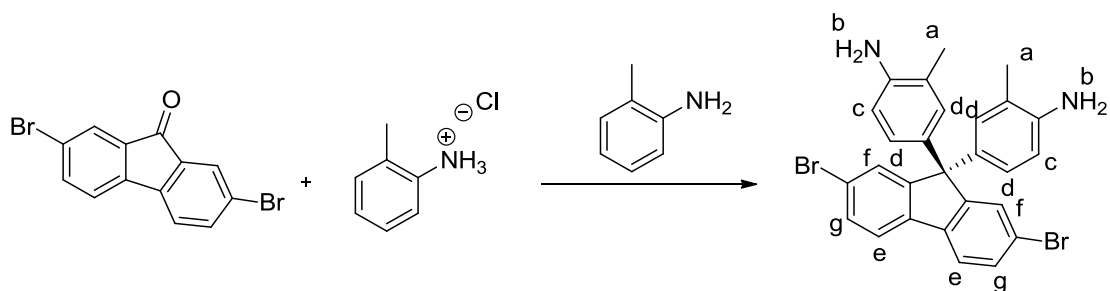
Preparation of 2,7-dibromo-9-fluorenone (73):



Following the procedure described by Y. Chen *et al.*¹⁶⁸, a mixture of 2,7-dibromo-9-fluorene (20.00 g, 61.77 mmol), chromium trioxide (15.44 g, 154.42 mmol) and acetic anhydride (450 ml) was stirred at 0 °C for an hour. It was then allowed to warm to room

temperature and stirred for a further 6 hours before the reaction was quenched by addition to dilute hydrochloric acid (2% wt., 2 L). The resulting precipitate was collected by filtration before being washed with water (500 ml) and methanol (100 ml). The solid was dried under vacuum before recrystallisation from diethyl ether was performed. The resulting solid was dried under vacuum, giving the product as a yellow powder (17.96 g, 53.17 mmol, 86.1%). Mp 182 – 184 °C; Lit. Mp = 202 – 204 °C¹⁶⁸; ¹H NMR (400 MHz, CDCl₃) δ ppm 7.36 (2H, d, J = 8.0 Hz, H_a), 7.61 (2H, d, J = 8.0 Hz, H_b), 7.74 (2H, s, H_c); ¹³C NMR (100 MHz, CDCl₃) δ ppm 121.8, 123.3, 127.9, 135.3, 137.5, 142.3, 190.1; LRMS *m/z* (EI, M⁺) = 337.87; IR (NaCl): 3056, 1724, 1708, 1592, 1445, 1418, 1275, 1244, 1225, 1206, 1181, 1153, 1118, 1056, 1033 cm⁻¹.

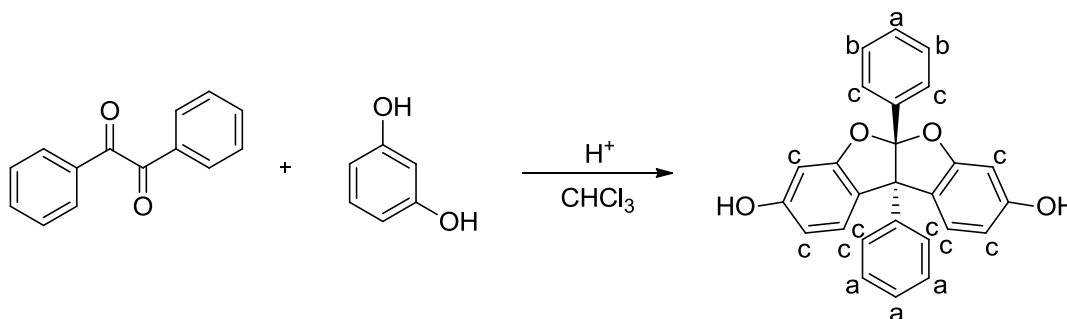
Preparation of 2,7-dibromo-9,9'-(3-methyl-4-aminophenyl)-fluorene (74):



2,7-Dibromo-9-fluorenone (15.00 g, 44.40 mmol), 2-methylaniline (45.00 ml, 419.93 mmol) and 2-methylaniline hydrochloride (14.03 g, 97.68 mmol) were mixed together at room temperature. The mixture was heated to 170 °C and stirred for 48 hours under a nitrogen atmosphere. The temperature was then reduced to 140 °C and the reaction quenched by addition of water (200 ml). After stirring for 30 minutes the mixture was cooled to room temperature and aqueous ammonia (35%, 200 ml) added. This was stirred briefly before the product was extracted with chloroform (3 x 200 ml). The chloroform solution was washed with water (200 ml) and concentrated to a dark oil under reduced pressure. The oil was passed through a silica column (7:3 hexane:ethyl acetate), which removed most of the impurities and gave the crude product as a brown solid. This was passed through a second silica column (7:3 hexane:ethyl acetate) before drying under vacuum. This gave the product as an off-white powder (20.54 g, 38.48 mmol, 86.7%). Mp 256 – 258 °C; ¹H NMR (400 MHz, CDCl₃) δ ppm 2.06 (6H, s, H_a), 3.58 (4H, br. s, H_b), 6.55 (2H, d, J = 8.8 Hz, H_c), 6.82 (4H, m, H_d), 7.44 (2H, d, J = 8.0 Hz, H_e), 7.48 (2H, s,

H_f), 7.55 (2H, d, J = 8.0 Hz, H_g); ¹³C NMR (100 MHz, CDCl₃) δ ppm 17.6, 64.5, 114.9, 121.4, 121.7, 122.3, 126.7, 129.3, 129.9, 130.5, 134.6, 137.9, 143.5, 154.3; HRMS Calc. for C₂₇H₂₂N₂Br₂m/z = 534, found 533.9861 gmol⁻¹; IR (NaCl): 3384, 2945, 1622, 1504, 1449, 1412, 1395, 1286, 1249, 1216, 1156, 1108, 1061, 1006 cm⁻¹. Crystals were prepared by a slow diffusion of hexane into a solution of the compound in chloroform. Crystal properties: system = Monoclinic, space group = *P* 21/*n*, *a* = 11.7990(5), *b* = 14.0900(5), *c* = 15.2150(5), *α* = 90.00(5), *β* = 110.80(5), *γ* = 90.00(5), *V* = 2364.65 Å³; *Z* = 4.

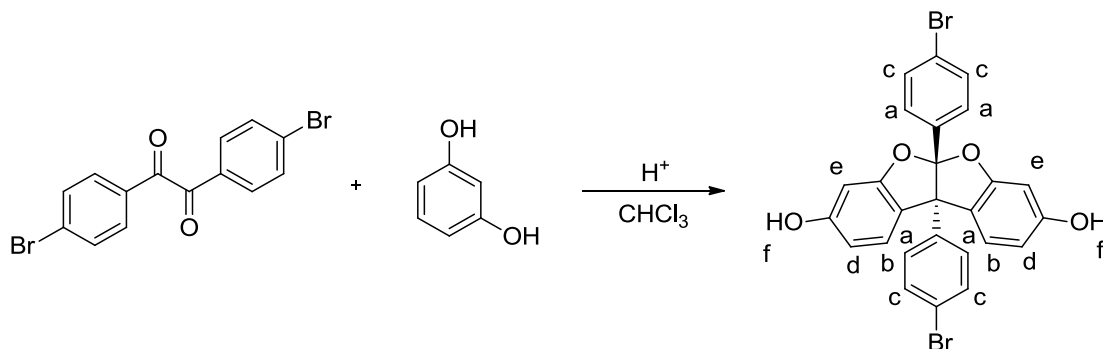
Preparation of 3,8-dihydroxy-5a,10b-diphenylcoumarano-2,2',3,3'-coumaron (75):



Based upon the procedure reported by J. C. McGowan *et al.*¹⁶⁹, resorcinol (4.19 g, 38.10 mmol), benzil (2.00 g, 9.52 mmol), glacial acetic acid (2 ml), chloroform (8 ml) and concentrated hydrochloric acid (37%, 1.5 ml) were mixed together at room temperature. The mixture was heated to 62 °C and stirred for 48 hours. The reaction was then quenched by addition to water (150 ml); this was stirred for an hour before the precipitated product was collected by filtration. The solid was washed with chloroform (100 ml) before being boiled in chloroform (100 ml) for a few minutes. Finally, after cooling to room temperature the product was collected by filtration and dried under vacuum. This gave the product as an off-white powder (3.16 g, 8.02 mmol, 84.2%). Mp 244 – 246 °C; Lit. Mp = 262 °C¹⁶⁹; ¹H NMR (400 MHz, *d*₆-acetone) δ ppm 6.55 (4H, m, H_a), 6.77 (2H, m, H_b), 7.05 (10H, m, H_c); ¹³C NMR (100 MHz, *d*₆-acetone) δ ppm 70.1, 98.3, 110.6, 124.1, 126.3, 127.4, 127.8, 128.2, 129.3, 129.9, 138.1, 141.4, 159.4, 160.9, 206.7; LRMS *m/z* (EI, M + 2H⁺) = 396.12; IR (NaCl): 3386, 2108, 1689, 1619, 1481, 1449, 1346, 1283, 1211, 1164, 1142, 1079, 1033, 1015 cm⁻¹. Crystals were prepared by a slow diffusion of hexane into a solution of the compound in THF. Crystal properties: system = Orthorhombic, space group = *P* 2₁2₁2₁,

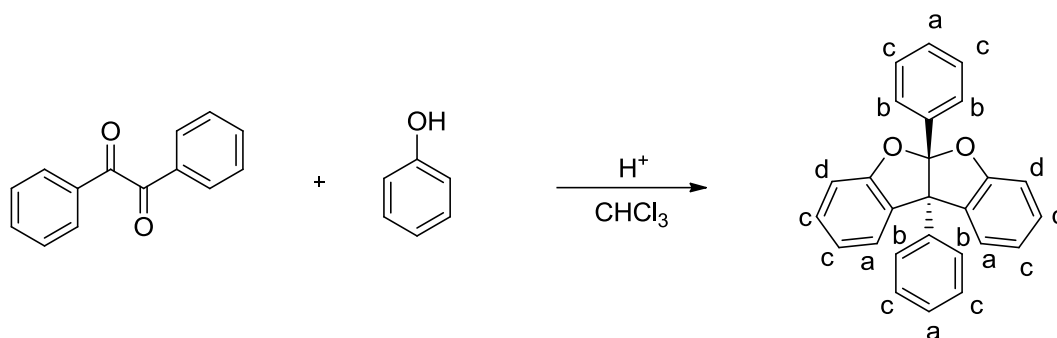
$a = 8.1590(3)$, $b = 12.3460(4)$, $c = 19.1230(5)$, $\alpha = 90.00$, $\beta = 90.00$, $\gamma = 90.00$, $V = 1926.28\text{\AA}^3$; $Z = 4$.

Preparation of 3,8-dihydroxy-(4,4'-dibromo)-5a,10b-diphenylcoumarano-2,2',3,3'-coumaron (76):



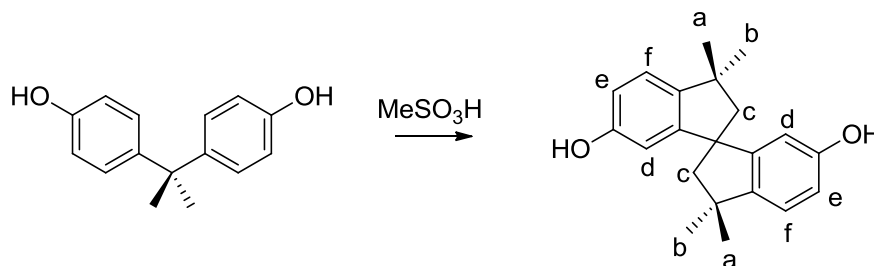
A mixture of resorcinol (3.59 g, 32.61 mmol), 4,4'-dibromobenzil (3.00 g, 8.15 mmol), glacial acetic acid (3 ml), chloroform (12 ml) and concentrated hydrochloric acid (37%, 2.5 ml) was heated to 62 °C. The mixture was left stirring for 96 hours before it was cooled to room temperature. The reaction was then quenched by addition to water (150 ml). This was stirred for an hour before the solid was collected by filtration and washed with chloroform (100 ml). The solid was dried under vacuum before being stirred in boiling in chloroform (100 ml) for a few minutes, before the mixture was cooled to room temperature. The solid was collected by filtration and dried under vacuum. This gave the product as an off-white powder (4.20 g, 7.58 mmol, 93.0%). Mp 234 – 236 °C; ¹H NMR (400 MHz, *d6*-acetone) δ ppm 6.57 (4H, m, H_a), 6.73 (2H, m, H_b), 7.09 (4H, m, H_c), 7.23 (2H, m, H_d), 7.32 (2H, m, H_e), 8.67 (2H, s, H_f); ¹³C NMR (100 MHz, *d6*-acetone) δ ppm 69.8, 98.5, 111.0, 121.7, 123.3, 126.2, 126.7, 129.5, 130.2, 131.6, 132.1, 137.4, 140.1, 159.7, 160.7; HRMS Calc. for C₂₆H₁₆O₄Br₂*m/z* = 552, found 551.9130 gmol⁻¹; IR (NaCl): 3382, 2082, 1623, 1487, 1464, 1395, 1365, 1280, 1232, 1146, 1113, 1074, 1005 cm⁻¹. Crystals were prepared by a slow diffusion of hexane into a solution of the compound in THF. Crystal properties: system = Triclinic, space group = *P* - *I*, $a = 9.8227(4)$, $b = 11.1614(6)$, $c = 13.6996(10)$, $\alpha = 71.67(3)$, $\beta = 82.16(4)$, $\gamma = 73.91(3)$, $V = 1367.91\text{\AA}^3$; $Z = 2$.

Preparation of 5a,10b-diphenylcoumarano-2,2',3,3'-coumaron (77):



A mixture of phenol (5.38 g, 57.14 mmol), benzil (3.00 g, 14.29 mmol), glacial acetic acid (3 ml), chloroform (12 ml) and concentrated hydrochloric acid (37%, 2.5 ml) was heated to 62 °C and stirred for 48 hours. The reaction was then quenched in water (100 ml) and stirred for an hour. The crude material was extracted with dichloromethane (3 x 50 ml), and the solution the solvent removed under reduced pressure. The resulting solid was passed through a silica column (6:4 hexane:ethyl acetate), which gave the product as a white powder (1.03 g, 2.85 mmol, 19.9%). Mp 208 – 210 ° C; ^1H NMR (400 MHz, CDCl_3) δ ppm 6.56 (4H, d, $J = 8.8$ Hz, H_a), 6.92 (4H, d, $J = 8.8$ Hz, H_b), 7.07 (8H, m, H_c), 7.55 (2H, d, $J = 7.9$ Hz, H_d); ^{13}C NMR (100 MHz, CDCl_3) δ ppm 30.8, 69.9, 114.8, 126.4, 127.6, 130.6, 131.0, 131.7, 135.0, 137.4, 143.8, 154.4; HRMS Calc. for $\text{C}_{26}\text{H}_{20}\text{O}_2$ [$\text{M} + 2\text{H}^+$] $m/z = 364$, found 364.1460 gmol^{-1} ; IR (NaCl): 3391, 3060, 3022, 1666, 1612, 1595, 1578, 1510, 1446, 1366, 1221, 1179, 1114, 1034, 1016 cm^{-1} .

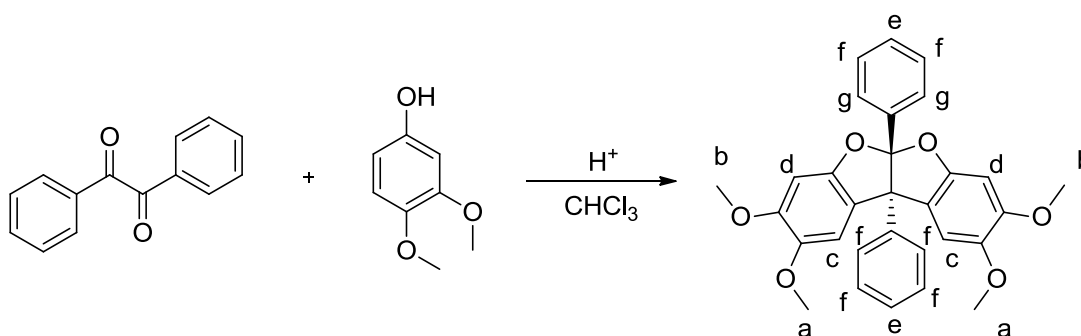
Preparation of 3,3,3',3'-tetramethyl-2,2',3,3'-tetrahydro-1,1'-spirobi[indene]-6,6'-diol (78):



Based upon the procedure described by Y. Han *et al.*⁹⁹, a solution of Bisphenol A (100.00 g, 0.44 mmol) in methanesulphonic acid (551.45 g, 5.74 mol) was stirred at 25 °C for 3

days under a nitrogen atmosphere. The reaction was then quenched in water (2000 ml) and stirred for 2 hours, causing a solid to crash out. The solid was collected by filtration, washed with water (500 ml) and dried under vacuum, giving the crude product as a pink solid. The solid was recrystallised from aqueous ethanol (60%, 500 ml), giving the product as an off-white solid (40.62 g, 131.88 mmol, 90.3%). Mp 172 – 174 °C; Lit. Mp = 184 – 186 °C²⁰⁰; ¹H NMR (400 MHz, *DMSO*) δ ppm 1.24 (6H, s, H_a), 1.31 (6H, s, H_b), 2.08 (1H, s, H_c), 2.11 (1H, s, H_c), 2.23 (1H, s, H_c), 2.27 (1H, s, H_c), 6.10 (2H, s, H_d), 6.59 (2H, d, J = 8.0 Hz, H_e), 6.99 (2H, d, J = 8.0 Hz, H_f); ¹³C NMR (100 MHz, *CDCl*₃) δ ppm 30.5, 31.6, 42.3, 56.9, 59.4, 110.0, 114.4, 122.1, 142.2, 151.5, 156.7; LRMS *m/z* (EI, M⁺) = 308.05; IR (NaCl): 3390, 2950, 2861, 1604, 1471, 1361, 1288, 1208, 1153, 1118 cm⁻¹.

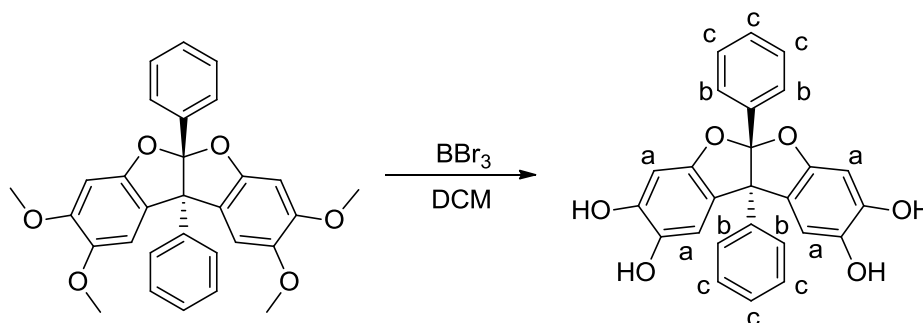
Preparation of 2,3,8,9-tetramethoxy-5a,10b-diphenylcoumarano-2,2',3,3'-coumaron (79):



A mixture of 3,4-dimethoxyphenol (7.75 g, 50.27 mmol), benzil (3.52 g, 16.76 mmol), chloroform (48 ml), glacial acetic acid (12 ml) and concentrated hydrochloric acid (37%, 10 ml) was heated to 60 °C and stirred for 96 hours. The reaction was then quenched by addition to water (150 ml), and the mixture stirred for 30 minutes. The crude material was extracted with chloroform (3 x 100 ml), and the solvent removed under reduced pressure, giving a dark oil. This was triturated in boiling methanol for 2 hours, filtered and dried under vacuum to give the product as a white powder (4.74 g, 9.83 mmol, 58.7%). Mp 162 – 164 °C; ¹H NMR (400 MHz, *CDCl*₃) δ ppm 3.79 (6H, s, H_a), 3.90 (6H, s, H_b), 6.71 (2H, s, H_c), 6.75 (2H, s, H_d), 6.78 (2H, m, H_e), 7.02 (6H, m, H_f), 7.14 (2H, m, H_g); ¹³C NMR (100 MHz, *CDCl*₃) δ ppm 56.2, 57.1, 71.0, 95.4, 108.3, 121.4, 126.5, 126.7, 127.1, 127.4, 127.7, 128.4, 129.4, 136.7, 139.8, 145.2, 150.3, 153.2; HRMS Calc. for C₃₀H₂₆O₆ *m/z* = 482, found 482.1726 gmol⁻¹; IR (NaCl): 3061, 3020, 2937, 2865, 2833, 1621, 1503, 1453, 1416, 1303, 1212, 1167, 1135, 1109, 1077, 1015 cm⁻¹. Crystals were prepared by a slow

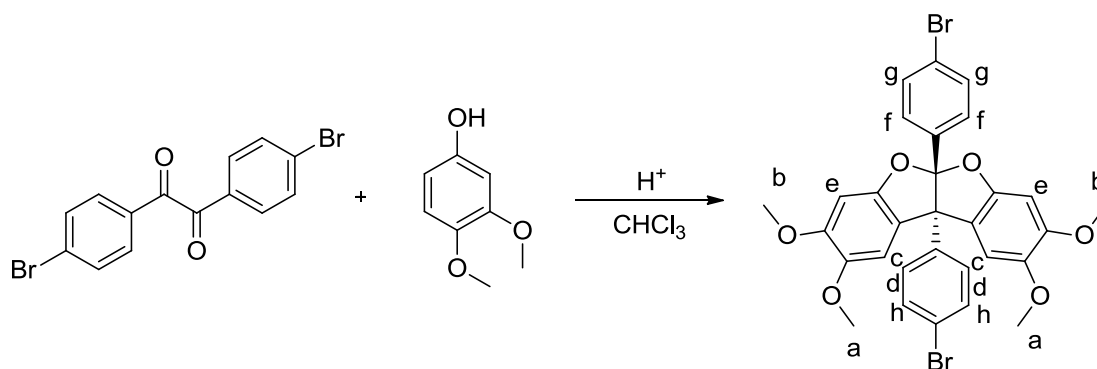
diffusion of hexane into a solution of the compound in chloroform. Crystal properties: system = Triclinic, space group = $P-1$, $a = 9.0570(3)$, $b = 11.5819(3)$, $c = 12.6859(4)$, $\alpha = 82.76(2)$, $\beta = 70.84(2)$, $\gamma = 76.31(2)$, $V = 1219.57\text{\AA}^3$; $Z = 2$.

Preparation of 2,3,8,9-tetrahydroxy-5a,10b-diphenylcoumarano-2,2',3,3'-coumaron (80):



2,3,8,9-Tetramethoxy-5a,10b-diphenylcoumarano-2,2',3,3'-coumaron (1.00 g, 2.07 mmol) was dissolved in anhydrous dichloromethane (75 ml) and the solution purged with nitrogen for 2 hours. It was then cooled down to $-78\text{ }^\circ\text{C}$ in an acetone/dry ice bath and boron tribromide (0.60 ml, 6.22 mmol) slowly added. The reaction mixture immediately turned red and was left stirring for 4 hours whilst warming to room temperature. The reaction was quenched by the addition of de-ionised water (50 ml), which caused the solution to immediately turn black. The precipitate was collected by filtration, washed with fresh dichloromethane (30 ml) and dried under vacuum. This gave the product as a blue powder (0.29 g, 0.68 mmol, 32.9%). $\text{Mp} > 360\text{ }^\circ\text{C}$; $^1\text{H NMR}$ (400 MHz, d_6 -acetone) δ ppm 6.57 (4H, s, H_a), 6.92 (4H, m, H_b), 7.01 (6H, m, H_c); $^{13}\text{C NMR}$ (100 MHz, d_6 -acetone) δ ppm 98.1, 104.5, 112.8, 119.6, 128.0, 128.2, 140.2, 140.8, 149.0, 155.4; HRMS Calc. for $\text{C}_{26}\text{H}_{18}\text{O}_6$ $m/z = 426$, found 426.1106 gmol^{-1} ; IR (NaCl): 3399, 2519, 2416, 2257, 1667, 1605, 1508, 1463, 1309, 1160, 1119, 1022 cm^{-1} .

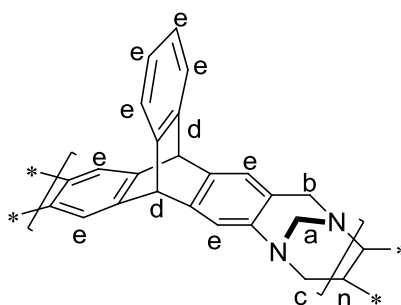
Preparation of 2,3,8,9-tetramethoxy-(4,4'-dibromo)-5a,10b-diphenylcoumarano-2,2',3,3'-coumaron (**81**):



A mixture of 3,4-dimethoxyphenol (1.76 g, 11.41 mmol), 4,4'-dibromobenzil (2.00 g, 5.43 mmol), *o*-dichlorobenzene (50 ml), glacial acetic acid (20 ml), and concentrated hydrochloric acid (37%, 10 ml) was heated to 120 °C for 48 hours. The reaction was then cooled to room temperature and quenched by addition to water (200 ml). After stirring for 30 minutes the crude product was extracted with chloroform (3 x 50 ml). The chloroform solution was dried under reduced pressure, leaving a dark oil, which was triturated in methanol for 2 hours. The resulting solid was collected by filtration and dried under vacuum to give the product as a white powder (1.09 g, 1.70 mmol, 31.4%). Mp 240 – 242 °C; ¹H NMR (400 MHz, CDCl₃) δ ppm 3.78 (6H, s, H_a), 3.89 (6H, s, H_b), 6.62 (2H, s, H_c), 6.65 (2H, d, J = 8.4 Hz, H_d), 6.71 (2H, s, H_e), 7.01 (2H, d, J = 8.6 Hz, H_f), 7.17 (2H, d, J = 8.6 Hz, H_g), 7.22 (2H, d, J = 8.4 Hz, H_h); ¹³C NMR (100 MHz, CDCl₃) δ ppm 56.2, 57.0, 70.6, 95.5, 108.0, 120.6, 121.6, 123.1, 125.9, 128.2, 130.9, 135.7, 138.7, 145.4, 150.5, 152.9; HRMS Calc. for C₃₀H₂₄O₆Br₂ *m/z* = 640, found 639.9930 gmol⁻¹; IR (NaCl): 3003, 2935, 2834, 1621, 1491, 1455, 1416, 1394, 1306, 1213, 1136, 1107, 1074, 1004 cm⁻¹. Crystals were prepared by a slow diffusion of methanol into a solution of the compound in chloroform. Crystal properties: system = Triclinic, space group = *P* -1, *a* = 10.6474(2), *b* = 12.0149(3), *c* = 13.2690(2), α = 75.68(2), β = 66.66(10), γ = 71.67(10), *V* = 1464.59 Å³; *Z* = 2.

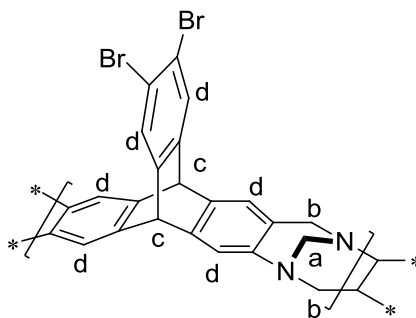
6.3 Polymer synthesis

Polymerisation of 2,6(7)-diaminotriptycene (82):



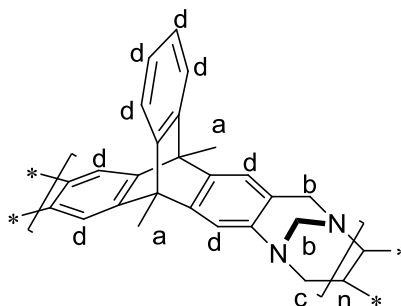
2,6(7)-Diaminotriptycene (1.43 g, 5.04 mmol) was dissolved in a mixture of dimethoxymethane (2.23 ml, 25.22 mmol) and dichloromethane (1.5 ml). Once dissolved trifluoroacetic acid (14.3 ml) was added dropwise over 2 hours. The clear red solution was left stirring for 168 hours before the reaction was quenched with water (100 ml). After stirring briefly, aqueous ammonia (35%, 100 ml) was added and the solution stirred vigorously for a further 2 hours before the precipitate was collected by filtration. The solid was washed with water (100 ml) and acetone (100 ml) before being ground to a fine powder. The polymer was dissolved in chloroform (150 ml), reprecipitated with hexane (150 ml) and collected by filtration, this process was repeated twice more. The solid was then refluxed in acetone and twice in methanol, each time for 16 hours. Filtration gave the polymer as a cream powder (1.28 g, 4.01 mmol based on repeating unit, 79.6%). BET surface area = 725 m² g⁻¹; total pore volume = 0.51 ml g⁻¹ at $p/p^o = 0.98$; TGA (nitrogen): weight loss due to thermal degradation started at 400 °C and totalled 30.5%; GPC (based on polystyrene standard) $M_n = 21,200$, $M_w = 50,700$ gmol⁻¹; ¹H NMR (400 MHz, CDCl₃) δ ppm 3.89 (2H, br. s, H_a), 4.41 (2H, br. s, H_b), 4.80 (2H, br. s, H_c), 5.07 (2H, br. s, H_d), 6.97 (8H, m, H_e); ¹³C NMR (100 MHz, *solid state*) δ ppm 53.7, 58.4, 67.0, 124.2, 145.0. Elemental analysis calc. (%) for repeating unit [C₂₃H₁₆N₂]: C 86.22, H 5.03, N 8.74 (calculated), C 76.63, H 4.15, N 7.69 (found).

Polymerisation of 2,3-dibromo-6(7),14-diaminotriptycene (83):



2,3-Dibromo-6(7),14-diaminotriptycene (2.00 g, 4.52 mmol) was dissolved in trifluoroacetic acid (20 ml) at 0 °C with stirring before dimethoxymethane (2.00 ml, 22.62 mmol) was added. The reaction mixture was left stirring under nitrogen for 72 hours. The reaction was then quenched by addition of water (100 ml), and stirred for 1 hour before aqueous ammonia (35%, 100 ml) was added. After stirring for a further 3 hours the precipitate was collected by filtration and washed with acetone. The solid was refluxed in acetone, THF and methanol, each for 16 hours, giving the product as a brown powder (0.78 g, 1.62 mmol based on repeating unit, 35.7%). BET surface area = 10 m²/g; total pore volume = 0.01 ml g⁻¹ at $p/p^o = 0.98$; TGA (nitrogen): weight loss due to thermal degradation started at 350 °C and totalled 41.0%; ¹H NMR (400 MHz, DMSO) δ ppm 3.36 (2H, br. s, H_a), 3.88 (2H, br. s, H_b), 4.38 (2H, br. s, H_b), 5.31 (2H, br. s, H_c), 7.00 (3H, br. m, H_d), 7.70 (3H, br. m, H_d); ¹³C NMR (100 MHz, solid state) δ ppm 53.2, 59.2, 67.5, 121.2, 145.5.

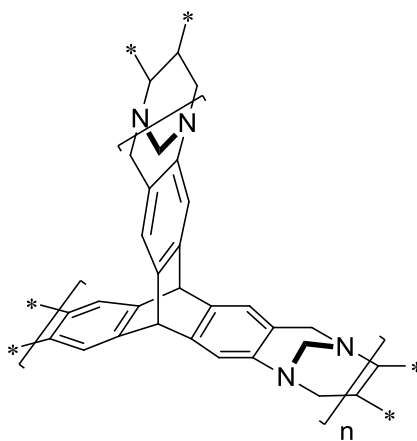
Polymerisation of 2,6/7-diamino-9,10-dimethyltriptycene (84):



2,6(7)-Diamino-9,10-dimethyltriptycene (2.32 g, 7.44 mmol) was dissolved in trifluoroacetic acid (23 ml) with stirring at 0 °C. Once dissolved, dimethoxymethane (3.29

ml, 37.18 mmol) was slowly added over a few minutes and the reaction mixture left stirring for 96 hours under a nitrogen atmosphere. The reaction was then quenched by addition of water (100 ml) and aqueous ammonia (35%, 100 ml), before the mixture was stirred vigorously for 16 hours. The precipitated solid was then collected by filtration, washed with water (200 ml) and acetone (200 ml) before being dried under reduced pressure. After the polymer was refluxed in acetone (100 ml) for an hour it was dissolved in chloroform (200 ml) and reprecipitated with hexane (250 ml). This was performed two additional times, before the polymer was refluxed in acetone (100 ml) and methanol (100 ml), both for 16 hours. This gave the polymer as a cream coloured powder (2.17 g, 6.23 mmol, 83.7%). BET surface area = 775 m²/g; total pore volume = 0.57 ml g⁻¹ at p/p⁰ = 0.98; TGA (nitrogen): weight loss due to thermal degradation started at 376 °C and totalled 33.0%; GPC (based on polystyrene standard) M_n = 6.000, M_w = 13,600 gmol⁻¹; ¹H NMR (400 MHz, CDCl₃) δ ppm 2.19 (6H, br. s, H_a), 3.92 (4H, br. m, H_b), 4.46 (2H, br. s, H_c), 6.93 (8H, br. m, H_d); ¹³C NMR (100 MHz, *solid state*) δ ppm 12.9, 47.6, 58.5, 66.9, 118.4, 124.4, 145.0. Elemental analysis calc. (%) for repeating unit [C₂₅H₂₀N₂]: C 86.18, H 5.79, N 8.04 (calculated), C 77.78, H 5.00, N 7.13 (found).

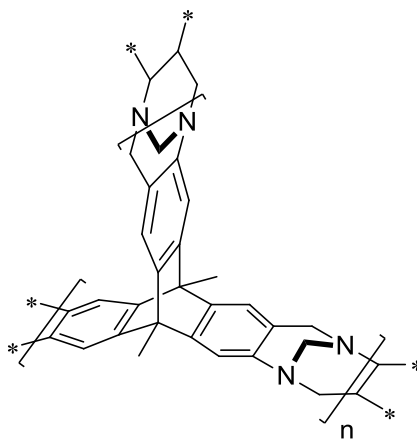
Polymerisation of 2,6(7),14-triaminotriptycene (85):



2,6(7),14-Triaminotriptycene (0.85 g, 2.84 mmol) was dissolved in trifluoroacetic acid (10 ml) at 0 °C. To this solution dimethoxymethane (1.76 ml, 19.90 mmol) was added dropwise before the mixture was left stirring for 48 hours. The reaction was then quenched with water (100 ml), stirred briefly then aqueous ammonia (35%, 100 ml) added. After stirring for 24 hours the solid was collected by filtration. The polymer was refluxed in

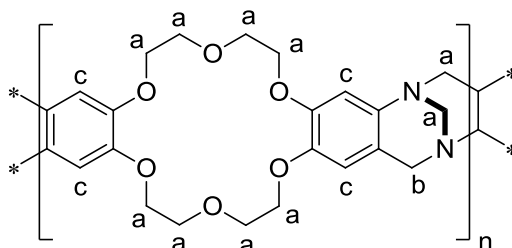
acetone, THF, chloroform and methanol, each time for 16 hours. Finally, the product was dried under vacuum, giving the product as a brown powder (0.74 g, 69.2% based on repeating unit). BET surface area = 1035 m² g⁻¹; total pore volume = 0.63 ml g⁻¹ at $p/p^0 = 0.98$; TGA (nitrogen): weight loss due to thermal degradation started at 423 °C and totalled 21.2%, solvent loss started at 23.4 °C and totalled 5.6%; ¹³C NMR (100 MHz, *solid state*) δ ppm 54.0, 59.5, 67.7, 111.1, 123.1, 145.3. Elemental analysis calc. (%) for repeating unit [C₂₄H₁₆N₃]: C 83.21, H 4.66, N 12.12 (calculated), C 78.04, H 4.88, N 11.89 (found).

Polymerisation of 2,6(7),14-triamino-9,10-dimethyltritycene (86):



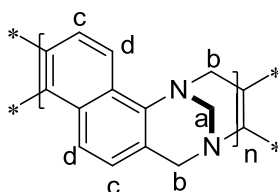
2,6(7),14-Triamino-9,10-dimethyltritycene (2.34 g, 7.16 mmol) was dissolved in trifluoroacetic acid (23 ml) with stirring at 0 °C. Once dissolved, dimethoxymethane (4.43 ml, 50.10 mmol) was slowly added, the mixture was left stirring for 72 hours under a nitrogen atmosphere. The reaction was then quenched by addition of water (100 ml) and aqueous ammonia (35%, 100 ml). This was stirred for 16 hours, with the solid broken up regularly with a spatula, before the precipitated polymer was collected by filtration, washed with water (200 ml) and washed with acetone (200 ml). The polymer was dried under vacuum before being refluxed in acetone, THF and methanol (100 ml), each for 16 hours. Drying under vacuum gave the product as a light brown powder (2.43 g, 6.38 mmol, 89.1%). BET surface area = 750 m²/g; total pore volume = 0.48 ml g⁻¹ at $p/p^0 = 0.98$; TGA (nitrogen): weight loss due to thermal degradation started at 294 °C and totalled 29.0%; ¹³C NMR (100 MHz, *solid state*) δ ppm 12.6, 30.3, 39.1, 47.3, 59.4, 67.3, 109.2, 117.8, 123.2, 144.9. Elemental analysis calc. (%) for repeating unit [C₂₆H₂₀N₃]: C 83.40, H 5.38, N 11.22 (calculated), C 74.29, H 5.60, N 9.62 (found).

Polymerisation of 2,13-diaminodibenzo-18-crown-6 (87):



2,13-Diaminodibenzo-18-crown-6 (0.75 g, 1.92 mmol) was dissolved in a mixture of trifluoroacetic acid (10 ml) and chloroform (10 ml) at 0 °C. Once dissolved, dimethoxymethane (0.51 ml, 5.77 mmol) was slowly added and the reaction left stirring for 72 hours. The reaction was then quenched in a mixture of ice water (100 ml) and aqueous ammonia (35%, 50 ml). This was stirred for 2 hours before the yellow precipitate was collected by filtration. The precipitate was finely ground before being refluxed in acetone for 16 hours. Final filtration gave the polymer as a yellow powder (0.40 g, 0.93 mmol based on repeating unit, 48.4 %). BET surface area = 3 m²/g; total pore volume = 0.02 ml g⁻¹ at $p/p^o = 0.98$; TGA (nitrogen): weight loss due to thermal degradation started at 201 °C and totalled 55.4%. ¹H NMR (400 MHz, CDCl₃) δ ppm 3.98 (20H, br. s, H_a), 4.46 (2H, br. s, H_b), 6.46 (2H, br.s, H_c), 6.52 (2H, br.s, H_c); ¹³C NMR (100 MHz, *solid state*) δ ppm 58.5, 70.0, 100.3, 108.3, 120.0, 141.0, 144.8, 148.1.

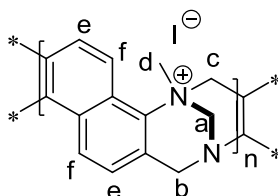
Polymerisation of 1,5-diaminonaphthalene (88):



1,5-Diaminonaphthalene (1.00 g, 6.32 mmol) was stirred in diethyl ether (50 ml) for an hour before being collected by filtration, giving a red coloured solution and purified 1,5-diaminonaphthalene, which was dried in a vacuum oven at 40 °C for 5 hours. The dry powder was mixed with paraformaldehyde (0.95 g, 31.60 mmol) and the mixture slowly added to trifluoroacetic acid (10 ml) at 0 °C. The reaction was left stirring for 72 hours before being quenched in saturated sodium hydroxide solution (50 ml) and stirred for a

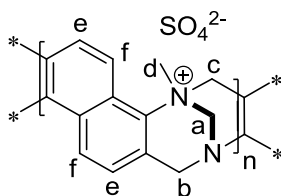
further 3 hours. The precipitate was then filtered off and refluxed in THF and acetone, each for 2 hours. The powder was then refluxed in methanol for 16 hours, giving the polymer as a cream coloured powder (0.85 g, 69% based on repeating unit). BET surface area = $700 \text{ m}^2 \text{ g}^{-1}$; total pore volume = 0.32 ml g^{-1} at $p/p^o = 0.98$; TGA (nitrogen): weight loss due to thermal degradation started at $400 \text{ }^\circ\text{C}$ and totalled 70.5%. ^1H NMR (400 MHz, CDCl_3) δ ppm 4.30 (2H, br. s, H_a), 4.55 (2H, br. s, H_b), 4.90 (2H, br. s, H_b), 7.04 (2H, br. s, H_c), 8.03 (2H, br. s, H_d); ^{13}C NMR (100 MHz, *solid state*) δ ppm 56.3, 67.5, 118.9, 124.0, 129.0, 143.2.

Preparation of iodine stabilised quaternary naphthalene TB polymer (89):



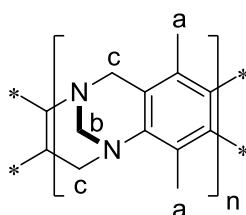
Based upon the procedure described by Lenev et al.¹⁷⁷, TB naphthalene polymer (**88**, 0.40 g, 2.06 mmol based on repeating unit), DMSO (20 ml), and methyl iodide (2.57 ml, 41.22 mmol) were mixed together and stirred for 72 hours. During this time a colour change from red to brown was observed but the polymer remained insoluble. After this time the reaction was quenched in water (100 ml) and the resulting mixture stirred for two hours. The polymer was filtered off, washed with acetone and refluxed in methanol for 16 hours. This gave the product as a red brown powder (0.73 g, 2.03 mmol, 98.7%). BET surface area = $3 \text{ m}^2/\text{g}$; total pore volume = 0.03 ml g^{-1} at $p/p^o = 0.98$; TGA (nitrogen): weight loss due to thermal degradation started at $35 \text{ }^\circ\text{C}$ and totalled 51.8%. ^1H NMR (400 MHz, CDCl_3) δ ppm 4.27 (2H, br. s, H_a), 4.39 (2H, br. s, H_b), 4.57 (2H, br. s, H_c), 4.89 (3H, br. s, H_d), 7.04 (2H, br. s, H_e), 8.04 (2H, br. s, H_f); ^{13}C NMR (100 MHz, *solid state*) δ ppm 56.6, 67.5, 119.4, 124.3, 128.6, 143.1.

Preparation of sulphate stabilised quaternary naphthalene polymer (90):



TB naphthalene polymer (**88**, 0.40 g, 2.06 mmol based on repeating unit), DMSO (20 ml) and dimethyl sulphate (3.91 ml, 41.22 mmol) were mixed together and stirred for 72 hours. During this time a colour change from red to brown was completed but the polymer remained insoluble. After this time the reaction was quenched in water (100 ml) and the resulting mixture stirred for two hours. The polymer was filtered off, washed with acetone and refluxed in methanol for 16 hours. This gave the product as a dark brown powder (0.66 g, 2.01 mmol, 97.6%). BET surface area = 0 m²/g; total pore volume = 0.01 ml g⁻¹ at $p/p^o = 0.98$; TGA (nitrogen): weight loss due to thermal degradation started at 184 °C and totalled 33.6%. ¹H NMR (400 MHz, DMSO) δ ppm 4.26 (2H, br. m, H_a), 4.53 (2H, br. s, H_b), 4.90 (2H, br. s, H_c), 5.11 (3H, br. s, H_d), 7.13 (2H, br. m, H_e), 7.97 (2H, br. s, H_f); ¹³C NMR (100 MHz, solid state) δ ppm 56.4, 67.8, 125.1, 143.1.

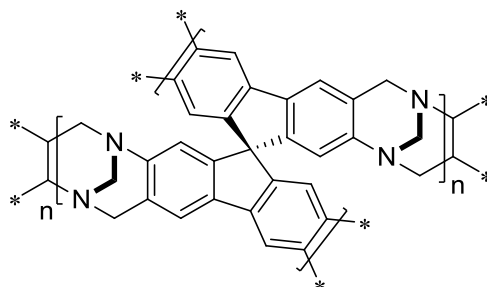
Polymerisation of 1,4-dimethyl-2,5-phenylenediamine (91):



2,5-Dimethyl-1,4-phenylenediamine (1.00 g, 7.34 mmol) was dissolved in trifluoroacetic acid (10 ml) with stirring at 0 °C. Once dissolved, dimethoxymethane (1.95 ml, 22.03 mmol) was added and the reaction left stirring for 48 hours. The reaction was quenched by addition of saturated sodium hydroxide solution (100 ml) and then left stirring for 3 hours. The resulting light brown precipitate was filtered off and washed with acetone. The crude polymer (0.57 g) was refluxed in acetone and methanol, each for 16 hours. The polymer was then reprecipitated from chloroform (50 ml) with hexane (100 ml) three times, each

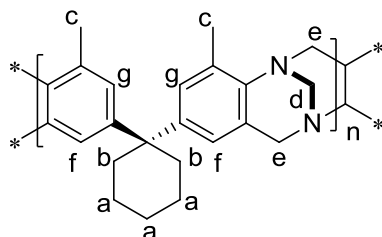
time filtering off the resulting solid. Finally, the material was refluxed in acetone for 16 hours and filtered, giving the polymer as a cream powder (0.44 g, 2.53 mmol based on repeating unit, 34.4%). BET surface area = 430 m²/g; total pore volume = 0.35 ml g⁻¹ at p/p⁰ = 0.98; TGA (nitrogen): weight loss due to thermal degradation started at 304 °C and totalled 37.5%; GPC (based on polystyrene standard) $M_n = 600$, $M_w = 3,300$ gmol⁻¹; ¹H NMR (400 MHz, CDCl₃) δ ppm 2.15 (6H, br. m, H_a), 4.26 (6H, br. m, H_b and H_c); ¹³C NMR (100 MHz, *solid state*) δ ppm 11.74, 54.77, 66.32, 126.49, 142.79.

Polymerisation of 2,2',7,7'-tetraamino-9,9'-spirobisfluorene (92):



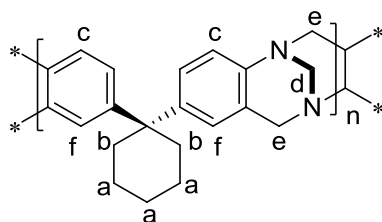
2,2',7,7'-Tetraaminospirobisfluorene (2.00 g, 5.32 mmol) was dissolved in trifluoroacetic acid (20 ml) at 0 °C; this was accompanied almost immediately by a colour change from yellow to dark red. Once dissolved, dimethoxymethane (4.24 ml, 47.87 mmol) was slowly added. The mixture was then left stirring for 24 hours under a nitrogen headspace. After this time, the reaction mixture, now a dark jelly, was quenched by addition of water (100 ml) and aqueous ammonia (35%, 100 ml). This was left stirring overnight before the precipitated solid was broken up with a spatula and collected by filtration. The polymer was refluxed in acetone, THF and methanol, each for 16 hours. BET surface area = 0 m²/g; total pore volume = 0.00 ml g⁻¹ at p/p⁰ = 0.98; TGA (nitrogen): weight loss due to thermal degradation started at 34 °C and totalled 29.0%; ¹³C NMR (100 MHz, *solid state*) δ ppm 29.2, 47.3, 60.2, 66.5, 119.4, 148.2, 162.7. Elemental analysis calc. (%) for repeating unit [C₃₁H₂₀N₄]: C 83.01, H 4.49, N 12.49 (calculated), C 72.80, H 4.71, N 11.72 (found).

Polymerisation of 2,2-bis(3-methyl-4-aminophenyl)cyclohexane (93):



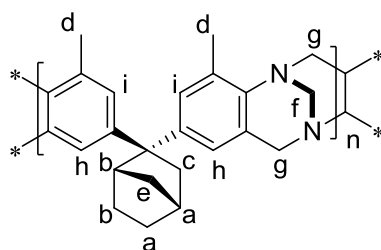
2,2-Bis(3-methyl-4-aminophenyl)cyclohexane (2.00 g, 6.80 mmol) was dissolved in trifluoroacetic acid (20 ml) with stirring at 0 °C. Once dissolved dimethoxymethane (3.00 ml, 34.01 mmol) was added before the mixture was left stirring under nitrogen for 72 hours. The reaction was then quenched by addition of water (100 ml), and after stirring for an hour aqueous ammonia (35%, 100 ml) was added. After stirring for a further hour the mixture was filtered and the precipitated polymer washed with acetone (50 ml). The polymer was then ground up before being refluxed in acetone for 16 hours. It was then dissolved in chloroform (100 ml) and reprecipitated with hexane (150 ml), this was performed two additional times. Finally the polymer was refluxed in methanol for 16 hours, giving the product as a cream powder (1.80 g, 5.96 mmol based on repeating unit, 87.6%). BET surface area = 30 m²/g; total pore volume = 0.09 ml g⁻¹ at p/p⁰ = 0.98; TGA (nitrogen): weight loss due to thermal degradation started at 332 °C and totalled 59.4%, GPC (based on polystyrene standard) $M_n = 44,300$, $M_w = 118,400$ gmol⁻¹; ¹H NMR (400 MHz, CDCl₃) δ ppm 1.43 (6H, br. s, H_a), 2.10 (4H, br. s, H_b), 2.32 (6H, br. s, H_c), 3.90 (2H, br. m, H_d), 4.22 (2H, br. s, H_e), 4.48 (2H, br. m, H_e), 6.63 (2H, br. s, H_f), 6.83 (2H, br. s, H_g); ¹³C NMR (100 MHz, *solid state*) δ ppm 17.4, 23.2, 26.8, 37.6, 44.5, 47.2, 55.5, 67.9, 128.0, 144.0, 136.7. Elemental analysis calc. (%) for repeating unit [C₂₃H₂₆N₂]: C 83.59, H 7.93, N 8.47 (calculated), C 81.21, H 8.07, N 8.10 (found).

Polymerisation of 1,1-bis(3-methyl-4-aminophenyl)cyclohexane (94):



1,1-Bis(4-aminophenyl)cyclohexane (2.00 g, 7.51 mmol) was dissolved in trifluoroacetic acid (20 ml) with stirring at 0 °C. Once dissolved, dimethoxymethane (3.32 ml, 37.57 mmol) was added before the mixture was left stirring under nitrogen for 40 hours. The reaction was then quenched by addition of water (100 ml) and aqueous ammonia (35%, 100 ml). After stirring for 4 hours the mixture was filtered and the precipitated polymer washed with water (100 ml) and acetone (100 ml). The polymer was then ground up before being refluxed in acetone, THF, chloroform and methanol (100 ml), each for 16 hours. After drying under vacuum the product appeared as a cream coloured powder (2.07 g, 6.85 mmol, 91.2%, based on repeating unit). BET surface area = 50 m²/g; total pore volume = 0.21 ml g⁻¹ at $p/p^o = 0.98$; GPC (based on polystyrene standard, using a small soluble portion) $M_n = 5,800$, $M_w = 35,300$ gmol⁻¹; ¹³C NMR (100 MHz, *solid state*) δ ppm 23.8, 36.8, 44.0, 47.4, 58.9, 66.9, 127.5, 141.0, 146.9.

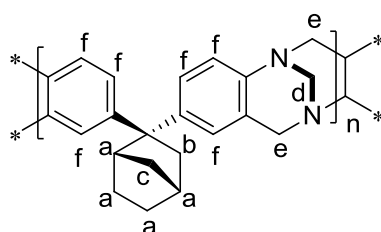
Polymerisation of 2,2-bis(3-methyl-4-aminophenyl)bicyclo[2.2.1]heptane (95):



2,2-Bis(3-methyl-4-aminophenyl)bicyclo[2.2.1]heptane (3.00 g, 9.80 mmol) was dissolved in trifluoroacetic acid (30 ml) with stirring at 0 °C. Once dissolved dimethoxymethane (4.33 ml, 49.02 mmol) was added before the mixture was left stirring under nitrogen for 72 hours. The reaction was then quenched by addition of water (150 ml), and after stirring for an hour aqueous ammonia (35%, 150 ml) was added. After brief stirring the mixture was filtered and the precipitated polymer washed with acetone (100 ml). The polymer was ground up and refluxed in acetone for 16 hours. It was then dissolved in chloroform (150 ml) and reprecipitated with hexane (200 ml); this was performed two additional times. Finally the polymer was refluxed in methanol for 16 hours. This gave the polymer as a cream powder (1.94 g, 5.67 mmol based on repeating unit, 57.9%). BET surface area = 70 m²/g; total pore volume = 0.37 ml g⁻¹ at $p/p^o = 0.98$; TGA (nitrogen): weight loss due to thermal degradation started at 350 °C and totalled 58.5%, GPC (based on polystyrene

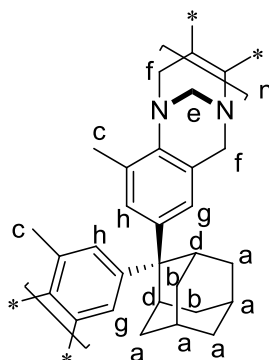
standard) $M_n = 13,900, M_w = 31,600 \text{ gmol}^{-1}$; $^1\text{H NMR}$ (400 MHz, CDCl_3) δ ppm 1.15 (3H, br. m, H_a), 1.44 (3H, br. m, H_b), 2.08 (3H, br. m, $\text{H}_c + \text{H}_e$), 2.31 (6H, br. s, H_d), 3.03 (1H, br. s, H_e), 3.88 (2H, br. s, H_f), 4.17 (2H, br. s, H_g), 4.47 (2H, br. m, H_g), 6.69 (2H, br. m, H_h), 6.91 (2H, br. m, H_i); $^{13}\text{C NMR}$ (100 MHz, *solid state*) δ ppm 17.2, 25.0, 39.0, 43.6, 55.6, 67.6, 126.8, 143.6, 148.3. Elemental analysis calc. (%) for repeating unit $[\text{C}_{24}\text{H}_{26}\text{N}_2]$: C 84.17, H 7.65, N 8.18 (calculated), C 79.99, H 7.32, N 7.79 (found).

Polymerisation of 2,2-bis(4-aminophenyl)bicyclo[2.2.1]heptane (96):



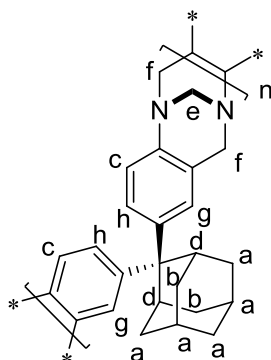
2,2-Bis(4-aminophenyl)bicyclo[2.2.1]heptane (2.00 g, 7.19 mmol) was dissolved in trifluoroacetic acid (20 ml) with stirring at 0 °C. Once dissolved, dimethoxymethane (3.18 ml, 35.97 mmol) was added before the mixture was left stirring under nitrogen for 40 hours, eventually becoming too viscous to stir. The reaction was quenched by addition of water (100 ml) and aqueous ammonia (35%, 100 ml). After stirring for 16 hours the mixture was filtered and the precipitated polymer washed with water (100 ml) and acetone (100 ml). After drying under vacuum, the polymer was ground up and refluxed in acetone (100 ml) for 16 hours. The polymer was then dissolved in chloroform (100 ml) and reprecipitated using hexane (150 ml), this was performed two additional times. Finally, the polymer was refluxed in acetone and methanol (100 ml), each for 16 hours. After drying under vacuum the product appeared as a brown powder (1.30 g, 4.14 mmol, 57.6%, based on repeating unit). BET surface area = $4 \text{ m}^2 \text{ g}^{-1}$; total pore volume = 0.03 ml g^{-1} at $p/p^o = 0.98$; GPC (based on polystyrene standard) $M_n = 1,700 M_w = 4,500 \text{ gmol}^{-1}$; $^1\text{H NMR}$ (400 MHz, CDCl_3) δ ppm 1.30 (6H, br. m, H_a), 2.16 (3H, br. m, H_b, H_c), 2.99 (1H, br. s, H_e), 4.11 (4H, br. m, H_d, H_e), 4.57 (2H, br. s, H_e), 6.87 (6H, br. m, H_f); $^{13}\text{C NMR}$ (100 MHz, *solid state*) δ ppm 26.2, 39.1, 42.2, 45.9, 55.7, 56.7, 67.3, 127.3, 145.9.

Polymerisation of 2,2-bis(3-methyl-4-aminophenyl)adamantane (97):



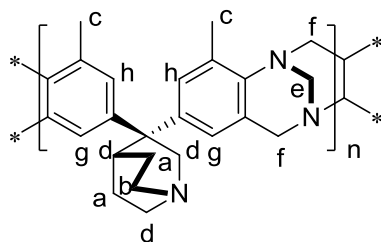
2,2-Bis(3-methyl-4-aminophenyl)adamantane (5.00 g, 14.43 mmol) was dissolved in trifluoroacetic acid (50 ml) with stirring at 0 °C. Once dissolved, dimethoxymethane (6.38 ml, 72.14 mmol) was added before the mixture was left stirring under nitrogen for 72 hours. The reaction was then quenched by addition of water (200 ml), and after stirring for an hour aqueous ammonia (35%, 200 ml) was added. After brief stirring the mixture was filtered and the precipitated polymer washed with acetone (100 ml). The polymer was ground up and refluxed in acetone for 16 hours. It was then dissolved in chloroform (250 ml) and reprecipitated with hexane (300 ml), this was performed two additional times. Finally, the polymer was refluxed in methanol for 16 hours, giving the polymer as a cream powder (3.19 g, 8.36 mmol based on repeating unit, 57.9%). BET surface area = 615 m² g⁻¹; total pore volume = 0.41 ml g⁻¹ at $p/p^o = 0.98$; TGA (nitrogen): weight loss due to thermal degradation started at 470 °C but violently degraded so no measurement could be taken, GPC (based on polystyrene standard) $M_n = 31,500$, $M_w = 113,000$ gmol⁻¹; ¹H NMR (400 MHz, CDCl₃) δ ppm 1.67 (8H, br. m, H_a), 1.91 (4H, br. s, H_b), 2.29 (6H, br. s, H_c), 3.03 (2H, br. s, H_d), 3.88 (2H, br. m, H_e), 4.13 (2H, br. m, H_f), 4.46 (2H, br. s, H_f), 6.74 (2H, br. s, H_g), 7.00 (2H, br. s, H_h); ¹³C NMR (100 MHz, *solid state*) δ ppm 16.7, 28.5, 33.9, 38.5, 50.0, 55.7, 67.9, 121.7, 127.6, 132.3, 143.7. Elemental analysis calc. (%) for repeating unit [C₂₇H₃₀N₂]: C 84.77, H 7.90, N 7.32 (calculated), C 80.26, H 7.90, N 6.98 (found).

Polymerisation of 2,2-bis(3-methyl-4-aminophenyl)adamantane (98):



2,2-Bis(4-aminophenyl)adamantane (2.00 g, 6.06 mmol) was dissolved in trifluoroacetic acid (20 ml) with stirring at 0 °C. Once dissolved, dimethoxymethane (2.68 ml, 30.30 mmol) was added before the mixture was left stirring under nitrogen for 16 hours. The reaction was then quenched by addition of water (100 ml) and aqueous ammonia (35%, 100 ml). After stirring for 6 hours the mixture was filtered and the precipitated polymer washed with water (100 ml) and acetone (100 ml). The polymer was then ground up before being refluxed in acetone, chloroform, THF and methanol (100 ml), each for 16 hours. This gave the polymer as a cream powder (1.94 g, 5.30 mmol based on repeating unit, 87.5%). BET surface area = 50 m²/g; total pore volume = 0.25 ml g⁻¹ at $p/p^o = 0.98$; GPC (based on polystyrene standard, small soluble portion) $M_n = 4,200$, $M_w = 14,800$ gmol⁻¹; ¹³C NMR (100 MHz, *solid state*) δ ppm 28.5, 33.7, 45.0, 50.4, 60.6, 68.4, 124.8, 127.7, 144.7, 145.7.

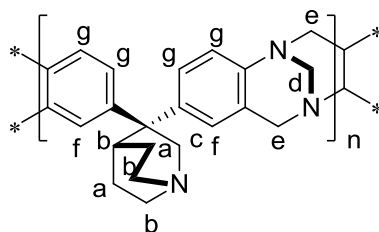
Attempted polymerisation of 3,3-bis(3-methyl-4-aminophenyl)-1-azabicyclo[2,2,2]octane (99):



3,3-Bis(3-methyl-4-aminophenyl)-1-azabicyclo[2,2,2]octane (2.00 g, 6.23 mmol) was dissolved in trifluoroacetic acid (20 ml) with stirring at 0 °C. Dimethoxymethane (2.76 ml,

31.15 mmol) was then added and the reaction mixture stirred for 120 hours under a nitrogen atmosphere. The reaction was quenched by addition of water (100 ml) and aqueous ammonia (35%, 100 ml). This mixture was stirred for two hours before the precipitated polymer was collected by filtration, washed with water (100 ml) and washed with acetone (100 ml) before being dried under vacuum. The polymer was dissolved in chloroform (100 ml) and reprecipitated by addition of hexane (150 ml). This was performed two additional times, before the polymer was refluxed in acetone and methanol (100 ml), each for 16 hours. After drying under vacuum the product was obtained as a light brown powder (1.68 g, 5.14 mmol, 82.5%). BET surface area = 55 m²/g; total pore volume = 0.21 ml g⁻¹ at p/p⁰ = 0.98; TGA (nitrogen): weight loss due to thermal degradation started at 349 °C and totalled 58.0%; GPC (based on polystyrene standard) M_n = 890, M_w = 910 g mol⁻¹; ¹H NMR (400 MHz, CDCl₃) δ ppm 1.79 (4H, br. s, H_a), 2.05 (2H, br. s, H_b), 2.30 (6H, br. s, H_c), 2.71 (5H, br. s, H_d), 3.85 (2H, br. s, H_e), 4.15 (2H, br. s, H_f), 4.45 (2H, br. s, H_f), 6.65 (2H, br. s, H_g), 6.90 (2H, br. s, H_h); ¹³C NMR (100 MHz, *solid state*) δ ppm 16.6, 24.8, 28.8, 44.9, 55.7, 67.3, 127.4, 144.3.

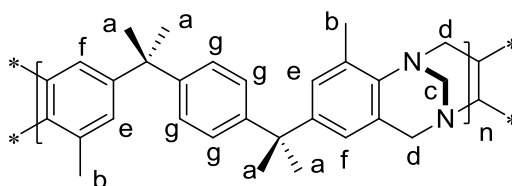
Attempted polymerisation of 3,3-bis(4-aminophenyl)-1-azabicyclo[2,2,2]octane (100):



3,3-Bis(4-aminophenyl)-1-azabicyclo[2,2,2]octane (2.00 g, 6.83 mmol) was dissolved in trifluoroacetic acid (20 ml) with stirring at 0 °C. Dimethoxymethane (3.02 ml, 34.13 mmol) was then added and the reaction mixture stirred for 120 hours under a nitrogen atmosphere. The reaction was then quenched by addition of water (100 ml) and aqueous ammonia (35%, 100 ml). This was stirred for 2 hours before the precipitated polymer was collected by filtration, washed with water (100 ml) and washed with acetone (100 ml) before being dried under vacuum. The polymer was dissolved in chloroform (100 ml) and reprecipitated by addition of hexane (150 ml). This was performed two additional times, before the polymer was refluxed in acetone and methanol (100 ml), each for 16 hours.

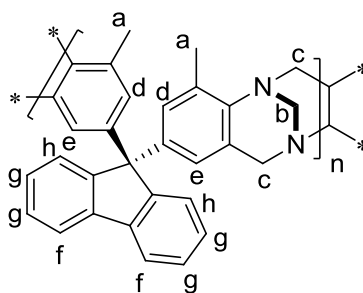
After drying under vacuum the product was obtained as a cream coloured powder (1.82 g, 5.53 mmol, 81.0%). BET surface area = 10 m²/g; total pore volume = 0.05 ml g⁻¹ at $p/p^0 = 0.98$; TGA (nitrogen): weight loss due to thermal degradation started at 368 °C and totalled 59.0%; GPC (based on polystyrene standard) $M_n = 900$, $M_w = 930$ gmol⁻¹; ¹H NMR (400 MHz, CDCl₃) δ ppm 1.47 (4H, br. s, H_a), 2.68 (5H, br. s, H_b), 4.04 (2H, br. m, H_c), 4.15 (2H, br. s, H_d), 4.55 (2H, br. s, H_e), 4.77 (2H, br. s, H_e), 6.79 (2H, br. m, H_f), 6.97 (4H, br. s, H_g); ¹³C NMR (100 MHz, *solid state*) δ ppm 23.8, 45.3, 58.2, 66.2, 127.3, 145.9.

Polymerisation of 1,1',4,4'-tetramethyl-1,4-(3-methyl-4-aminophenyl)benzene (101):



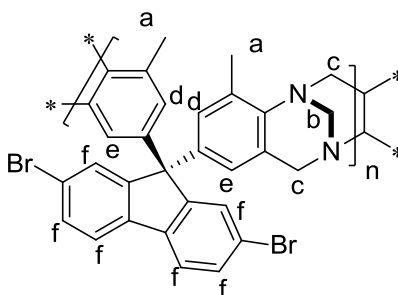
1,1',4,4'-Tetramethyl-1,4-(3-methyl-4-aminophenyl)benzene (3.00 g, 8.06 mmol) was dissolved in trifluoroacetic acid (30 ml) with stirring at 0 °C. Once dissolved, dimethoxymethane (3.57 ml, 40.32 mmol) was slowly added before the mixture was left stirring for 72 hours. The reaction was then quenched by addition of water (100 ml) and aqueous ammonia (35%, 100 ml). This was stirred for an hour before the precipitated polymer was collected by filtration, and then washed with water (100 ml) and acetone (100 ml). The polymer was dried under vacuum before being dissolved in chloroform (200 ml) and reprecipitated with hexane (250 ml); this was performed three additional times. Finally the polymer was refluxed in acetone and methanol (100 ml), each for 16 hours. This gave the polymer as a white powder (1.98 g, 4.85 mmol, 60.2%, based on repeating unit). BET surface area = 6 m²/g; total pore volume = 0.02 ml g⁻¹ at $p/p^0 = 0.98$; GPC (based on polystyrene standard) $M_n = 51,900$, $M_w = 99,600$ gmol⁻¹; ¹H NMR (400 MHz, CDCl₃) δ ppm 1.59 (12H, br. s, H_a), 2.33 (6H, br. s, H_b), 3.93 (2H, br. m, H_c), 4.27 (2H, br. s, H_d), 4.52 (2H, br. m, H_d), 6.66 (2H, br. s, H_e), 6.85 (2H, br. s, H_f), 7.10 (4H, br. s, H_g); ¹³C NMR (100 MHz, *solid state*) δ ppm 17.0, 30.9, 42.1, 55.5, 68.2, 127.1, 144.7. Elemental analysis calc. (%) for repeating unit [C₂₉H₃₂N₂]: C 85.25 H 7.89, N 6.85 (calculated), C 82.51, H 8.05, N 6.68 (found).

Polymerisation of 9,9'(3-methyl-4-aminophenyl)-fluorene (102):



9,9'(3-Methyl-4-aminophenyl)-fluorene (3.50 g, 9.31 mmol) was dissolved in trifluoroacetic acid (35 ml) with stirring at 0 °C. Once dissolved, dimethoxymethane (4.12 ml, 46.54 mmol) was added before the reaction mixture was left stirring for 96 hours under a nitrogen atmosphere. The reaction was quenched by addition of water (100 ml) and aqueous ammonia (35%, 100 ml). After stirring for 2 hours the precipitated solid was collected by filtration, and then washed with water (100 ml) and acetone (100 ml). The polymer was dried under vacuum before being dissolved in chloroform (200 ml) and reprecipitated with hexane (250 ml), this was performed two additional times. Finally, the polymer was refluxed in acetone and methanol (100 ml), each for 16 hours. This gave the polymer as a white powder (2.90 g, 7.04 mmol, 75.6%, based on repeating unit). BET surface area = 400 m² g⁻¹; total pore volume = 0.47 ml g⁻¹ at $p/p^o = 0.98$; TGA (nitrogen): weight loss due to thermal degradation started at 393 °C and totalled 52.0%; GPC (based on polystyrene standard) $M_n = 13,800$, $M_w = 33,600$ gmol⁻¹; ¹H NMR (400 MHz, CDCl₃) δ ppm 2.17 (6H, s, H_a), 3.70 (2H, br. s, H_b), 4.15 (2H, br. s, H_c), 4.34 (2H, br. s, H_c), 6.38 (2H, s, H_d), 6.85 (2H, s, H_e), 7.22 (2H, br. m, H_f), 7.32 (4H, m, H_g), 7.71 (2H, d, J = 7.2 Hz, H_h); ¹³C NMR (100 MHz, *solid state*) δ ppm 16.8, 55.6, 64.8, 119.9, 127.3, 140.5, 144.7, 152.5. Elemental analysis calc. (%) for repeating unit [C₃₀H₂₄N₂]: C 87.38, H 5.83, N 6.80 (calculated), C 84.63, H 5.70, N 6.38 (found).

Polymerisation of 2,7-dibromo-9,9'(3-methyl-4-aminophenyl)-fluorene (103):



2,7-Dibromo-9,9'(3-methyl-4-aminophenyl)-fluorene (3.00 g, 5.62 mmol) was dissolved in trifluoroacetic acid (30 ml) with stirring at 0 °C. Once dissolved, dimethoxymethane (2.49 ml, 28.10 mmol) was added before the mixture was left stirring for 72 hours under a nitrogen atmosphere. At this stage the product had crashed out of solution, so the reaction was quenched by addition of water (100 ml) and aqueous ammonia (35%, 100 ml). After stirring for a few hours the mixture was filtered before the precipitated polymer was washed with water (200 ml) and acetone (100 ml). The polymer was dissolved in chloroform (150 ml) and reprecipitated with hexane (200 ml), this was performed two additional times. The polymer was then refluxed in acetone and methanol (100 ml), each for 16 hours. After drying the polymer under vacuum the product appeared as a cream coloured powder (2.40 g, 4.21 mmol, 74.9%, based on repeat unit). BET surface area = 390 m²/g; total pore volume = 0.44 ml g⁻¹ at $p/p^o = 0.98$; TGA (nitrogen): weight loss due to thermal degradation started at 376 °C and totalled 41.0%; GPC (based on polystyrene standard) $M_n = 20,400$, $M_w = 43,300$ gmol⁻¹; ¹H NMR (400 MHz, CDCl₃) δ ppm 2.21 (6H, br. s, H_a), 3.76 (2H, br. s, H_b), 4.17 (2H, br. s, H_c), 4.38 (2H, br. s, H_c), 6.35 (2H, br. s, H_d), 6.82 (2H, br. s, H_e), 7.46 (6H, m, H_f); ¹³C NMR (100 MHz, *solid state*) δ ppm 16.8, 55.7, 65.3, 121.6, 129.6, 138.5, 145.1, 154.1. Elemental analysis calc. (%) for repeating unit [C₃₀H₂₂N₂Br₂]: C 63.16, H 3.86, N 4.91, Br 28.07 (calculated), C 61.85, H 3.72, N 4.56, Br 25.14 (found).

Bibliography

- (1) <http://oxforddictionaries.com/definition/english/pore?q=pore>
- (2) Rouquerol, J.; Avnir, D.; Fairbridge, C. W.; Everett, D. H.; Haynes, J. H.; Pernicone, N.; Ramsay, J. D. F.; Sing, K. S. W.; Unger, K. K.; *Pure and Applied Chemistry*, **1994**, 66, 1739.
- (3) Burwell, R. L.; *Pure and Applied Chemistry*, **1976**, 46, 71.
- (4) Oterhals, Å.; Solvang, M.; Nortvedt, R.; Berntssen, M. H. G. *European Journal of Lipid Science and Technology*, **2007**, 109, 691.
- (5) Sawaki, T.; Dewa, T.; Aoyama, Y.; *Journal of the American Chemical Society*, **1998**, 120, 8539.
- (6) Wang, D. *Separation and Purification Technology*, **2004**, 35, 125.
- (7) Murray, L. J.; Dinca, M.; Long, J. R. *Chemical Society reviews*, **2009**, 38, 1294.
- (8) Dawson, R.; Stöckel, E.; Holst, J. R.; Adams, D. J.; Cooper, A. I. *Energy & Environmental Science*, **2011**, 4, 4239.
- (9) Langmuir, I.; *Journal of the American Chemical Society*, **1916**, 38, 2221.
- (10) Brunauer, S.; Emmett, P. H.; Teller, E.; *Journal of the American Chemical Society*, **1938**, 60, 309.
- (11) Barton, T. J.; Bull, L. M.; Klemperer, W. G.; Loy, D. A.; McEnaney, B.; Misono, M.; Monson, P. A.; Pez, G.; Scherer, G. W.; Vartuli, J. C.; Yaghi, O. M.; *Chemistry of Materials*, **1999**, 11, 2633.
- (12) Farha, O. K.; Eryazici, I.; Jeong, N. C.; Hauser, B. G.; Wilmer, C. E.; Sarjeant, A. A.; Snurr, R. Q.; Nguyen, S. T.; Yazaydin, A. O.; Hupp, J. T. *Journal of the American Chemical Society*, **2012**, 134, 15016.
- (13) Furukawa, H.; Ko, N.; Go, Y. B.; Aratani, N.; Choi, S. B.; Choi, E.; Yazaydin, A. O.; Snurr, R. Q.; O'Keeffe, M.; Kim, J.; Yaghi, O. M. *Science*, **2010**, 329, 424.
- (14) Meek, S. T.; Greathouse, J. A.; Allendorf, M. D. *Advanced Materials*, **2011**, 23, 249.
- (15) Tanabe, K. K.; Cohen, S. M. *Chemical Society Reviews*, **2011**, 40, 498.
- (16) Lee, J.; Farha, O. K.; Roberts, J.; Scheidt, K. A.; Nguyen, S. T.; Hupp, J. T. *Chemical Society Reviews*, **2009**, 38, 1450.
- (17) Horcajada, P.; Serre, C.; Vallet-Regi, M.; Sebban, M.; Taulelle, F.; Ferey, G. *Angewandte Chemie International Edition English*, **2006**, 45, 5974.
- (18) Li, J. R.; Kuppler, R. J.; Zhou, H. C. *Chemical Society Reviews*, **2009**, 38, 1477.
- (19) Harbuzaru, B. V.; Corma, A.; Rey, F.; Atienzar, P.; Jorda, J. L.; Garcia, H.; Ananias, D.; Carlos, L. D.; Rocha, J. *Angewandte Chemie International Edition English*, **2008**, 47, 1080.
- (20) Liu, B.; Pang, L.-Y.; Hou, L.; Wang, Y.-Y.; Zhang, Y.; Shi, Q.-Z. *CrystEngComm*, **2012**, 14, 6246.
- (21) Sumida, K.; Rogow, D. L.; Mason, J. A.; McDonald, T. M.; Bloch, E. D.; Herm, Z. R.; Bae, T. H.; Long, J. R. *Chemical Reviews*, **2012**, 112, 724.
- (22) Shah, M.; McCarthy, M. C.; Sachdeva, S.; Lee, A. K.; Jeong, H.-K. *Industrial & Engineering Chemistry Research*, **2012**, 51, 2179.
- (23) Mastalerz, M. *Angewandte Chemie International Edition English*, **2008**, 47, 445.
- (24) Wang, L.; Wang, L.; Zhao, J.; Yan, T. *Journal of Applied Physics*, **2012**, 111, 112628.
- (25) Koo, B. T.; Dichtel, W. R.; Clancy, P. *Journal of Materials Chemistry*, **2012**, 22, 17460.

- (26) Ding, S. Y.; Gao, J.; Wang, Q.; Zhang, Y.; Song, W. G.; Su, C. Y.; Wang, W. *Journal of the American Chemical Society*, **2011**, *133*, 19816.
- (27) Tilford, R. W.; Mugavero, S. J.; Pellechia, P. J.; Lavigne, J. J. *Advanced Materials*, **2008**, *20*, 2741.
- (28) Han, S. S.; Furukawa, H.; Yaghi, O. M.; Goddard, W. A. *Journal of the American Chemical Society*, **2008**, *130*, 11580.
- (29) Wan, S.; Guo, J.; Kim, J.; Ihee, H.; Jiang, D. *Angewandte Chemie International Edition English*, **2008**, *47*, 8826.
- (30) Lan, J.; Cao, D.; Wang, W.; Smit, B. *ACS Nano*, **2010**, *4*, 4225.
- (31) Furukawa, H.; Yaghi, O. M. *Journal of the American Chemical Society*, **2009**, *131*, 8875.
- (32) Masters, A. F.; Maschmeyer, T. *Microporous and Mesoporous Materials*, **2011**, *142*, 423.
- (33) Quintelas, C.; Rocha, Z.; Silva, B.; Fonseca, B.; Figueiredo, H.; Tavares, T. *Chemical Engineering Journal*, **2009**, *152*, 110.
- (34) Velu, S.; Ma, X.; Song, C. *Industrial and Engineering Chemical Research*, **2003**, *42*, 5293.
- (35) Qiu, W.; Zheng, Y. *Journal of Hazardous Materials*, **2007**, *148*, 721.
- (36) Corma, A.; Diaz-Cabanás, M. J.; Martínez-Triguero, J.; Rey, F.; Rius, J., *Nature*, **2002**, *418*, 514.
- (37) Van Der Waal, J. C.; Van Bekkum, H., *Journal of Porous Materials*, **1998**, *5*, 289.
- (38) Zheng, Y.; Li, X.; Dutta, P. K. *Sensors (Basel)*, **2012**, *12*, 5170.
- (39) Hyun, S. H.; Song, J. K.; Kwak, B. I.; Kim, J. H.; Hong, S. A., *Journal of Materials Science*, **1999**, *34*, 3095.
- (40) Zecchina, A.; Bordiga, S.; Vitillo, J. G.; Ricchiardi, G.; Lamberti, C.; Spoto, G.; Bjorgen, M.; Lillerud, K. P., *Journal of the American Chemical Society*, **2005**, *127*, 6361.
- (41) Grancaric, A.; Tarbuk, A.; Kovacek, I. *Chemical Industry and Chemical Engineering Quarterly*, **2009**, *15*, 203.
- (42) Chatti, R.; Bansiwal, A. K.; Thote, J. A.; Kumar, V.; Jadhav, P.; Lokhande, S. K.; Biniwale, R. B.; Labhsetwar, N. K.; Rayalu, S. S. *Microporous and Mesoporous Materials*, **2009**, *121*, 84.
- (43) Ströbel, R.; Garche, J.; Moseley, P. T.; Jörissen, L.; Wolf, G. *Journal of Power Sources*, **2006**, *159*, 781.
- (44) Sawa, E. *Fullerene Science and Technology*, **1999**, *7*, 637.
- (45) Areerachakul, N.; Vigneswaran, S.; Ngo, H. H.; Kandasamy, J. *Separation and Purification Technology*, **2007**, *55*, 206.
- (46) López, F.; Medina, F.; Prodanov, M.; Güell, C. *Journal of Colloid and Interface Science*, **2003**, *257*, 173.
- (47) Eddleston, M.; Juszczak, E.; Buckley, N. A.; Senarathna, L.; Mohammed, F.; Allen, S.; Dissanayake, W.; Hittarage, A.; Azher, S.; Jeganathan, K.; Jayamanne, S.; Sheriff, M. H.; Warrell, D. A. *BMC Emergency Medicine*, **2007**, *7*, 2.
- (48) van den Berg, A. W. C.; Areán, C. O. *Chemical Communications*, **2008**, 668.
- (49) Zhao, Y.; Zhao, L.; Yao, K. X.; Yang, Y.; Zhang, Q.; Han, Y. *Journal of Materials Chemistry*, **2012**, *22*, 19726.
- (50) Sobiesiak, M.; Gawdzik, B.; Puziy, A. M.; Poddubnaya, O. I. *Applied Surface Science*, **2010**, *256*, 5355.
- (51) Himeno, S.; Komatsu, T.; Fujita, S., *Journal of Chemical Engineering Data*, **2005**, *50*, 369.
- (52) Sevilla, M.; Fuertes, A. B. *Energy & Environmental Science*, **2011**, *4*, 1765.

- (53) Dawson, R.; Cooper, A. I.; Adams, D. J. *Progress in Polymer Science*, **2012**, *37*, 530.
- (54) Tsyurupa, M. P.; Davankov, V. A., *Reactive & Functional Polymers*, **2002**, *53*, 193.
- (55) Ahn, J.-H.; Jang, J.-E.; Oh, C.-G.; Ihm, S.-K.; Cortez, J.; Sherrington, D. C., *Macromolecules*, **2006**, *39*, 627.
- (56) Wood, C. D.; Tan, B.; Trewin, A.; Niu, H.; Bradshaw, D.; Rosseinsky, M. J.; Khimiyak, Y. Z.; Campbell, N. L.; Kirk, R.; Stockel, E.; Cooper, A. I., *Chemical Materials*, **2007**, *19*, 2034.
- (57) Rose, M.; Bohlmann, W.; Sabo, M.; Kaskel, S. *Chemical Communications (Cambridge)*, **2008**, 2462.
- (58) Fritsch, J.; Rose, M.; Wollmann, P.; Böhlmann, W.; Kaskel, S. *Materials*, **2010**, *3*, 2447.
- (59) Pan, B. C.; Xiong, Y.; Li, A. M.; Chen, J. L.; Zhang, Q. X.; Jin, X. Y.; *Reactive & Functional Polymers*, **2002**, *53*, 63.
- (60) Chang, C. F.; Chang, C. Y.; Hsu, K. E.; Lee, S. C.; Holl, W. *Journal of Hazardous Materials*, **2008**, *155*, 295.
- (61) Li, B.; Su, F.; Luo, H.-K.; Liang, L.; Tan, B. *Microporous and Mesoporous Materials*, **2011**, *138*, 207.
- (62) Beth, M.; Unger, K. K.; Tsyurupa, M. P.; Davankov, V. A., *Chromatographia*, **1993**, *36*, 351.
- (63) Lee, J.-Y.; Wood, C. D.; Bradshaw, D.; Rosseinsky, M. J.; Cooper, A. I., *Chemical Communications*, **2006**, 2670.
- (64) Luo, Y.; Li, B.; Wang, W.; Wu, K.; Tan, B. *Advanced Materials*, **2012**.
- (65) Hittinger, E.; Kokil, A.; Weder, C. *Angewandte Chemie*, **2004**, *116*, 1844.
- (66) Jiang, J. X.; Su, F.; Trewin, A.; Wood, C. D.; Campbell, N. L.; Niu, H.; Dickinson, C.; Ganin, A. Y.; Rosseinsky, M. J.; Khimiyak, Y. Z.; Cooper, A. I. *Angewandte Chemie International Edition English*, **2007**, *46*, 8574.
- (67) Weder, C. *Angewandte Chemie International Edition English*, **2008**, *47*, 448.
- (68) Xie, Z.; Wang, C.; deKrafft, K. E.; Lin, W. *Journal of the American Chemical Society*, **2011**, *133*, 2056.
- (69) Li, A.; Lu, R. F.; Wang, Y.; Wang, X.; Han, K. L.; Deng, W. Q. *Angewandte Chemie International Edition English*, **2010**, *49*, 3330.
- (70) Chen, L.; Honsho, Y.; Seki, S.; Jiang, D., *Journal of the American Chemical Society*, **2010**, *132*, 6742.
- (71) Liu, Y.-R.; He, L.; Zhang, J.; Wang, X.; Su, C.Y., *Chemical Materials*, **2009**, *21*, 557.
- (72) Kou, Y.; Xu, Y.; Guo, Z.; Jiang, D. *Angewandte Chemie International Edition English*, **2011**, *50*, 8753.
- (73) Ren, S.; Dawson, R.; Laybourn, A.; Jiang, J.-x.; Khimiyak, Y.; Adams, D. J.; Cooper, A. I. *Polymer Chemistry*, **2012**, *3*, 928.
- (74) Trewin, A.; Cooper, A. I. *Angewandte Chemie International Edition English*, **2010**, *49*, 1533.
- (75) Ben, T.; Ren, H.; Ma, S.; Cao, D.; Lan, J.; Jing, X.; Wang, W.; Xu, J.; Deng, F.; Simmons, J. M.; Qiu, S.; Zhu, G. *Angewandte Chemie International Edition English*, **2009**, *48*, 9457.
- (76) Konstas, K.; Taylor, J. W.; Thornton, A. W.; Doherty, C. M.; Lim, W. X.; Bastow, T. J.; Kennedy, D. F.; Wood, C. D.; Cox, B. J.; Hill, J. M.; Hill, A. J.; Hill, M. R. *Angewandte Chemie International Edition English*, **2012**, *51*, 6639.

- (77) Ben, T.; Pei, C.; Zhang, D.; Xu, J.; Deng, F.; Jing, X.; Qiu, S. *Energy & Environmental Science*, **2011**, *4*, 3991.
- (78) McKeown, N. B.; Budd, P. M.; Msayib, K. J.; Ghanem, B. S.; Kingston, H. J.; Tattershall, C. E.; Makhseed, S.; Reynolds, K. J.; Fritsch, D. *Chemistry*, **2005**, *11*, 2610.
- (79) Ghanem, B. S.; Hashem, M.; Harris, K. D. M.; Msayib, K. J.; Xu, M.; Budd, P. M.; Chaukura, N.; Book, D.; Tedds, S.; Walton, A.; McKeown, N. B. *Macromolecules*, **2010**, *43*, 5287.
- (80) McKeown, N. B.; Budd, P. M. *Chemical Society reviews*, **2006**, *35*, 675.
- (81) McKeown, N. B.; Budd, P. M. *Macromolecules*, **2010**, *43*, 5163.
- (82) Budd, P. M.; Ghanem, B.; Msayib, K.; McKeown, N. B.; Tattershall, C. *Journal of Materials Chemistry*, **2003**, *13*, 2721.
- (83) McKeown, N. B.; Hanif, S.; Msayib, K.; Tattershall, C. E.; Budd, P. M. *Chemical Communications*, **2002**, 2782.
- (84) McKeown, N. B.; Budd, P. M.; Book, D. *Macromolecular Rapid Communications*, **2007**, *28*, 995.
- (85) Wang, Y.; McKeown, N. B.; Msayib, K. J.; Turnbull, G. A.; Samuel, I. D. *Sensors (Basel)*, **2011**, *11*, 2478.
- (86) Budd, P. M.; Ghanem, B. S.; Makhseed, S.; McKeown, N. B.; Msayib, K. J.; Tattershall, C. E. *Chemical Communications (Cambridge)*, **2004**, 230.
- (87) McKeown, N. B. *Journal of Materials Chemistry*, **2000**, *10*, 1979.
- (88) McKeown, N. B.; Makhseed, S.; Budd, P. M. *Chemical Communications*, **2002**, 2780.
- (89) Hashem, M.; Grazia Bezzu, C.; Kariuki, B. M.; McKeown, N. B. *Polymer Chemistry*, **2011**, *2*, 2190.
- (90) Ghanem, B. S.; Msayib, K. J.; McKeown, N. B.; Harris, K. D.; Pan, Z.; Budd, P. M.; Butler, A.; Selbie, J.; Book, D.; Walton, A. *Chemical Communications (Cambridge)*, **2007**, 67.
- (91) Budd, P. M.; Elabas, E. S.; Ghanem, B. S.; Makhseed, S.; McKeown, N. B.; Msayib, K. J.; Tattershall, C. E.; Wang, D., *Advanced Materials*, **2004**, *16*, 456.
- (92) Budd, P.; McKeown, N.; Ghanem, B.; Msayib, K.; Fritsch, D.; Starannikova, L.; Belov, N.; Sanfirova, O.; Yampolskii, Y.; Shantarovich, V. *Journal of Membrane Science*, **2008**, *325*, 851.
- (93) Yong, W. F.; Li, F. Y.; Xiao, Y. C.; Li, P.; Pramoda, K. P.; Tong, Y. W.; Chung, T. S. *Journal of Membrane Science*, **2012**, *407-408*, 47.
- (94) Mason, C. R.; Maynard-Atem, L.; Al-Harbi, N. M.; Budd, P. M.; Bernardo, P.; Bazzarelli, F.; Clarizia, G.; Jansen, J. C. *Macromolecules*, **2011**, *44*, 6471.
- (95) Liaw, D.-J.; Wang, K.-L.; Huang, Y.-C.; Lee, K.-R.; Lai, J.-Y.; Ha, C.-S. *Progress in Polymer Science*, **2012**, *37*, 907.
- (96) Ghanem, B. S.; McKeown, N. B.; Budd, P. M.; Al-Harbi, N. M.; Fritsch, D.; Heinrich, K.; Starannikova, L.; Tokarev, A.; Yampolskii, Y. *Macromolecules*, **2009**, *42*, 7881.
- (97) Ma, X.; Swaidan, R.; Belmabkhout, Y.; Zhu, Y.; Litwiller, E.; Jouiad, M.; Pinnau, I.; Han, Y. *Macromolecules*, **2012**, *45*, 3841.
- (98) Robeson, L. M. *Journal of Membrane Science*, **1991**, *62*, 165.
- (99) Robeson, L. M. *Journal of Membrane Science*, **2008**, *320*, 390.
- (100) Seinfeld, J. H. *AIChE Journal*, **2011**, *57*, 3259.
- (101) Lee, Z. H.; Lee, K. T.; Bhatia, S.; Mohamed, A. R. *Renewable and Sustainable Energy Reviews*, **2012**, *16*, 2599.

- (102) Canadell, J. G.; Le Quere, C.; Raupach, M. R.; Field, C. B.; Buitenhuis, E. T.; Ciais, P.; Conway, T. J.; Gillett, N. P.; Houghton, R. A.; Marland, G. *Proceedings of the National Academy of Sciences of the United States of America*, **2007**, *104*, 18866.
- (103) Wolff, E. W., *Nature*, **2012**, *484*, 41.
- (104) Honisch, B.; Ridgwell, A.; Schmidt, D. N.; Thomas, E.; Gibbs, S. J.; Sluijs, A.; Zeebe, R.; Kump, L.; Martindale, R. C.; Greene, S. E.; Kiessling, W.; Ries, J.; Zachos, J. C.; Royer, D. L.; Barker, S.; Marchitto, T. M., Jr.; Moyer, R.; Pelejero, C.; Ziveri, P.; Foster, G. L.; Williams, B. *Science*, **2012**, *335*, 1058.
- (105) Hansen, J.; Sato, M.; Kharceda, P.; Beerling, D.; Berner, R.; Masson-Delmotte, V.; Pagani, M.; Raymo, M.; Royer, D. L.; Zachos, J. C., *The Open Atmospheric Science Journal*, **2008**, *2*, 217.
- (106) Gibbins, J.; Chalmers, H. *Energy Policy*, **2008**, *36*, 4317.
- (107) Oh, T. H. *Renewable and Sustainable Energy Reviews*, **2010**, *14*, 2697.
- (108) Samanta, A.; Zhao, A.; Shimizu, G. K. H.; Sarkar, P.; Gupta, R. *Industrial & Engineering Chemistry Research*, **2012**, *51*, 1438.
- (109) Drage, T. C.; Snape, C. E.; Stevens, L. A.; Wood, J.; Wang, J.; Cooper, A. I.; Dawson, R.; Guo, X.; Satterley, C.; Irons, R. *Journal of Materials Chemistry*, **2012**, *22*, 2815.
- (110) Lee, K. B.; Beaver, M. G.; Caram, H. S.; Sircar, S., *Industrial & Engineering Chemistry Research*, **2008**, *48*, 8048.
- (111) Sayari, A.; Belmabkhout, Y., *Journal of the American Chemical Society*, **2010**, *132*, 6312.
- (112) Drage, T. C.; Arenillas, A.; Smith, K. M.; Snape, C. E. *Microporous and Mesoporous Materials*, **2008**, *116*, 504.
- (113) Tröger, J., *Journal für Praktische Chemie*, **1887**, *36*, 227.
- (114) Spielman, M. A., *Journal of the American Chemical Society*, **1935**, *57*, 583.
- (115) Didier, D.; Tylleman, B.; Lambert, N.; Vande Velde, C. M. L.; Blockhuys, F.; Collas, A.; Sergeev, S. *Tetrahedron*, **2008**, *64*, 6252.
- (116) Sergeev, S., *Helvetica Chimica Acta*, **2009**, *92*, 415.
- (117) Larson, S. B.; Wilcox, C. S., *Acta Crystallographica Section C: Crystal Structure Communication*, **1986**, *42*, 224.
- (118) Webster, B. M., *Recueil Des Travaux Chimiques Des Pays-Bas-Journal of the Royal Netherlands Chemical Society*, **1953**, *72*, 661.
- (119) Marquis, E.; Graton, J.; Berthelot, M.; Planchat, A.; Laurence, C.; *Canadian Journal of Chemistry*, **2004**, *82*, 1413.
- (120) Poli, E.; Merino, E. b.; Díaz, U.; Brunel, D.; Corma, A. *The Journal of Physical Chemistry C*, **2011**, *115*, 7573.
- (121) Dolensky, B.; Havlik, M.; Kral, V. *Chemical Society reviews*, **2012**, *41*, 3839.
- (122) McKeown, N. B.; Carta, M.; Croad, M., UK Patent Applied PCT/GB2011/051703; WO 2012/035327 (2010).
- (123) Carta, M.; Malpass-Evans, R.; Croad, M. J.; Rogan, Y.; Jansen, J. C.; Bernado, P.; Bazzarelli, F.; McKeown, N. B., *Science*, **2013**, *339*, 303.
- (124) Abella, C. A.; Benassi, M.; Santos, L. S.; Eberlin, M. N.; Coelho, F. *The Journal of Organic Chemistry*, **2007**, *72*, 4048.
- (125) Bag, B. G.; Maitra, U., *Synthetic Communications*, **1995**, *25*, 1849.
- (126) Johnson, R. A.; Gorman, R. R.; Wnuk, R. J.; Crittenden, N. J.; Aiken, J. W. *Journal of Medicinal Chemistry*, **1993**, *36*, 3202.
- (127) Qian, X.; Li, Z.; Xu, X.; Peng, Y.; Jiang, Z.; Ding, C. *Synthesis*, **2005**, 1228.
- (128) Furst, A.; Berlo, R. C.; Hooton, S. *Chemical Reviews*, **1965**, *65*, 51.

- (129) Furst, A.; Balcom, D. *Journal of the American Chemical Society*, **1953**, 75, 4334.
- (130) Vione, D.; Maurino, V.; Minero, C.; Pelizzetti, E. *Environmental Science and Technology*, **2005**, 39, 1101.
- (131) Halder, R.; Lawal, A.; Damavarapu, R. *Catalysis Today*, **2007**, 125, 74.
- (132) Klanderman, B. H.; Perkins, W. C. *The Journal of Organic Chemistry*, **1969**, 34, 630.
- (133) Crivello, J. V. *The Journal of Organic Chemistry*, **1981**, 46, 3056.
- (134) Chen, Z.; Swager, T. M. *Macromolecules*, **2008**, 41, 6880.
- (135) Chong, J. H.; MacLachlan, M. J. *Inorganic Chemistry Communication*, **2006**, 45, 1442.
- (136) Zhang, C.; Chen, C. F. *The Journal of Organic Chemistry*, **2006**, 71, 6626.
- (137) Hart, H.; Bashir-Hashemi, A.; Luo, J. Meador, M. A. *Tetrahedron*, **1986**, 42, 1641.
- (138) Friedman, L.; Logullo, F. M. *Journal of the American Chemical Society*, **1963**, 85, 1549.
- (139) Chance, J. M.; Geiger, J. H. Okamoto, Y.; Aburatani, R.; Mislow, K. *Journal of the American Chemical Society*, **1990**, 112, 3540.
- (140) Allen, C. F. H.; Bell, A. *Organic Syntheses*, **1955**, 3, 310.
- (141) Zhang, C.-Z.; Yang, H.; Wu, D.-L.; Lu, G.-Y. *Chinese Journal of Chemistry*, **2007**, 25, 653.
- (142) Sangaiah, R.; Gold, A. *The Journal of Organic Chemistry*, **1987**, 52, 3205.
- (143) Marquadt, D. J.; McCormick, F. A. *Tetrahedron Letters*, **1994**, 35, 1131.
- (144) He, N.; Chen, Y.; Doyle, J.; Liu, Y.; Blau, W. J. *Dyes and Pigments*, **2008**, 76, 569.
- (145) Brändstrom, A.; Carlsson, S. A. I. *Acta Chemica Scandinavica*, **1967**, 21, 983.
- (146) Xu, H.; Wolf, C. *Chemical Communications (Cambridge)*, **2009**, 3035.
- (147) Chen, J.; Yuan, T.; Hao, W.; Cai, M. *Tetrahedron Letters*, **2011**, 52, 3710.
- (148) Wu, Z.; Jiang, Z.; Wu, D.; Xiang, H.; Zhou, X. *European Journal of Organic Chemistry*, **2010**, 2010, 1854.
- (149) Zhao, H.; Fu, H.; Qiao, R. *The Journal of Organic Chemistry*, **2010**, 75, 3311.
- (150) Godinez, C. E.; Zepeda, G.; Mortko, C. J.; Dang, H.; Garcia-Garibay, M. A. *The Journal of Organic Chemistry*, **2004**, 69, 1652.
- (151) Hess, H.-J.; Cronin, T. H.; Scriabine, A. *Journal of Medicinal Chemistry*, **1968**, 11, 130.
- (152) Teng, M.; Johnson, M. D.; Thomas, C.; Kiel, D.; Lakis, J. N.; Kercher, T.; Aytes, S.; Kostrowicki, J.; Bhumralkar, D.; Truesdale, L.; May, J.; Sidelman, U.; Kodra, J. T.; Jorgensen, A. S.; Olesen, P. H.; de Jong, J. C.; Madsen, P.; Behrens, C.; Pettersson, I.; Knudsen, L. B.; Holst, J. J.; Lau, J. *Bioorganic & Medicinal Chemistry Letters*, **2007**, 17, 5472.
- (153) Guenzi, A.; Johnson, C. A.; Cozzi, F.; Mislow, K. *Journal of the American Chemical Society*, **1983**, 105, 1438.
- (154) Yagodkin, E.; Douglas, C. J. *Tetrahedron Letters*, **2010**, 51, 3037.
- (155) Fieser, L. F.; Webber, T. G. *Journal of the American Chemical Society*, **1940**, 62, 1360.
- (156) Sergeev, S.; Stas, S.; Remacle, A.; Vande Velde, C. M. L.; Dolenský, B.; Havlík, M.; Král, V.; Čejka, J. *Tetrahedron: Asymmetry*, **2009**, 20, 1918.
- (157) Shopsowitz, K.; Lelj, F.; MacLachlan, M. J. *The Journal of Organic Chemistry*, **2011**, 76, 1285.
- (158) ChlChak, K.; Jacquemard, U.; Branda, N. R. *European Journal of Inorganic Chemistry*, **2002**, 357.
- (159) Lee, H.; Oh, J.; Chu, H. Y.; Lee, J.-I.; Kim, S. H.; Yang, Y. S.; Kim, G. H.; Do, L.-M.; Zyung, T.; Lee, J.; Park, Y. *Tetrahedron*, **2003**, 59, 2773.

- (160) Pei, J.; Ni, J.; Zhou, X.-H.; Cao, X.-Y.; Lai, Y.-H. *The Journal of Organic Chemistry*, **2002**, *67*, 4924.
- (161) Fournier, J.-H.; Maris, T.; Wuest, J. D. *The Journal of Organic Chemistry*, **2004**, *69*, 1762.
- (162) Choi, K.-Y.; Yi, M. H. *Macromolecules Symposia*, **1999**, *142*, 193.
- (163) Gao, C.; Zhang, S.; Gao, L.; Ding, M. *Macromolecules*, **2003**, *36*, 5559.
- (164) Yi, M. H.; Huang, W.; Lee, B. J.; Choi, K.-Y. *Journal of Polymer Science: Part A: Polymer Chemistry*, **1999**, *37*, 3449.
- (165) Vygodskii, Y. S.; Churochkina, N. A.; Panova, T. A.; Fedotov, Y. A. *Reactive & Functional Polymers*, **1996**, *30*, 241.
- (166) Kim, I. C.; Park, K. W.; Tak, T. M. *Journal of Applied Polymer Science*, **1999**, *73*, 907.
- (167) Huang, W. Y.; Chang, M. Y.; Han, Y. K.; Huang, P. T. *Journal of Polymer Science Part A: Polymer Chemistry*, **2010**, *48*, 5872.
- (168) Wu, J.-R.; Chen, Y.; Wu, T.-Y. *Journal of Applied Polymer Science*, **2011**, *119*, 2576.
- (169) Niederl, J. B.; Nagel, R. H. *Journal of the American Chemical Society*, **1941**, *63*, 580.
- (170) Ma, X.; Swaidan, R.; Belmabkhout, Y.; Zhu, Y.; Litwiller, E.; Jouiad, M.; Pinnau, I.; Han, Y. *Macromolecules*, **2012**, *45*, 3841.
- (171) Vickery, E. H.; Pahler, L. F.; Eisenbraun, E. J. *The Journal of Organic Chemistry*, **1979**, *44*, 4444.
- (172) Carter, K. R. *Macromolecules*, **1995**, *28*, 6462.
- (173) Bunnett, J. F.; Zahler, R. E. *Chemical Reviews*, **1951**, *49*, 273.
- (174) Carothers, W. H. *Transactions of the Faraday Society*, **1936**, *32*, 39.
- (175) Dolensky, B.; Elguero, J.; Král, V.; Pardo, C.; Valík, M. *Advances in Heterocyclic Chemistry*, **2007**, *93*, 1.
- (176) Smith, M.; March, J. *Advanced Organic Chemistry: Reactions, Mechanisms and Structure (5th ed.)*, **2001**, New York: Wiley-Interscience, ISBN 0-471-58589-0.
- (177) Lenev, D. A.; Golovanov, D. G.; Lyssenko, K. A.; Kostyanovsky, R. G. *Tetrahedron: Asymmetry*, **2006**, *17*, 2191.
- (178) Weber, E.; Müller, U.; Worsch, D.; Vögtle, F.; Will, G.; Kirfel, A. *Journal of the Chemical Society, Chemical Communications*, **1985**, 1578.
- (179) Sayari, A.; Belmabkhout, Y.; Serna-Guerrero, R. *Chemical Engineering Journal*, **2011**, *171*, 760.
- (180) Ruthven, D. M.; Brandani, S.; Kanellopoulos, N. K. *Recent Advances in Gas Separation by Microporous Ceramic Membranes*, Elsevier: Amsterdam, **2000**, ISBN: 978-0-444-50272-8, 187.
- (181) Brandani, F.; Ruthven, D.; Coe, C. G. *Industrial and Engineering Chemical Research*, **2003**, *42*, 1451.
- (182) Poli, E.; Merino, E. b.; Díaz, U.; Brunel, D.; Corma, A. *The Journal of Physical Chemistry C*, **2011**, *115*, 7573.
- (183) Unpublished work, Professor Neil McKeown research group, Cardiff University.
- (184) Irwin, L. J.; Reibenspies, J. H.; Miller, S. A. *Journal of the American Chemical Society*, **2004**, *126*, 16716.
- (185) Klanderman, B. H.; Criswell, T. R. *The Journal of Organic Chemistry*, **1969**, *34*, 3426.
- (186) Netka, J.; Crump, S. L.; Rickborn, B. *The Journal of Organic Chemistry*, **1986**, *51*, 1189.

- (187) Dhayalan, V.; Clement, J. A.; Jagan, R.; Mohanakrishnan, A. K. *European Journal of Organic Chemistry*, **2009**, 2009, 531.
- (188) Wang, X.; Zhang, Y.; Sun, X.; Bian, Y.; Ma, C.; Jiang, J. *Inorganic Chemistry*, **2007**, 46, 7136.
- (189) Naghipur, A.; Reszka, K.; Sapse, A.-M.; Lown, J. W. *Journal of the American Chemical Society*, **1989**, 111, 258.
- (190) Stock, L. M.; Wasielewski, M. R. *Journal of the American Chemical Society*, **1977**, 99, 50.
- (191) Konieczny, M.; Harvey, R. G. *The Journal of Organic Chemistry*, **1980**, 45, 1308.
- (192) Zeng, W. *Synthesis*, **2004**, 7, 1011.
- (193) Nose, M.; Suzuki, H. *Synthesis*, **2000**, 11, 1539.
- (194) Doornbos, T. *Organic Preparations and Procedures*, **1969**, 1, 287.
- (195) Errazuriz, B.; Tapia, R.; Valderrama, J. A. *Tetrahedron Letters*, **1985**, 26, 819.
- (196) Markiewicz, J. T.; Wiest, O.; Helquist, P. *The Journal of Organic Chemistry*, **2010**, 75, 4887.
- (197) Poriel, C.; Ferrand, Y.; Juillard, S.; Le Maux, P.; Simonneaux, G. *Tetrahedron*, **2004**, 60, 145.
- (198) Ryashentseva, M. A. Patent SU 170998, **1965**.
- (199) Lu, H. H.; Ma, Y. S.; Yang, N. J.; Lin, G. H.; Wu, Y. C.; Chen, S. A. *Journal of the American Chemical Society*, **2011**, 133, 9634.
- (200) Molteni, V.; Rhodes, D.; Rubins, K.; Hansen, M.; Bushman, F. D.; Siegel, J. S. *Journal of Medicinal Chemistry*, **2000**, 43, 2031.

Appendix 1: Solid state crystal structure analysis

As part of the synthesis for this project crystals were grown for interesting compounds, including TB model compounds, bis-aniline monomers and coumaron derivatives. The technique chosen for crystal growth was slow diffusion, which works by the diffusion of a non-solvent into a solution of the purified compound. The crystals were analysed by single-crystal X-ray diffraction (XRD) and, after resolution, the crystal structures were analysed using various software, such as Mercury 3.0.

An attempt to grow crystals for each model compound, bis-aniline monomer and coumaron derivative was made using a suitable solvent (THF, DCM and ethyl acetate) and a range of non-solvents (such as hexane, petroleum ether and methanol). Typically, the best conditions for crystal growth were found to be when chloroform or THF was used as the solvent and hexane used as the non-solvent.

A1.1 Crystal structures from TB model compounds

The TB model compound is made from a mono-aniline derivative which was reacted using the TB condensation procedure but, having only one amino moiety it forms a dimer instead of polymerising. This allows for crystals to be grown of these interesting compounds, which is not possible for the amorphous polymers, thus enabling an investigation of their structural properties, which share many similarities with those of the corresponding polymers, if the model compound is imagined as a repeat unit of the polymer.

A1.1.1 Tröger's base

A good starting point for this analysis are the crystal structures of unsubstituted TB and dimethyl-TB (Figure 58), which have previously been resolved and reported^{115, 117}. The structures show the expected V-shaped framework with an angle around the nitrogen atoms, formed by the intersection of the two phenyl rings (α) of 95.4° for unsubstituted TB and 92.9° and 97.4° for dimethyl-TB.

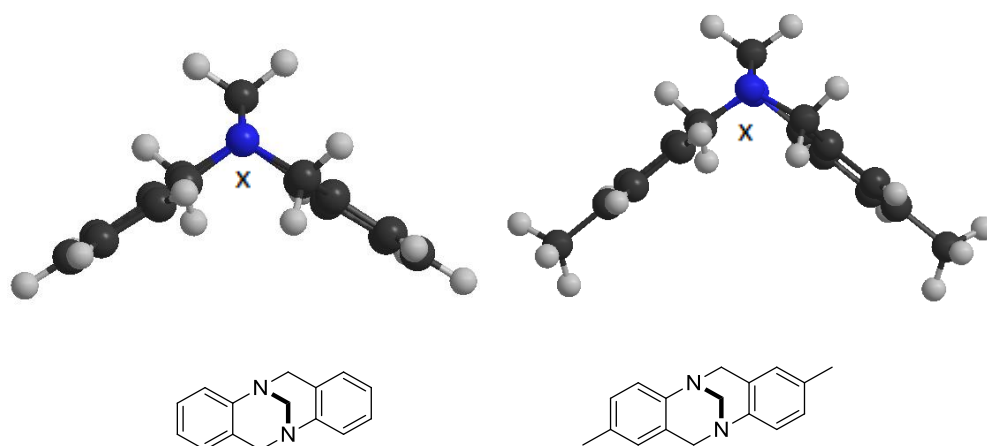


Figure 58: The structure of TB Model compounds 1 and 2 (3D images made using Chem3D Pro).

A1.1.2 TB 1,4-dimethoxytetrahydronaphthalene model compound (Compound 6)

Crystals of compound **6** were prepared using the slow-diffusion method with chloroform as the solvent and hexane as the non-solvent. The crystal structure (Figure 59) shows the non-planarity of the molecule, with the V-shape which is typical of the TB unit, particularly evident when viewed from the side. The crystal formed as a clathrate, since a molecule of chloroform was present in the unit cell, but was omitted from the figure for clarity. The angle around the nitrogen atoms, formed by the intersection of the two phenyl rings (x) was found to be 113.65° .

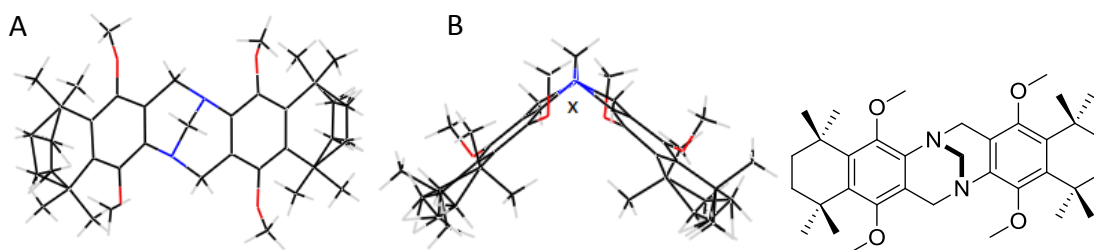


Figure 59: The solid state crystal structure of compound **6**, A. Facial view, B. Side view. Also shown is the ChemDraw representation of the compound.

The packing of several unit cells ($2 \times 2 \times 2$) shows an interesting pattern, with the molecules unable to pack closely together, resulting in large spaces between molecules (Figure 60). Unfortunately, this analysis is less useful for this model compound because no corresponding polymer could be synthesised, but it does prove that the presence of the TB

unit prevents space efficient packing, although for this compound the bulky phenyl substituents clearly have some effect.

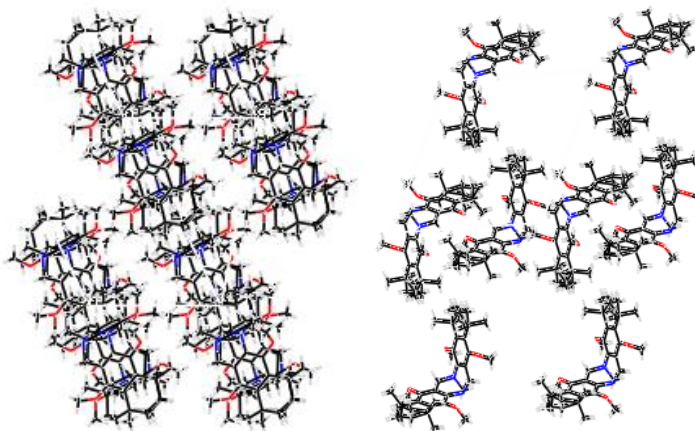


Figure 60: The bulk packing of compound **6**, observed from different angles.

A1.1.3 TB triptycene model compound (Compound 13)

Crystals of compound **13** were grown by slow diffusion of hexane into a solution of the compound dissolved in ethyl acetate. The crystal grew as a clathrate (Figure 61), with two molecules of hexane present in the unit cell, but these were omitted from the figure for simplicity. The typical V-shape can be clearly seen from the side view, which also shows the shape of the rigid triptycene framework. The angle formed by the intersection of the phenyl rings around the TB unit (x) was found to be 113.86° .

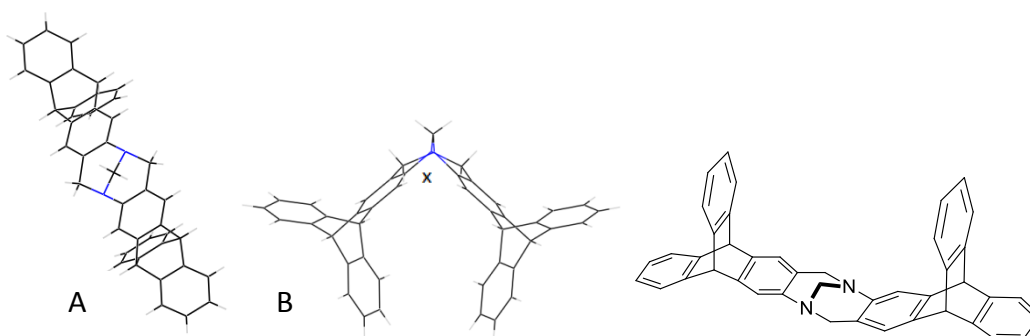


Figure 61: The solid state crystal structure of compound **13**. A. Facial view, B. Side view. Also shown is a ChemDraw representation of the compound.

The packing of several unit cells ($2 \times 2 \times 2$) of the solid state crystal structure shows that the bulk packing of compound **13** is very inefficient, with large cavities and pores left between molecules (Figure 62). This helps to explain why polymer **82** exhibits high microporosity, since the polymer chains should behave similarly. The effect of the additional site of contortion, provided by the triptycene framework can quite clearly be seen from both images, confirming that triptycene is a useful building block for PIMs.

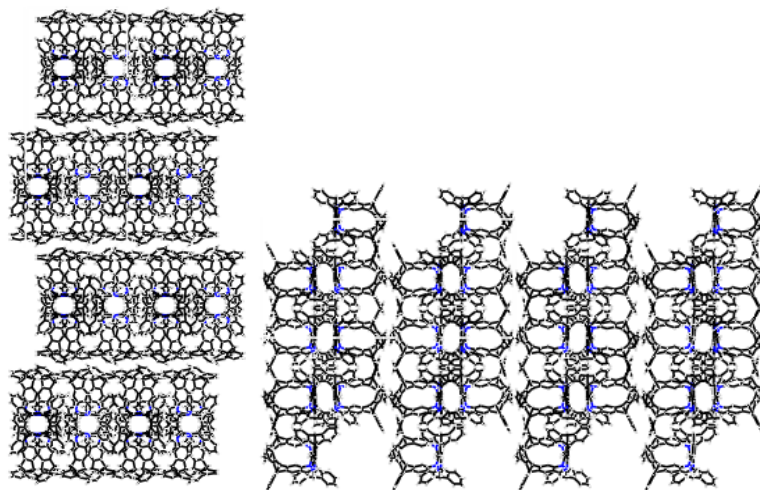


Figure 62: The packing of several unit cells of compound **13**, observed from different angles.

A1.1.4 TB naphthalene model compound (Compound 53)

Crystals of compound **53** were prepared using the slow-diffusion method with THF as the solvent and hexane as the non-solvent. The crystal structure (Figure 63) shows the expected V-shape with the naphthalene ring systems pointing in opposite directions. The angle formed by the intersection of the phenyl rings around the TB unit (x) was found to be 111.32° .

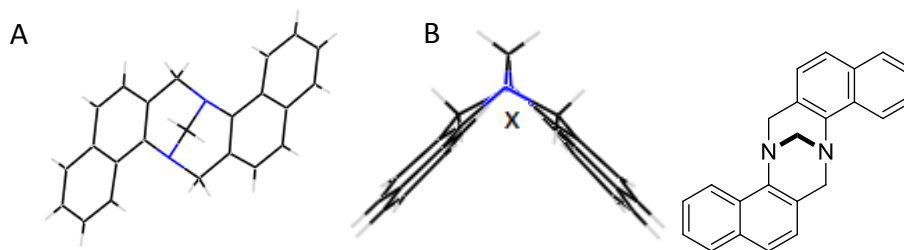


Figure 63: The solid state crystal structure of compound **53**. A. Facial view, B. Side view, also shown is the ChemDraw representation of the compound.

When analysing the packing between unit cells ($2 \times 2 \times 2$) for this solid state crystal structure the general trend of poor space efficient packing can once again be observed, resulting in channels and cavities present between molecules (Figure 64), which in this case were not occupied by solvent molecules. It appears that the presence of the rigid TB links ensure poor packing for compound **53**, despite the potential for good π -stacking between conjugated ring systems on neighbouring molecules, which would enhance intermolecular cohesion and facilitate efficient packing. This may help to explain the high microporosity displayed by polymer **88**.

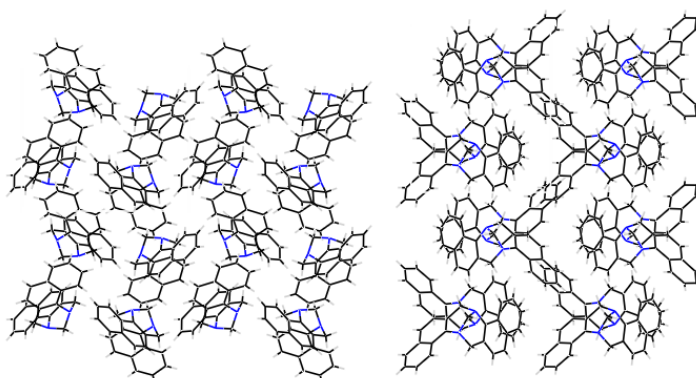


Figure 64: The packing of compound **53**, observed from different angles.

A1.1.5 TB 1,4-dimethylbenzene model compound (Compound **54**)

Crystals of compound **54** were grown using the slow-diffusion method with chloroform as the solvent and hexane as the non-solvent. The crystal structure (Figure 65) shows that the compound exhibits the expected V-shape, but no solvent was present in the unit cell showing the decreased ability to form hydrogen bonding and short contact. The angle

formed by the intersection of the phenyl rings around the TB unit (x) was found to be 112.67°.

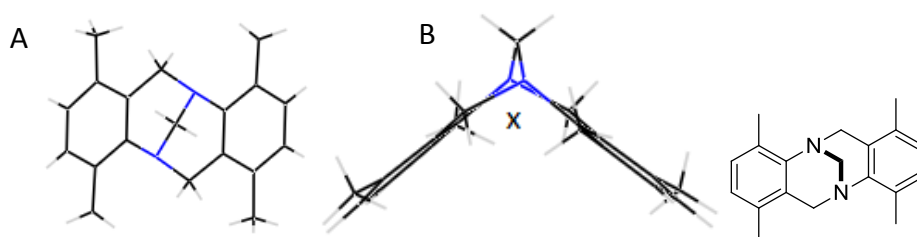


Figure 65: The solid state crystal structure of compound **54**, A. Facial view, B. Side view. Also shown is the ChemDraw representation of the compound.

Once again, the packing of several unit cells (2 x 2 x 2) shows that the molecules of this model compound are unable to pack closely together, resulting in solvent-filled space existing as channels between molecules (Figure 66). This analysis again proves that the presence of TB links hinder space efficient packing, which may help to explain the moderate microporosity observed in the related polymer **91**.

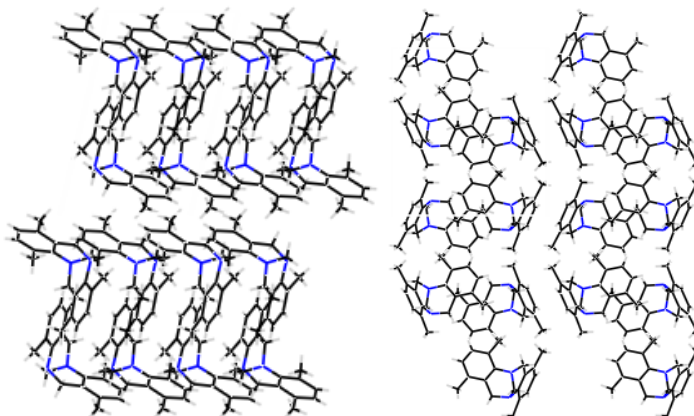


Figure 66: The packing of compound **54**, from different angles.

A1.1.6 Summary of bond angles and solid state crystal structure properties for the TB model compounds

The angles around the TB unit for the compounds discussed and the crystal cell parameters are summarised below in tables 18 and 19. All of these angles for the prepared model compounds are substantially larger than the angle reported for unsubstituted TB, although it should be stated that angles derived from single crystal X-ray diffraction can be greatly affected by crystal effects. This data suggests a general and logical linear trend of increasing intersection angle when the bulkiness of the phenyl ring substituents is increased, but no obvious trend exists between the size of this angle and the degree of microporosity exhibited by the corresponding polymers, confirming that these model compounds are not true representations of the structure of their related polymers.

Model compound	N°	Intersection Angle	Polymer surface area (m ² /g)
Unsubstituted TB	-	95.4°	-
Dimethyl TB	-	92.9° and 97.4°	-
1,4-Dimethoxytetrahydronaphthalene	6	113.65°	-
Triptycene	13	113.86°	725 (ladder) 1035 (network)
Naphthalene	53	111.32°	700
1,4-Dimethylbenzene	54	112.67°	430

Table 18: The bond angles around the TB unit.

Model compound	N°	Space group	Crystal system	Cell parameters	Cell volume (Å ³)	Z
1,4-Dimethoxytetrahydronaphthalene	6	P -1	Orthorhombic	a =9.6255(3) b =13.8598(6) c=14.8971(6) α =111.57(2) β =101.44(2) γ =100.77(2)	1736.37	2
Triptycene	13	P bca	Orthorhombic	a =19.6400(2) b =17.8250(19) c =41.9200(5) α= β =γ =90.00	14675.5	16
Naphthalene	53	P 21/c	Monoclinic	a =10.9661(5) b =13.1191(8) c =11.3187(5) β =93.95(3)	1624.5	0
1,4-Dimethylbenzene	54	P 21/c	Monoclinic	a =13.0370(3) b =13.8370(3) c =8.2433(16) β =103.32(3)	1447.03	4

Table 19: Solid state crystal structure parameters for TB model compounds.

A1.2 Bis-aniline monomers

The bis-aniline monomer series was synthesised using a solvent-free dehydration reaction between a suitable ketone or alcohol and aniline or *o*-toluidine hydrochloride salt, producing a compound with two amino groups, which possesses more structural flexibility than usual for PIM monomers owing to the lack of fused ring skeleton. Despite the majority of these compounds have been previously synthesised in published literature, their structures have not been resolved by single-crystal XRD. Therefore, crystal formation was attempted for each of the monomers, this proved successful for most of the series, but despite numerous attempts high quality crystals could not be synthesised for compounds **63**, **68** or **69**.

A1.2.1 Monomer 1: Compound 62

Crystals of monomer **62** were grown from the slow diffusion of hexane into a solution of chloroform containing the monomer. The resulting crystal structure exhibits a V-shape with the cyclohexane ring in the low energy chair conformation (Figure 67). Analysis found that the angle made from the intersection of the two phenyl rings (x) was 107.84° , which serves as a good reference point for the rest of the series as the cyclohexane ring is the least bulky of the different ring systems.

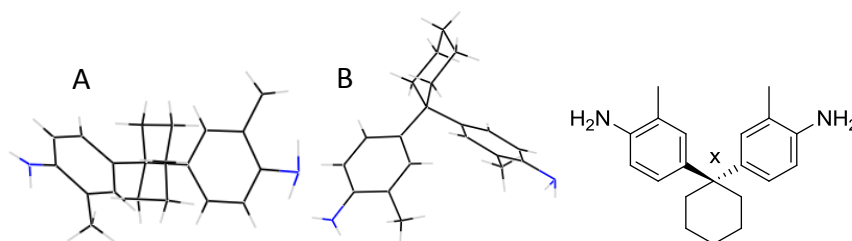


Figure 67: The solid state crystal structure of compound **62**. A. Facial view, B. Side view. Also shown is the ChemDraw representation of the compound.

A1.2.2 Monomer 2: Compound 64

Crystals of compound **64** were prepared from the slow diffusion of hexane into a solution of the monomer in THF. Similar to compound **62** the crystal structure was found to have a V-shape, with the norborane ring system clearly more bulky than the cyclohexane ring (Figure 68). The bond angle formed by the intersection of the phenyl rings (x) was found to be 106.37° .

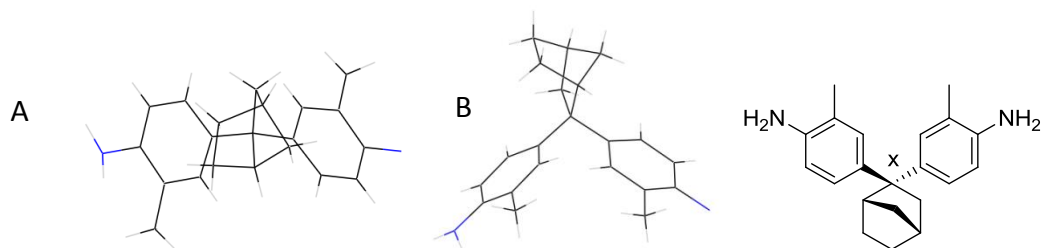


Figure 68: The solid state crystal structure of compound **64**. A. Facial view, B. Side view. Also shown is a ChemDraw representation of the compound.

A1.2.3 Monomer 3: Compound 65

Crystals of compound **65** were grown from the slow diffusion of hexane into a solution of the monomer in THF. The crystal structure exhibits the familiar V-shape, but the norborane group was not as easy to resolve as for compound **64**, resulting in a disordered appearance (Figure 69). The bond angle between the two phenyl rings (x) was found to be 107.59° .

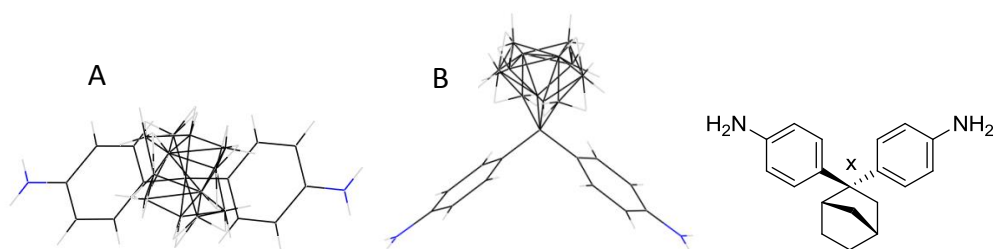


Figure 69: The solid state crystal structure of compound **65**. A. Facial view, B. Side view. Also shown is a ChemDraw representation of the compound.

A1.2.4 Monomer 4: Compound 66

Crystals of compound **66** were prepared from the slow diffusion of hexane into a solution of the monomer in chloroform. The crystal structure clearly shows the familiar V-shape formed by the phenyl rings, and the cage-like structure of adamantane unit (Figure 70). The angle formed by the intersection of the phenyl rings (x) was found to be 104.41° .

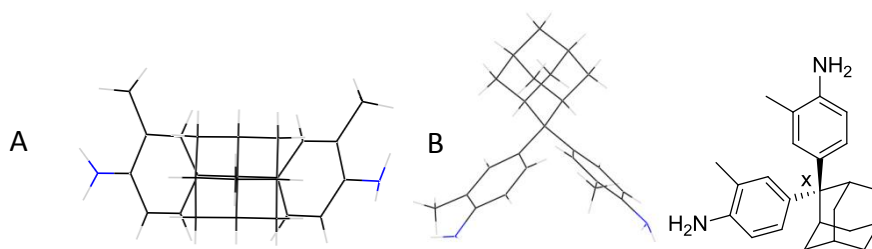


Figure 70: The solid state crystal structure of compound **66**. A. Facial view, B. Side view. Also shown is the ChemDraw representation of the compound.

A1.2.5 Monomer 5: Compound 67

Crystals of compound **67** were prepared using the slow-diffusion method with hexane as the non-solvent and THF as the solvent. The crystal structure shows a similar molecular structure to that of compound **66**, with the phenyl rings forming a V-shape and the bulky cage structure of the adamantane unit (Figure 71). The angle of intersection between the two phenyl rings (x) was found to be 106.31° .

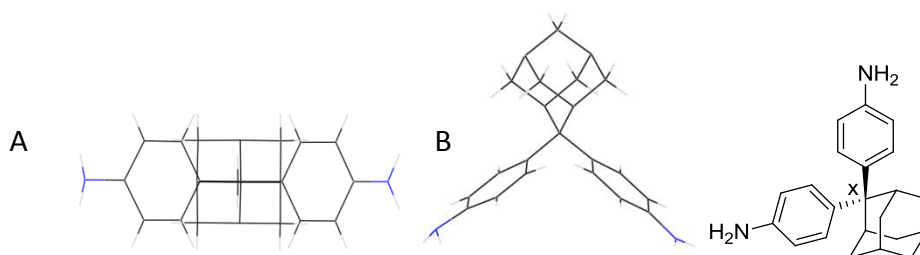


Figure 71: The solid state crystal structure of compound **67**. A. Facial view, B. Side view. Also shown is the ChemDraw representation of the compound.

A1.2.6 Monomer 6: Compound 70

Crystals of compound **70** were grown from the slow diffusion of hexane into a solution of the monomer in THF. The crystal structure (Figure 72) shows a structure unlike that for any of the other monomers, simply because a diol rather than a ketone was used as the starting material, meaning that the two 2-methylaniline groups are not bonded to the same carbon. The angle between the amino substituted phenyl rings and the central phenyl rings (x) was found to be 109.70° on both sides of the symmetrical molecule.

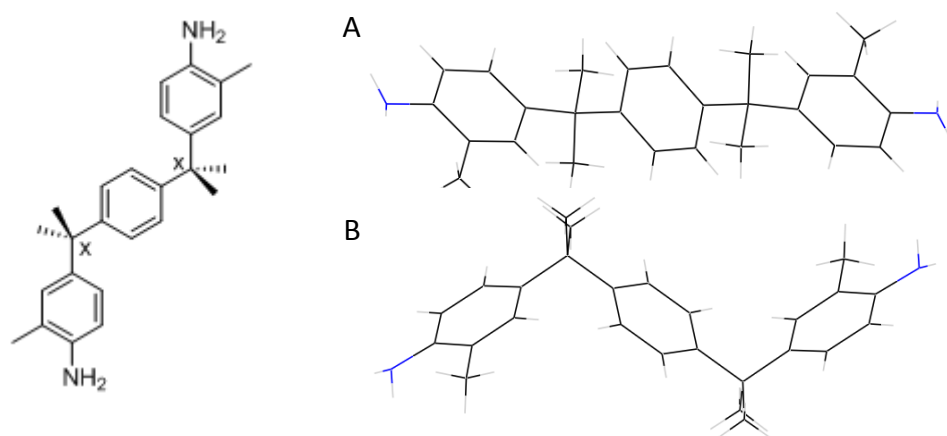


Figure 72: The solid state crystal structure of compound **70**. A. Facial view, B. Side view. Also shown is the ChemDraw representation of the compound.

A1.2.7 Monomer 7: Compound 71

Crystals of compound **71** were prepared from the slow diffusion of hexane into a solution of the monomer in THF. The crystal structure (Figure 73) shows that the molecule adopts a tetrahedral conformation with the phenyl rings adopting the familiar V-shape and lying perpendicular to the fluorene ring system. The angle formed by the intersection of the phenyl rings around the fluorene ring system (x) was found to be 114.13° .

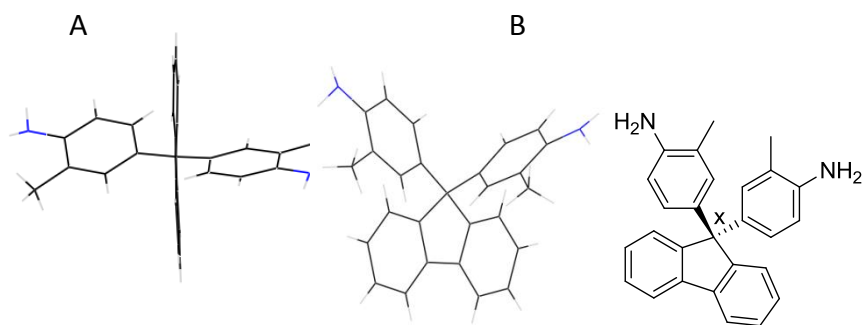


Figure 73: The solid state crystal structure of compound **71**. A. Facial view, B. Side view. Also shown is a ChemDraw representation of the compound.

A1.2.8 Monomer 8: Compound 74

Crystals of compound **74** were grown from the slow diffusion of hexane into a solution of the monomer in chloroform. The crystal structure shows a similar structure to that of compound **71**, a tetrahedral conformation with the phenyl rings adopting a V-shape and lying in a plane perpendicular to that occupied by the fluorene ring system (Figure 74). The angle of intersection between the phenyl rings and the fluorene ring system (x) was found to be 112.94° .

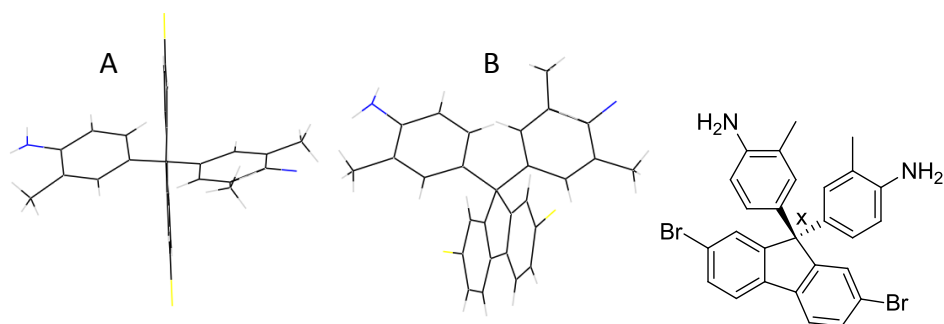


Figure 74: The solid state crystal structure of compound **74**. A. Facial view, B. Side view. Also shown is a ChemDraw representation of the compound.

3.2.9 Summary of intersection angles and solid state crystal structure properties for the bis-aniline monomers

The angles formed by the intersection of the phenyl rings for the monomers discussed and the crystal cell parameters are summarised below in tables 20 and 21. There appears to be two main trends related to the angle of intersection: a linear connection between the size of the angle and size of the group between the two phenyl rings, and secondly, an increase in the angle when methyl substituents are absent from the phenyl rings. However, the difference between the intersection angles for the 8 bis-aniline monomers is small enough that other factors could be responsible for the discrepancy, including instrument error and crystal effects.

Bis-aniline monomer	N°	Angle	Polymer surface area (m ² /g)
Cyclohexanone bis-methylaniline	62	107.84	30
Norcamphor bis-methylaniline	64	106.37	70
Norcamphor bis-aniline	65	107.59	4
Adamantanone bis-methylaniline	66	104.41	615
Adamantanone bis-aniline	67	106.31	50
Bis(hydroxyisopropyl)benzene bis-methylaniline	70	109.70	6
Fluorenone bis-methylaniline	71	114.13	400
Dibromofluorenone bis-methylaniline	74	112.94	390

Table 20: The summary of the intersection angles for the bis-aniline monomers.

Bis-aniline monomer	N°	Space group	Crystal system	Cell parameters	Cell volume (Å ³)	Z
Cyclohexane-bismethylaniline	62	I 41/a	Tetragonal	a = 31.3432(18) b = 31.4883(18) c = 6.5834(5) α = 89.88 β = 89.82 γ = 89.83	6497.37	18
Norcamphor-bismethylaniline	64	C 2/c	Monoclinic	a = 29.7279(8) b = 6.9561(3) c = 18.1863(8) β = 114.29	3427.94	8
Norcamphor-bis-aniline	65	P 2 ₁ 2 ₁ 2 ₁	Orthorhombic	a 6.4087(4) b 10.7718(7) c 10.7814(6) α = β = γ = 90.00	744.28	-
Adamantanone-bismethylaniline	66	I -42d	Tetragonal	a 14.8398(14) b 14.8373(18) c 36.1380(5) α = β = γ = 90.00	7956.96	18

Bis-aniline monomer	N°	Space group	Crystal system	Cell parameters	Cell volume (Å ³)	Z
Adamantanone-bis-aniline	67	P nma	Orthorhombic	a =12.2760(4) b =12.6251(3) c =21.4990(8) $\alpha =\beta =\gamma =90.00$	3331.25	8
Bis(hydroxyisopropyl)benzene-bismethylaniline	70	P 21/n	Monoclinic	a =10.0150(5) b =10.3320(5) c =10.7710(5) $\beta =111.37(5)$	1037.87	2
Fluorenone-bismethylaniline	71	P 21/n	Monoclinic	a =13.4303(7) b =11.9346(6) c =13.4861(5) $\beta =114.21(3)$	1971.49	4
Dibromofluorenone-bismethylaniline	74	P 21/n	Monoclinic	a =11.7990(5) b =14.0900(5) c =15.2150(5) $\beta =110.80(5)$	2364.65	-

Table 21: The solid state crystal structure parameters for the series of bis-aniline monomers.

A1.3 Coumaron derivatives

Where possible crystals were grown for the coumaron derivatives because the structure of this interesting framework had not been previously investigated by XRD and this would provide useful information on the rigidity and shape of the framework. Furthermore, this enabled an assessment of the viability of using the framework as a building block for PIM synthesis.

A1.3.1 Coumaron 1: Compound 75

Crystals of compound **75** were prepared from the slow diffusion of hexane into a solution of the compound in THF. The crystal structure (Figure 75) shows a highly rigid molecule adopting a shape with the two phenyl rings from the benzil pointing upwards in such a way that they appear to overlap when the molecule is viewed from the side, whilst the other two phenyl rings are angled downwards due to the contortion of the fused ring system. The fused ring unit provides the structure with its high rigidity and the site of contortion that would be useful in a coumaron-based PIM.

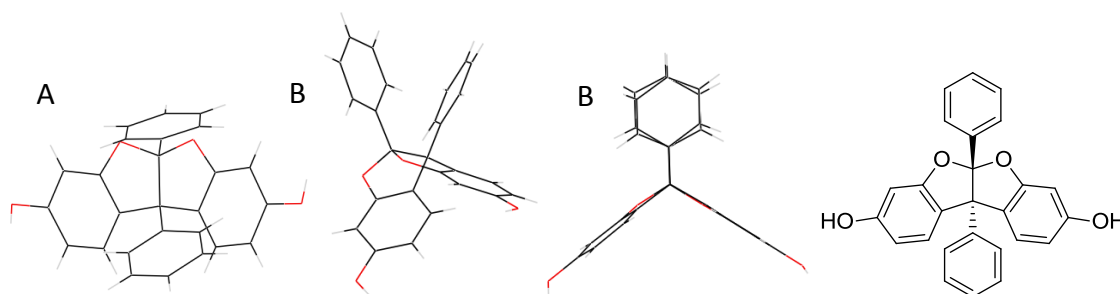


Figure 75: The solid state crystal structure of compound **75**. A. Facial view, B. Side views. Also shown is a ChemDraw representation of the compound.

Analysis showed that the angles formed by the intersection of the phenyl rings with the two five-membered rings (Figure 76) were different (115.93° and 116.47°) and the angles formed by the connection of the two five-membered rings are also different (110.42° and 108.19°).

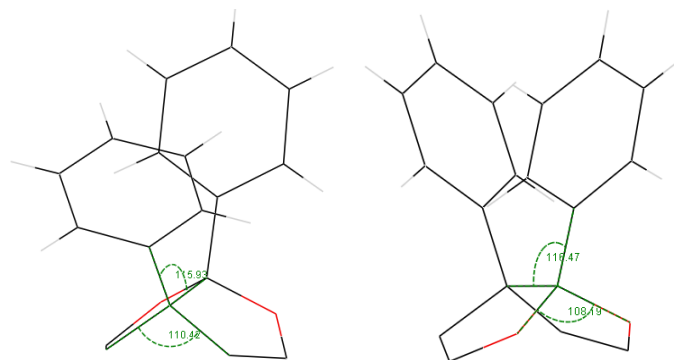


Figure 76: Fragments of the wireframe structures of compound **75**, showing the important angles.

A1.3.2 Coumaron 2: Compound 76

Crystals of compound **76** were grown from the slow diffusion of hexane into a solution of the compound in THF. The crystals were found to be clathrates, with a molecule of acetic acid included in the unit cell, although this was omitted for clarity. The crystal structure again shows a rigid framework with a four membered fused-ring skeleton component and two additional phenyl rings pointing in the opposite direction (Figure 77). This time these two phenyl rings do not overlap greatly, presumably to minimise the steric interaction between the two bulky bromine atoms.

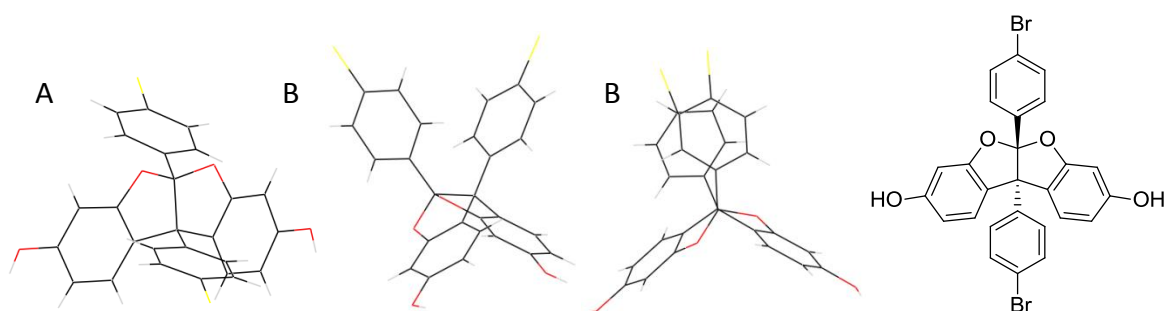


Figure 77: The solid state crystal structure of compound **76**. A. Facial view. B. Side views. Also shown is a ChemDraw representation of the compound.

Analysis of the angles within the framework showed that there is greater variation between the two sides of the structure (Figure 78); with the angles formed by the connection of the two five-membered rings differing at 111.94° and 106.83° , whilst the angles formed by the intersection of the free phenyl rings with the fused-ring component are also quite different at 115.34° and 118.92° .

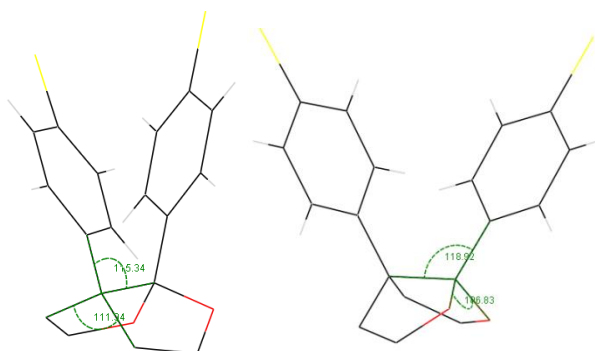


Figure 78: Fragments of the wireframe structures of compound **76**, showing the important angles.

A1.3.3 Coumaron 3: Compound **79**

Crystals of compound **79** were grown by the slow diffusion method with chloroform as the solvent and hexane as the non-solvent. The crystal structure shows that the compound adopts the familiar rigid framework structure (Figure 79) and bears close resemblance to that of compound **75**, as the two free phenyl rings do not overlap greatly. Each pair of methoxy groups appears to have the methyl groups pointing in opposite directions, presumably to minimise steric interaction, but the carbon-oxygen bonds appear free to rotate.

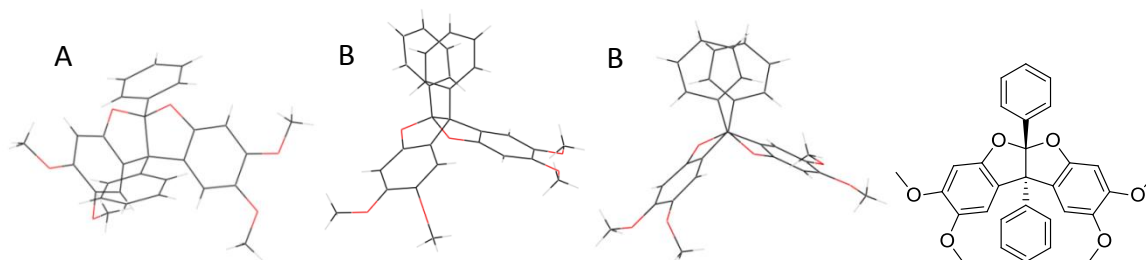


Figure 79: The solid state crystal structure of compound **79**. A. Facial view, B. Side views. Also shown is a ChemDraw representation of the compound.

Analysis of the angles within the framework showed the compound is unsymmetrical (Figure 80), with the angles formed by the intersection of the phenyl rings with the fused ring component at 118.89° and 114.56° , and the angles formed by the linking of the two five-membered rings of 108.25° and 110.63° .

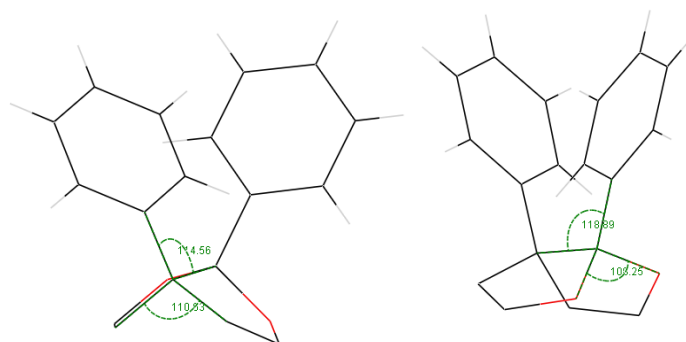


Figure 80: Fragments of the wireframe structures of compound **79**, showing the important angles.

A1.3.4 Coumaron 4: Compound **81**

Crystals of compound **81** were prepared from the slow diffusion of methanol into a solution of the compound in chloroform. The crystals grew as a clathrate with a molecule of dichloroethane present in the unit cell. The crystal structure shows the typical coumaron shape (Figure 81), with the rigid four membered ring fused component pointing in an opposite direction to the two free bromine substituted phenyl rings, which show poor overlap, presumably to minimise steric interaction between the two bulky bromine atoms. Each pair of methoxy substituents has the methyl groups angled in different directions to minimise steric interaction, but carbon-oxygen bonds appear free to rotate.

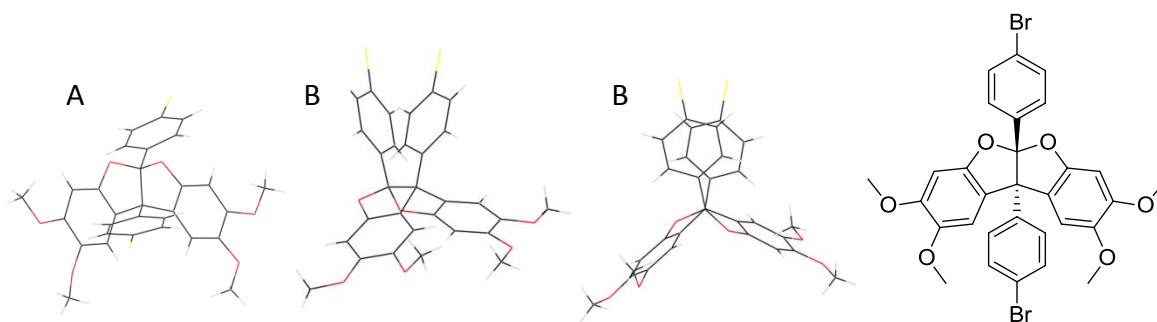


Figure 81: The solid state crystal structure of compound **81**. A. Facial view, B. Side views. Also shown is a ChemDraw representation of the compound.

The analysis of the angles within the framework showed the same unsymmetrical pattern as for the other coumaron derivatives (Figure 82). The angles of the links between the two five-membered rings are 107.49° and 111.91° , whilst the angles of intersection between the phenyl rings and the fused ring component are 117.16° and 114.96° .

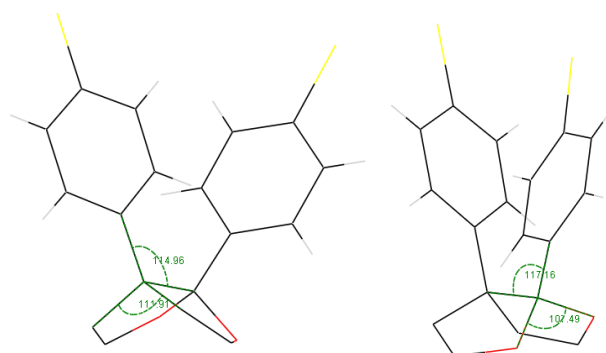


Figure 82: Fragments of the wireframe structure of compound **81**, showing the important angles.

A1.3.5 Summary of coumaron derivative crystal structures

With no prior investigation into the coumaron framework this crystal analysis study has proven useful for providing information on the shape and rigidity of the framework. The crystal structures of the coumaron derivatives show the rigidity of the coumaron unit, arising from the four membered fused ring components, which should make the framework suitable for incorporation into a PIM. The angles within the four frameworks show no obvious trend, merely suggesting that the framework is not symmetrical. The crystal parameters from these crystal structures are shown in tables 22 and 23.

Coumaron derivative	N°	Intersection angle between phenyl ring and five-membered fused ring component	Angle between five-membered rings
Dihydroxy-coumaron	75	115.93° and 116.47°	108.19° and 110.42 °
Dibromodihydroxy-coumaron	76	115.34° and 118.92°	106.83° and 111.94°
Dimethoxy-coumaron	79	114.56° and 118.99 °	108.25° and 116.63°
Dibromodimethoxy-coumaron	81	114.89° and 117.15°	107.63° and 112.12°

Table 22: A summary of the angles within the coumaron framework for each derivative.

Coumaron derivative	N°	Space group	Crystal system	Cell parameters	Cell volume (Å ³)	Z
Dihydroxy-coumaron	75	P 2 ₁ 2 ₁ 2 ₁	Orthorhombic	a = 8.1590(3) b = 12.3460(4) c = 19.1230(5) α = β = γ = 90.00	1926.28	4
Dibromodihydroxy-coumaron	76	P -1	Triclinic	a = 9.8227(4) b = 11.1614(6) c = 13.6996(10) α = 71.67(3) β = 82.16(4) γ = 73.91(3)	1367.91	2
Dimethoxy-coumaron	79	P -1	Triclinic	a = 9.0570(3) b = 11.5819(3) c = 12.6859(4) α = 82.76(2) β = 70.84(2) γ = 76.31(2)	1219.57	2
Dibromodimethoxy-coumaron	81	P -1	Triclinic	a = 10.6474(2) b = 12.0149(3) c = 13.2690(2) α = 75.68(2) β = 66.66(10) γ = 71.67(10)	1464.59	2

Table 23: The crystal parameters for the coumaron derivative crystal structures.